Geochimica et Cosmochimica Acta

JOURNAL OF THE GEOCHEMICAL SOCIETY

Executive Editors

C. W. CORRENS, *Göttingen.* E. INGERSON, *Austin, Texas.* L. R. WAGER, *Oxford.*

Editors

L. H. AHRENS, *Capetown.* S. R. NOCKOLDS, *Cambridge.* H. C. UREY, *La Jolla, Calif.*
JOHN VERHOOGEN, *Berkeley, Calif.* A. P. VINOGRADOV, *Moscow.*
W. A. WAHL, *Helsingfors.*

UNIVERSITY OF HAWAII LIBRARY

CONTENTS VOLUME 18, NOS. 1/2 JANUARY 1960

W. COMPSTON: The carbon isotopic compositions of certain marine invertebrates and coals from the Australian Permian 1
N. YAMAGATA, Y. MURAKAMI and T. TORII: Biogeochemical investigation in serpentine-chromite ore district 23
U. SCHINDEWOLF and M. WAHLGREN: The rhodium, silver and indium content of some chondritic meteorites 36
C. E. ADAMS, N. H. FARLOW and W. R. SCHELL: The compositions, structures and origins of radioactive fall-out particles 42
E-AN ZEN: Carbonate equilibria in the open ocean and their bearing on the interpretation of ancient carbonate rocks 57
H. FECHTIG, W. GENTNER und G. KISTNER: Räumliche Verteilung der Edelgasisotope im Eisenmeteoriten Treysa 72
A. P. TUDGE: A method of analysis of oxygen isotopes in orthophosphate—its use in the measurement of paleotemperatures 81
M. S. CROWLEY and R. ROY: The effect of formation pressures on sheet structures—a possible case of Al–Si ordering 94
G. L. BATE, H. A. POTRATZ and J. R. HUIZENGA: Scandium, chromium and europium in stone meteorites by simultaneous neutron activation analysis 101
J. R. MERRILL, E. F. X. LYDEN, M. HONDA and J. R. ARNOLD: The sedimentary geochemistry of the beryllium isotopes 108
E. A. VINCENT and J. H. CROCKET: Studies in the geochemistry of gold—I. The distribution of gold in rocks and minerals of the Skaergaard intrusion, East Greenland 130
E. A. VINCENT and J. H. CROCKET: Studies in the geochemistry of gold—II. The gold content of some basic and ultrabasic rocks and stone meteorites 143
Letter to the Editor:
D. M. KEMP and A. A. SMALES: Neutron activation results for vanadium and scandium in G-1 and W-1 149
Geochemical Note:
H. C. UREY: On the chemical evolution and densities of the planets 151
Book Review:
The Planet Earth, Edited by D. R. BATES. (Reviewed by H. HUGHES) 154
Errata 155
Papers to be published in future issues 156

QE351
.425

PERGAMON PRESS NEW YORK • LONDON • PARIS • LOS ANGELES

GEOCHIMICA ET COSMOCHIMICA ACTA

EXECUTIVE EDITORS

PROF. C. W. CORRENS (1959) *Sedimentpetrographisches Institut der Universität, Lotzestr.* 13, *Göttingen, Germany*
PROF. E. INGERSON (1959–1960) *Department of Geology, University of Texas, Austin* 12, *Texas, U.S.A.*
PROF. L. R. WAGER, F.R.S. (1959–1961) *Department of Geology and Mineralogy, The University Museum, Oxford, England*

EDITORS

PROF. L. H. AHRENS (1959–1960) *Department of Chemistry, University of Capetown, Rondebosch, Cape Province, South Africa*
Dr. S. R. NOCKOLDS (1959) *Department of Mineralogy and Petrology, The University, Cambridge, England*
PROF. H. C. UREY, For. Mem. R. S. (1959) *University of California, La Jolla, California, U.S.A.*
Dr. JOHN VERHOOGEN (1959–1961) *Department of Geology, University of California, Berkeley, California, U.S.A.*
PROF. A. P. VINOGRADOV (1959–1961) *Vernadsky Institute, Moscow, U.S.S.R.*
PROF. W. A. WAHL (1959–1961) *Observatoriegaten* 8, *Helsingfors, Finland*

EDITORIAL ADVISORY BOARD

AMERICAN CONTINENT

A. F. BUDDINGTON, *Princeton*
D. GUIMARÃES, *Belo Horizonte*
G. E. HUTCHINSON, *New Haven*
B. H. MASON, *New York*
F. WHIPPLE, *Cambridge*
R. WILDT, *New Haven*
H. S. YODER, *Washington*

EUROPE

T. F. W. BARTH, *Oslo*
L. CAPDECOMME, *Toulouse*
E. J. CONWAY, *Dublin*
P. ESKOLA, *Helsinki*
P. GALLITELLI, *Modena*
A. HADDING, *Lund*
O. HAHN, *Göttingen*
H. W. HARVEY, *Plymouth*
F. HEIDE, *Jena*
A. HOLMES, *Edinburgh*
W. Q. KENNEDY, *Leeds*
PH. H. KUENEN, *Gröningen*
S. LANDERGREN, *Stockholm*
F. MASHATSCHKI, *Vienna*
A. MUIR, *Harpenden*
J. ORCEL, *Paris*
E. RAGUIN, *Paris*
E. REINHARD, *Basle*
TH. G. SAHAMA, *Helsinki*
C. E. TILLEY, *Cambridge*
T. VOGT, *Trondheim*

FAR EAST

T. WATANABE, *Tokyo*

Publishing Office: Pergamon Press, Inc., 122 East 55th Street, New York 22, N.Y. (Plaza 3-9651)

Four issues per volume, three volumes per year

Subscription *per annum* (including postage) (A) $51.00; (B) For individual subscribers who write directly to the publisher certifying that the Journal is for their private use, $21.50. Members of the Geochemical Society, or non-members who occasionally publish papers in the Journal, $10.00 *per annum*.

Back numbers, $28.00 per volume

Single issues, $7.00 each

PERGAMON PRESS, INC.

122 EAST 55TH STREET, NEW YORK 22, N.Y. 4 & 5 FITZROY SQUARE, LONDON W.1

PRINTED IN NORTHERN IRELAND AT THE UNIVERSITIES PRESS, BELFAST.

PERGAMON PRESS

specialized journals for *specialized advertising!*

Advertise in GEOCHIMICA ET COSMOCHIMICA ACTA—

Space is available to all manufacturers of suitable products—the range which will appeal to readers of this journal is extensive and includes spectrometers, seismographs, seismic amplifiers and detectors, hydrometers, humidity instruments, monometers, galvanometers, radiation detectors and pyrometers, colorimeters, fluorometers, petrographic and other microscopes, flame photometers, surveying instruments, voltmeters, lenses and optical elements, mine ventilation instruments, X-ray microanalysers, pumps, pipe-lines, gas detection and measurement apparatus, microphotometers, X-ray films, plates and equipment, samplers of airborne dust and bacteria, telecommunications equipment, gyroscopic instruments, petroleum testing equipment, thermometers of all types, chemicals, oil boring equipment, electronic equipment . . . this list could easily be trebled!

We shall be happy to provide impartial advice as to the suitability of products not listed.

THIS IS ONE OF MORE THAN 50 INTERNATIONAL SCIENTIFIC JOURNALS. SPECIAL REDUCED "COMBINED RATES" ARE OFFERED TO MANUFACTURERS ADVERTISING IN MORE THAN ONE JOURNAL.

For details WRITE OR PHONE to

R. D. MILLER
Advertisement Manager
PERGAMON PRESS LIMITED
Pergamon House,
4 Fitzroy Square,
London W.1
Phone: EUSton 4455

H. L. WOUDHUYSEN
Advertisement Manager
PERGAMON PRESS INC.
122 East 55th Street,
New York 22, N.Y.,
U.S.A.
Phone: Plaza 3-9651

A selection of new titles from our 1959-60 catalogue

CUMULUS DYNAMICS

Edited by **Charles E. Anderson**

Proceedings of the first conference on Cumulus Convection held in May 1959 under the auspices of the Geophysics Research Directorate, U.S. Air Force Cambridge Research Center, Bedford, Mass.

In preparation

DYNAMICS OF CLIMATE

Edited by **Richard L. Pfeffer**

Proceedings of a conference on the application of numerical integration techniques to the problem of the general circulation, sponsored jointly by the Institute for Advanced Study and the U.S. Air Force Geophysics Research Directorate.

35s. net ($6.50)

ORGANIC GEOCHEMISTRY

Edited by **Irving A. Breger**

This treatise will be the first undertaken in the field, and will assure a complete synthesis between the application of the principles of organic chemistry and geology.

In preparation

PRINCIPLES OF METEORITICS

By **E. L. Krinov,** *Academy of Sciences of the U.S.S.R.*

In preparation

A SHORT OUTLINE OF THE GEOLOGY OF THE U.S.S.R.

By **D. V. Nalivkin**

Translated from the Russian by **S. I. Tomkeieff**

An outstanding Russian monograph of great topical interest.

Approx. 50s. net ($7.50)

PERGAMON PRESS

London New York Paris Los Angeles

4 & 5 Fitzroy Square, London, W.1 122 East 55th Street, New York 22, N.Y.

24 Rue des Écoles, Paris V^e^.

Geochimica et Cosmochimica Acta, 1960, Vol. 18, pp. 1 to 22. Pergamon Press Ltd. Printed in Northern Ireland

The carbon isotopic compositions of certain marine invertebrates and coals from the Australian Permian*

W. Compston
Department of Physics, University of Western Australia, Perth

Abstract—δC^{13} analyses are reported for Permian and Devonian brachiopods, Permian crinoids and Permian coals. δO^{18} analyses of the marine invertebrates are also given. Only the Permian brachiopods are isotopically preserved. Their mean δC^{13} value is significantly more positive than Cretaceous and Recent brachiopods and molluscs measured elsewhere. A single coal seam sampled in detail was very constant in δC^{13}, and a trend towards values some 2·5‰ more negative from lower to upper Permian was observed for a sequence of seams. The lower Permian coal δC^{13} was approximately the same as upper Carboniferous coal measured elsewhere. The meaning of this Permian isotopic distribution is discussed in terms of an age-effect, but there are other possible explanations.

Introduction

Attention has been drawn recently to the possible existence of age-effects in carbon isotopic abundance during post-Cambrian time. Wickman (1953) observed an apparent unidirectional trend in coal isotopic composition from upper Carboniferous to Pliocene, and Jeffery *et al.* (1955) suggested that their data for post-Cambrian coal and limestone could be interpreted in terms of fluctuations in the mean isotopic composition of the surface carbon reservoir. In neither case was the evidence conclusive: it merely indicated that no positive statement in either direction could then be made.

This paper describes analyses of Australian coals and marine invertebrates, chiefly of Permian age. It is intended as the beginning of systematic sampling of carbon fixed into these specific forms during the Permian, with the hope of contributing to an ultimate solution of the age-effect problem. The isotopic preservation of the marine invertebrates is explored in detail, and the instrumental accuracy of the analyses evaluated by measurement of isotopic reference standards. Analyses of preserved Permian material are then contrasted with those for other geological periods (measured elsewhere), and any significant grouping of the data in respect to time assessed in age-effect terms.

Materials

The fine-grained calcite found in most limestones is isotopically lighter (lower C^{13}/C^{12} ratio) on the average, than associated marine invertebrates (Urey *et al.*, 1951; Jeffery *et al.*, 1955). In contrast, calcareous algae are usually heavier (Craig, 1953; Lowenstam and Epstein, 1957), and it is possible that other phylogenetic groups of organisms may fractionate their carbon in characteristic ways. In view of this heterogeneity, it did not seem profitable to extend the earlier surveys of marine limestones in searching for an age-effect. Instead, attention was focused on the use of specific types of organisms.

Apparently both brachiopods and crinoids have always deposited calcite

* This work forms part of a thesis submitted to the University of Western Australia for the degree of Doctor of Philosophy.

rather than aragonite, which is metastable, as their shell material (STEHLI, 1956). This favours isotopic preservation since any recrystallization process, such as the inversion of aragonite to calcite, would be almost certainly accompanied by redistribution of the carbon and oxygen isotopes between the various chemical phases in the sediment. Since brachiopod shell structure, in contrast to the crinoids, consists of closely packed fibres or prisms with little interstitial space available for subsequent infilling by secondary calcite, these particular animals appeared quite promising as regards isotopic preservation. They were therefore selected as the most suitable available material for the possible detection of age-effects.

Representative samples of drill cores rather than hand-specimens of coal were chosen to avoid again any effects due to possible isotopic heterogeneity of the individual coal seams.

ACCURACY OF THE ISOTOPIC ANALYSES

Before data from different mass spectrometers may be accurately compared, it is essential to place all analyses on a common reference scale, and to demonstrate the absence or upper limit of possible systematic error in the particular measurement system employed. These requirements can be effected by the use of isotopic reference standards (CRAIG, 1957) together with proper handling of the raw experimental data.

The mass spectrometer

The mass spectrometer used here has been briefly described by JEFFERY *et al.* (1955). For this work, gas inlet switching valves (McKINNEY *et al.*, 1950) and new d.c. amplifiers (one a vibrating reed electrometer) were added. Instrumental technique and performance are described in detail by COMPSTON (1957).

Carbon dioxide was prepared by reacting carbonates with anhydrous phosphoric acid (McCREA, 1950), and organic carbon with the VAN SLYKE and FOLCH combustion fluid. Standard Dolomite was again used as the working reference gas (JEFFERY *et al.*, 1955).

Both carbon and oxygen isotope ratios were determined for each sample. These were measured relative to the ratios of a local reference gas, and expressed as per mil differences, δC^{13} and δO^{18}. The δ values are defined as

$$\delta = \frac{R \text{ sample} - R \text{ reference}}{R \text{ reference}} 1000$$

in which R denotes the ratio $C^{13}O_2{}^{16}/C^{12}O_2{}^{16}$ for δC^{13}, or the ratio $C^{12}O^{16}O^{18}/C^{12}O_2{}^{16}$ for δO^{18}. For comparison with earlier data, the δ values have been recalculated relative to the Chicago reference gas PDB1 (UREY *et al.*, 1951; CRAIG, 1957).

Corrections to the measured δ values

The ion beam ratios recorded by the mass spectrometer were the quantities

$$R'\left(\frac{45}{44}\right) = \frac{C^{13}O_2{}^{16} + C^{12}O^{16}O^{17} + f_1(C^{12}O_2{}^{16})}{C^{12}O_2{}^{16}}$$

and

$$R'\left(\frac{46}{44}\right) = \frac{C^{12}O^{16}O^{18} + f_2(C^{12}O_2{}^{16})}{C^{13}O_2{}^{16} + C^{12}O^{16}O^{17} + C^{12}O_2{}^{16}},$$

where f_1 and f_2 denote the small fractions of the intense mass 44 beam scattered into the mass 45 and mass 46 collector; δ' values were defined in terms of these experimental ratios, and corrections then applied in order to attain the true δC^{13} and δO^{18}. Correction was also applied for the mixing between sample and reference gases which occurs during measurement.

With the exception of the gas-scatter terms, these corrections have been evaluated by CRAIG (1957). For the mass spectrometer used in the present work, some 4 per cent on the average of both the mass 45 and mass 46 beams were contributed by scattered mass 44 ions. This produced a correction factor of 1·04, by which the δ' values were multiplied to normalize to zero scatter. The factor ranged in value from 1·02 to 1·06 according to the ion source efficiency, which was not maintained constant in this machine from day to day.

Gas mixing at the inlet valves amounted to 2 per cent. Using CRAIG'S derivation for the other factors, the relationship between $\delta'C^{13}$ as measured in this work and the true δC^{13} values becomes

$$\delta C^{13} = 1{\cdot}132\ \delta' C^{13} - 0{\cdot}034\ \delta O^{18}$$

with small variation in the $\delta'C^{13}$ factor according to the particular value taken for the gas-scatter term. Similarly, the relationship between $\delta'O^{18}$ and δO^{18} becomes

$$\delta O^{18} = 1{\cdot}062\ \delta' O^{18} + 0{\cdot}009\ \delta C^{13}$$

Reproducibility of analysis

Noise on the ratio traces contributed an uncertainty not greater than $\pm 0{\cdot}1‰$ to all $\delta'C^{13}$ values. The average difference in δC^{13} found between several independent preparations and measurements of the same sample gas was $\pm 0{\cdot}2‰$, both for carbonates and coals.

Initially in this study, rough δO^{18} analyses were made solely to correct the $\delta'C^{13}$ values. No attempt was made to control the temperature of carbonate decomposition, and standard dolomite in particular was sometimes heated to speed the reaction. Later, the value of precise δO^{18} determinations was realized. Through the courtesy of Dr. S. EPSTEIN, the writer subsequently re-analysed a number of specimens at the California Institute of Technology, where it was found, as expected, that the original δO^{18} values were irregularly too positive by amounts ranging from 0·5 up to 2·0‰ in the extreme case. All analyses here in which this uncertainty remains are indicated in the tables by an asterisk.

Measurement of isotopic reference standards

The corrected δ values relative to Standard Dolomite, $\delta_{S/SD}$, have been expressed as δ's relative to PDB1, $\delta_{S/PDB}$, through the relationship

$$\delta_{S/PDB} = \delta_{S/SD}\left(1 + \frac{\delta_{SD/PDB}}{1000}\right) + \delta_{SD/PDB}$$

The value for $\delta_{SD/PDB}$ was found indirectly by measurement of three isotopic reference standards, whose δ values on the PDB1 scale have been determined by CRAIG (1957). These analyses and CRAIG's are shown together in Table 1. The δO^{18} values, marked as described above, may differ systematically from analyses of the same samples decomposed at constant temperature. However, in this case, they are self-consistent, in that the three calcitic standards were prepared at room temperature, and measured relative to a single preparation of standard dolomite gas.

Table 1. Reference standards measurements

	SD scale		PDB scale (CRAIG, 1957)	
	δC^{13}	δO^{18}	δC^{13}	δO^{18}
NBS Std.	−1·1	+4·9*	−1·06	−4·14
Baertschi Std.	+2·6	+7·8*	+2·77	−1·62
Wickman Std.	−10·2	−6·6*	−10·32	−15·38

* See text for explanation of asterisks.

It is evident from Table 1 that the origins of the SD and PDB1 δC^{13} scales happen to be identical. If there is no systematic error between the two analysis systems, the scales will be identical throughout the entire δ range.

The upper limit for possible systematic error was evaluated by computing "standard differences" between pairs of reference standards analyses, since the δ value of a standard A relative to another standard B as calculated from the δ values of each relative to some reference sample S, must be independent of the choice of S and of the measuring system employed to obtain $\delta_{A/S}$ and $\delta_{B/S}$. Table 2 shows such standard differences calculated from the data of Table 1.

Table 2. Reference sample "standard differences"

	This work		CRAIG (1957)	
	δC^{13}	δO^{18}	δC^{13}	δO^{18}
$\delta_{W/B}$	−12·8	−14·4	$-13{\cdot}0_5$	$-13{\cdot}7_8$
$\delta_{W/NBS}$	−9·1	−11·5	$-9{\cdot}3_0$	$-11{\cdot}2_9$
$\delta_{B/NBS}$	$+3{\cdot}7_5$	+2·9	$+3{\cdot}8_0$	$+2{\cdot}5_3$

Subscripts: W, Wickman reference sample; B, Baertschi reference sample; NBS, National Bureau of Standards reference sample.

All equivalent values in Table 2 are equal to within the compounded possible errors in each δ determination. However, if the data are read literally it suggests that the Perth δC^{13} values might be systematically some 2 per cent lower than the Chicago values. This error, if it exists, amounts to 0·5‰ in a coal δ value of −25‰, which has little geochemical significance for the range of coal δ values used in this paper. For the marine invertebrate values the maximum error, 0·12‰, is quite negligible.

Table 3a. Permian specimens, Carnarvon Basin, Western Australia

No.	Specimen	δC^{13}	δO^{18}	Portion analyses	Stratigraphic unit	Locality
ML122	*Neospirifer*	+5·1	−1·2	Interior pedicle valve near beak	Coolkilya formation	S. Southern Cross Mill
ML51	*Neospirifer* 1	+5·8	−0·4	Section pedicle valve beak ridge	Norton greywacke	Minilya Syncline
ML51	*Neospirifer* 2	+5·0	—	Section near centre pedicle valve	Norton greywacke	Minilya Syncline
ML51	*Neospirifer* 3	+3·8	−0·2	Section pedicle valve, beak ridge	Norton greywacke	Minilya Syncline
ML44	*Neospirifer*	+2·9	−0·5	Section, fold pedicle valve	Wandagee formation	Minilya Syncline
ML87	*Calceolispongia*	−11·2	−10·8*	Section, basal plate	Bulgadoo shale	Lyndon River
ML26	*Neospirifer* 1	+5·3	−0·5	Section, anterior margin, pedicle valve	Callytharra formation	SE Donnelly's Well
ML26	*Neospirifer* 2	+4·8	—	Section, anterior margin, pedicle valve	Callytharra formation	SE Donnelly's Well
CW132	*Neospirifer*	+3·8	−0·1	Section, pedicle valve towards beak	Callytharra formation	SE Donnelly's Well
CW132	*Neospirifer*	+3·6	−0·4	Lamellar layer only pedicle valve	Callytharra formation	SE Donnelly's Well
CW87	*Neospirifer* 1	+4·8	+0·7	Section pedicle valve beak	Callytharra formation	Callytharra Springs
CW87	*Neospirifer* 2	+4·6	+0·5	Section pedicle valve beak	Callytharra formation	Callytharra Springs
CW87	*Neospirifer* 3	+4·9	—	Section pedicle valve beak	Callytharra formation	Callytharra Springs
CW84	Crinoid	+2·0	−15·5*	Basal plate	Callytharra formation	Callytharra Springs
ML94	*Calceolispongia* 1	−8·5	−6·8	Section, basal plate	Callytharra formation	Minilya Syncline
	Calceolispongia 2	−6·0	−4·7*	Section, basal plate	Callytharra formation	Minilya Syncline
	Calceolispongia 3	−7·3	−4·2*	Section, basal plate	Callytharra formation	Minilya Syncline
	Calceolispongia 4	+3·7	−7*	Stem ossicles	Callytharra formation	Lyndon river
ML107	Spiriferid	+2·0	+0·2	Section beak ridge, pedicle valve	Lyons Group, 1500 ft below top of group	Lyndon river
		$-2{\cdot}7_4$	−3·7	Section through beak	Lyons Group, 1500 ft below top of group	Lyndon river
		+4·0	+2·2	Section through beak	Lyons Group, 1500 ft below top of group	Lyndon river
	Calceolispongia	+4·7	−8*	Basal plates	Lyons Group, 1500 ft below top of group	Lyndon river

Marine Invertebrate Data

Table 3 shows δC^{13} and δO^{18} for the brachiopods and other fossil marine invertebrates analysed in this work. The location, stratigraphic horizon, genus and portion analysed of each specimen are listed opposite its δ value. Sample locations of both marine invertebrates and coals are shown on Fig. 12, p. 19. The material analysed usually represented the thickest part available macroscopically free from the sedimentary matrix. In most cases a section was cut approximately normal to the growth lines, so that at least 1 year's shell growth should be sampled.

Figs. 1 and 2 illustrate the relative ranges in δC^{13} of the Permian and Devonian samples, and the frequency distribution of the two brachiopod groups. Fig. 3

Table 3b. Permian specimens, Fitzroy Basin, Western Australia

No.	Specimen	δC^{13}	δO^{18}	Portion analysed	Stratigraphic unit	Locality
KLB11	*Neospirifer*	+5·3	−0·2	Interior, pedicle valve, beak ridge	Upper Liveringa Group	Mt. Hardman
	Crinoid	−13·3	−8·8*	Basal plate section	Upper Liveringa Group	Mt. Hardman
KLB57	*Neospirifer*	+5·3	+0·7*	Interior, pedicle valve, inter area	Upper Liveringa Group	Mt. Hardman
KNB53	*Neospirifer*	+5·0	−2·6*	Section, anterior pedicle valve	Lower Liveringa Group	NE Mt. Fenton
	Calceolispongia	−17·0	−9·8*	Section, basal plate	Top, Noonkanbah Formation	Mt. Marmion
KNF88	*Neospirifer*	+4·8	+0·5	Section, pedicle valve toward beak	2300 ft Noonkanbah Formation	Bruten's Yard Christmas Creek
KNF76	*Neospirifer*	+5·3	Table 4	Section, posterior margin, pedicle valve	Noonkanbah formation 2150 ft	Bruten's Yard Christmas Creek
KNF73	*Neospirifer*	+3·9	−1·5	Section, posterior margin, pedicle valve	Noonkanbah formation 750 ft	Bruten's Yard Christmas Creek
KNF83	*Neospirifer*	+4·0	−1·6	Section, middle of pedicle valve	Noonkanbah formation 575 ft	Bruten's Yard Christmas Creek
KNF84	*Neospirifer*	+4·1	−1·3	Section, towards anterior unident. valve	Noonkanbah formation 500 ft	Bruten's Yard Christmas Creek
KNA44	*Neospirifer*	+5·2	+0·2	Section, middle pedicle valve	Noonkanbah formation 1240 ft	So. Grant Range
KNA39	*Strophalosia*	+4·0	−0·2	Section, beak pedicle valve	Noonkanbah formation 1200 ft	So. Grant Range
KNA28	*Neospirifer*	+4·2	−0·4	Section, middle of pedicle valve	Noonkanbah formation 900 ft	So. Grant Range
		+3·9	—	Section, middle of pedicle valve	Noonkanbah formation	So. Grant Range
KNA22	*Taeniothaerus*	+2·8	−1·1	Section, valve unident.	Noonkanbah formation 815 ft	So. Grant Range
		+2·6	−1·0	Section, valve unident.	Noonkanbah formation 815 ft	So. Grant Range
KNA17	*Dictyoclostus*	+1·3	−1·4	Section, valve unident.	Noonkanbah formation 770 ft	So. Grant Range
KNuA1	*Neospirifer*	+3·9	−0·8*	Section, brachial valve	Nura Nura limestone	Mt. Wynne

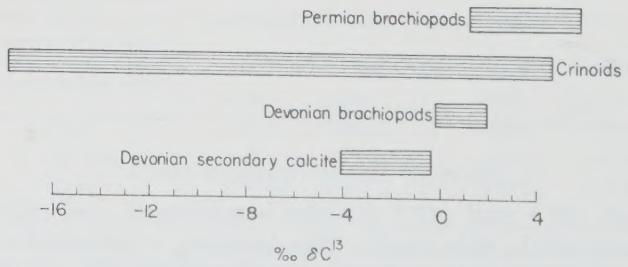

Fig. 1. δC^{13} ranges of Palaeozoic marine invertebrates. Recrystallized Devonian invertebrates are included as "Secondary calcite."

shows a series of analyses of successive portions of a single Permian brachiopod. It is evident from Fig. 2 that this particular group of Permian brachiopods can be characterized in carbon isotopic composition by a mean value of +4·3‰, since half of the analyses fall within ±0·7‰ of this figure, and their distribution is roughly normal. The range of the Devonian brachiopod analyses is also short,

Table 3c. Devonian specimens

No.	Specimen	δC^{13}	δO^{18}	Portion analysed	Stratigraphic unit	Locality
17408	Rhynchonellid 1	+0·8 +1·1	−5·2 —	Lamellar layer, pedicle valve	Gneudna formation	Williambury, W. Australia
	Rhynchonellid 2	+0·2	—	Lamellar layer, pedicle valve	Gneudna formation	Williambury, W. Australia
	Rhynchonellid 3	−0·1	−6·0*	Section, pedicle valve	Gneuda formation	Williambury, W. Australia
17355	*Cyrtospirifer* 1	+1·6	−3·6	Section beak, plus adjacent lamellar layers	Gneudna formation	Williambury, W. Australia
	Cyrtospirifer 2	−0·2	−5·5	Section beak	Gneudna formation	Williambury, W. Australia
17315	*Cyrtospirifer*	−0·1	−5·6*	Lamellar layer, pedicle valve	Gneudna formation	Williambury, W. Australia
	Secondary calcite	−0·3	−8·9*	Filling to above	Gneudna formation	Williambury, W. Australia
17294	Rhynchonellid (recrystallized)	−4·1	−7·0*	Portion pedicle valve	Gneudna formation	Williambury, W. Australia
17291	Nautiloid (recrystallized)	−1·4	−9·1*	Outer shell wall	Gneudna formation	Williambury, W. Australia
C1	*Austrospirifer variablis*	+0·7	−6·1*	Section, pedicle valve	Gneudna formation	Williambury, W. Australia
C?	*Hypothyridina*	+1·9	−4·8	Section, pedicle valve	Gneudna formation	Williambury, W. Australia
[C2	Secondary calcite	−0·8	−5·8*	Filling to above	Gneudna formation	Williambury, W. Australia
C3	*Austrospirifer variablis*	+0·6	−6·2*	Section, pedicle valve	Gneudna formation	Williambury, W. Australia

* May contain an irregular error in the range 0·0 to +2·0‰

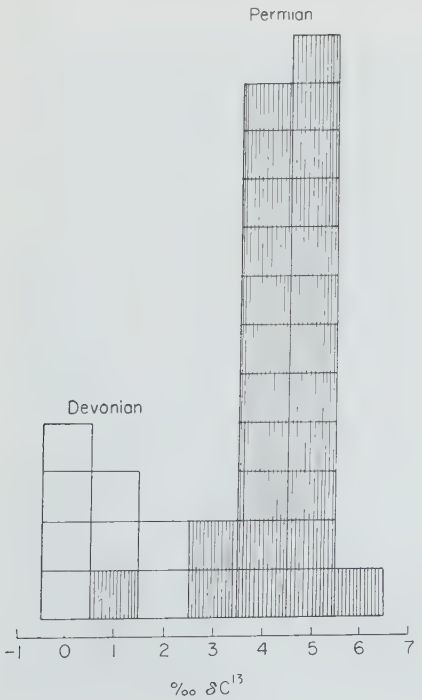

Fig. 2. Brachiopod δC^{13} distributions.

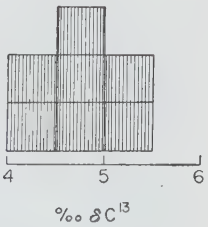

Fig. 3. δC^{13} distribution within a single Permian brachiopod.

and differs significantly from the Permian, but there are hardly enough samples to give a reliable picture of any characteristic internal distribution (Fig. 2). Similarly, the Permian crinoid analyses are too few in number and spread over too wide a range to reveal any possible isotopic characterization (other than the wide range).

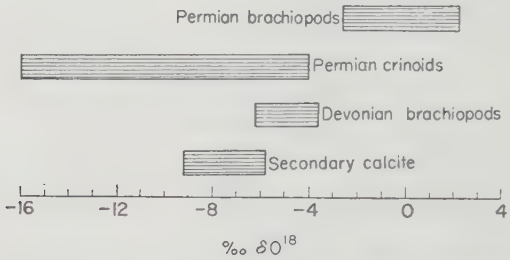

Fig. 4. δO^{18} ranges of Palaeozoic marine invertebrates. Recrystallized Devonian invertebrates included in "Secondary calcite."

Figs. 4 and 5 show the equivalent information for the δO^{18} values. The crinoid values again exhibit a very wide spread, while those of the Permian and Devonian brachiopods form two distinct groups. However, the frequency distributions of the two latter are skewed in the negative δO^{18} direction, particularly for the Devonian group.

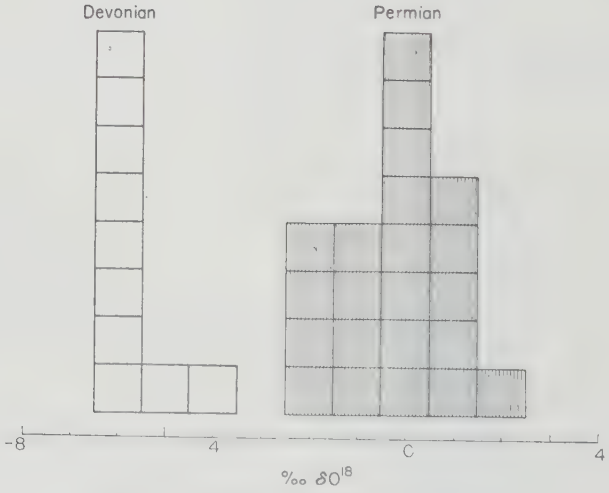

Fig. 5. Brachiopod δO^{18} distributions.

δO^{18} analyses of successive increments of single specimens are currently in progress and will be reported in detail elsewhere. So far variations of about 0·5‰ have been observed in a single Permian brachiopod.

Preservation of the original isotopic composition

Before considering the δ values in terms of a possible time-effect, it is essential to establish the degree to which they represent the original isotopic compositions

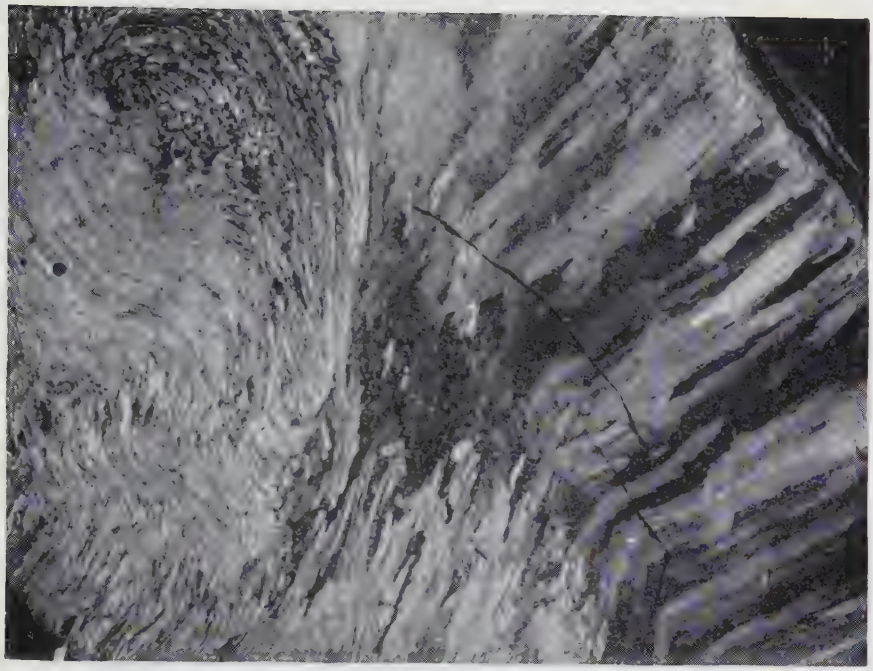

Fig. 6(a). *Neospirifer* CW87, showing external lamellar zone (top right-hand corner), internal prismatic zone, and contorted fibrous calcite of the hinge line ($\times 35$).

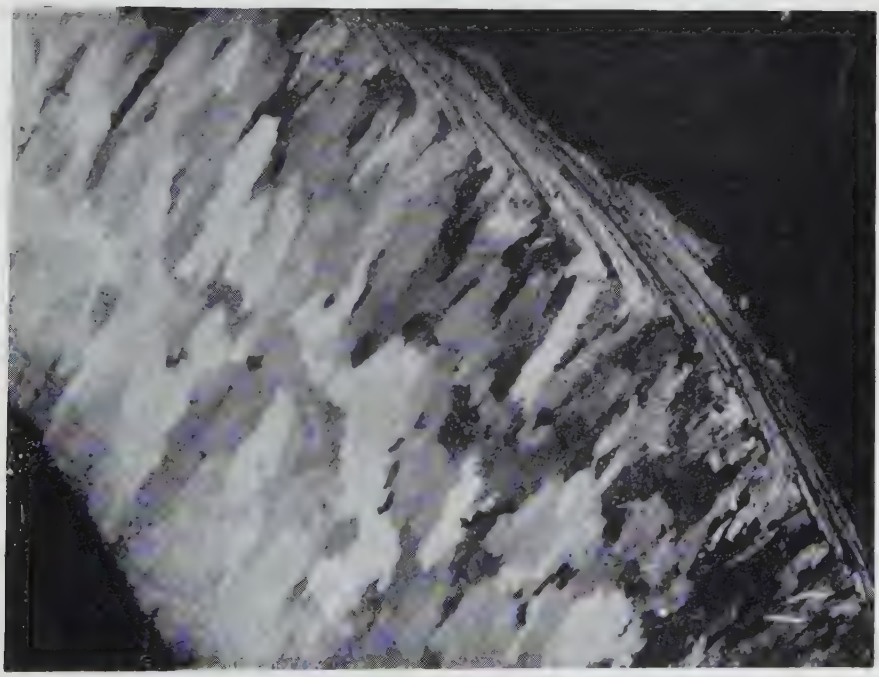

Fig. 6(b). *Neospirifer* CW87, showing lamellar and prismatic zones towards the anterior.

Fig. 6(c). *Strophalosia* KNA39, showing entirely fibrous texture, and secondary calcite filling a crack.

of the shells. This must be achieved by some criterion independent of the δ values themselves, or independent at least of the δC^{13}.

1. *Shell microstructure.* The absence of appreciable recrystallization within the shell material is apparently one necessary condition for isotopic preservation. For example, the analyses of all partially recrystallized specimens reported by Lowenstam and Epstein (1954) deviate significantly in δO^{18} (more negative) from those of unrecrystallized specimens. This has also been the experience of the present work. Since recrystallization implies that the material has approached

Table 4. Analyses of inner and outer layers in *Neospirifer* valve material

	Outer layer		Inner layer	
	δC^{13}	δO^{18}	δC^{13}	δO^{18}
KNF76	$+5{\cdot}1_5$	$+0{\cdot}3$	$+5{\cdot}1$	$+0{\cdot}6$
ML44	$+2{\cdot}6$	$-0{\cdot}6$	$+3{\cdot}4$	$-0{\cdot}4$
CW132	$+3{\cdot}6$	$-0{\cdot}4$	$+3{\cdot}8$	$-0{\cdot}1$

thermodynamic equilibrium with some post-depositional environment, the carbon isotopes must also be expected to exchange with any foreign carbon present in the system. It is also necessary to observe whether any secondary calcite is present in cavities in the shell structure, which may significantly contaminate the primary material.

Recrystallization is readily recognized in thin section by disappearance of the distinctive animal microstructure; secondary calcite has a characteristic granular texture.

Figs. 6(a) and (b) typify a number of sections of the brachiopod genus *Neospirifer*. In all specimens examined, there was an outer zone of fine fibres oriented nearly parallel to the valve surface, and a relatively thick inner zone of coarse prismatic crystals whose length was approximately normal to the fibrous layer. In most cases this structure could also be detected by the naked eye. It is evidently original, since there was no significant difference in either δC^{13} or δO^{18} between the two zones (Table 4). So far it seems to be peculiar to the spiriferid group: the Devonian *Cyrtospirifer* exhibits a thin prismatic zone in the process of recrystallization, but *Strophalosia* (Fig. 6c) *Taeniothaerus*, *Dictyoclostus* and the several rhynoconellids examined have an entirely fibrous structure. All recent brachiopods so far examined are also composed entirely of fibrous material (Lowenstam, personal communication).

Secondary calcite was observed in the Permian thin-sections only in *Strophalosia* (Fig. 6c) where it fills a crack in one valve. Apparently recrystallization was totally absent. In the Devonian brachiopods, both secondary calcite and recrystallization were observed, the former being in very intimate contact with the original material. Since, in addition, the valves of the Devonian specimens were thin, so that even a macroscopic separation from the matrix became rather difficult, it seems quite probable that in some specimens appreciable secondary

calcite was included in the material for isotopic analysis. The values in Table 3c would therefore represent mixtures of original and secondary material.

The analyses of specimen ML107 (Table 3a), a dwarfed spiriferid from the lower Permian glacial sequence, demonstrate the effects of secondary calcite contamination. This individual was fragmented and also thin-walled (in contrast to the remainder of the Permian specimens, which were very thick), and difficult to separate from a red calcareous matrix. However, the colour of the powdered sample proved a good index of the amount of matrix included. As expected, the whitest powder gave the most positive δ values, and significantly, δC^{13} and δO^{18} for these three analyses were linearly related.

The punctate brachiopods, *Taeniothaerus* and *Dictyoclostus*, appeared free of secondary calcite in thin section. It is believed that no secondary calcite is present in the remainder of the *Neospirifer* specimens.

Thin sections of two crinoids (*Calceolispongia* ML107, and the Mt. Marmion specimen) revealed both recrystallization of the original material and its abundant impregnation with secondary calcite.

2. *Isotopic temperature.* The occurrence of post-depositional oxygen isotope exchange in a marine invertebrate specimen can be safely assumed if its δO^{18} analysis yields an absurd isotopic temperature value. In such circumstances, it is highly probable that the original carbon isotopic composition also has been changed. On the other hand, if cyclic δO^{18} variation corresponding to seasonal sea-water temperature variation can be observed, there is considerable confidence that the isotopic preservation is complete or very nearly so (Urey *et al.*, 1951).

All the Permian brachiopods analysed here present reasonable isotopic temperatures, as calculated from the expression

$$T^\circ \text{ C} = 16{\cdot}5 - 4{\cdot}3(\delta O^{18} - A) + 0{\cdot}14(\delta O^{18} - A)^2$$

(Epstein *et al.*, 1953).

It must be assumed that the isotopic composition, A, of the local sea-water in which the specimen grew was equal to that of modern mean ocean water. On this basis, the isotopic temperature ranged from about 6·5°C to 28°C. Furthermore, these temperatures correspond well with the values deduced for the various stratigraphic units from other evidence, which will be described in detail elsewhere. No definitely cyclic δO^{18} variation has been observed so far, but this is probably due to the unfavourable morphology of the particular specimens used. (The valves are very thick with the zoned structure already described, and always incomplete.) In addition, the observation of Lowenstam and Epstein (1954), that brachiopods apparently deposit shell material only in the higher range of the annual temperature variation, suggests that their cyclic δO^{18} variation may be small and not distinctly sinusoidal, and therefore difficult to observe experimentally. However, it is significant that real variations in both δO^{18} and δC^{13} do exist, which would hardly be the case if isotopic equilibrium at some post-depositional temperature had been achieved.

The isotopic temperature of the heaviest Devonian brachiopod, 34°C, lies at the upper limit of the reasonable range, but that of the next heaviest, 40°C, is well beyond. The remainder all give even higher temperatures (Fig. 5)

suggesting that some post-depositional process or processes have changed the original isotopic composition of probably all of these specimens. As discussed earlier, contamination by secondary calcite is probably responsible for at least part of this effect. On the other hand, it is possible that the δ value of the local Devonian sea-water was more negative than that of present day mean ocean water.

As regards Devonian water isotopic composition, it seems most unlikely that the maximum possible negative δ value would be more than 1‰ relative to mean Devonian ocean water (Compston, 1959). It also seems unlikely that the mean isotopic composition of the oceans has changed significantly between Devonian and the present day (Urey *et al.*, 1951). Nevertheless, allowing for a possible value of −2‰ for A in the palaeotemperature equation, the lowest Devonian isotopic temperatures could be 24°C, 29·6°C, 31·7°C and 33°C. However, only the first of these values is in reasonable accordance with present day experience (i.e. water temperature of 24°C, marine water isotopic composition −1‰). It still appears that the Devonian specimens have suffered post-depositional isotopic exchange.

It is conceivable that significant isotopic exchange of individual shell fibres may occur without visible recrystallization. The smaller the fibrous crystals, the larger is their surface area, and thus the larger will be the amount of surface calcite in isotopic equilibrium with interstitial water at some diagenetic temperature. Granted sufficient time, solid state diffusion may proceed far enough to equilibrate a significant fraction of the original material. Such a process is more likely to be effective with the Devonian than the Permian brachiopods, since the former are much more finely fibrous, and there has been approximately double the time available to the solid state diffusion process.

Isotopic preservation of the Devonian specimens can be proved therefore only by the discovery of cyclic δO^{18} variation within a single specimen, which has not yet been done. Similarly, it is clear that very few if any of the crinoid specimens can be isotopically preserved since the lowest isotopic temperature registered is approximately 34°C.

Comparison of the Permian with other δC^{13} *data*

On the basis of their reasonable isotopic temperatures and compact unrecrystallized shell structure, it is believed that at least the majority of these Permian brachiopods are isotopically preserved. In contrast, most of the Devonian brachiopods and Permian crinoids appear either contaminated with secondary calcite or isotopically exchanged by a solid state diffusion process. On the same basis, the Cretaceous brachiopod analyses of Urey *et al.* (1951) also represent original compositions. In addition, several unpublished analyses of Recent brachiopods have been made available to the writer through courtesy of S. Epstein and H. Lowenstam. The distributions of these data are shown together in Fig. 7. The Permian specimens on the average are some 2·5‰ more positive than the rest, despite the overlap in δC^{13} range.

Fig. 8 shows the ranges and frequency distribution of published analyses of Recent marine calcareous material.

The oolites, believed to be formed by direct inorganic precipitation, possess

a restricted δC^{13} range and yield good isotopic temperatures (Lowenstam and Epstein, 1957). In contrast, the δC^{13} values of calcareous algae cover a wide range (although with approximately the same mean value as the oolites), their δO^{18} values do not correspond to isotopic equilibrium, and the algal heads are significantly enriched in the heavier isotopes relative to the stalks (Lowenstam and Epstein, 1957). Clearly there is a biological effect in the isotopic fractionation of both carbon and oxygen in the algal calcite.

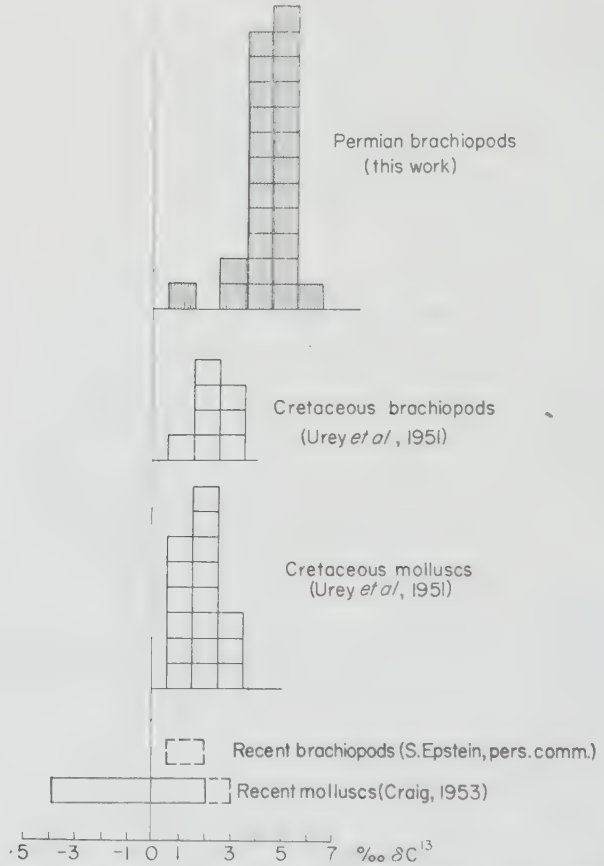
Permian brachiopods
(this work)
Cretaceous brachiopods
(Urey et al, 1951)
Cretaceous molluscs
(Urey et al, 1951)
Recent brachiopods (S. Epstein, pers. comm.)
Recent molluscs (Craig, 1953)
-5 -3 -1 0 1 3 5 7 ‰ δC13

Fig. 7. δC^{13} distribution for Recent, Cretaceous and Permian brachiopods and molluscs.

It is possible that a similar biological effect in carbon isotopic fractionation exists in mollusc and brachiopod shell materials, despite the fact that their oxygen is in isotopic equilibrium with sea-water (Epstein and Lowenstam, 1953). This is suggested by the significantly more negative δC^{13} average of this group when compared to the oolites, which latter might be expected to be closest of all groups to isotopic equilibrium with the sea-water–bicarbonate system. The situation in this respect is obscure at present because the equilibrium distribution of the carbon isotopes in sea-water has not been experimentally determined. In addition, there is no certainty that the data of Fig. 8 is a representative sample of the

"normal marine environment." Nevertheless, it is empirically valid on the present sampling to assume at least partial phylogenetic control in the carbon isotopic fractionation. In view of this possibility, it becomes necessary to contrast similar phylogenetic groups only, in tracing a possible age-effect in carbon isotopic composition.

Comparing therefore the brachiopod δC^{13} values in Permian, Cretaceous and Recent times (Fig. 7) it appears that the mean carbon isotopic composition of

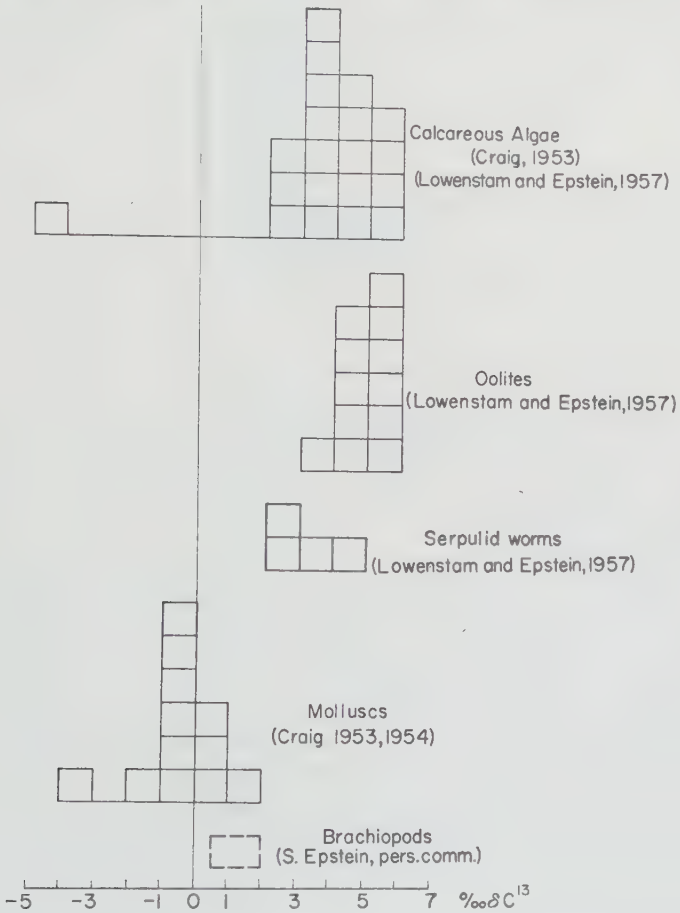

Fig. 8. δC^{13} distribution for Recent calcareous materials.

the particular Permian sea-water sampled by these organisms was some 2‰ more positive than the Recent. If, in addition, the Permian and Recent sampling are representative on a worldwide scale, then a difference is indicated between the mean isotopic compositions of the surface exchange reservoirs of these periods. Since the Cretaceous values appear to be intermediate, a unidirectional trend with time is suggested.

Such a general age-effect would be registered by the preserved carbon of other members of the surface exchange reservoir. Plant carbon, for example, preserved

as coal, should exhibit a parallel variation in mean isotopic composition. Such a correlation is essential to support an age-effect hypothesis.

Coal Data

A suite of Permian coals was analysed to increase the body of data available for consideration of the age-effect problem. Previously Wickman (1953) observed significant differences in the mean δC^{13} values of three coal basins of different age: Carboniferous, Cretaceous and Pliocene coals were successively more negative (Fig. 10). Despite the ambiguity of a possible biotope-effect,

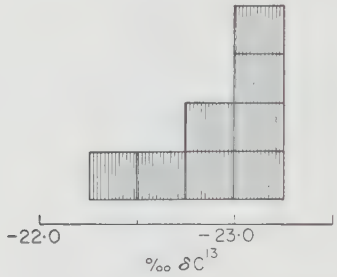

Fig. 9. Artie's Seam δC^{13} analyses.

this result is in the direction required to support the age-effect suggested by the brachiopod data. On the other hand, Craig (1953) found no time or spatial distribution in the analyses of a number of individual specimens ranging through the upper Paleozoic and Tertiary.

The considerable spread in isotopic composition of contemporary plants (Wickman, 1952; Craig, 1953) indicates that many specimens must be analysed to specify a mean value for any given interval of time. For this reason, Wickman's (1953) data for coals may be more representative than Craig's (1953) "spot" sampling of the same periods. In this work, representative sampling per coal seam was obtained by the use of drill cores, which were averaged through the seam over lengths of several feet (Table 5b). Fig. 9 shows eight samples of the same seam taken over a length of approximately 10 miles. The mean C^{13} value was $-22{\cdot}9‰$ with half the analyses falling within $\pm 0{\cdot}2‰$ of this value. Such a scatter is barely greater than the mass-spectrometric reproducibility, and is less than the scatter found in a number of coal component analyses by a factor of 3 (Table 5a).

Fig. 10 gives the frequency distribution of the analyses of different seams through the Permian and also, for comparison, Wickman's 1953 data, replotted on the PDB scale. It is evident that the Permian distribution is distinctly non-Gaussian, in contrast to those of the Carboniferous and Cretaceous, and probably possesses a double maximum. Fig. 11 shows the analyses in their correct stratigraphic succession. The lower Permian values are on the average some $2{\cdot}5‰$ more positive than the upper, which is evidently responsible for the double-maximum in the frequency distribution figure.

The "fixed carbon" of the drill core specimens, calculated on the dry, ash-free basis, from the proximate analyses, and percentages of carbon and hydrogen

from ultimate analyses of the coal maceral specimens, are also shown in Table 5(a). Both the fixed carbon and ultimate carbon are indices of coal rank, and thus may provide a qualitative indication of the relative amounts of carbon lost by the original plant material since deposition. Isotopic fractionation may potentially occur during the carbon loss, but there is definitely no visible correlation between

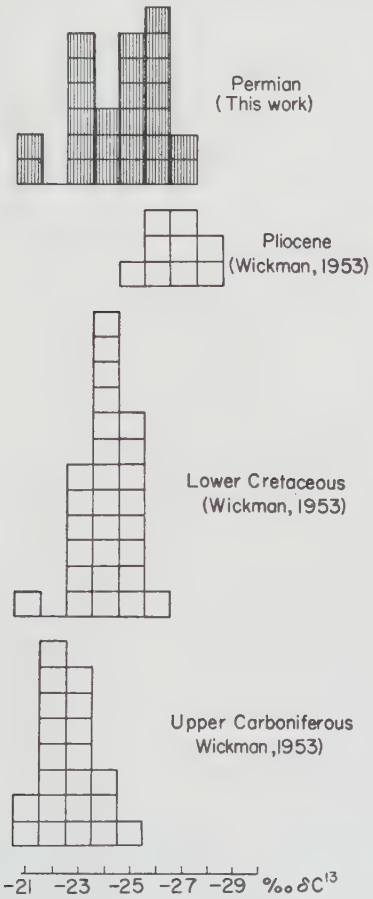

Fig. 10. Coal δC^{13} data.

the δC^{13} and carbon analyses. The fixed carbon of Artie's Seam, for instance, extends over almost the complete range observed for all seams, yet its δC^{13} is essentially constant.

The percentage hydrogen of the ultimate analysis is considered an indication of coal type (Raistrick and Marshall, 1939, p. 200). There was no correlation observed between δC^{13} and percentage hydrogen for the coal macerals. Unfortunately there are no ultimate analyses available for the particular drill-core specimens analysed. It is believed however that the fraction of canneloid constituents in the Greta Coal measures is in general greater than the Tomago and Newcastle measures (Wade, 1925). Since Permian torbanites, the most

canneloid coal type, possess δC^{13} values some 8‰ more positive than the mean Permian value (Jeffery *et al.*, 1955), it is possible that the Greta Coals may be slightly more positive in δC^{13} on this account. However, the more positive δC^{13} values persist beyond the Greta to the lower Tomago specimens.

These findings, that there is no apparent correlation of coal δC^{13} with rank and chemical composition, agree with those of Wickman (1953).

Table 5a. Coal maceral analyses, Newcastle coal measures

Sample	C (%)	H (%)	C^{13} (‰)
Vitrain 1 Bulli seam	89·3	5·2	−26·3
Vitrain 2 Bulli seam	89·6	5·1	−26·1
Clarain 1 Bulli seam	88·7	5·1	−25·6
Duroclarain 1 Bulli seam	87·2	4·7	−24·6
Vitrain 1 Wongawilli seam	86·8	5·4	−25·6
Vitrain 2 Wongawilli seam	87·4	5·2	−24·8
Vitrain 3 Wongawilli seam	86·9	5·4	−23·5
Durain 1 Wongawilli seam	87·0	6·0	−25·3
Durain 2 Wongawilli seam	85·5	4·8	−26·1

Discussion of the coal data

There may be some doubt with the present data that the gross δC^{13} trend in the Muswellbrook coals (Fig. 11) is real. At the same time, the detailed isotopic distribution is definitely more complicated, as demonstrated by the single very light Greta specimen No. 2925, Fleming Seam. More extensive sampling of each seam is necessary to determine the significant variations. Similarly, sampling of the various Permian sedimentary basins must be greatly increased to explore the possible generality of the trend observed in the single Muswellbrook area. At present, the few specimens analysed do group into heavy lower Permian and light upper Permian, but with one pronounced exception (Fig. 8), the Mt. Mulligan coal from northern Queensland (Fig. 12).

The surveys of Wickman (1952) and Craig (1953) show that on the average rain-forest trees are some 3‰ more negative in δC^{13} than temperate zone trees. No conclusive explanation for this effect has appeared. It may be that the lower ratios of photosynthesis rate/respiration rate in tropical plants is responsible (Craig, 1954), and it is also possible that the difference may be due to the

Table 5b. Drill core analyses, Muswellbrook District, N.S.W.

Sample	Core length	Fixed carbon* (%)	Stratigraphic horizon	δC^{13} (‰)
1734 Bore 4S Anderson's Gap	2 ft 7 in.	58·7	Seam 40, Tomago formation	−26·3
1387 Bore 7S Blakefield	3 ft 0 in.	60·0	Seam 39 Tomago formation	−26·1
1393 Bore 7S Blakefield	2 ft 7 in.	66·7	Seam 36 Tomago formation	−26·3
1224 Bore 1S Mt. Arthur	1 ft 7 in.	62·4	Seam 26 Tomago formation	−27·3
1230 Bore 1S Mt Arthur	2 ft 6 in.	64·0	Seam 23 Tomago formation	−26·4
2086 Bore 1S Edinglassie	2 ft 11 in.	65·0	Seam 20 Tomago formation	−25·4
2092 Bore 1S Edinglassie	3 ft 10 in.	65·3	Seam 14 Tomago formation	−25·0
2354 Bore 4S Edinglassie	2 ft 9 in.	61·8	Seam 10 Tomago formation	−24·0
930 Bore 2S Pond's Creek	2 ft 4 in.	57·7	Artie's seam Tomago formation	−22·9 −22·8
932 Bore 2S Pond's Creek	2 ft 5 in.	62·7	Artie's seam Tomago formation	−22·8
935 Bore 2S Pond's Creek	2 ft 5 in.	70·1	Artie's seam Tomago formation	−22·3
1474 Bore 1S Ravensworth	1 ft 0 in.	61·6	Artie's seam Tomago formation	−23·2
1476 Bore 1S Ravensworth	3 ft 0 in.	64·7	Artie's seam Tomago formation	−23·2
1995, Bore 6S Parnell's Creek	2 ft 1 in.	58·4	Artie's seam Tomago formation	−22·7 −22·5
1997, Bore 6S Parnell's Creek	3 ft 2 in.	61·7	Artie's seam Tomago formation	−23·1
1999, Bore 6S Parnell's Creek	4 ft 4 in.	57·9	Artie's seam Tomago formation	−23·2 −23·1
498, Bore 1S Pond's Creek	1 ft 11 in.	58·1	Upper Liddell seam Tomago formation	−25·1

* Computed from proximate analysis.

Table 5b (*contd.*)

Sample	Core length	Fixed carbon* (%)	Stratigraphic horizon	δC^{13} (‰)
2000, Bore 6S			Upper Liddell seam	
Parnell's Creek	1 ft 10 in.	62·5	Tomago formation	−25·1
501, Bore 1S			Lower Liddell seam	
Pond's Creek	2 ft 7 in.	57·4	Tomago formation	−24·1
2925, Bore 1S				
St. Heliars	3 ft 0 in.	61·1	Fleming seam	−27·1
2929, Bore 1S				
St. Heliars	1 ft 10 in.	62·4	Hallett seam	−23·3
			Greta coal measures	
2935, Bore 1S			Muswellbrook seam	
St. Heliars	3 ft 0 in.	61·8	Greta coal meas.	−23·4
2941, Bore 1S			St. Heliars seam	
St. Heliars	3 ft 0 in.	59·6	Greta coal meas.	−23·8
2948, Bore 1S			St. Heliars seam	
St. Heliars	3 ft 0 in.	63·0	Greta coal meas.	−25·2
2953, Bore 1S			Lewis seam	
St. Heliars	2 ft 3 in.	63·3	Greta coal meas.	−25·0
2956, Bore 1S			Loder seam	
St. Heliars	2 ft 0 in.	58·4	Greta coal meas.	−23·0

* Computed from proximate analysis

Table 5c. Permian hand-specimen samples (Jeffery *et al.*, 1955)

Sample	Stratigraphic horizon	Location	C^{13} (%)
S7	Bulli seam Newcastle coal meas.	Bulli, N.S.W.	−25·8
Q4	Upper Bowen series	Bluff coalfield Qld.	−25·8
Q11	Upper Bowen series	Mt. Mulligan Qld.	−20·3
Q10	Bowen seam Middle Bowen series	Collinsville Qld.	−21·1
7463	Irwin coal measures	Irwin River, W.A.	−22·6
8133	Collieburn seam, Collieburn formation	Collie, W.A.	−22·8

significantly more restricted mixing of the rain-forest atmosphere with oceanic air (cf. the data for atmospheric carbon dioxide from Keeling, 1957).

Either of these mechanisms can be linked with the Permian situation. Apparently the climate changed from frigid in the underlying formations to cool temperate and temperate "possibly pluvial," respectively, in the Tomago and Newcastle Coal Measures (Banks, 1952). Moreover, the Greta Coal Measures were formed during a cool temperate period with trees of relatively stunted

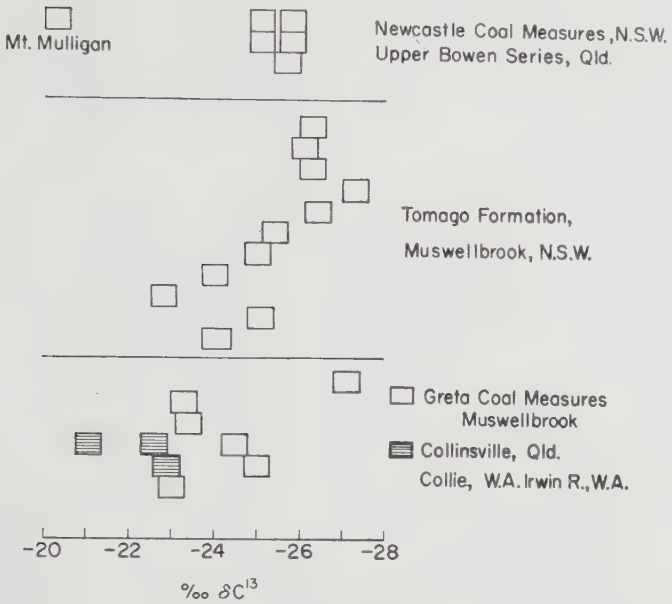

Fig. 11. Coal δC^{13} vs. stratigraphy.

Fig. 12. Specimen localities.

growth, whereas "forests of lofty trees" grew in the later periods (David, 1950). An explanation in these terms, connected with local or regional events, should in principle be preferred to a possible age-effect during Tomago time, which would involve the worldwide surface exchange reservoir. Moreover, such an interpretation allows for the detailed variations within the Muswellbrook sequence and even for the distinct departure from the mean Greta value registered in the Fleming Seam.

In view of this δC^{13} trend (or grouping) observed within the Permian coals, these coal analyses cannot provide substantial support for the age-effect suggested by the Permian brachiopods. No criterion is known by which only one of the two Permian coal groups might be favoured for comparison with the coals of different age analysed by Wickman (1953).

Summary and Conclusions

From study of thin sections, and from the δO^{18} analyses, it is concluded that all the Permian brachiopods examined are isotopically preserved. On the other hand, most of the Devonian brachiopods and probably all the Permian crinoids have undergone isotopic re-equilibration at some post-depositional temperature. The crinoids in addition are probably completely impregnated with diagenetic calcite, which is isotopically more negative than the original material, and a few of the Devonian brachiopods also may be appreciably contaminated.

Therefore the δC^{13} analyses of the Permian brachiopods only may be employed for the assessment of any possible time variation in the isotopic composition of the surface carbon reservoir.

Using an analysis system of measured reproducibility ($\pm 0{\cdot}2‰$) and negligible systematic error (2% of the ratio differences), the twenty-seven Permian brachiopods analysed were found to have a mean δC^{13} value of $+4{\cdot}3‰$, with individual values approximately normally distributed, and with a "probable error" of $\pm 0{\cdot}7‰$.

Analyses made elsewhere show that Recent oolites and calcareous algae are on the average more positive in δC^{13} than Recent molluscs and brachiopods. This suggests at least partial phylogenetic control of the isotopic fractionation. If this is true (that is, if sampling of the present biosphere has been adequate), then it is necessary to confine comparisons of the Permian brachiopod data to other brachiopods and molluscs only, in order to make a valid assessment for any time-effect. The Permian brachiopods are significantly more positive in δC^{13} than Cretaceous and Recent analyses.

It is not yet known whether there are generic effects in carbon isotopic fractionation within the brachiopod group sufficiently large to explain the above distribution. It may perhaps be significant then, that nearly all the Permian specimens were of the genus *Neospirifer*. Otherwise, assuming again that sampling of Recent material has been representative, it could be concluded that the sea-water in which these particular specimens lived was isotopically heavier than at the present. This would indicate either an age-effect, in which the entire Permian exchange reservoir was enriched in carbon-13 relative to the present,

or else a comparatively local enrichment apparently not obtained in present marine environments.

The δC^{13} analyses of Permian coals, sampled both as pure component macerals and as drill-corings representative of several feet of each seam, showed no correlation with rank or chemical composition. It is believed that the coal δC^{13} values represent the average isotopic compositions of the original plant constituents.

Sampling by drill core specimens apparently gives representative δC^{13} values for an entire coal seam: the analyses of a single seam sampled over an extended area possessed much smaller scatter than the range exhibited by an entire sequence of seams. The analyses of a suite of specimens from the one district seem to correlate with stratigraphic location: the upper Permian specimens were some 2·5‰ more negative than the lower Permian, although there was one pronounced exception. It is suggested that the general climatic amelioration which reputably occurred in Australia during this time may be directly responsible for the δC^{13} trend.

The δC^{13} values of the lower Permian coals are approximately the same as the upper Carboniferous specimens analysed by Wickman (1953), and fit well into the apparent trend with time observed by Wickman from heavy coals in the Palaeozoic to lighter coals in Mesozoic and Tertiary. This correlates with the possible age-effect suggested by the brachiopod data. However, the discovery of the more negative δC^{13} values for upper Permian coals, which were not paralleled by variation in brachiopod δC^{13}, shows that coal isotopic composition is in part determined by some unknown factor, possibly climate, which is subject to significant regional change.

It is therefore concluded that much more extensive sampling of preserved fossil and Recent carbon, both coals and marine invertebrates, must be made before an empirical age-effect can be determined. At the same time, experimental studies of carbon isotopic fractionation are essential in order to reduce the number of variables which currently obscure the solution to this problem.

Acknowledgements—The writer wishes to thank P. M. Jeffery for advice and practical assistance with the mass spectrometry, and C. J. B. Clews for his continued interest throughout the project. Criticism of the manuscript by S. Erstein (California Institute of Technology) was greatly appreciated.

K. Malinowski, B. R. F. Kendall and D. Greenhalgh also contributed to the experimental work. G. Thomas and M. C. Konecki (Commonwealth Bureau of Mineral Resources), B. F. Glenister (University of Western Australia) and C. E. Marshall (University of Sydney) kindly provided the fossil material.

The experimental work was carried out during the tenure of a CSIRO studentship, and the manuscript written at the California Institute of Technology.

Financial support for the project was provided by the Research Grants Committee of the University of Western Australia.

References

Banks M. R. (1952) *Nineteenth Int. Geol. Congr., Algiers.* Symposium on the Gondwana Series p. 10.

Compston W. (1957) Ph.D. Thesis, University of Western Australia.

Compston W. (1960) *The Isotopic Temperatures of Some Permian and Devonian Brachiopods from Western Australia.* In preparation.

Craig H. (1953) *Geochim. et Cosmochim. Acta* **3**, 53.
Craig H. (1954) *J. Geol.* **62**, 115.
Craig H. (1957) *Geochim. et Cosmochim. Acta* **12**, 133.
David T. W. E. (1950) *The Geology of the Commonwealth of Australia.* Edward Arnold, London.
Epstein S., Buchsbaum R., Lowenstam H. A. and Urey H. C. (1953) *Bull. Geol. Soc. Amer.* **64**, 1315.
Epstein S. and Lowenstam H. A. (1953) *J. Geol.* **61**, 424.
Jeffery P. M., Compston W., Greenhalgh D. and de Laeter J. (1955) *Geochim. et Cosmochim. Acta* **7**, 255.
Keeling C. D. (1957) *Geochim. et Cosmochim. Acta* **13**, 322.
Lowenstam H. A. and Epstein S. (1954) *J. Geol.* **62**, 207.
Lowenstam and Epstein S. (1957) *J. Geol.* **65**, 364.
McKinney C. R., McCrea J. M., Epstein S., Allen H. A. and Urey H. C. (1950) *Rev. Sci. Instrum.* **21**, 724.
Raistrick A. and Marshall C. E. (1939) *The Nature and Origin of Coal and Coal Seams.* English Universities Press, London.
Stehli F. G. (1956) *Science* **123**, 1031.
Urey H. C., Lowenstam H. A., Epstein S. and McKinney C. R. (1951) *Bull. Geol. Soc. Amer.* **62**, 399.
Wade A. (1925) Cited by Booker F. W., Ph.D. Thesis, University of Sydney.
Wickman F. (1952) *Geochim. et Cosmochim. Acta* **2**, 243.
Wickman F. (1953) *Geochim. et Cosmochim. Acta* **3**, 244.

Geochimica et Cosmochimica Acta, 1960, Vol. 18, pp. 23 to 35. Pergamon Press Ltd. Printed in Northern Ireland

Biogeochemical investigation in serpentine–chromite ore district

Noboru Yamagata*, Yukio Murakami† and Tetsuya Torii‡

(*Received* 20 *February* 1959)

Abstract—Chemical analyses were made of stream and underground waters, soils and vegetation from a serpentine–chromite ore district. The distribution of several elements in plant and soil was examined statistically and soil–plant relationships were discussed. Of eighteen species of plant examined, *Clethra* and *Castanea* showed great accumulation of cobalt and manganese, respectively. Lognormal distribution was assumed in plant for several elements.

Introduction

In Japan, investigations were initiated in 1946 into the possibility of geochemical prospecting for ores by Prof. Kenjiro Kimura§ at the University of Tokyo and his collaborators. Since then, many investigators have carried out reconnaissance seeking methods of mineral exploration by use of natural waters, soils and vegetation for a variety of minerals and elements. As indicators natural waters and soils have principally been taken up by them and the minerals examined have extended to copper, zinc, lead, gold, mercury, iron, manganese, sulphur, phosphorus, coal, petroleum and natural gases (Kimura and Shima, 1954; Shima, 1955). However, vegetation has rarely been taken up. Kimura and Murakami (1950) discussed the possibility of prospecting for manganese ore by vegetation and recently Yamagata and Yamagata (1957) have carried out fundamental studies on the biogeochemical prospecting for manganese.

Prospecting for chromite ore by use of chemical or biological methods have rarely been reported (Buck, 1949; Hedström and Nordström, 1945). In 1954, the writers attempted to seek for the law of distribution of several elements in an area of serpentine–chromite mineralization, and the results and discussion are presented in this paper.

Description of the Area of Investigation

The biogeochemical studies described in this paper were carried out in the Hinokami mining district which is situated in the south-west corner of Tottori Prefecture. The geological map of the neighbouring district is shown in Fig. 1 (Kitahara, 1958). The Palaeozoic sediments are intruded by chromite-bearing ultra-basic rocks which consist largely of serpentinite originated from dunite and harzburgite. The granitic rocks are also intruded into the Palaeozoic sediments and the intrusion of serpentine rocks is presumed by Kitahara (1958) to have taken place later than that of granite. Chromite ores which have been formed along fissures in serpentinite masses form ore bodies of various shapes and magnitude. The area examined falls within the zone of serpentinite masses, and

* Kiriu College of Technology, Gunma University, Kiriu, Japan
† The Isotope School, Japan Atomic Energy Research Institute, Komagome, Tokyo; formerly at Department of Chemistry, University of Tokyo.
‡ Chemical Institute, Faculty of Literature and Science, Chiba University, Chiba
§ At present, Japan Atomic Energy Research Institute.

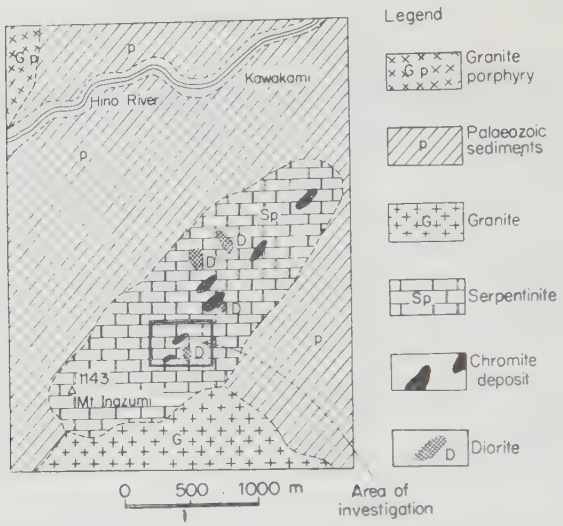

Fig. 1. The geological map of the district. Mt. Inazumi is located at latitude 35° 06′ N and longitude 133° 14′ E.

elongates 260 m from east to west and 200 m from south to north, including two of the chromite ore bodies under operation.

The climate is temperate with a moderate rainfall and weathering of the rocks have produced a development of reddish- or greyish-yellow clay soil which is extended to a thickness of from 20 cm to 1 m in the examined area except for on the debris of wastes. A thick vegetation is found all over the area composed mostly of *Quercus*, *Castanea*, *Deutzia*, *Lindera* and various kinds of herbs. Several streams run through the area and some of them disappear in dry seasons.

Analytical Procedure

The air-dried soil samples were passed through a sieve of about mesh 10 and dried at 110°C in an oven. About 10 g of dried sample were ground in an agate mortar to fine powder. From this amount, about 1 g was taken into a platinum crucible and heated at dull red heat for 15 min to destroy organic matter. The powder was mixed with 5 g of sulphuric acid.

The plant ashes prepared by incineration at 450–500°C of approximately 20 g samples of air-dried plant material were decomposed with hydrochloric and nitric acid mixture. The mixture was heated to fuming after the addition of sulphuric acid.

Cr *and* Mn. An aliquot of sample solution was used for the determination of chromium and manganese after the removal of iron and vanadium by carbon tetrachloride extraction in the presence of cupferron. Manganese was determined colorimetrically by the permanganate method by use of silver peroxide as an oxidant (Kimura and Murakami, 1951). Chromium was determined by a diphenylcarbazide colorimetric method after the decomposition of permanganate with sodium azide.*

Fe *and* Ni. The usual thiocyanate method was applied for iron determination and nickel was determined by the dimethylglyoxime method (Sandell, 1950).

Co *and* V. The *o*-nitrosoresorcinol monomethylether method (Torii, 1955) was applied. The specific orange-red colour of cobalt complex with the reagent was extracted with carbon tetrachlorides and measured at 373 mμ. The presence of 5000 parts of iron and 1000 parts of

* The method used will appear in a paper by Murakami in another journal in the near future.

nickel did not interfere with the determination of 1 part of cobalt. The improved colorimetric method was applied for vanadium (MURAKAMI, 1950).

Cu *and* Zn. A dithizone titration technique was employed for the semiquantitative analysis of soil samples. For plant samples, a polarographic method was devised and applied.

NATURAL WATERS

The area of investigation on natural waters extended wider than that on soils and plant. In the fall of 1957, about one hundred samples of surface and underground waters were collected and analysed for pH, zinc and iron on the field. Most of the samples showed slightly acid reaction (pH 5·8–6·0). The range of variation of iron and zinc contents of surface waters were from 57 to 1060 μg/l. and from 8 to 32 μg/l., respectively. Thirty-five of these samples were sent to the laboratory to be analysed for manganese, chromium, nickel and vanadium. Twenty-nine samples of surface water contained on average (in μg/l.) Cr 2·8, Mn $<$ 2·0, V $<$ 2·4, Fe 194, Ni 2·6 and Zn 16. Of the six samples of underground waters inside of ore bodies, four contained more than 3 μg/l. of chromium and one of them showed the maximum value of 134 μg/l. Three samples contained more than 3 μg/l. of vanadium but nickel did not show any anomalous high values in proximity to mineralization. Locations of sampling of surface waters are shown in Fig. 2 and the results for the limited area are shown in Table 1.

The Japanese normal river water contains less than 10 μg/l. of manganese, 100–200 μg/l. of iron and 0·1–3·0 (average 1·0) μg/l. of vanadium (SUGAWARA,

Table 1. Ore-metal content of waters
(μg/l.)

Sample no.	pH	Cr	Mn	V	Fe	Ni	Zn
			Surface waters				
26	5·8	1·4	<2·0	<1·0	90	1·8	17
28	5·8	2·1	<2·0	2·7	120	1·9	15
32	5·8	0·9	<2·0	1·6	130	5·9	32
33	5·8	0·7	<2·0	3·1	99	3·5	14
34	5·8	3·5	<2·0	2·8	140	2·7	12
37	5·9	12·7	<2·0	1·6	140	3·9	13
Average for 29 samples	5·9	2·8	<2·0	<2·4	194	2·6	16
			Underground waters inside of ore bodies				
14	5·9	3·9	11·1	4·6	55	1·8	18
71	6·2	1·5	<2·0	3·1	110	2·3	—
72	7·8	134	<2·0	6·6	290	1·5	—
95	—	3·3	10·0	<1·0	160	1·8	—
96	—	4·1	5·4	9·5	460	1·7	—
97	—	2·3	2·0	10·0	300	2·5	—

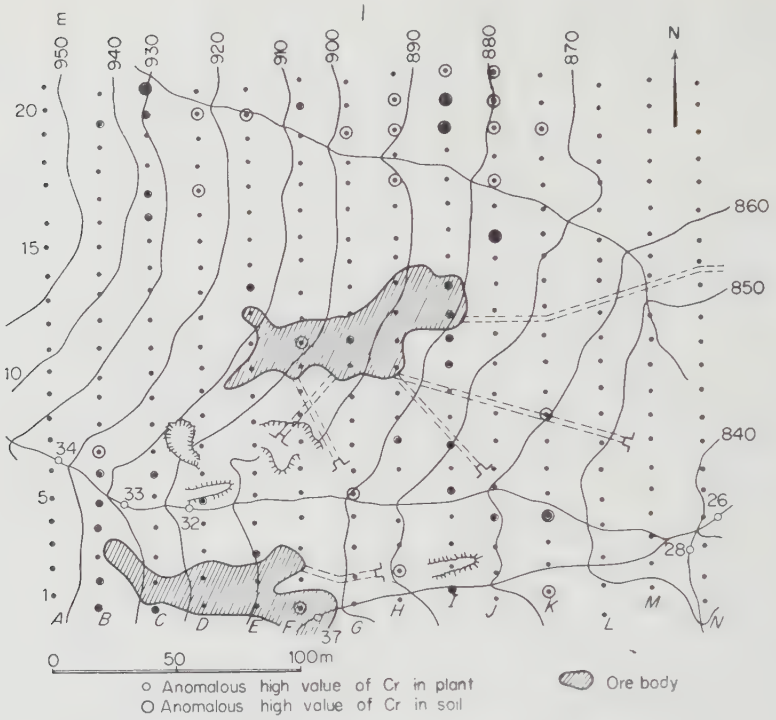

Fig. 2. Locations of sampling of soil, plant and surface water.

1956). We have no information on the normal chromium content of surface water. However, it appears to us that vanadium and chromium may be considered as the indicating elements for chromite ore body.

Soil

The soil samples were collected in the *B* horizon (20–60 cm) over the examined area along the fourteen north to south traverses (*A* to *N* in Fig. 2) every 10 m and analysed for chromium, manganese, iron, nickel, cobalt, copper and zinc. The range of values recorded is as follows on dry basis: for Cr, 50–15,000 p.p.m., for Mn, 220–7310 p.p.m., for Fe, 0·93–17·8 per cent, for Ni, less than 100–3580 p.p.m., for Co, 10–9250 p.p.m. for Cu, 1–420 p.p.m. and for Zn, 50–630 p.p.m. The average values for 250 samples are shown in Table 2 in comparison with the values for normal soil given by Vinogradov (1957). Soils derived from ultrabasic rocks are known to be high in total content of chromium, nickel and cobalt. The characteristic feature of the area in metal content of soil is clearly shown by the factors of anomalies as shown in Table 2.

Thirty-one soil profiles were analysed for selective distribution of metals in the three soil horizons, *A*, *B* and *C*. Soil sampling was carried out at depths of 10–20 cm (*A*), 20–60 cm (*B*), and 80–185 cm (*C*). In most cases (twenty-six of iron, twenty-nine of Mn, and twenty-eight of Ni of the thirty-one) the concentrations of the metals increased in the deeper layers of the soil profile. Chromium

Table 2. Average metal contents in the soil horizons and comparison with the values for normal soil

Metal	Metal in dried sample (p.p.m.)				Factor of anomaly (*B*-horizon)
	Serpentine–chromite mineralized soil			Normal soil*	
	A-horizon	*B*-horizon	*C*-horizon		
Cr	2634	3441	6410	20	170
Mn	1000	1432	3160	850	1·7
Fe(%)	4·56	6·09	12·23	3·8	1·6
Ni	728	1001	2291	40	25
Co	708	621	782	8	78
Cu	36	70	170	20	3·5
Zn	240	260	300	50	5·2

* Vinogradov (1957).

and cobalt did not show such a distinct distribution. In seventeen cases of the thirty, the chromium content was found to be $C > B,A$, in ten cases $B > A,C$ and in the remaining three $A > B,C$. Cobalt was found to be enriched in the *A* horizon in nine cases of the thirty, and in the *B* horizon in eight cases. The average values for the thirty-one profile samples are shown in Table 2.

Vegetation

In the autumn of 1955, plant samples were collected over the concerned area. Considering the sensitivity of the small herbaceous plants to microvariations in metal content of the soil, the leaves of big trees were collected. The dominant woody species in the area are *Quercus crispula* and *Q. serrata*, although they could not always be found growing just on the soils corresponding to the sampling positions. Of the 199 foliar samples collected in the area, *Quercus* occupied sixty-nine. It was necessary to substitute other woody species for *Quercus* to get samples on the localities as closely as possible to the soil sampling positions. Twenty-six samples were *Deutzia crenata*, twenty-four each of *Cynoxylon japonica* and *Castanea crenata*, seventeen of *Clethra barbinervis* and eleven of *Lindera umbellata*. The remaining twenty-eight samples were composed of eleven woody species, *Hydrangea serrata*, *Ilex pedunculosa*, *Rhus japonica*, *Pieris japonica*, *Carpinus Tschonoskii*, *Lyonia Neziki*, *Magnolia*, *salicifolia*, *Acer sp.*, *Lindera obtusiloba* and two undetermined species.

Those samples were analysed for the seven elements; the recorded values is as follows (in p.p.m. of leaf ash): for Cr, 1·1 (*Cynoxylon*), 218 (*Deutzia*); for Mn, 81·6 (*Quercus*), 28,400 (*Ilex*); for Fe, 141 (*Cynoxylon*), 8060 (*Deutzia*); for Ni, 5·4 (*Lindera*), 304 (*Clethra*); for Co, 0·2 (*Quercus*), 2200 (*Clethra*); for Cu, 50 (several species), 630 (*Quercus*); and for Zn, 80 (*Deutzia*), 1500 (*Deutzia*). The metal concentrations averaged for plant species are shown in Table 3.

Although the biological occurrence of chromium was suspected by Rankama and Sahama (1955), this element was found in all plant leaves examined. Difference

Table 3. Average metal concentrations in plant and the underlying soil (p.p.m. dry matter for soil and p.p.m. ash for plant unless otherwise indicated)

Element	Total	*Clethra barbinervis*	*Castanea cretana*	*Cynoxylon japonica*	*Deutzia crenata*	*Lindera umbellata*	*Quercus*
	(199*)	(17)*	(24)	(24)*	(26)*	(11)*	(69)*
soil (%)	5·91	6·28	4·49	4·78	6·08	7·19	6·17
Fe plant	681	548	846	688	791	696	614
soil	1005	1125	759	774	1132	1021	973
Ni plant	33·4†	140	31·8	24·6	24·0	26·7	42·2
soil	562	511	396	931	620	538	555
Co plant	3·3†	661	3·6	2·0	5·3	4·3	2·6
soil	1506	1723	1208	1422	1536	1902	1416
Mn plant	6356	8128	11,108	675	1269	3485	8084
soil	3476	2928	1813	3251	3441	4039	3497
Cr plant	20·5	23·8	18·5	12·2	31·2	44·4	16·5
soil	85	100	45	75	140	140	70
Cu plant	123	192	168	79	96	101	132
soil	256	280	230	270	250	240	260
Zn plant	397	790	398	260	431	524	332

* No. of samples.
† Other than *Clethra*.

of metal concentrations in the different plant species will be discussed later in relation to metal content of the underlying soil. However, it must be mentioned here, as briefly described in the previous report (Yamagata and Murakami, 1958), that the most conspicuous specific anomaly was found in *Clethra barbinervis* for cobalt concentration. As clearly shown in Table 3, more than one hundred times as much cobalt and several times as much nickel were found in *Clethra* as in other plant species, although the soil on which *Clethra* was growing did not show any anomalous levels in these elements. This anomaly was found by chance, although the inequality of response of different plants to metal uptake has been naturally expected. We must carefully select plant species when the vegetation is used for prospecting.

Soil–Plant Interrelationships

The concentrations of trace elements in plants are primarily dependent upon the species and the nature of the soil on which they are growing. Plant uptake can not be related directly to the total trace-element content of a soil, but it is strongly affected by several factors such as the type and the reactions of soil. However, it will be possible to rule out the effects of those factors when the area of investigation is limited to a small one as in the present case, and the mineral composition of a plant may be considered to be a reflection, in the first approximation, of the composition of the soil on which it has grown.

The plant/soil ratios in concentration of an element will be a relative measure for the response of a plant to uptake of the element. The ratio has been calculated for each of the 199 locations on the basis of the same concentration unit (plant ash/dry soil) and averaged for the plant species. The results are shown in Table 4.

Table 4. Difference of plant/soil ratios in metal concentration (plant ash/dry soil)

Plant	Fe	Ni	Co	Mn	Cr
Average	0·0159	0·0607*	0·0168*	6·12	0·0277
Clethra barbinervis	0·0108	0·156	1·37	6·08	0·0127
Castanea crenata	0·0207	0·0643	0·0236	12·14	0·0466
Cynoxylon japonica	0·0190	0·0573	0·0114	0·566	0·0115
Deutzia crenata	0·0255	0·0375	0·0413	1·52	0·0217
Lindera umbellata	0·0122	0·0524	0·0225	2·78	0·0252
Quercus	0·0119	0·0679	0·0124	7·76	0·0434

* Other than *Clethra*.

The plant/soil ratios for iron and chromium indicate an invariable response between the six plant species. However, those for cobalt and manganese show considerable variability. Besides the previously mentioned peculiar nature of *Clethra* concerning cobalt accumulation, the great response of *Castanea* and the small response of *Cynoxylon* to manganese uptake are to be noticed. Generic or specific differences in the major element contents of plants growing under the same soil conditions have long been known. Similar differences in trace-elements have also been recorded by several workers; among them aluminium (Yoshii and Jimbo 1932; Webb, 1954 and Chenery, 1955) and manganese (Olsen, 1934, 1937) have been most extensively investigated. These facts will be of interest in the field of comparative biochemistry and of plant taxonomy. However, for the purpose of biogeochemical prospecting for ores, such an element as manganese or aluminium, which shows a variability of response between plant species,

appears unsuitable as an indicator element unless samples of the same species are collected for examination.

Frequency Distribution of Elements in Plant and Soil

The statistical nature of the distribution of concentration of several elements in plant and soil has been studied to solve the problem of biogeochemical prospecting. Preliminary drawing of the histograms by the use of an arithmetic interval revealed very asymmetric nature and positive skewness for all of the elements examined both in plant and soil. Accordingly, the arithmetic mean is found to be greater than the geometric mean in all cases. Statistical information is shown in Table 5 using the same symbols as used by Ahrens (1954). The

Table 5. Statistical data on the distribution of several elements in soil and plant

Element			Standard deviation of log-conc. (λ)	Antilog of λ (λ')	Arithmetic mean / Geometric mean
Cr	soil		0·52	3·3	1·71
	plant		0·33	2·1	1·31
Mn	soil		0·28	1·91	1·16
	plant	total	0·64	4·4	2·20
		Q	0·46	2·9	1·41
		D	0·36	2·3	1·74
		Cj	0·42	2·6	1·71
		Cc	0·34	2·2	1·24
		Cb	0·27	1·88	1·16
Fe	soil		0·25	1·78	1·06
	plant		0·27	1·88	1·24
Ni	soil		0·42	2·6	1·44
	plant	*Clethra*	0·22	1·66	1·13
		others	0·26	1·82	1·18
Co	soil		0·46	2·9	1·57
	plant	*Clethra*	0·35	2·2	1·39
		others	0·42	2·6	1·43

Q, Quercus; D, Deutzia crenata; Cj, Cynoxylon japonica; Cc, Castanea crenata; Cb, Clethra barbinervis.

histograms using a geometric interval are illustrated in Figs. 3–9; in the case of zinc and copper in soil, the determinations are only semiquantitative and hence greater intervals are taken.

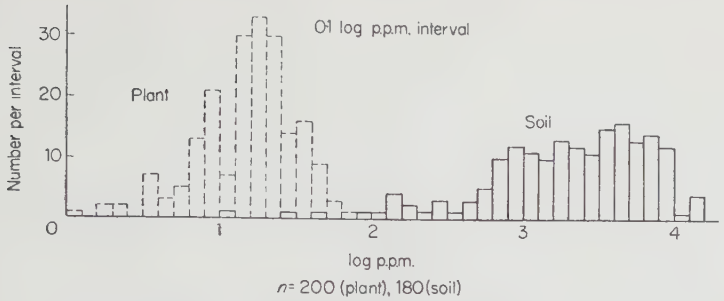

Fig. 3. Frequency distribution diagram of Cr in plant and soil.

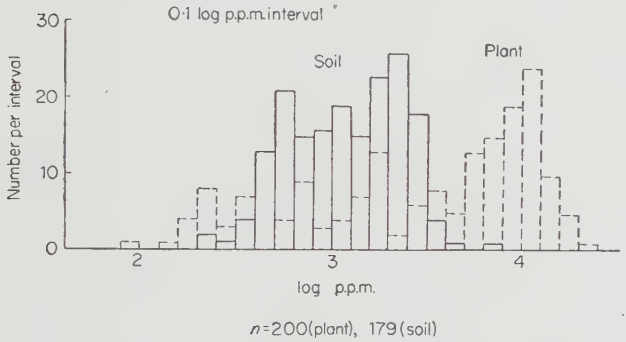

Fig. 4. Frequency distribution diagram of Mn in plant and soil.

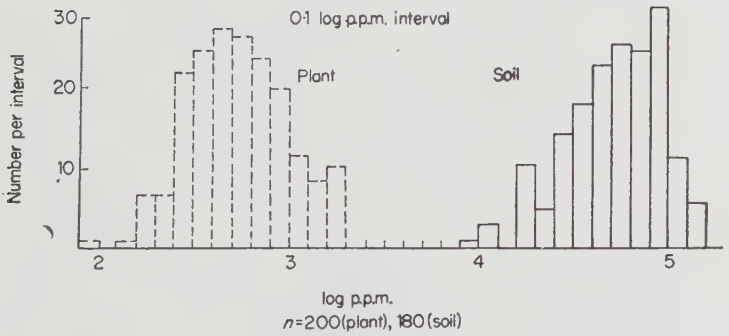

Fig. 5. Frequency distribution diagram of Fe in plant and soil.

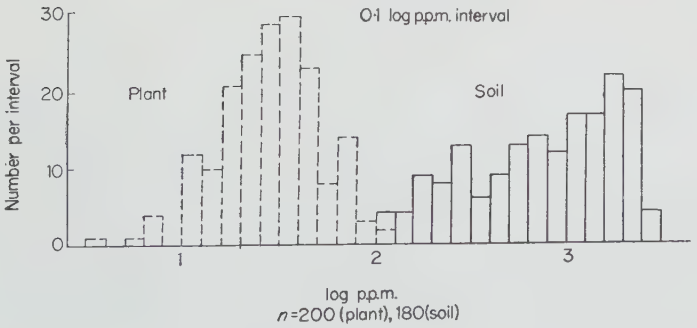

Fig. 6. Frequency distribution diagram of Ni in plant and soil.

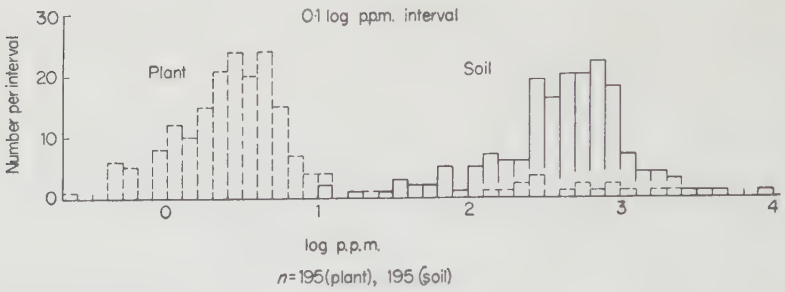

Fig. 7. Frequency distribution diagram of Co in plant and soil.

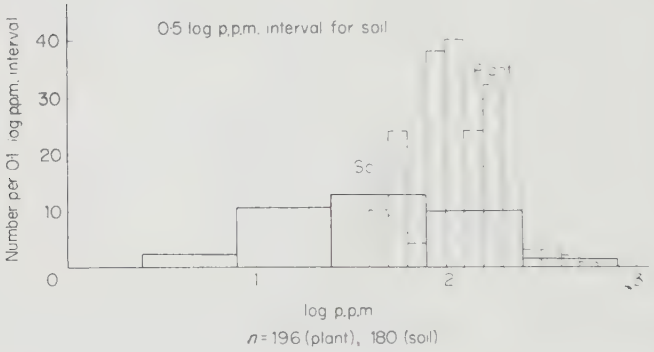

Fig. 8. Frequency distribution diagram of Cu in plant and soil.

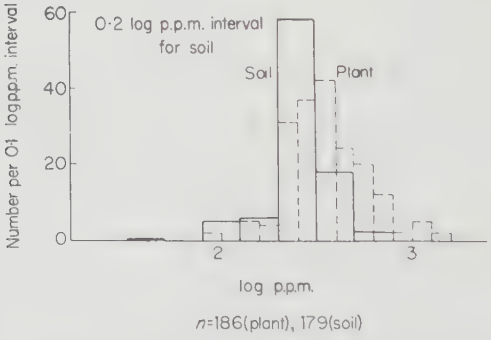

Fig. 9. Frequency distribution diagram of Zn in plant and soil.

Positive skewness has been strongly reduced by the use of a geometric interval and in most cases of plant, the distribution becomes fairly symmetrical and a lognormality may be assumed (or very nearly so). The distribution of manganese in plant (Fig. 4) appears to be composed of several independent distributions resulted from the specific variability of response of plant to manganese uptake as has been described in the preceding paragraph (Table 4). Hence, the antilog of standard deviation λ', an estimate of dispersion, is very large (4·4) for the whole plant species as compared with those for the individual ones (1·88–2·9). Similarly,

the anomalous nature of *Clethra* in cobalt accumulation is shown in Fig. 7 as the independent distribution pattern separate from the normal one.

Negative skewness is observed in the histograms of log-concentration of chromium, nickel and iron in soil. However, the size of dispersion may be compared and predictions can be made on the basis of assumed lognormal distribution. One of the factors that determine the size of dispersion of an element in the soil of a restricted area is the variation of concentration of an element in the mother-rocks. Thus, the large dispersion of chromium in soil ($\lambda' = 3{\cdot}3$) can be attributed to the large variation of concentration of this element in parent materials, i.e. serpentine and chromite ore as shown in Table 6. In contrast, the other elements showing

Table 6. Metal contents of representative specimens of serpentinite and chromite ore (%)

Specimen	Ni	Co	Fe	Cr	Mn
Black serpentinite (Kuro-Jamon)	0·228	0·122	6·56	0·288	0·1080
Red serpentinite (Aka-Jamon)	0·133	0·099	4·72	0·185	0·0963
Greasy serpentinite (Abura-Jamon)	0·188	0·071	4·17	0·424	0·0587
Serpentinite* (4 specimens)	—	—	3·60–7·12	0·34–0·95	tr.–0·50
Chromite ore	0·139	0·084	9·09	4·29	0·0817
Chromite* (8 specimens)	—	—	8·29–19·88	22·4–30·5	0·15–0·70

* Kitahara (1958).

relatively small dispersion in soil do not appear to be selectively associated with chromite.

The dispersion of an element in plant will be primarily governed by that in soil. However, the secondary biogeochemical mechanisms are complicated. It is of interest to compare the size of dispersion (λ') of an element in soil and plant in Table 5. Nickel and cobalt show smaller dispersion in plant than in soil in contrast to iron which is the closest relative of these elements in the Periodic System. Similar trend is found in chromium–manganese and copper–zinc (Fig. 9), respectively. The clearest difference in geochemical properties between these pairs of elements is easiness of liberation and migration during weathering; iron, manganese and zinc go readily into solution compared with nickel and cobalt, chromium and copper, respectively, and are able to migrate for considerable distances under proper conditions. It is probably permissible to consider this as one of the factors which determine the size of dispersion.

Suggestions for Prospecting

Soils derived from serpentinite masses are characteristic in the high concentrations of chromium, nickel and cobalt; among them, chromium may be the only indicator element associated with chromite ore. Detailed description of distribution patterns of elements in soil and plant has been avoided but only peak points of chromium concentration are indicated in Fig. 2. Values higher than (geometric mean) $\times \lambda'$, namely 6630 p.p.m. for soil and 32·9 p.p.m. for plant, are provisionally taken as anomalous; thus we reduce and fix the number of anomalous values about one-sixth of the total for both soil and plant. Several peak points in the southeastern part of the area probably indicate disturbances by mining, especially by debris of wastes. Striking indication observed in the northern part of the area suggested probable existence of unknown ore bodies, which was partly confirmed by recent test borings.

Soils as well as plant leaves can be used as indicator. However, the disadvantage of the former is the rather troublesome methods of gaining a representative sample and of decomposing for analysis. The plant method of prospecting has its disadvantage in that the variation of total chromium concentration in soil is diminished in plant leaves, although the lower concentration of this element in plant than in soil matters but little.

Acknowledgement—The writers thank those who co-operated or assisted in the collection of samples, especially Mr. Y. Adachi of the Nisttetsu Kogyo Co. Ltd. Thanks are also due to Mrs. T. Yamagata, Miss Y. Susuki, Mr. S. Murata, Mr. A. Yamada and Mr. I. Satake for their assistance in laboratory work.

References

Ahrens L. H. (1954) The lognormal distribution of the elements. *Geochim. et Cosmochim. Acta* **5**, 49–89.

Buck L. J. (1949) Association of plants and minerals. *J. N.Y. Bot. Gdn.* **50,** 265–269. Cited by Harbaugh J. W.

Chenery E. M. (1955) A preliminary study of aluminum and the tea bush. *Plant and Soil* **6,** 174.

Harbaugh J. W. (1952) Contributions to geochemical prospecting for minerals. *U.S. Geol. Survey.*

Hedström H. and Nordström A. (1945) Malmletningsteknikens nuvarande ståndpunkt. *Med. Jernkontorets Gruvbyra* (*Uppsala*) **39,** 1–10. Cited by Harbaugh J. W.

Kimura K. and Murakami Y. (1950) Geochemical prospecting by the use of vegetation. Read at the Symposium on Geochemistry and Analytical Chemistry held by Japan Chemical Society.

Kimura K. and Murakami Y. (1951) *Mikrochemie* **36/37,** 727–40.

Kimura K. and Shima M. (1945) Geochemical prospecting for ore deposits. *J. Sci. Res. Inst.* **48,** No. 1, 347.

Kitahara J. (1958) Studies on the chromites and their occurrences in the Tari district, Tottori Prefecture. *Ganseki Kobutsu Kosho Gakukaishi* **42,** 2–10, 90–100, 114–128.

Murakami Y. (1950) *Bull. Chem. Soc. Japan* **23,** 153.

Olsen C. (1934) *Biochem. Z.* **269,** 329.

Olsen C. (1937) *Ber. wiss. Biol.* **40,** 339.

Rankama K. and Sahama G. (1955) *Geochemistry* p. 624. The University of Chicago Press., Chicago.

Sandell E. B. (1950) *Colorimetric Determination of Traces of Metals* p. 474. Interscience, New York.

Shima M. (1955) *Geochemical Prospecting* p. 174. Maruzen, Tokyo. (In Japanese).

Sugawara K. (1956) *Geochemistry* p. 87. Iwanami Book Company, Tokyo. (In Japanese).
Torii T. (1955) New colorimetric determination of cobalt with *o*-nitrosoresorcin-monomethylether. *Nippon Kagaku Zasshi* **76,** 328–333; *Chem. Abstr.* **50,** 4717b.
Vinogradov A. P. (1954) *Geochemie seltener und nur in Spuren vorhandener chemischer Elemente im Boden* p. 214. Akademie-Verlag Berlin.
Vinogradov A. P. (1957) *Geochemistry of Rare and Disperse Chemical Elements in Soils* p. 216. Academy of Science, U.S.S.R., Moscow. (In Russian).
Webb L. J. (1954) Aluminium accumulation in the Australian–New Guinea flora. *Austr. J. Bot.* **2,** 176.
Yamagata N. and Murakami Y. (1958) A cobalt-accumulator plant, *Clethra barbinervis* Sieb. et Zucc. *Nature, Lond.* **181,** 1808.
Yamagata N. and Yamagata T. (1957) Fundamental studies on the biogeochemical prospecting for manganese. *Bull. Chem. Soc. Japan* **30,** 900–904.
Yoshii Y. and Jimbo T. (1932) Mikrochemischer Nachweis von Aluminium und sein Vorkommen in Pflanzenreiche. *Sci. Rep. Tohoku Imp. Univ.* Ser. 4, **7,** 65.

Geochimica et Cosmochimica Acta, 1960, Vol. 18, pp. 36 to 41. Pergamon Press Ltd. Printed in Northern Ireland

The rhodium, silver and indium content of some chondritic meteorites

U. Schindewolf* and M. Wahlgren
Department of Chemistry, University of Michigan, Ann Arbor, Michigan

(*Received* 23 *April* 1959)

Abstract—By neutron activation analysis the rhodium, silver and indium content of five chondritic meteorites has been determined. The average data are 0·186 and 0·094 p.p.m. for rhodium and silver. The upper limit for the indium content is 0·001 p.p.m. The values for rhodium and silver are in fair agreement with the data estimated by Suess and Urey; the indium values, however, are lower by a factor of 100 or more.

Introduction

Knowledge of the abundance distribution of nuclear species on a cosmic scale is a prerequisite to the formulation of any theory of the formation of the elements. Suess and Urey (1956) in a critical discussion of available abundance data taken mainly from analyses of stony meteorites have reported the apparent unreliability of previous analytical data for a number of trace elements. By activation analysis new abundance data for five chondritic meteorites have been obtained in this laboratory for three of these elements (rhodium, silver and indium), utilizing their neutron capture products 4·4 min Rh^{104}, 2·3 min Ag^{108} and 54 min In^{116m}. The short half-lives and favourable cross-section for the formation of these nuclides permit the use of relatively short irradiations but require rapid and simple chemical separations. Use was made of the Ford Nuclear Reactor of the Phoenix Memorial Laboratory with its pneumatic tube system (Meinke, 1959) which allowed short and precisely timed irradiations and fast delivery of the samples after the irradiation.

A fusion technique was developed to achieve rapid dissolution of the finely powdered meteoritic samples and the existing radiochemical separation methods for the three elements of interest were modified to allow their fast chemical separation. The flux available for these studies was 10^{11} neutrons/cm^{-2}/sec^{-1} at a power level of 0·1 MW. On the basis of some earlier estimations (Schindewolf, 1958) it was expected that with this neutron flux and irradiation times of one half-life of the nuclides of interest a sensitivity of 10^{-8} g for rhodium and for silver and 10^{-9} g for indium could be obtained allowing for a separation time of two half-lives. This seemed to be sufficient because corresponding to the calculations of Suess and Urey the abundance of these elements should be in the order of 10^{-7} g/g of meteorite.

Experimental

Preparation of the meteoritic material

After etching the surface with HCl and rinsing it with distilled water, the meteorites were ground to a very fine powder with a steel mortar and a vibrating

* Present address: Institut für Kernuerfahrenstechnik der Technischen Hochschule, Karlsruhe, Germany.

electric ball mill.* Samples of 0·5–1·0 g were weighed out and transferred to a small lusteroid capsule which was placed inside a rapid opening pull-cap nylon "rabbit" for irradiation. Its design was such that the samples could be removed and the chemical separation started within a few seconds after the end of the irradiation.

Dissolution of the meteoritic material

The samples were dissolved in about 8 g of molten sodium peroxide in a nickel crucible which was brought to a dull red heat over a Meker burner just before the end of the irradiation. Care had to be taken not to decompose the peroxide by heating too long or too vigorously before adding the meteorite powder, for otherwise it might not dissolve the material completely. The fusion was allowed to proceed for 1–1½ min, then the outside of the crucible was cooled by dipping it in a beaker of cold water, and the melt was made to solidify in a thin, readily dissolved coating by manipulation of the crucible. The melt was then dissolved by immersion into an aqueous solution (about 100 ml) containing sufficient HCl to neutralize all the sodium peroxide and leave a slightly acid solution.

Chemical separations

(a) *Rhodium.* About 20 mg of rhodium carrier were added to the solution before adding the solidified melt. After its quick dissolution saturated sodium nitrite solution was added to the boiling solution until it was slightly basic. Rhodium is complexed by the nitrite ions whereas all iron and also silica, the main constituents of the stony meteorites, are precipitated. The iron so removed acts as a scavenger for many trace elements. After fast filtration in a large Buchner glass fritted funnel a few grammes of potassium nitrite were added to the solution and the precipitated potassium–rhodium–nitrite complex filtered off and washed. It then was dissolved in hot 6–8 N HCl, the rhodium reduced to the metallic state by adding zinc powder, filtered in a filter chimney, washed with dilute acid, water and alcohol, and finally mounted on a counting card. The determination of the chemical yield was done after the counting by weighing the metallic rhodium. From the end of the bombardment until the beginning of the counting not more than 9 min were required. The isotopic exchange between the rhodium carrier and the activated rhodium traces of the meteorite was confirmed with 220 day Rh^{102}. The separation factors for the elements tested (one representative for each group of the periodic table, Cs, Sr, Ce, Zr, Nb, W, Tc, Ru, Ag, Zn, In, Sn, Sb, Se, Re) were greater than 10^5.

(b) *Silver.* The silver carrier was added to the nickel crucible and dried before addition of the sodium peroxide and the preliminary fusion. After fusion the melt was dissolved in HCl, the resulting silver chloride was filtered off, washed and dissolved in hot ammonia. A few milligrams of iron-III were added as scavenger. Finally, the silver was reduced with zinc powder, filtered in a filter chimney, washed with dilute acid, water and alcohol, and mounted on a counting card. The chemical yield was determined after counting by titration with thiocyanate.

* High speed vibration mill with agate sample tube and balls, available from Jarrell Ash Co., Newtonville, Mass.

The elapsed time between the end of the bombardment and the beginning of the counting was about 5 min. The completeness of the chemical exchange of added carrier and the activated traces was checked with 210-day Ag^{110}. The separation factors from other elements were not determined, however, the procedure described here has been proven to be very useful for the effective and clean separation of short-lived silver isotopes from fission products (Alexander *et al.*, 1958).

(c) *Indium.* After dissolving the cooled melt in water containing 20 mg of indium carrier, an equal amount of 9 N HBr was added and the solution heated to boiling. $InBr_3$ was extracted twice with 40 ml portions of ether and the combined portions were washed twice with 20 ml of 4·5 N HBr. The indium was then stripped from the ether phase with 30 ml of 6 N HCl. The solution was boiled down almost to dryness, taken up in 2 N HCl and passed through an anion exchange column (Dowex 1, 8 per cent cross-linking, 100 to 200 mesh). This step very effectively separates indium from iron which goes with the indium into the ether but is absorbed very strongly on the column. The eluted indium solution is scavenged with a palladium sulphide precipitation. After buffering the solution with acetate the indium was precipitated as the sulphide, filtered off and air-dried. When necessary the scavenging step and indium sulphide precipitation were repeated. The sulphide precipitate was weighed for the chemical yield determination. The procedure takes about 1 hr. The separation factors from other elements have not been determined, however, they are estimated to be in the order of 10^5 (Sunderman *et al.*, 1959).

Preparation of the standards

The standards were prepared by pipetting a suitable aliquot of the standard solution on to a small square of tissue paper dried under a heat lamp and carefully wrapped in two more layers of tissue paper. Owing to the short half-lives of the isotopes of interest the standards and the unknowns could not be irradiated simultaneously. Therefore each one was combined with a weighed gold foil (1 mg), in which the induced activity of 2·8 day Au^{198} served as a neutron monitor. For the experiments described here no neutron flux variations could be detected over the small errors of the foil weighings and the counting statistics.

Counting techniques

The dried samples on filter paper were centred on a cardboard counting card and covered with cellophane. The samples were counted in a side window flow-type β-proportional counter and the decay followed to a constant background. This required about 20–30 min for the rhodium and silver samples; for indium see below.

Reproducibility of the procedure

The validity of the analysis was confirmed for each isotope by adding a known amount of the standard to the meteorite sample and carrying through the complete irradiation and separation. When from 5 to 10 μg of the elements of interest were added to 1 g of meteoritic material the results were accurate to within 10 to 15%. The precision of the data in pure meteoritic samples will be much lower

because of the smaller abundance of these elements. The relatively good agreement between the amount of rhodium, silver or indium added to the meteorites and the ones found by activation analysis confirms that there is no appreciable absorption or slowing down of neutrons in the meteorite or the added gold foil which might change the neutron flux. Owing to the difficulties of working with short-lived nuclides a better agreement can hardly be expected.

Results and Discussion

The abundance data (in p.p.m.) obtained in the experiments for the five chondrites investigated are listed in Table 1. The data for rhodium and silver are the averages of three and two determinations, respectively, for each meteorite. The relative error for the rhodium analysis does not exceed 30 per cent, the silver results are good by a factor of 2 only. The indium data which are an upper limit only are the results of one run for each meteorite. The counting rate of the indium samples was so low that neither good counting statistics could be achieved nor an unambiguous analysis of the decay curves could be obtained.

Table 1. Abundance of rhodium, silver and indium (p.p.m.)

	Rhodium	Silver	Indium
Beardsley	0·21	0·12	0·0013
Forest City	0·21	0·13	0·0010
Hessly	0·20	0·06	0·0008
Holbrook	0·15	0·04	0·0003
Modok	0·16	0·12	0·0006
Averages	0·186	0·094	0·001

Table 2. Atomic abundance of rhodium, silver and indium relative to silicon $= 10^6$

Source	Rhodium	Silver	Indium
Suess and Urey	0·214	0·26	0·11
Goldschmidt	0·75	3·2	0·25
This paper	0·27	0·131	0·0013

The counting rates obtained in the experiments with Beardsley are: 6000 c/min of 4·4 min Rh^{104} 10 min after the end of the bombardment with a background of long lived contaminations of 350 c/min, 3300 c/min of 2·3 min Ag^{108} 5·5 min after the end of bombardment with a long-lived background of 180 c/min. The constant normal background of the counter was 65 c/min. In all experiments for rhodium and silver the decay curve could be analysed without difficulties with the expected half-lives resulting.

From the average data of Table 1 the atomic abundance of the three elements relative to silicon = 10^6 have been calculated and compared with the ones listed by Suess and Urey (1956) and Goldschmidt (1954). The agreement of the new rhodium data and the ones estimated by Suess and Urey is good. Silver seems to be a factor of 2 lower than estimated. (Suess and Urey state that the results of most trace silver determinations are too high due to contamination of equipment and hands of the experimentors. During the course of the analysis we have avoided any handling of silver coins, tableware, etc. to exclude contamination of this kind.) Indium seems to be lower by a factor of 100 or more than the estimations based on interpolation by Suess and Urey.

The apparent low abundance of indium in the meteorites as compared to the estimations cannot be understood easily. In the activation analysis described for indium only the concentration of the one isotope In^{115} was measured. The assumption normally can be made that the isotopic composition of matter is very uniform, and even for meteorites (which might come from other solar systems) no exceptions have been observed.

Because In^{115} has a metastable state (1/2-), 335 keV above ground state which decays by β-emission with a partial half-life of 100 hr to Sn^{115}, it might be conceivable that via thermal excitation In^{115} has been depleted. This could explain the very low abundance of In^{115} in meteorites. However, the temperatures necessary for the thermal excitation are of the order of 10^{10} degrees and it seems very unlikely that the matter has been at such a temperature for a time long enough to allow the In^{115} to decay.

Nevertheless, an experiment has been performed to determine the abundance of In^{113} by activation and counting its neutron capture product 50 day In^{114m}, which is formed with a capture cross-section of 61 barns. After irradiating 1 g samples of Modok for a week with a flux of 10^{13} neutrons-sec^{-1}-cm^{-2} together with a standard of 1 μg of indium at the Argonne CP5 Reactor and processing them in a manner similar to that described above, here too only an upper limit of 0·001 p.p.m. for indium can be set. This confirms that the isotopic ratio of indium in meteorites is not much different from that on earth, it probably is even the same, and that the abundance of indium in chondrites is very low indeed.

By using spectrographic analysis with a sensitivity of 0·02 p.p.m. Shaw (1952a) also was unable to detect any indium in chondrites. So far there is not any reasonable explanation for the low indium content of the meteorites. Because in nucleogenesis In^{115} has the same chance to be formed as the other unshielded nuclides with odd mass numbers of this mass area one only can conclude that indium was depleted in the meteorites by some chemical or physical fractionation. The reported low value for thallium (Shaw, 1952b) is also of interest in this connexion.

Acknowledgements—This work was supported by the U.S. Atomic Energy Commission and the Michigan Memorial Phoenix Project. Thanks are due to the reactor staffs of the Ford Nuclear Reactor at the University of Michigan and of the CP5 Reactor at Argonne National Laboratory for arranging for the irradiations. The writers are very much obliged to Dr. W. W. Meinke for his help and encouragement. They are greatly indebted to Professor E. W. Heinrich, the Curator of Mineralogical Collections, at the University of Michigan for most of the samples

used. The interest of Professors H. C. Urey and J. H. Huizenga in this work is also acknowledged. One of us (U. S.) is grateful to Dr. Meinke for the invitation to work in the Nuclear Chemistry Group of the Chemistry Department of the University of Michigan.

References

Alexander J. M., Schindewolf U. and Coryell C. D. (1958) *Phys. Rev.* **111,** 248.
Goldschmidt V. M. (1954) *Geochemistry.* Clarendon Press, Oxford.
Meinke W. W. (1959) Rapid activation analysis with the Ford nuclear reactor. *Nucleonics* **17,** 86.
Schindewolf U. (1958) *Angew. Chem.* **70,** 181.
Shaw D. M. (1952a) *Geochim. et Cosmochim. Acta* **2,** 118.
Shaw D. M. (1952b) *Geochim. et Cosmochim. Acta* **2,** 185.
Suess H. E. and Urey H. C. (1956) *Rev. Mod. Phys.* **28,** 53.
Sunderman D. N., Ackermann I. B. and Meinke W. W. (1959) *Analyt. Chem.* **31,** 40.

Geochimica et Cosmochimica Acta, 1960, Vol. 18, pp. 42 to 56. Pergamon Press Ltd. Printed in Northern Ireland

The compositions, structures and origins of radioactive fall-out particles

C. E. Adams, N. H. Farlow and W. R. Schell
U.S. Naval Radiological Defense Laboratory, San Francisco, California

(*Received* 1 *April* 1959)

Abstract—The chemical compositions, structures and modes of origin of several different types of radioactive fall-out particles have been determined through petrographic techniques, X-ray diffraction analysis, radioautography and specially prepared reagent films for liquid fall-out. The fall-out particles studied were collected following the detonation of nuclear weapons under various conditions at both the Nevada Test Site and the Eniwetok Proving Grounds. Radioactive fall-out particles were formed by the interaction of the condensing vaporized metals and fission products derived from the bomb and associated structures with the surface material swept up into the cooling fireball. Descriptions of the various types of fall-out particles are given and their modes of origin are qualitatively related by a simplified thermodynamic treatment.

Introduction

With a continuing programme of nuclear weapons testing, the importance of the radioactive fall-out associated with these detonations has been realized. As this radioactive fall-out can in some cases constitute a serious immediate danger to human beings and in all cases must be regarded as a grave potential hazard, it is desirable to know something of its physical and chemical characteristics and its modes of origin. Samples of radioactive fall-out originating from the detonation of nuclear weapons in various environments have been collected during the course of several field operations at both the Nevada Test Site and the Eniwetok Proving Grounds. This fall-out occurs in the form of small radioactive particles and it is with the study of these individual radioactive fall-out particles that this paper is concerned.

Method of Study

Collection

The methods of collecting the fall-out particles have varied considerably. In some instances soil containing radioactive fall-out particles has been scooped up with a shovel, placed in a suitable container, and returned to the Laboratory. Sometimes open pans or trays have been placed in areas receiving radioactive fall-out and the pans, or liners from the pans, returned to the Laboratory. At the Eniwetok Proving Grounds, where most of the fall-out particles are susceptible to alteration by rain or sea-water, many collections have been made with collectors which open during the period of fall-out; at all other times the collectors are closed thereby protecting the samples.

Most of the fall-out collections were made at many points scattered over hundreds of square miles of fall-out area. In some instances fall-out samples were collected at only one or a few points within the fall-out field. It is not felt that this is a serious bias against the representativeness of the sample, as it has been found in studying fall-out particles from the most widespread collections that the compositions and structures of the particle do not change appreciably over wide areas.

Identification

Two methods have been used for identifying the radioactive particles in the inert soil materials with which they are usually mixed. The simpler method consists of isolating a radioactive particle by repeatedly subdividing a small sample of soil and discarding those subdivisions which indicate no radioactivity when checked with a Geiger counter. When the soil sample containing the radioactive particle has been reduced to a small size, it is examined under a low-power binocular microscope. The radioactive fall-out particles usually have such distinctive appearances that they can be immediately recognized and can be removed manually and checked for radioactivity.

When the above method is not practicable, because the particles are either too small, or too slightly radioactive, or do not differ in appearance from the inactive soil grains, the other method is to fasten the sample in a dispersed condition on the backs of pieces of photographic sheet film. This is accomplished by spraying the back of the film with a liquid plastic and then sprinkling the radioactive soil sample onto the wet plastic. The plastic hardens in a few minutes, firmly binding the particles to the film. After an appropriate exposure for a few hours to a few days, depending upon the intensity of the radioactivity of the individual fall-out particles, the film is developed and fixed by brushing the appropriate solutions onto the emulsion side of the film, care being taken not to disturb the particles cemented to the back. The exposed film is examined with a low-power binocular microscope and the radioactive particles are identified by the dark areas of exposed film surrounding them. Eastman NTB stripping film and single-coated X-ray film have been used successfully for this purpose. If the film has a coloured dye backing, before mounting the particles it is necessary to remove this backing by brushing with photographer's hypo followed by a water rinse.

Composition and structure

The method used for studying the internal compositions and structures of the solid fall-out particles was to make thin sections through the centres of the particles and to study these thin sections under the petrographic microscope. This was done by first placing the individual radioactive fall-out particles in moulds prepared by drilling cylindrical cavities in blocks of paraffin and then pouring in a liquid plastic similar to those used for mounting biological specimens. The plastic, to which a hardening catalyst had previously been added, set in a few hours. The cylindrical plastic pellets containing the fall-out particles were then removed from the moulds and completely hardened by baking at 60°C for 1 hr.

Thin sections were then prepared by first grinding away the plastic pellets on one end until plane sections through the centres of the enclosed fall-out particles were exposed. These semi-sections were then cemented with Canada balsam, particle side down, on to glass microscope slides and the other side of the pellets were ground down until the thicknesses of the thin sections of plastic and enclosed particles were about 30 μ.

The coarse grinding was done on a horizontal, motor driven, iron wheel with

carborundum abrasive nos. 280 and 400. The final stage of grinding was done by hand on a glass plate with emery abrasives nos. 1000 and 1600. In cases where the fall-out particles contained no water-soluble components, water was used as an abrasive lubricant. In cases where the fall-out particles did contain water-soluble components, silicone diffusion pump oil was found to be suitable as an abrasive lubricant as it neither dissolved the soluble parts of the fall-out particles nor the Canada balsam cement.

The thickness of the thin sections was estimated by observing under the petrographic microscope the birefringence of grains of quartz which had been included in the plastic pellets with the fall-out particles. The sections were ground down until the quartz grains exhibited a greyish white or grey interference colour. With increasing experience the investigator was able to judge the thicknesses of the thin seictons by the birefringence and general appearance of the compounds in the fall-out particles themselves without the use of the quartz grains.

Examination of the completed thin sections under the petrographic microscope revealed the structures and, in many cases, the chemical compositions of the fall-out particles. The compositions of the particles were determined also by X-ray diffraction analysis. Either whole single particles or several particles ground together were placed in the X-ray apparatus and powder diffraction patterns obtained. The distribution of radioactivity within the fall-out particles was determined by radioautography of the thin sections with Eastman NTB stripping films.

A limitation on the technique is that only particles greater in diameter than about 150 μ can be made into thin sections. This is not a serious disadvantage as most of the radioactivity in areas of high level radioactive fall-out is found on particles larger than about 100 μ in diameter. Individual radioactive fall-out particles have been collected and identified whose sizes range down to a few microns. They were too small to yield much information as to their compositions and structures; however, except for size, they did not differ in physical appearance from the larger particles described in this report.

Liquid particles

A special method had to be devised for the collection and study of liquid fall-out particles. A reagent film was developed as a surface upon which the liquid drops were collected. This film was cut into circular pieces about 3 in. in diameter and placed in the trays of collecting machines. The machines exposed a series of individual trays, one at a time for a predetermined time interval, to the radioactive fall-out. Each tray was completely protected from outside contamination when not being exposed to the fall-out. The film was treated so that the amount of water and soluble chloride content of the fall-out drops could be determined and an estimate made of the amount of included insoluble solids.

The amount of soluble chloride was determined by impregnating one side of a commercially prepared gelatin coated film (Eastman Kodak Co., Type K-509) with red silver dichromate. In the presence of soluble chloride the red silver dichromate reacts to give colourless silver chloride. It was found that the area of reaction could be easily observed and measured under the microscope and that

the reaction area was proportional to the amount of soluble chloride available. A calibration curve was then established relating reaction area to weight of chloride. The measurable range of sodium chloride by this method is from 10^{-6} to 10^{-12} g (Farlow, 1957).

The determination of the water content of the drops was based on the observation that when a drop strikes the reagent film it spreads over a certain area related to the volume of water in the drop. Insoluble solids within each fall-out drop outlined this maximum spread on the collecting film. The visible residue is called an "artifact". A calibration curve was constructed giving the volume of water in a drop as a function of the area covered by the insoluble solids trace. This calibration was based on the chloride determination described above. A solution of known chloride content was prepared containing some suspended insoluble material. The solution was aspirated on to the reagent film, then dried and the relationship between the original volume of the drop, as measured from its chloride reaction area on the film, and the area on the film outlined by the insoluble material was determined. The smallest water volume measurable by this technique is about 10^{-10} cm^3.

Estimations of the volumes of the insoluble solid material originally suspended in the liquid fall-out particles were made by visually comparing the aggregate volume of the solids remaining in each drop artifact on the reagent film with those made by a series of standard volumes. The standard volumes were prepared by aspirating and collecting on a reagent film small slurry drops from aluminium oxide suspensions of known concentrations. Aluminium oxide was chosen as its density was close to that of the residual solids in the fall-out drops. Also the particle sizes of the aluminium oxide used were approximately equal to the particle sizes of the residual solid material. The volume of aluminium oxide in each drop could be determined by first measuring the water content of the drop as described above and then calculating the volume of included aluminium oxide from the known concentration data. Five standard aluminium oxide artifacts ranging in volume from 10^{-7} to 10^{-9} cm^3 were prepared and mounted on a microscope slide. Each fall-out drop artifact was visually compared with the standard aluminium oxide volumes and an estimate of the volume of the insoluble matter in the fall-out drop was made.

Formation and Description of Radioactive Fall-out Particles

Radioactive fall-out particles are formed by the interaction of the condensing bomb materials, vaporized in the fireball, with surface materials swept up into the hot, radioactive cloud by atmospheric turbulence.

Condensation of vaporized materials

Let us consider first the condensation of the materials vaporized in the fireball. Because of the number of components in the fireball and the lack of high-temperature vapour pressure data, even an approximate analysis of the condensation of the fireball can be made only by assuming a very simplified model. Assume that the major constituents of the fireball are vaporized iron, derived from the construction material of the bomb and associated structures, and air

engulfed in the fireball. This condition is approximately true for high tower bursts.

To describe the condensation of the iron in this simplified model it is necessary to know what the vapour and liquid species of iron are in an oxidizing atmosphere and what the pressure of this vapour over the liquid is as a function of temperature. The data on iron used in this paper have been taken from a report on the iron–oxygen system by Darken and Gurry (1946). These authors conclude that iron oxide vaporizes predominantly by decomposition to free metal atoms and oxygen molecules.

It is assumed, therefore, that in the cooling fireball the iron vapour exists as free iron atoms but during condensation the iron is oxidized and that the liquid phase consists of iron oxide whose composition is determined by the temperature and oxygen pressure. The actual mechanism of the condensation of the iron vapour to liquid iron oxide is not known. It seems improbable that the iron vapour condenses to liquid iron which is subsequently oxidized. The saturation vapour pressure of iron over liquid iron is much higher than that over liquid iron oxide at the same temperature, that, if the fireball were to cool sufficiently so that the iron vapour was just saturated with respect to liquid iron, it would be highly supersaturated with respect to liquid iron oxide. Stewart (1956) in considering the condensation of vaporized iron in an atomic fireball, suggests that clusters of iron atoms and oxygen molecules form which pass directly into iron oxide nuclei.

To find the saturation vapour pressure of iron over liquid iron oxide it is necessary to know the activity of iron in the oxide melt as a function of the temperature and oxygen pressure. These data are available from Darken and Gurry for the temperature range of from 1400 to 1600°C. Unfortunately the temperatures of interest in considering the condensation of the fireball are about 1000°C higher and it is necessary to make a rather bold extrapolation of the Darken and Gurry data up to this region. This extrapolation is justified only by the approximate nature of the fireball model that is being considered. From these extrapolated data on the activity of iron in liquid iron oxide and from the vapour pressure data for iron over liquid iron from the *International Critical Tables*, a graph has been made showing the equilibrium vapour pressure of iron over liquid iron oxide as a function of temperature at oxygen pressures of 0·2, 1·0 and 2·1 atmospheres (Fig. 1).

Let us consider next the detonation of a moderate yield bomb on a 300 ft steel tower. It will be assumed that the only significant metallic constituent of the fireball will be the iron from the tower. The weight of the tower will be estimated at 100 tons and the fireball radius will be assumed to be 600 ft. During the short period of time ($1\frac{1}{2}$–$2\frac{1}{2}$ sec after fission) while the fireball cools through the temperature range at which condensation of the iron occurs, the fireball volume remains essentially constant (Glasstone, 1950). With the assumption that at these high temperatures and low pressures the iron vapour behaves ideally, the pressure of the iron vapour within the fireball has been computed as a function of temperature and the result is plotted on the graph of Fig. 1. The point at which the curve representing the vapour pressure of iron over liquid iron oxide intersects the curve of the pressure of iron vapour in the fireball indicates the

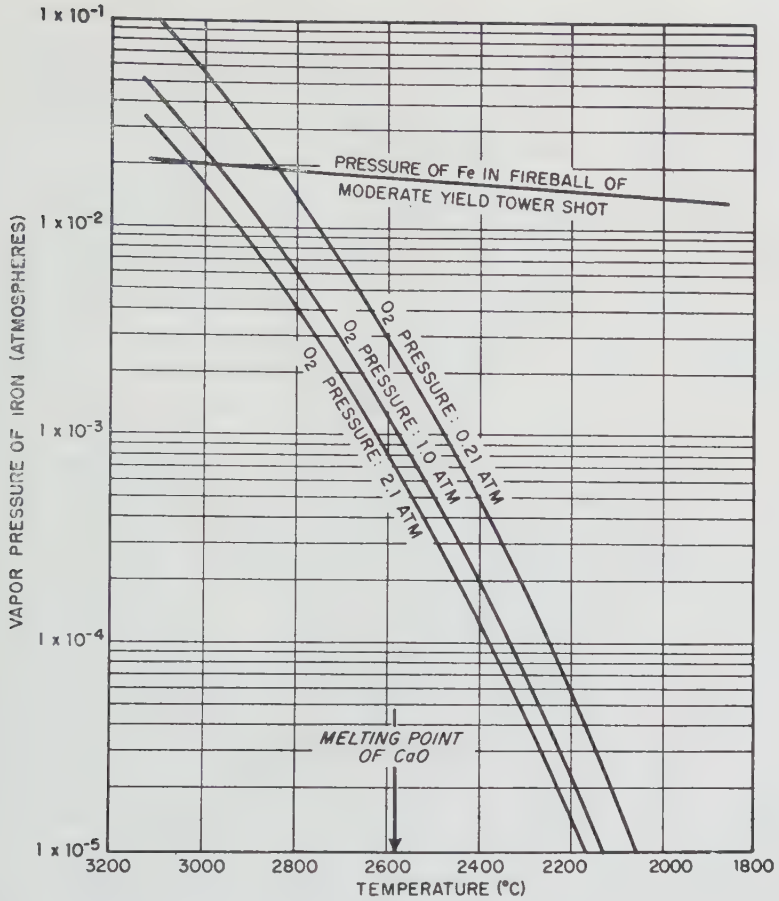

Fig. 1. Vapour pressure of iron over liquid iron oxide at various oxygen pressures as a function of temperature.

temperature at which the iron vapour in the fireball reaches saturation with respect to liquid iron oxide and begins to condense. This point is seen to vary from about 2830°C at an oxygen pressure of 0·2 atm to about 3030°C at an oxygen pressure of 2·1 atm. There is uncertainty as to what the oxygen pressure is within the fireball but it probably falls somewhere between these limits. It is further seen from inspecting the decrease of the equilibrium iron vapour pressure with temperature that about 90 per cent of the iron will have condensed by the time the temperature has dropped about 300°C. This analysis has assumed uniform mixing throughout the fireball and has neglected any effect of supersaturation. The radioactive fission products, owing to their extremely small concentration, would condense as trace impurities in the liquid iron oxide and would have no effect on the main course of condensation.

Stewart, using much the same assumptions as those made above, has analysed the condensation of a fireball composed of iron vapour and air into droplets of liquid iron oxide for the purpose of establishing the size distribution of the

resulting particles. Using an assumed fireball radius of about 500 ft and an iron content of about 25 tons, and by considering the particles to grow by both condensation and coagulation processes, Stewart arrives at a modal diameter for the resulting iron oxide particles of 0·2 μ. The probability that a particle would attain a diameter of a few hundred microns during the short time available for growth would be very small.

The condensation model described above and Stewart's calculations should be approximately true where the conditions are similar to an air burst in which the entire bomb is vaporized. However, the case of a moderate yield tower shot is complicated by the relatively large mass of iron in the tower which may not vaporize completely and by the introduction into the cooling fireball of important amounts of soil material swept up by atmospheric turbulence associated with the explosion.

Under actual conditions the cooling fireball from a moderate yield tower shot will contain not only iron vapour but drops of melted soil materials and may contain liquid iron or iron oxide drops derived from the incomplete vaporization of the tower. By failure of the entire tower to vaporize, the vapour pressure of iron in the fireball will be less than that indicated in Fig. 1, and the corresponding saturation temperature lower. For example, if only one half of the 100 ton tower were vaporized, the condensation temperature would drop approximately 80°C. What is more important, however, is that the addition of liquid soil and iron oxide particles to the fireball will change the size distribution and character of the resulting fall-out particles. The vaporized iron and fission products not only will condense into very small particles of the sizes described by Stewart but important amounts will condense on to the comparatively large drops of iron oxide and soil materials. Hence it is possible to end up with three species of particles: (1) very small iron oxide particles formed by direct condensation from the vapour with subsequent growth by coagulation; (2) large iron oxide particles originally formed by the melting of the steel tower with subsequent growth by condensation of the vaporized iron and by collisions with previously condensed particles; and (3) large particles of liquid soil materials which have grown by the condensation of the iron and by collisions with previously condensed iron oxide particles.

Fall-out samples have been collected and thin sections prepared of individual fall-out particles from tower shots at Eniwetok and at Nevada. The weight and height of the tower and the size of the fireball of the shot at Eniwetok approximated the assumed dimensions of the tower and fireball which were used in the computations establishing the line indicating the vapour pressure of iron in the fireball of a moderate yield tower shot in Fig. 1. In the case of fall-out from the Eniwetok tower shot, the three types of radioactive fall-out particles described above were found.

Variety of particles—tower shots

The most common type of particle collected at Eniwetok was black, spheroidal, weakly magnetic, and usually cracked and veined with calcium salts. These particles varied in size from about $\frac{1}{4}$ to 1 mm in diameter. They were composed

of a core of what originally had been calcium oxide but which had been altered by hydration and carbonation to calcium hydroxide and calcium carbonate, (a mixture of calcite and vaterite). This core was surrounded by a thick, outer zone of dicalcium ferrite ($2CaO \cdot Fe_2O_3$). The dicalcium ferrite was veined with the calcium hydroxide and carbonate and there was often a superficial surface coating of these materials. Radioautographs of the thin sections revealed that most of the radioactivity was confined to the areas of dicalcium ferrite and that the calcium oxide core was apparently inactive (Fig. 2).

These particles were formed by the direct condensation of iron and by the impaction of previously condensed small liquid iron oxide drops on to the drops of liquid calcium oxide. The calcium oxide is derived from the coral sand which forms the surface material of the Pacific atolls. The coral is calcium carbonate, largely in the form of aragonite, which decarbonates at about 800–900°C to form calcium oxide. The calcium oxide melts at 2570°C. It can be seen from Fig. 1 that most of the iron vapour in the fireball will have condensed by the time the temperature has dropped to the melting point of calcium oxide. Therefore most of the fall-out particle formation process will proceed while the calcium oxide drops are still liquid. The iron oxide and the calcium oxide reacted while crystallizing to form dicalcium ferrite. The fission products condensed with the iron making the iron-rich areas of the particles radioactive. The calcium oxide in the particles subsequently reacted with water and carbon dioxide to form calcium hydroxide and calcium carbonate. These processes are accompanied by a twofold increase in volume so that cracks were formed in the particles, which were filled by the calcium compounds, forming veins.

The second type of fall-out particle found was black, usually shiny with a metallic lustre, spherical and magnetic. These particles were composed wholly of magnetite (Fe_3O_4), with the radioactivity distributed homogeneously throughout the particle (Fig. 3). They were found up to about $\frac{1}{2}$ mm in diameter and it seems unlikely, owing to their large size, that they were formed by a condensation process as described by STEWART but were probably originally liquid iron drops formed by the melting and incomplete vaporization of the steel tower. During the course of condensation of the fireball materials, these drops oxidized and accumulated additional iron oxide and fission products which dissolved and were distributed throughout their volumes. The drops crystallized as magnetite, which is the stable form of iron oxide at high temperatures under normal atmospheric oxygen pressure.

The third type of radioactive particle observed was small black spheres ranging in size from about 10 μ in diameter to submicroscopic. These small spheres did not fall by themselves but were found adhering to the surfaces of unaltered coral sand grains or coral grains which had been heated sufficiently to be converted to the unmelted oxide (Fig. 4). Because of their small size nothing is known of their structure or composition but presumably they are the particles formed by direct condensation from the vapour state with subsequent growth by coagulation.

The fall-out particles collected following tower shots at Nevada were similar to the first type described above. These particles were black spheres ranging in size from 1–2 mm to about $\frac{1}{4}$ mm in diameter. They had a metallic or glossy

lustre and many were magnetic. Thin sections showed that the spheres were composed mostly of transparent glass, colourless to pale yellow-brown, with an outer layer of dark brown to black glass. The densities of several of these particles were measured and were found to vary from 1·38 to 2·56 g/cm³. The variation is largely due to numerous air bubbles included within the glassy particles. The radioactivity was usually confined to the dark areas of the glass but often was found in smaller amounts distributed through the lighter coloured glass (Fig. 5).

The source of the glass was the silicate minerals which form the surface material of the Nevada Test Site. These soil materials were melted by the heat of the bomb and carried up into the cooling fireball by atmospheric turbulence. There these liquid soil drops collected on their surfaces the iron and fission products from the fireball. Whether the collection of the iron and fission products was by direct condensation from the vapour state or by the impaction of previously condensed particles is not known, as both the iron and fission products dissolved completely in the liquid glass.

Large fall-out particles consisting only of iron oxide were not found. Whether the occurrence of this type of particle in the Eniwetok fall-out was unusual or whether its absence in the Nevada fall-out was due to non-representative sampling is not known.

Variety of particles—ground shots

In the case of fall-out particles originating from nuclear bombs detonated on or near the surface of the ground the situation is more complicated. Large amounts of soil as well as the bomb and associated structures are vaporized. Also very large amounts of unvaporized soil materials are turbulently mixed throughout the fireball during the cooling process.

Widespread fall-out collections have been made following the surface detonations of very large bombs at Eniwetok and Bikini atolls. The assumptions that underlie the model describing the condensation process for air and tower shots cannot be used. Because of the extremely large size of the fireball uniform mixing of the vaporized constituents throughout the fireball can no longer be assumed. The vaporized iron will probably be concentrated near the centre of the fireball and will decrease in concentration outward. The amount of vaporized soil will be important but no reliable estimate of this quantity can be made.

The characteristic feature of the ground surface shot is the existence in the cooling fireball of such large amounts of material swept up from the ground by the explosion that condensation of the vaporized materials seems to proceed in large measure upon the surfaces provided by these soil particles.

The fall-out particles from the Eniwetok and Bikini surface shots consisted of two types which were both derived from coral sand grains. These particles were white to pale yellow or grey, and varied in size from 1–2 mm to several microns in diameter. The densities varied from 2·0 to 2·8 g/cm³, the variation being due to differences in densities and distribution of the calcium compounds from which the particles were formed.

The first type was angular in shape and consisted almost wholly of fine grained calcium hydroxide with a thin outer layer of calcium carbonate (calcite structure).

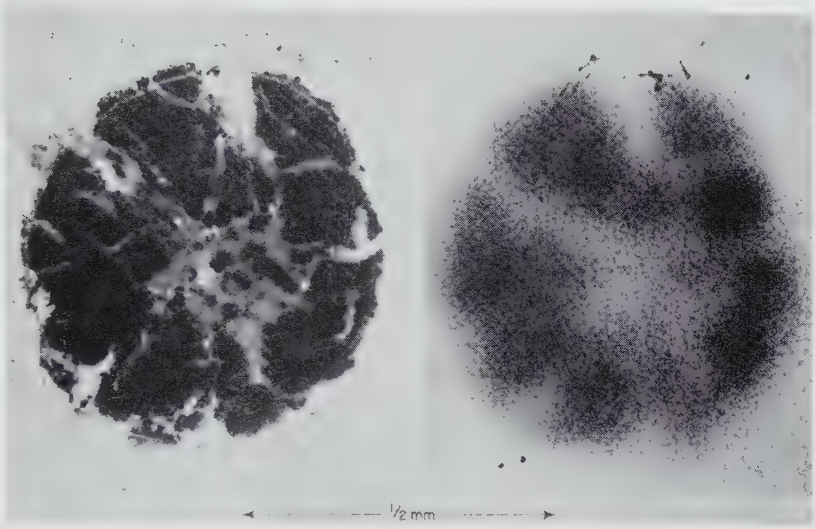

Fig. 2. Thin section and radioautograph of a fall-out particle from a moderate yield tower shot at Eniwetok. The grey central area and veins are remnants of the original inactive calcium oxide drop. The dark areas are radioactive dicalcium ferrite.

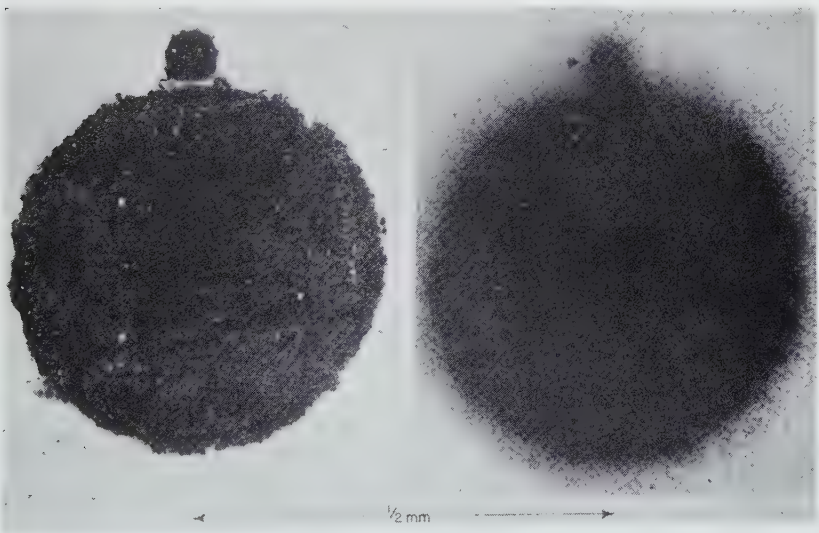

Fig. 3. Thin section and radioautograph of a fall-out particle from a moderate yield tower shot at Eniwetok. This particle is composed entirely of magnetite and the radioactivity is distributed homogeneously throughout its volume.

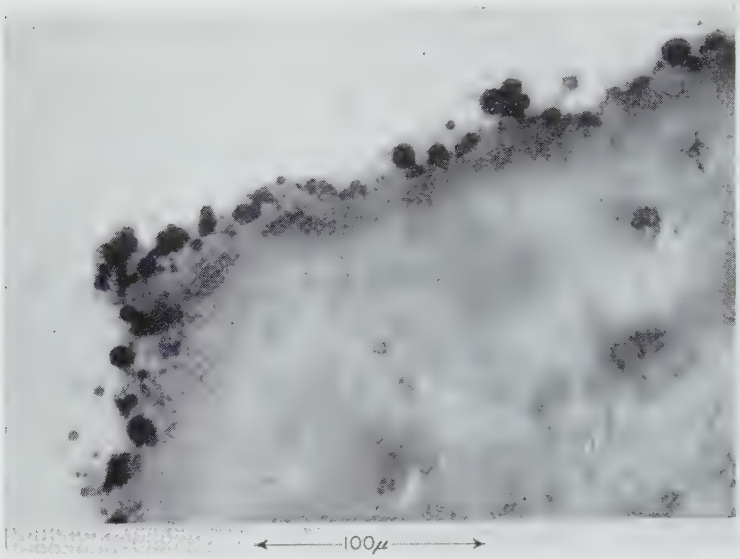

Fig. 4. Small, black, radioactive spheres adhering to the surface of what was originally a coral sand grain. These spheres are formed by the direct condensation, with subsequent growth by coagulation, of material vaporized in the fireball.

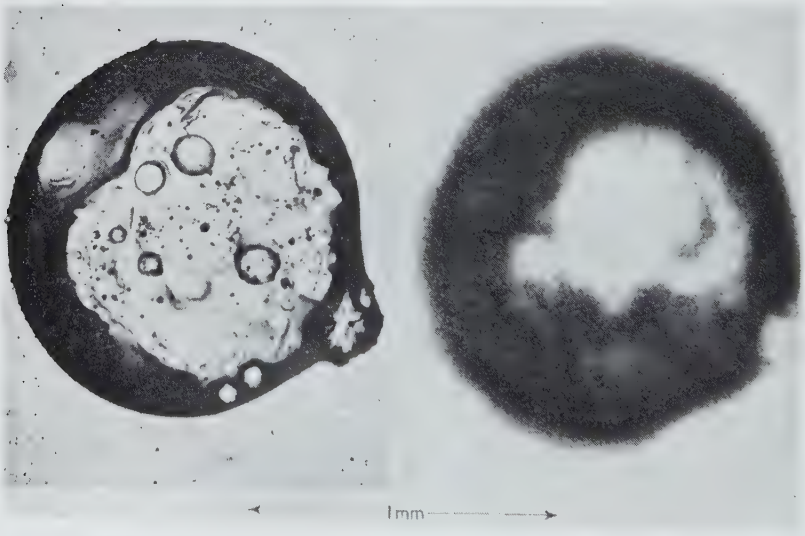

Fig. 5. Thin section and radioautograph of a fall-out particle from a moderate yield tower shot in Nevada. This particle is composed of a transparent glass with a darkly coloured, radioactive outer zone. The circular areas shown in the thin section are gas bubbles.

Some of these angular particles retained a core of unaltered coral (calcium carbonate) surrounded by an outer zone of calcium hydroxide. The radioactivity always occurred as a more or less homogeneous coating on the surfaces of the particles with a tendency to diffuse slightly into the interior of the particles (Fig. 6). Even under high magnification there were no visible sources for the radioactivity except in some cases where many small spheres were found adhering to the surfaces of the large particles of calcium hydroxide or, occasionally, to particles of unaltered coral. These small spheres were black to reddish orange in colour and varied in size from about 10 μ in diameter to submicroscopic (Fig. 4).

The second type of particle was spherical and composed of calcium oxide which had been partially hydrated to calcium hydroxide. The particles had a thin outer layer of calcium carbonate (calcite). The radioactivity was usually found distributed irregularly throughout the volumes of these particles but in some cases it was concentrated near the outer zones of the particles (Fig. 7).

The angular particles were formed by heating of the coral sand grains sufficiently to decarbonate them (800–900°C) but not sufficiently to melt the resulting oxide (2570°C). This calcination formed grains of microporous calcium oxide which were rapidly hydrated upon cooling by water vapour derived from the evaporation of large quantities of sea-water by the heat of the explosion. A thin surface layer of calcium carbonate was formed by the carbon dioxide in the atmosphere. The existence of distinct cores of unaltered coral in some of the particles indicated that these particles were derived from individual coral sand grains and were not formed by the agglomeration of smaller particles.

Many of the coral particles entered the fireball at earlier times or in hotter areas so that the resulting calcium oxide melted and formed the spherical type fall-out particles. During the melting and subsequent freezing the fused calcium oxide particles lost the porous structure characteristic of the unmelted calcium oxide so that the hydration process was slow and incomplete. Many of the particles still consisted of about 90 per cent unaltered calcium oxide several weeks after their collection.

This hydration process is accompanied by a 100 per cent increase in volume. Many of the particles during a period of slow hydration over several weeks were observed to swell and develop a crumbly, fluffy structure. Fragile, fluffy particles similar to these were collected and observed at the time of fall-out. Probably these were originally dense calcium oxide particles which had been more or less completely hydrated while descending through the air by encountering concentrations of water vapour or droplets.

Even though data are not available to make any reliable estimate of the pressures of the vaporized constituents in the fireball, some qualitative estimates can be made. It is known that the weight of iron used in the bomb and associated structures is of the same order of magnitude as that which was assumed to have been used in the tower shot described above for which the iron pressure curve in Fig. 1 is computed. However, the volume of the fireball from a large-yield surface shot is several hundred times the volume of the fireball from the tower shot. As far as iron vapour is concerned, its average concentration is considerably less than that used in computing the condensation temperature in Fig. 1. Owing to the

inhomogeneous mixing in the large fireball there undoubtedly exists a concentration gradient with iron, calcium oxide and fission-product vapours being concentrated relatively near the centre of the fireball and diminishing to much lower pressures in the outer zone.

The existence of calcium oxide vapour in the fireball also will modify the condensation process in that the condensate will be mixed iron–calcium oxides and the temperature of condensation will be affected by the vapour pressure of the calcium oxide.

In the outer regions of the fireball the pressures of the iron and calcium oxide should be low enough so that condensation from the vapour would not occur until comparatively low temperatures had been reached. For example, it is seen from an examination of the graph in Fig. 1 that if the vapour pressure of iron in the fireball is decreased to about one-tenth its value as shown, the condensation process will not start until the fireball has cooled approximately to the melting point of calcium oxide. In the outer zone of the fireball from a large surface shot, the concentrations of the vaporized constituents are probably low enough so that condensation does not occur until temperatures below the melting point of calcium oxide have been reached. This means that it is possible for condensation of the vaporized fission products, or radioactive elements formed by the decay of the fission products, to occur directly on to the unmelted calcium oxide particles which were introduced at comparatively late times into the cooling fireball.

Apparently in some regions of the fireball the concentration of vaporized iron and calcium oxide was sufficently large so that small, micron-size spheres condensed independently. These spheres, probably composed of mixed iron, calcium and fission-product oxides, collected on and adhered to the surfaces of some of the angular calcium oxide particles and account in large measure for their radioactivity. Small spheres of this nature striking the surfaces of liquid calcium oxide particles would dissolve and lose their identity.

Electron micrographs were made of material taken from the surfaces of some of the angular particles which did not carry any small black spheres which could be seen with the optical microscope. Some small spheres were found a few tenths of a micron in diameter; however, there did not seem to be enough of them present to account for the observed radioactivity of the large, angular particles.

In view of the obvious difference in thermal environment between the angular and spherical particles it is of interest to determine whether or not there was a corresponding difference in their radiological environment. Measurements of the amount of included radioactivity and of the weight of a few individual particles indicated that the spherical particles had a higher specific activity than the irregular particles.

There also appear to be differences in the γ-spectra of the two classes. If the angular particles collected their radioactivity in cooler parts of the fireball and at later times than the spherical particles, it is reasonable to assume that they would collect less radioactivity and that a fractionating effect would occur whereby the later condensates would be richer in the more volatile radioactive elements or radioactive elements formed by decay from volatile, short-lived precursors. For example radiochemical, as well as γ-spectrometer, measurements on the

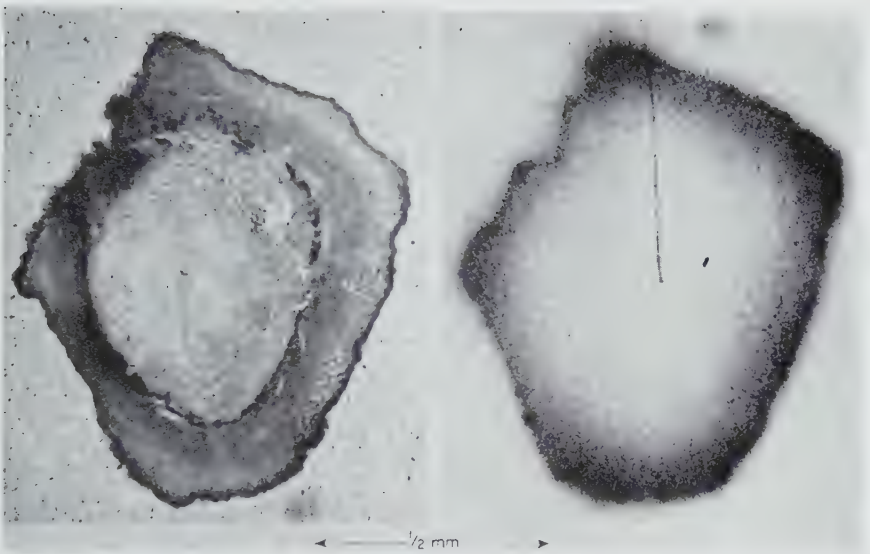

Fig. 6. Thin section and radioautograph of an angular fall-out particle from a large yield surface shot at Bikini. This particle is composed almost wholly of calcium hydroxide with a thin outer layer of calcium carbonate. The radioactivity has collected on the surface and has diffused a short distance into the particle.

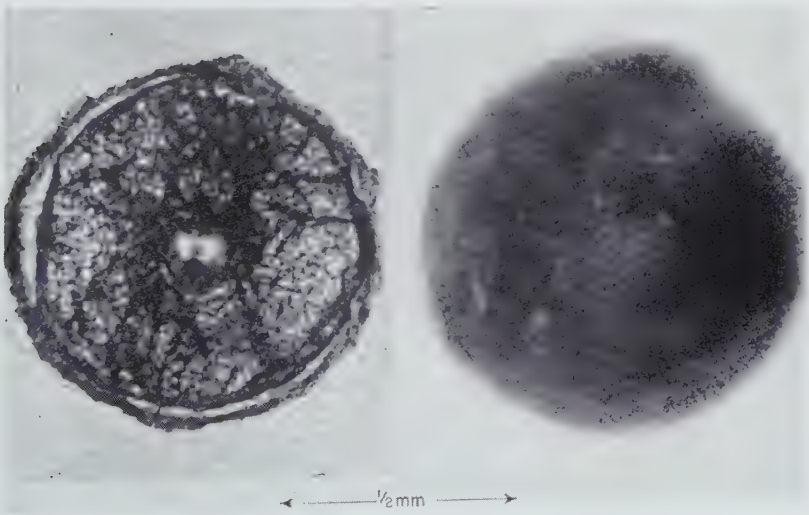

Fig. 7. Thin section and radioautograph of a spherical fall-out particle from a large yield surface shot at Bikini. This particle is composed almost wholly of unaltered calcium oxide with a thin surface layer of calcium hydroxide and calcium carbonate. The radioactivity is distributed irregularly throughout the volume of the particle.

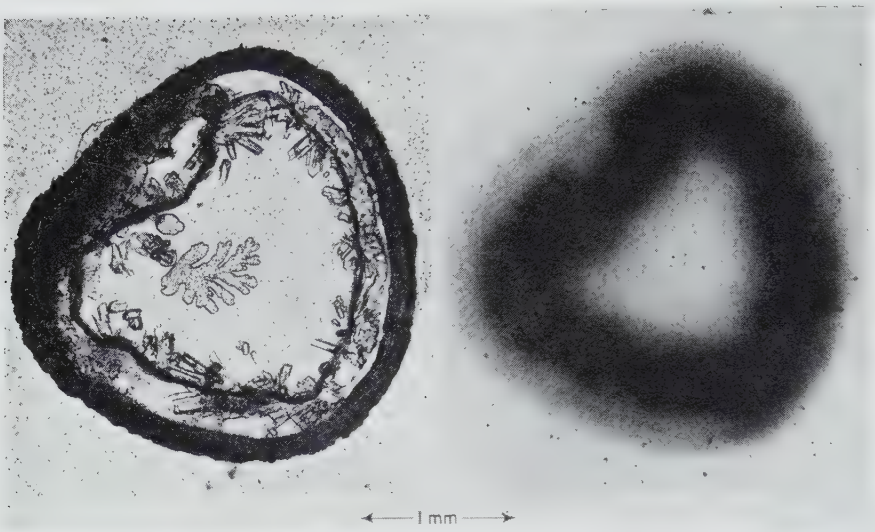

Fig. 8. Thin section and radioautograph of a fall-out particle from a large yield surface shot at Eniwetok which was subjected to wetting by sea-water. The outer shell is composed of magnesium hydroxide and calcium carbonate. The inner shell is composed of calcium sulphate dihydrate crystals with some residual, radioactive calcium hydroxide. The fern shaped object in the centre is a defect in the thin section.

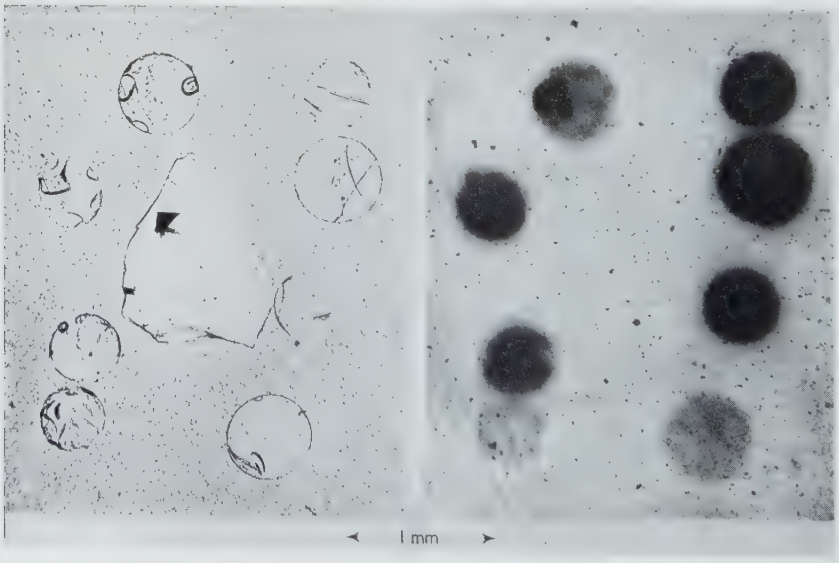

Fig. 9. Thin sections and radioautographs of some fall-out particles from a small yield surface shot at Nevada. The particles are a transparent, green-yellow glass with their radioactivity distributed more or less evenly throughout their volumes. The irregular shaped particle in the centre is a quartz grain used to gauge the thickness of the thin section.

two types of particles showed that the spherical particles contained less Ba^{140} and Sr^{89} (relative to Mo^{99} and Np^{239}) than did the angular particles. Ba^{140} is formed by the decay of the volatile radio-elements Xe^{140} (16 sec half-life) and Cs^{140} (66 sec half-life); Sr^{89} is formed by the decay of the volatile radio-elements Kr^{89} (3·16 min half-life) and Rb^{89} (15·4 min half-life). At comparatively early times after fission most of those volatile elements have not yet decayed into Ba^{140} and Sr^{89}. The spherical calcium oxide particles which entered the fireball during these earlier times received a larger proportion of their radioactive contamination by the condensation of the less volatile radio-elements. The angular calcium oxide particles which entered the fireball at later times received their radioactive contamination from the condensation of radio-elements enriched in Ba^{140} and Sr^{89} and their volatile precursors.

That this fractionation effect occurs to some extent indicates that the large fall-out particles received at least part of their radioactivity by direct condensation rather than by the collection of previously condensed small particles. Small particles which had condensed earlier in the hotter parts of the fireball probably would have a more uniform composition and, if collected indiscriminately by both angular and spherical calcium oxide particles, would not lead to any marked fractionation effect between the two classes. This phenomenon has been observed when radiochemical analyses of bulk fall-out samples from large land surface shots and from large water surface shots have been compared. The solid, radio-active phase of the fall-out particles from the water surface shots, which will be described in detail later, consists of small, black spheres formed by the direct condensation of the vaporized material of the bomb and the platform barge. In this case there were no solid or melted soil particles entering the fireball to act as condensation surfaces for the vaporized materials and the condensation of these vaporized materials proceeded uninterruptedly, forming the small, radioactive spheres. The fall-out from this type of shot compared with the fall-out from the large land surface shots exhibited markedly less fractionation of the radio-elements.

An interesting reaction occurred where calcium oxide or calcium hydroxide particles fell on to surfaces wet with sea-water. These particles were found adhering tenaciously to the surfaces upon which they had fallen. Examination of the thin sections of these particles showed that they consisted of an outer, hard shell of magnesium hydroxide and some intercalated calcium carbonate which surrounded an inner zone of bladed crystals of calcium sulphate-dihydrate (gypsum). The centre of the particles usually consisted of a hollow space containing some calcium hydroxide. The radioactivity was always associated with the calcium hydroxide (Fig. 8).

This type of particle was formed by the partial solution and reprecipitation of the original calcium hydroxide particle. The calcium hydroxide, being slightly soluble in sea-water, started to dissolve slowly. The hydroxyl ions which were released reacted immediately with magnesium ions, the second most abundant cation in sea-water, to form a shell of very insoluble magnesium hydroxide. The calcium ions which were released reacted with sulphate ions, the second most abundant anion in sea-water, to form calcium sulphate-dihydrate. Some of the calcium ions also reacted with the bicarbonate ions in the sea-water to form

calcium carbonate. The undissolved calcium hydroxide remained near the centre of the particle and held the residual radioactivity.

Fall-out particles also were collected following a low-yield surface shot in Nevada. These particles consisted of glass derived from the melting of the silicate minerals of the soil. In most cases there was no pronounced colouring of the glass by the solution of large amounts of iron oxide. The fall-out particles were of two types: transparent spheres of a yellow-green colour and irregular, opaque grains which were brown in colour and did not differ in appearance from the unaltered mineral grains of the original soil. Both types of particle were found up to 2–3 mm in diameter.

The transparent spheres contained radioactivity more or less homogeneously distributed throughout their volumes. Apparently they were formed from drops of liquid soil minerals heated to a very fluid state (Fig. 9).

The irregular particles, as revealed in thin sections, were composed of a transparent, light brown to colourless glass with occasional areas of dark brown to black glass. They contained many inclusions of unmelted mineral grains and air bubbles and looked as if they had been formed from a frothy, viscous mixture of melted and unmelted soil material. The radioactivity was scattered irregularly throughout the particles, being most intense in areas of strong colouring (Fig. 10).

As was the case with the particles from the surface shots at Eniwetok and Bikini, the difference between the spherical particles and the irregular particles was due to the greater heating of the former. The spherical particles apparently originated from soil material which was closer to the centre of the explosion and hence heated to a higher degree of fluidity than the irregular particles.

Electron micrographs of some of the fall-out samples from this shot showed the presence of some small spheres about $\frac{1}{10}\ \mu$ in diameter. It seems probable that these particles were formed by direct condensation of vaporized material.

Variety of particles—water shots

An interesting situation arose when large bombs were detonated on barges anchored in the lagoon at Bikini atoll. In this case the water at the anchorage was sufficiently deep so that little or no material from the lagoon bottom was swept up into the fireball. The sea-water that was evaporated did not condense until very low temperatures had been reached, so that the condensation of the vaporized metals approximated that which would occur at an air burst where there were no complications due to the mixing of relatively non-volatile surface materials with the vaporized material in the fireball.

The major components of the barge assembly were steel and an almost equal weight of coral sand used as ballast. In view of the large sizes of the bombs involved, it may be assumed that most of the materials in the barge were vaporized. The cooling fireball would consist predominantly of iron and calcium oxide vapours with an indeterminate amount of vaporized water and sodium chloride. The initial condensation product should then be small radioactive spheres of mixed iron–calcium oxide. At a later time when cooling has progressed sufficiently, water will condense out forming drops which, combining with sodium chloride, will collect some of the radioactive spheres and eventually reach the surface as fall-out particles.

This type of fall-out particle has been collected and studied on the chloride-sensitive reagent films (Fig. 11). These particles consist of a slurry drop of a saturated solution of sodium chloride in water containing in suspension crystals of sodium chloride and small radioactive spheres. These slurry drops, at the time of and in the meteorological environment of collection, range in size from about 50 to 250 μ in diameter and have a density of from 1·30 to 1·35 g/cm^3. By weight they are composed of about equal parts water and sodium chloride and about 4 per cent insoluble solids. The insoluble solids when examined microscopically are seen to be mostly small spheres varying in colour from black to a reddish orange and in size from about 30 μ in diameter down to submicroscopic. Spheres $\frac{1}{100}$ μ in diameter have been identified in the electron microscope (Fig. 12). Most of the radioactivity is associated with the insoluble solids. Only about 15 per cent of the activity is soluble enough to diffuse into the reagent film.

A small quantity of the insoluble spheres was laboriously accumulated from a large number of drops on the reagent films and an X-ray diffraction pattern obtained from them. The only compound identified was dicalcium ferrite. Judging from the variation in colour of the spheres, there is probably a corresponding variation in composition although no other compounds were detected.

The details of the mechanism of the initial formation of the slurry drops are in doubt. It seems likely, considering the high salt content of the drops, that water was collected by condensation from the vapour on to small aggregates of hygroscopic salt crystals. These slurry drops then collected radioactive spheres by impaction. During the course of descending from high elevations they went through various climatic conditions including a freezing level. The water content of the drops should vary, depending upon the temperature and humidity of the air through which they passed so that the drops probably changed in size and density as they fell.

Conclusions

From a consideration of the examples of fall-out particle formation which have been described above it is evident that the origin of fall-out particles lies in the interaction of two processes: the condensation of the vaporized material in the fireball and the entrainment and heating of surface material in the fireball. The process of condensation alone would produce particles too small to descend in appreciable quantities. It is only when the material vaporized in the fireball combines with the surface materials, either by direct condensation on to the surface materials or by first condensing into discrete particles and then impacting and collecting on to the surface materials, that particles of sufficient size to fall in a relatively short time are formed.

In the absence of unvaporized surface material in the fireball, the condensation process is governed by the saturation vapour pressures of the most abundant constituents. In the simplest cases these consist mainly of iron with lesser amounts of other metals from the bomb and associated structures and vaporized soil all of which condense into small, liquid drops of mutually soluble oxides.

If soil particles are introduced into the cooling fireball before the condensation of the vaporized material is complete, condensation will proceed on these surfaces

and will no longer be governed by the saturation vapour pressures of the major vaporized species but by their abilities to condense on to the heated soil materials.

Because of their extreme dilution, the individual radioactive elements are never concentrated sufficiently to condense as individual metal or oxide particles but only condense on to the particles which are being formed by the major vaporized constituents and by the soil materials. Their condensation behaviour is not governed by their saturation vapour pressures or volatilities but by their ability to condense on to the surfaces of the hot, liquid oxide or silicate particles.

References

Darken L. S. and Gurry R. W. (1946) The system iron–oxygen—II. Equilibrium and thermodynamics of liquid oxide and other phases. *J. Amer. Chem. Soc.* **68,** 798–816.

Farlow N. H. (1957) Quantitative determination of chloride ion in 10^{-6} to 10^{-12} gram particles. *Analyt. Chem.* **29,** 883–885.

Glasstone S. (Editor) (1950) *The Effects of Atomic Weapons* p. 182. U.S. Government Printing Office, Washington, D.C.

Stewart K. (1956) The condensation of a vapour to an assembly of droplets or particles. *Trans. Faraday Soc.* **52,** 161–173.

Geochimica et Cosmochimica Acta, 1960, Vol. 18, pp. 57 to 71. Pergamon Press Ltd. Printed in Northern Ireland

Carbonate equilibria in the open ocean and their bearing on the interpretation of ancient carbonate rocks

E-AN ZEN
Department of Geology and Geography, The University of North Carolina, Chapel Hill, North Carolina

(*Received* 9 *March* 1959)

Abstract—A model of steady-state equilibrium deposition of carbonates in the open sea, where exchange of material between the sediment and the water is permitted, is studied from the phase-equilibrium point of view. Allowing for the possibility of arbitrary variations in temperature, pressure and activity of CO_2 in the system, in general only one-carbonate deposits, either calcite or dolomite, should result. The contact between calcite beds and dolomite beds should be sharp although the two carbonates should be in mutual equilibrium. Changes in hydrographic conditions may result in onlap–offlap relations in the deposits and apparent interbedding of the strata.

Experimental results in the literature on the solubility of dolomite in water are not all internally consistent, although they do indicate that, under atmospheric conditions, the solution relations are sensitive to the value of the CO_2 activity. Increases in total pressure (depth) favour the precipitation of dolomite. Available thermochemical data indicate that dolomite may be the carbonate phase in equilibrium with many sea-water compositions.

Modern carbonate deposits are either calcite or aragonite at the surface, but may change over, abruptly, to dolomite at depth. Two-carbonate deposits, where carefully studied, show evidence of incomplete reaction. The prevalence of one-carbonate deposits thus accord with theoretical considerations although the nature of the surface deposit is at variance with thermochemical data. In the sedimentary record, carbonate rocks with nearly equal amounts of calcite and dolomite are not uncommon; these beds cannot be due to direct chemical precipitation in the open sea.

INTRODUCTION

THE origin of dolomitic limestone and dolostone* in sedimentary rock sequences has long been a matter of debate. Many ideas on their origin have been advanced, for which summaries appear from time to time (e.g. VAN TUYL, 1914; FAIRBRIDGE, 1957); yet no generally accepted theory seems to exist.

In this paper, no novel theory will be advanced. Rather, an attempt will be made to apply concepts of physicochemical equilibrium to carbonate deposition, and thereby to deduce what resulting petrographic relations might be used to decide if a given rock could or could not have been precipitated at equilibrium.

PHASE EQUILIBRIUM IN AN OPEN SYSTEM

Consider a situation of chemical precipitation of carbonates in an area of free oceanic circulation, where the water is not stagnant. This condition ensures that, initially at least, the current may be regarded as being derived from a very large reservoir, the ocean itself, and thus the chemical activities of the dissolved matter will not depend on the immediate system of interest, which is the current at any given point in space, but depend only on their values in the reservoir. This is a situation that may be realized in an open sea; for this reason we will hereafter refer to the particular model as the model of the "open sea" although by "open" is not necessarily implied physical openness. A current flowing through a narrow strait, for instance, would qualify under the present definition.

* The term dolostone is used as proposed by SHROCK (1948, p. 126).

If the physical conditions, the composition of the incoming water, and the net rate of subsidence of the substratum (taking into account any effect of organic activity in building up the substratum as well), are such that these factors do not vary sensibly with time, within any reasonable length of time, then a steady state will be established and the physicochemical conditions of the water at any point will depend only on its spatial co-ordinates. Such a condition may be approximated, for example, at the Bahama Banks today (SMITH, 1940; NEWELL and RIGBY, 1957). This steady-state condition is the specific model that will be examined.

According to this model, the chemical activities of all the dissolved salts and gases are controlled by external conditions and thus are independently variable quantities. These external conditions may be, for example, the activities of the salts in the water body where the ocean current is generated; or, particularly for the gases, these may be their corresponding chemical activities in the atmosphere. The chemical activity of the component H_2O, however, will not then be independently variable, since it must then be connected to the activities of the other components through differential relations of the type:

$$\frac{(\partial \ln a_i/\partial N_i)_{T,P,N_k}}{(\partial \ln a_j/\partial N_i)_{T,P,N_k}} = -\frac{N_j}{N_i} \tag{1}$$

where N_i may be the mole fraction of H_2O in sea-water and N_j the mole fraction of any of the other salts or gaseous components.

The relation that governs the number of phases and number of independent components in an open system has been derived by KORZHINSKII (1950) and by THOMPSON (1955), and states that

$$w = c + 2 - \phi - c' \tag{2}$$

where w is the variance or number of thermodynamic degrees of freedom; c is the total number of independent components; ϕ is the number of phases; and c' is the number of "mobile" or "active" components whose chemical activities have externally-controlled values and are not dependent upon the initial bulk composition of the system itself. At arbitrary values of temperature and total pressure, we therefore have

$$\phi_{\max} = c - c' \tag{3}$$

Since $(c - c')$ for a completely open system is unity due to the relations (1), $\phi_{\max} = 1$, and in general for such a system only one phase will exist. This is a solution phase, or sea-water in our problem.

Consider the situation in which the activity of CO_3^{2-} ion is controlled by the equilibrium between dissolved and atmospheric CO_2, and let the sea-water be concentrated through evaporation, holding the *relative* concentrations of Ca^{2+} and Mg^{2+} ions at their ratio in normal sea-water. Through continued evaporation under equilibrium conditions, one carbonate phase, either calcite or dolomite, would eventually reach saturation and precipitate out of solution. We are not concerned at the moment which carbonate this will be; what matters is that with the Ca^{2+}/Mg^{2+} ratio controlled by *external* conditions, it is very unlikely for both carbonates to start to precipitate out simultaneously, inasmuch as such an event

demands that the Ca^{2+}/Mg^{2+} ratio in sea-water must be a unique quantity even though the actual ratio represents a random choice out of an infinite number of possibilities.

This situation is graphically represented in Fig. 1. In this figure, the solubilities of dolomite and calcite are shown schematically, as functions of total salinity and temperature, at some constant hydrostatic pressure and activity of carbon dioxide. Solubilities are measured in units of the mole fraction of $CaCO_3$ in solution, since such a unit is useful in comparing the relative solubilities of calcite and dolomite.

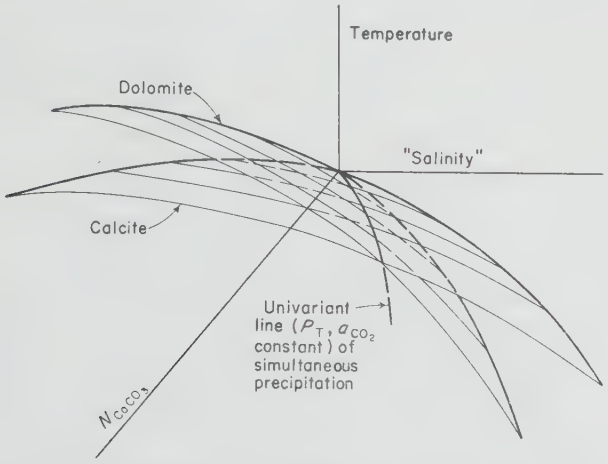

Fig. 1. Schematic representation of the solubilities of calcite and dolomite (in units of the mole fraction, N, of $CaCO_3$ in solution), as functions of temperature and total salinity at constant total pressure and activity of CO_2.

Each of the two solubilities describes a surface in the temperature–salinity–solubility space, and thus each surface is divariant. The two surfaces will, in general, intersect along a single line, a univariant line, along which both carbonates will be saturated simultaneously. The course of this univariant line in the solubility–temperature–salinity space will vary with temperature *or* salinity, but not both, as an independent variable. In terms of the Gibbs Phase Rule, with two solids and one solution present in a three-component system, at arbitrary total pressures the variance is unity.

At a given salinity of the system, controlled by external conditions corresponding to the particular circulation pattern, however, a plane surface normal to the "salinity" axis must describe the conditions of the system at a given point in space. Within this plane section, each of the two solubility surfaces will be reduced to a line, and their intersection is reduced to a point. The system described by two carbonates and a solution is thus invariant. Such an invariant condition is not likely to be fulfilled by the evaporation of a solution of random initial composition.

In a real system, of course, the relative proportions of the dissolved salts may vary independently of one another, so that we can no longer show them along a single "salinity" co-ordinate. For any body of sea-water, however, the activity

of each salt will be fixed by its own external conditions and for the system we should specify the value along each and all of these compositional co-ordinates. The net variance of the system thus is not altered.

The detailed chemical composition of the carbonate precipitating out of the solution may change with changing composition of the solution and with changing physical conditions, without destroying the homogeneity of the phase. We will consider the problem from two different points of view.

First, we may fix our attention on some particular volume of water in the

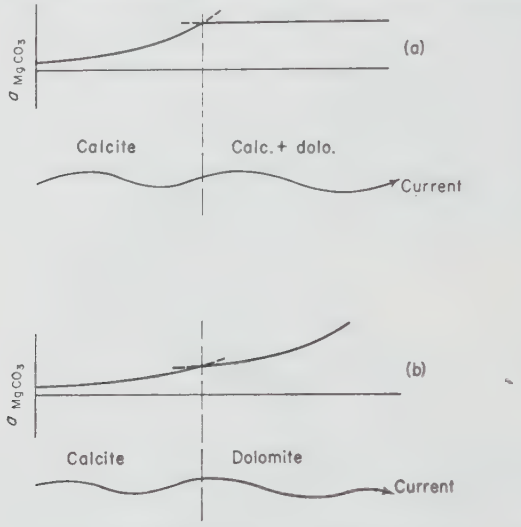

Fig. 2. Steady-state carbonate precipitation from an ocean current. The diagrams assume arbitrary but continuous variations of temperature, total pressure and activity of CO_2 along the course of the current. *A*, equilibrium precipitation. One-carbonate rock (here assumed to be calcite) is followed by two-carbonate rock. Lower diagram, "map view" of the current and its precipitate; upper diagram, schematic plot of the value of a_{MgCO_3}, relative to a_{CaCO_3}, along the course of the current. *B*, complete fractional crystallization. Only one-carbonate rocks will result; two-carbonate rocks will, in general, be confined to beds of negligible thickness and gaps may obtain, along any time-plane, between calcite rock and dolomite rock.

current and follow it along. As far as this volume of water is concerned, the system is *closed* unless mixing of waters of different origins occurs. Barring this, continued evaporation will lead to changes in its chemical composition and eventually to saturation and precipitation of a carbonate. Suppose this is calcite. Because of the relatively more rapid removal of $CaCO_3$, compared with $MgCO_3$, from the sea-water, the chemical activity of $MgCO_3$ will increase relative to that of $CaCO_3$. This increase will continue until the sea-water becomes saturated with dolomite as well, when both carbonates will simultaneously precipitate out and the activities of the two carbonates in solution will thereafter remain constant (Fig. 2*A*). This process, in theory, could give rise to two-carbonate rocks of chemical origin even in an open sea.

However, if, as the current flows along, it encounters different physical conditions, e.g. temperature changes, changes in hydrostatic pressure due to sinking or upwelling or changes in the activity of *atmospheric* CO_2 in equilibrium with

dissolved CO_3^{2-}, then the same solution may find itself actually becoming saturated in a second, different carbonate phase, while undersaturated with the original one. Thus a different carbonate will start to precipitate out. As the ocean current is continuously moving along, the solution is not in contact with the crystals already precipitated out and there is complete and perfect fractional crystallization; hence no resorption of older crystals can take place to keep the solution at a composition saturated with respect to both carbonates, as would be the case in a truly closed system.*† The contact between the calcite deposit and the dolomite deposit may be marked by an abrupt change, by a narrow zone of two-carbonate deposit, or even by a gap of no deposition (Fig. 2*B*).

In a real system, all physical variables must change *continuously* from point to point in space, and so the change from one carbonate to another will be transitional, in the following sense. The first carbonate will change in its detailed composition, continuously in space, until both carbonates are in mutual equilibrium and in equilibrium with the solution; after this point the first carbonate will disappear, due to the effect of fractional crystallization, and the second carbonate will remain. As simultaneous precipitation of two carbonates can occur only at very special values of the physical conditions, such precipitates should be of no practical spatial significance. The field geologist will thus see an abrupt change from a one-carbonate limestone to a one-carbonate dolostone, but the calcite in contact with the dolomite should be in chemical equilibrium therewith—provided, of course, that no gap existed in the original deposition as mentioned above.

In the second alternative, we fix our attention to a point in space. At steady state, every element of solution arriving there should precipitate out exactly the same carbonate and so a thick unit of this carbonate, probably also a really extensive (since a wide range of water composition may be expected to be in equilibrium with a given carbonate phase), may be expected. Along any given time plane, however, the carbonate may be expected to show chemical compositional changes in space as the composition of the solution is modified.

With shifts in hydrographic conditions, thus deviating from true steady-state, the current may sustain different rates of evaporation at different times, moreover the pressure and temperature at a given point may also change with time. As a result, apparent "onlap" and "offlap" relations may be realized; for instance an onlap if evaporation is speeded up, an offlap if retarded. Such a situation may well result in interbedded limestone and dolostone. Indeed, if the interlamination is on a fine scale, the rock may be incorrectly labelled a two-carbonate rock.

Experimental Results and Thermochemical Calculations

Quantitative data, based on experimental results or thermochemical determinations, are necessary in order to decide which carbonate, calcite or dolomite is to be expected to precipitate out of solution, at equilibrium, under a given set

* This concept can obviously be applied to evaporite deposits in general; the writer will publish a communication on that subject in the near future.

† Attention should be called to the analogy between the proposed mechanism and that suggested by Faust (1949) for the deposition of carbonates from hydrothermal solutions.

of conditions. At constant temperature and total hydrostatic pressure, the system $CaCO_3$–$MgCO_3$–H_2O may be treated as a ternary system provided that the activity of CO_2 is also kept constant. Solubility relations of the carbonates in water may then be determined. This is the experimental approach used by YANAT'EVA (1954), YANAT'EVA and DANILOVA (1956), and KRAMER (1959) in the study of this system.

YANAT'EVA (1954, p. 1) studied this system at 0°, 25° and 55°C, under 1 atm CO_2 pressure; and also at 25°C using laboratory air, $P_{CO_2} \simeq 0{\cdot}0012$ atm. The results, however, are not internally consistent, as they indicate that dolomite is stable relative to calcite plus magnesite, at 25°C and $P_{CO_2} = 1$ atm, but at the same temperature but 0·0012 atm CO_2 pressure the reverse relation is true. The relative stabilities of the solid phases of course are independent of the activity of CO_2. YANAT'EVA's data therefore cannot be fully accepted, although they do suggest that at 25°C and under atmospheric conditions concentration of sea-water would result in dolomite, rather than calcite precipitation. It is reasonable to expect that the solution relations of the carbonates should be sensitive to the activity of CO_2.

KRAMER's work (1959,) seems to confirm the incongruent solution relationships of dolomite at 25°C and under atmospheric conditions. His results also show that, under these conditions, concentration of normal sea-water should result in the equilibrium precipitation of dolomite. The value of the activity of CO_2 in KRAMER's experimental work, however, is not known other than it is "atmospheric".

The equilibrium relation between calcite and dolomite in sea-water may be given, at constant activity of CO_2, by the equation

$$2 \text{ calcite} + MgCO_3 \text{ (aq.)} = \text{dolomite} + CaCO_3 \text{ (aq.)} \tag{4}$$

and the change in Gibbs Free Energy is therefore

$$\Delta G = G_{dol} + \mu_{CaCo_3} - 2G_{cal} - \mu_{MgCO_3} \tag{5}$$

Since $(\partial \Delta G/\partial T)_{P,N} = -\Delta S$, the temperature effect on this reaction hinges on the entropy change. Entropies of the dissolved species, especially in a concentrated mixed solution such as sea-water, are little known and so the total entropy change cannot as yet be evaluated. The effect of temperature should not be very marked, however, owing to the small range of temperature variation to be expected in the open sea.

The effect of pressure depends on the volume change, since $(\partial \Delta G/\partial P)_{T,N} = \Delta V$; available data (ZEN, 1956, 1957) indicate that the reaction forming dolomite involves a volume decrease of about 8 cm^3 per dolomite formula (or half that value per calcite formula). This corresponds to a Gibbs Free Energy change of about 0·2 cal per atmosphere of pressure increase, or 0·7 cal per 100 ft of water, in favour of dolomite.

The Free Energy of Formation data for the solid carbonates have been compiled by ROBIE (private communication) and by GARRELS and SIEVER (1958). The

solubilities of calcite and magnesite are remeasured by GARRELS under atmospheric conditions (personal communication). The data at 25°C are as follows:

Phase	ΔG from the elements (ROBIE)
Calcite, $CaCO_3$	$-269{,}667 \pm 400$ cal
Dolomite, $CaMg(CO_3)_2$	$-518{,}676 \pm 900$ cal
Magnesite, $MgCO_3$	$-246{,}077 \pm 450$ cal

Phase	Activity product (GARRELS)
Calcite	$10^{-8.4}$
Magnesite	$10^{-8.0}$

From the activity products, the value of μ_{CaCO_3} and of μ_{MgCO_3} in sea-water can be computed by the formula, for example:

$$\mu_{CaCO_3} = G_{cal} + \Delta\mu = G_{cal} + RT \ln \frac{a_{CaCO_3,\ \text{sea-water}}}{a_{CaCO_3,\ \text{saturated}}} \qquad (6)$$

where the value of a_{CaCO_3} in sea-water can be calculated by using: (1) the composition data in SVERDRUP *et al.* (1942, p. 173), with $Mg^{2+} = 0{\cdot}0523$ mole/kg sea-water, $Ca^{2+} = 0{\cdot}0100$ mole/kg sea-water; (2) the formula of LYMAN and FLEMING for calculating the ionic strength of sea-water (SVERDRUP *et al.*, 1942, p. 205); and (3) the Debye–Hückel formula relating the ionic strength to the activity coefficient (MACDOUGALL, 1948, p. 509).* The value of $\Delta\mu$ for $MgCO_3$ is $+990$ cal, for $CaCO_3$ it is $+280$ cal. Hence ΔG for reaction (4) is $-3{\cdot}7$ kcal in favour of dolomite.†‡ The maximum uncertainty is about 5 kcal.

The results of thermochemical calculations thus agree with KRAMER's experimental results and they *might* eventually prove to accord with YANAT'EVA's data. The large uncertainty attached to the value of ΔG, however, indicate the need for further measurements, particularly under carefully specified values of the activity of CO_2 and with ascertainment of true chemical equilibrium. Nonetheless, it is likely that normal sea-water is in fact close to the boundary of equilibrium precipitation of calcite and dolomite. Petrographic data must next be examined.

PETROGRAPHIC EVIDENCE

Only a few of the studied modern carbonate deposits are attributable to direct chemical precipitation; the majority of these deposits are clearly organic in origin.

* Even though the Debye–Hückel theory probably ceases to be valid in solutions as concentrated as the sea-water, as long as the deviation is proportionally the same for $MgCO_3$ and for $CaCO_3$, this error will not affect the value of ΔG for reaction (4), since it appears on both sides of the equation and therefore will cancel out exactly.

† KRAMER (1959) calculated the free energy of formation for dolomite at 25°C to be $-516{\cdot}5(6)$ kcal. This value is based on his own experimental work. If this value is used, ΔG in equation (5) would be reduced to $-1{\cdot}6$ kcal. However, ROBIE's value is used because it constitutes a consistent set with the other values of ΔG.

‡ The effect of solid solution in the *equilibrium* carbonates will be negligibly small.

Nevertheless, even this latter type of deposit, when exposed to sea-water, may react therewith and approach chemical equilibrium in an open system; thus a mineralogical study of such carbonate deposits may yet be meaningful for our purposes.

Bahama Banks. This, perhaps the best studied modern carbonate deposit, has a complex origin. The surface material, at least west of Andros Island, is a mixture of aragonite and calcite and appears at least in part to be due to direct chemical precipitation (Black, 1933; Smith, 1940; Illing, 1954; Cloud, 1955; Newell and Rigby, 1957), in a sea whose salinity runs locally up to 43 per cent and rarely even to 46 per cent (Smith, 1940, p. 159; Cloud, 1955). The banks may be built upon ancient reefs (Newell and Rigby, 1957). Two drill-hole records are available. One, at North Andros Island, is calcite down to 530 ft level according to Spencer (*in* Eardley, 1951, p. 573), but only to 400 ft level according to Illing (1954, p. 91); then the mineralogy changes, apparently *abruptly*, to dolomite, which becomes the dominant carbonate phase as far as the bottom of the hole at 14,587 ft (Newell and Rigby, 1957, p. 64). Unfortunately, no data are given on whether the two carbonates ever occur together in the same bed.

In the second drill hole, on New Providence Island, pure limestone is encountered until 145 ft below the top, thence the rock changes abruptly to dolostone which persists to the bottom of the hole at about 400 ft level (Newell and Rigby, 1957, p. 64). Chemical analyses of the samples (*ibid.*, p. 65) bear out the mineralogical data, and there seems to be ample evidence for the recrystallization of the carbonates. The calcite–dolomite transition in this second core is said to be coincident with the boundary between the Pleistocene and the Miocene (*ibid.*, p. 65), thus marking a time gap.

Although the abrupt mineralogical change reported accords with the thermodynamic predictions, it is perhaps doubtful that a depth of a few hundred feet will suffice to effect the change in mineralogy. Water samples from the appropriate depths may help to clarify the issue and might also throw light on the alternation of calcite and dolomite at depth in the North Andros Island core (*ibid.*, p. 64). Finally, possible complications due to the reported gaps in fossil records cannot be ignored.

Florida. Hovey (1896) reports on a drill core record from the carbonate deposits of Key West, Florida. A total of about 2000 ft are penetrated and only "limestone" is reported. Hovey does not cite specific tests for dolomite, but from his table of chemical analyses (1896, p. 85), only one sample, at a depth of 775 ft, had as much as 6·7 per cent of MgO in a nearly pure carbonate rock, which is described as a hard, porous and highly fossiliferous limestone (*ibid.*, p. 76). All the other analyses have less than 2·5 per cent of MgO in nearly pure carbonate rocks. It appears then that in this record of up to 2000 ft, no dolomite is found. The limestone is virtually exclusively of demonstrably organic origin. This conclusion agrees with the results of more recent studies by Ginsburg (1957).

Funafuti. Cullis (in Sollas *et al.*, 1904, pp. 392–415) studies the mineralogy of the drill cores from this atoll. The three carbonates that are present, aragonite, calcite and dolomite, are distinguished by staining, "Lemberg's solution"

(aluminium chloride plus haematoxylin) being used for the distinction of dolomite (*ibid.*, p. 393). The results indicate that at depths above 638 ft, calcite and aragonite occur exclusively. Aragonite is clearly a metastable phase, and the deepest sample that contains it is at 220 ft (*ibid.*, p. 403). Somewhere between 638 ft and 650 ft dolomite takes over and occurs exclusively (*ibid.*, p. 407), a situation that persists down to 820 ft. Between 820 ft and 875 ft calcite and dolomite coexist (*ibid.*, p. 411); from 875 ft to 1050 ft dolomite alone is found (*ibid.*, p. 412); between 1050 ft and 1070 ft the two carbonates again co-exist, and below 1070 ft, down to the maximum depth of boring, 1114 ft, dolomite alone is found (*ibid.*, pp. 413–414). These mineralogical data correlate very well with the chemical data of Judd (*ibid.*, p. 364–365), except that Judd indicates relatively high $MgCO_3$ content in the depth interval between 10 ft and 35 ft, which is not traceable to the presence of dolomite.

The results are confirmed by the recent X-ray study of these samples by Schmalz (1956). The high $MgCO_3$ content in the 10–35 ft interval is shown to be due to high-magnesium calcite. The transition between calcite and dolomite at 640 ft is abrupt and complete, with a vanishingly small layer of two-carbonate rock, even though the sample on either side of the boundary is visibly the same organic material. This is in conformity with the thermodynamic predictions for dolomitization in an open system.

The complications between 820 ft and 875 ft, and again between 1050 ft and 1070 ft, are also confirmed by Schmalz's X-ray analysis. The situation, nevertheless, may not be quite so contradictory as it appears; for at least for some samples Cullis reports (in Sollas *et al.*, 1904, pp. 410–411) encrustations of alternating *layers* of calcite and dolomite, while each layer is monomineralic. Even for those samples which do not show this texture, calcite may be observed as relicts armoured by dolomite (*ibid.*, p. 406). These observations show that for much of the two-carbonate assemblages one of these carbonates was in fact metastable, and some of the samples, with alternating layers of encrustations, have undergone reactions in fluctuating environments, in which either calcite or dolomite, but not both, was stable.

Further complications are shown by X-ray work. Goldsmith and Graf (1958, pp. 682–683) report that some of the Funafuti dolomite samples show bimodal basal reflections, and for at least one sample, depth 985 ft, the (03·0) peak is also bimodal, indicating the presence of two distinct dolomites. The present writer has also observed the doubling of the (10·4) peak for dolomite from between 706 ft and 716 ft, with *d*-spacings of 2·92 Å and 2·90 Å; the latter corresponding to nearly pure, ideal Ca,Mg dolomite. Thus it is clear that stable chemical equilibrium has not been attained everywhere in the Funafuti core, although we must not therefore conclude that *metastable* equilibrium, relative to the original high-magnesium calcite, may not have been established in these samples, at least for those portions which had been exposed to sea-water. For the armoured relicts, the equilibrium, if any, must be studied as if the system were essentially closed; for these systems coexistence of two carbonates are permissible by the present theory.

Paleontological studies (Ladd, 1958, p. 196) show that the land–sea relation

at the Funafuti atoll had fluctuated during the Pleistocene. The depth level at which dolomitization occurred, thus, cannot be taken to be the depth at which dolomite first occurs today.

Bikini. The mineralogical results of the four cores drilled at Bikini Atoll have been reported by Emery, Tracey and Ladd (1954). Although the greatest depth penetrated, in hole 2-B, is 2556 ft, no sample is recovered from this hole. The deepest sample studied by X-ray diffraction, from core 2-A, is at a depth of 1135 ft; all the samples from cores 2, 2-A and 3 show either calcite or calcite plus aragonite (*ibid.*, p. 85, table 18). No dolomite is found (*ibid.*, p. 85). The chemical analyses of the samples from cores 2, 2-A and 2-B show remarkable uniformity of values, and down to a maximum depth of 2510 ft (*ibid.*, p. 84, table 15) the maximum $MgCO_3$ content is 3·46 per cent in a rock consisting nearly exclusively of carbonates. A near-surface beach sand, sample no. 2-1-4, contains over 8 per cent of $MgCO_3$ but this is due to fragments of *Lithothamnion* (*ibid.*, p. 84). Thus at Bikini Atoll evidently no dolomite is present.

Eniwetok. Ladd *et al.* (1953) report on three cores drilled at Eniwetok Atoll, nos. Kl-B, F-1 and E-1. Core Kl-B penetrates to 1285 ft and only limestone is encountered (*ibid.*, p. 2271). Core E-1 penetrates to 4222 ft, bottoming in olivine basalt, and only non-dolomitic limestone is found. Core F-1 penetrates to 4630 ft, and dolostone is first found below the 4320 ft level (*ibid.*, p. 2266). Unfortunately, no X-ray data are given, and the dolomite is identified on the basis of copper nitrate staining (*ibid.*, p. 2269). The details of the mineralogical changes thus cannot be ascertained. It appears, however, that the change to the highest unit of dolostone, from the calcite rock above, may be transitional over up to 4 ft of strata (*ibid.*, p. 2266) and that non-dolomitic limestone has been found farther below that level.

It is interesting to note that the material surrounding core F-1 is sufficiently porous that tidal fluctuations are observed in the drill core with no time lag and amplitude diminution (*ibid.*, p. 2259, 2262). Interaction of "fresh" sea-water with material of the reef is thus a distinct possibility.

Kita-Daito-Jima. A drill hole 1416 ft deep is put down on this island and the results are reported by Hanzawa (1940). Dolostone is found down to a depth of 340 ft, and limestone from there on down to the bottom of the hole. The situation, however, is complicated by the fact that the surface material is Plio-Pleistocene in age and no modern deposit exists. There is doubt thus as to the depth at which the dolomite has formed.

Borneo. Kuenen (1947, pp. 6–7, 34–36) reports two holes drilled on Maratoea Atoll near Borneo. Hole no. 3 reached about 860 ft and hole no. 4 reached 1410 ft. The materials are indurated limestone and loose reef detritus; no dolomite is reported and apparently none encountered.

The Great Barrier Reef. Two holes are drilled in the Great Barrier Reef (Richards and Hill, 1942). One, on Michaelmas Cay, goes to a depth of 600 ft, and the other, on Heron Island, to 732 ft. No dolomite is found in either core. Little direct precipitation of carbonate occurs today in this reef complex (Fairbridge, 1950), and Professor Fairbridge has informed the writer (1958, personal

communication) that no dolomite is known in the surface material of the reef complex.

The elevated islands of southern Pacific and Indian Oceans. Skeats (1903) reports on the chemical composition and mineralogy of an extensive series of limestones and dolostones from a number of elevated islands in southern Pacific Ocean, as well as from the Christmas Islands in southern Indian Ocean. The islands in the Pacific include: the Fiji group, the Niue Island, the Tonga group, the Paumotus group and the Ladrones. The geology of the Fiji group has been reported by Andrews (1901).

Both chemical and mineralogical data are given for each sample studied, and the minerals are identified by their optical properties and by staining test with "Lemberg's solution". From Skeat's descriptions, the rocks seem by and large to consist of either calcite alone, or dolomite alone through metasomatic alteration of calcitic skeletons; however, numerous samples are encountered which do have both carbonates, with calcite and dolomite crystals occasionally mantling each other in optical continuity. The situation is complicated by possible secondary growth of the crystals after elevation of the beds above the sea floor. A new X-ray examination of the specimens would be very desirable.

The Peru–Chile Trench area. Sediment cores collected from the Peru–Chile Trench area, by the research vessel *Atlantis* of the Woods Hole Oceanographic Institution, have been studied by X-ray diffraction methods. Calcite is common in many of these cores; most of this is organic in origin but some specimens are due to the devitrification of volcanic glass (Zen, 1959). Dolomite is indicated by the presence of the (10·4) peak in a number of samples in cores recovered from water depths ranging from 228 m (748 ft) to 5515 m (18,100 ft). The following three samples have yielded unequivocal dolomite. Core 29-2, near the coast of Callao, shows dolomite near the top of the core; depth of water is 1075 m (3530 ft). Core 64-6, from the mouth of Moreno Bay off Antofagasta, Chile, shows dolomite in the depth interval of from 107 to 112 cm from the top of the core, and questionably from there on down; the depth of water is 228 m. The best sample, however, is found in Core 53-5, on the seaward side of the Peru–Chile Trench off the coast of Arica, Chile (Zen, in press; see also Zeigler *et al.* 1957, Fig. 1). The water depth is given as 4597 m (uncorrected echo-sounding data) or about 15,100 ft. The sample occurs as a grey, compact, cement-like nodule about 5 cm across, at a depth of 104 -108 cm below the surface of the core. Similar material is found also to form septa about 1 mm thick, enclosing the brown argillaceous mud which is the bulk of the core. X-ray study shows the material to be largely dolomite, with $d(10{\cdot}4)$ just under 2·90 Å; quartz, chlorite, illite, kaolinite and mixed-layer clay predominantly montmorillonite are associated with the carbonate. The textural relation indicates that the dolomite is neither organic nor detrital in origin; whether it precipitated as dolomite directly, or as calcite later converted to dolomite is not known. If the phase dolomite is due to later alteration, the reaction is complete.

Isolated occurrence of authigenic dolomite in the open sea has also been reported by other workers. For example, Correns (in Trask, 1955, p. 385) reports dolomite

near shore in the Gulf of Guinea, and also in the Cape Verde basin amidst pelagic sediments.

Summary. Modern carbonate deposits are largely in the form of reef complexes. The preceding review shows that in shallow waters calcite is the only form of carbonate being deposited, if we ignore the obviously metastable aragonite; calcite of organic origin, however, may be metastable due to its high initial magnesium content.

The pattern of calcite and dolomite occurrences is at first glance very irregular. Nonetheless, these general conclusions seem to be valid.

(1) Dolomite virtually never occurs in shallow water surface deposits of modern age and of open-sea environment.

(2) Dolomite does occur, however, in the deeper levels of many complexes, due to metasomatic alteration of calcite in contact with sea-water. The available chemical analyses, from the Bikini Atoll, the Funafuti Atoll and the Fiji Island group, indicate that the $MgCO_3$ content in the rocks is not uncommonly too high for these rocks to have been formed by simple recrystallization of the original high-magnesium calcite, without exchange of matter with the surroundings. The data of Goldsmith *et al.* (1955) and of Chave (1954a, b) indicate that $MgCO_3$ content of high-magnesium calcites, even in algae, never exceeds 29 per cent. In other words, such dolomite as found in the reef complexes must be the result of reactions in the open system.

(3) The depth at which dolomite appears, however, is variable, ranging from over 4300 ft to just over 140 ft below the surface. Moreover, even in adjacent areas, such as in the Bahama Banks, this depth may vary from core to core.

(4) Dolomite deposition is probably going on today in the open sea at great water depth. The depth of 4600 m for the material from the Peru-Chile Trench corresponds to about 460 atm of hydrostatic pressure or about 100 cal in terms of the change in Gibbs Free Energy. Whether, given the temperature and the composition of the water, this suffices to shift the calcite-dolomite equilibrium, at present cannot be evaluated.

(5) Wherever detailed petrographic data are given, the dolomite–calcite transition occurs *abruptly*, with little or no two-carbonate zone in between. Although the transition may reverse several times at depth (e.g. Bikini, Funafuti, Bahama), the sharp contact and lack of two-carbonate beds strongly suggest the applicability of the model of an open system reaction outlined in the early part of this paper.

Interpretation of Ancient Carbonate Rocks

The concepts considered in the first part of this paper, and the petrographic evidence considered in the second part, may be utilized to enable us to draw the following conclusions on the interpretation of ancient carbonate rocks.

Firstly, rocks containing only one carbonate, whether calcite or dolomite, are consistent with the thermodynamic conditions for deposition in the open sea. Although it may be impossible to decide whether the deposit is primary or due to metasomatic reactions with sea-water, yet if a rock, say dolostone, is taken to be the result of reaction in the sea, then the theory predicts that its contact with

the unreacted calcite limestone will be abrupt. In this context, deposition of carbonates in evaporite sequences need not be excluded; in fact the detailed description by Stewart (1949; 1951a, b) of the Yorkshire evaporite beds is in accord with the above deductions. Here, either magnesite or dolomite, but rarely if ever both, occur in a given stratum. A criterion that may be used to test the hypothesis is that carbonates in direct contact with each other must be in mutual chemical equilibrium even though the lithological transition must be sharp.

Secondly, the presence of two-carbonate rocks does not prove that the site of deposition was not the open ocean—a point discussed in an early section. Although deposition of one-carbonate rocks has excellent chances to persist in the open ocean because of the possibility of changing physical environment and of mixing of waters of different origins as the current flows along, continued evaporation of a body of water nevertheless could lead to precipitation of two-carbonate rocks. However, the same criterion, namely that any two carbonates in mutual contact must also be in mutual equilibrium, must also apply in this case. Moreover, the two carbonates within the body of a two-carbonate rock must have constant compositions (barring the effect of ferrous iron) throughout the rock, reflecting constant physical conditions during the precipitation process, as discussions in an earlier section demonstrated.

Finally, a really extensive two-carbonate rocks, if deposited in the open ocean, and if showing compositional variations, cannot be directly chemical in origin. Such rocks more likely owe their origin either to later alteration in a closed system, or due to recrystallization of organic or detrital material during diagenesis. The petrographic observations of Cullis on the two-carbonate rocks of Funafuti, however, indicate that even in this case conclusions must be drawn with caution.

Summary

(1) Deposition of carbonates in the open sea, where exchange of material is possible between sea-water and the sediments, should result, in general, in one-carbonate deposits. Under equilibrium conditions, this carbonate may be either calcite or dolomite. Continued evaporation of the ocean current under steady-state conditions should result in a really extensive, thick beds of monomineralic carbonate rocks.

(2) Experimental data suggest that, under atmospheric conditions, dolomite dissolves incongruently into calcite and solution. Both thermochemical calculations and experimental data predict that normal sea-water should, upon concentration, precipitate dolomite, rather than calcite. However, the thermochemical data are accompanied by large uncertainties. The experimental results show that the dolomite–calcite transition is sensitive to the value of the activity of CO_2; sea-water may in fact be compositionally close to that for the calcite–dolomite transition under surface conditions.

(3) Petrographic data from modern carbonate deposits indicate that calcite is the equilibrium carbonate under surface conditions. Dolomite, however, becomes relatively more stable at depth, and—everything else being equal—forms from

calcite through reaction with sea-water. Dolomite may also be forming directly from sea-water at great depth.

(4) Application of the concept of open-sea deposition of carbonates to carbonate rocks in the sedimentary record shows that many two-carbonate rocks, which from geological evidence must have formed in open, shallow seas, cannot be the product of direct chemical precipitation. These rocks are more likely the results of later metasomatism in closed systems, or the result of recrystallization of organic or clastic detritus.

Acknowledgements—I am deeply indebted to P. E. Cloud, Jr., R. M. Garrels, R. F. Schmalz and J. B. Thompson, Jr., for the numerous stimulating discussions I had with them during the past several years on the problem of carbonate equilibria. These people also read my manuscript and suggested many improvements. Garrels pointed out a serious error in my original reading of Yanat'eva's results. Schmalz's study of the Funafuti cores gave impetus to my own thinking; he should therefore share much of the credit though none of the responsibility for this paper. J. R. Kramer sent me a preprint of his revised data, and Garrels and R. A. Robie gave me permission to use their unpublished thermochemical data. For their courtesy I am truly grateful.

References

Andrews E. C. (1901) Notes on the limestones and general geology of the Fiji Islands, with special reference to the Lau group. *Mus. Comp. Zool. Bull. Harv. Univ.* **38,** 1–50.

Black M. (1933) The precipitation of calcium carbonate on the Great Bahama Bank. *Geol. Mag.* **70,** 455–466.

Chave K. E. (1954a) Aspects of the biogeochemistry of magnesium—I. Calcareous marine organisms. *J. Geol.* **62,** 266–283.

Chave K. E. (1954b) Aspects of the biogeochemistry of magnesium—II. Calcareous sediments and rocks. *J. Geol.* **62,** 587–599.

Cloud P. E., Jr. (1955) Bahama Banks west of Andros Island. *Bull. Geol. Soc. Amer.* **66,** 1542. (Abstract).

Eardley A. J. (1951) *Structural Geology of North America.* Harper, New York.

Emery K. O., Tracey J. I., Jr. and Ladd H. S. (1954) Geology of Bikini and nearby atolls—I. Geology. *U.S. Geol. Surv. Prof. Pap.* 260-A.

Fairbridge R. W. (1950) Recent and Pleistocene coral reefs of Australia. *J. Geol.* **58,** 330–401.

Fairbridge R. W. (1957) The dolomite question. *S.E.P.M. Symposium, Spec. Publ.* No. 5, pp. 125–178.

Faust G. T. (1949) Dedolomitization, and its relation to a possible derivation of a magnesium-rich hydrothermal solution. *Amer. Min.* **34,** 789–823.

Garrels R. M. and Siever R. (1958) Stability of some carbonates in aqueous solutions. *Bull. Geol. Soc. Amer.* **69,** 1569. (Abstract).

Ginsburg R. N. (1957) Early diagenesis and lithification of shallow-water carbonate sediments in south Florida. *S.E.P.M. Symposium, Spec. Publ.* No. 5, pp. 80–100.

Goldsmith J. R., Graf D. L. and Joensuu O. I. (1955) The occurrence of magnesian calcite in nature. *Geochim. et Cosmochim. Acta* **7,** 212–230.

Goldsmith J. R. and Graf D. L. (1958) Structural and compositional variations in some natural dolomites. *J. Geol.* **66,** 678–693.

Hanzawa S. (1940) Micropalcontological studies of drill cores from a deep well in Kita-Daito-Jima. In *H. Yabe Jubilee Publ.* Vol. II, pp. 755–802.

Hovey E. O. (1896) Notes on the artesian well sunk at Key West, Florida, in 1895. *Mus. Comp. Zool. Bull., Harv. Univ.* **28,** 65–91.

Illing L. V. (1954) Bahaman calcareous sands. *Bull. Amer. Ass. Petrol. Geol.* **38,** 1–95.

Korzhinskii D. S. (1950) Phase rule and geochemical mobility of elements. *Proc. Eighteenth Int. Geol. Congr.* Sect. A, pp. 50–57.

Kramer J. R. (1959) Correction on some earlier data on calcite and dolomite in sea water. *J. Sediment. Petrol.* **29,** no. 3.

Kuenen Ph. H. (1947) Two problems of marine geology: atólls and canyons. *Verh. Akad. Wet. Amst.* **43,** 1–69.

Ladd H. S. (1958) Fossil land shells from western Pacific atolls. *J. Paleont.* **32,** 183–198.

Ladd H. S., Ingerson E., Townsend R. C., Russell M. and Stephenson H. K. (1953) Drilling on Eniwetok Atoll, Marshall Islands. *Bull. Amer. Ass. Petrol. Geol.* **37,** 2257–2280.

MacDougall F. H. (1948) *Physical Chemistry.* Macmillan, New York.

Newell N. D. and Rigby J. K. (1957) Geological studies of the Great Bahama Bank. In Regional Aspects of Carbonate Deposition. *S.E.P.M. Symposium, Spec. Publ.* No. 5, p. 15–79.

Richards H. C. and Hill D. (1942) Great Barrier Reef bores, 1926–1937. *Report Great Barrier Reef Committee,* Vol. 5 p. 122. Australian Government Printers, Brisbane.

Schmalz R. F. (1956) The mineralogy of the Funafuti drill cores and its bearing on the physico-chemistry of dolomite. *J. Paleont.* **30,** 1004–1005. (Abstract).

Shrock R. R. (1948) A classification of sedimentary rocks. *J. Geol.* **56,** 118–129.

Skeats E. W. (1903) The chemical composition of limestones from upraised coral islands, with notes on their microscopical structures. *Mus. Comp. Zool. Bull., Harv. Univ.* **42,** 1–126.

Smith C. L. (1940) The Great Bahama Bank. I—General hydrographical and chemical features; II—Calcium carbonate precipitation. *J. Mar. Res.* **3,** 147–170, 171–189.

Sollas W. J. *et al.* (1904) The atoll of Funafuti. Borings into a coral reef and the results. *Rep. of the Coral Reef Committee of the Royal Society.* The Royal Society, London.

Stewart F. H. (1949) The petrology of the evaporites of the Eskdale no. 2 boring, east Yorkshire —I. *Miner. Mag.* **28,** 621–675.

Stewart F. H. (1951a) The petrology of the evaporites of the Eskdale no. 2 boring, east Yorkshire—II. *Miner. Mag.* **29,** 445–475.

Stewart F. H. (1951b) The petrology of the evaporites of the Eskdale no. 2 boring, east Yorkshire—III. *Miner. Mag.* **29,** 557–572.

Sverdrup H. U., Johnson M. W. and Fleming R. H. (1942) *The Oceans.* Prentice-Hall, New York.

Thompson J. B., Jr. (1955) The thermodynamic basis for the mineral facies concept. *Amer. J. Sci.* **253,** 65–103.

Trask P. D. (Editor) (1955) Recent marine sediments. *S.E.P.M. Spec. Publ.* No. 4.

Van Tuyl F. M. (1914) The origin of dolomite. *Ann. Rep. Iowa Geol. Surv.* pp. 257–428.

Yanat'eva O. K. (1954) Solubility of dolomite in water in the presence of carbon dioxide. *Izv. Akad. Nauk SSSR, Otdel. Khim. Nauk* No. 6, 1119–1120 (English Translation ATS, RJ-310).

Yanat'eva O. K. and Danilova E. P. (1956) Application of the solubility diagram of the system $CaCO_3$-$MgCO_3$-H_2O to the characterization of some carbonate rocks. *Zh. prikl. Khim.* **29,** No. 8, 1152–1159 (English translation ATS, RJ-748).

Zeigler J. M., Athearn W. D. and Small H. (1957) Profiles across the Peru–Chile Trench. *Deep-sea Res.* **4,** 238–249.

Zen E. (1956) Correlation of chemical composition and physical properties of dolomite. *Amer. J. Sci.* **254,** 51–60.

Zen E. (1957) Partial molar volumes of some salts in aqueous solutions. *Geochim. et Cosmochim. Acta* **12,** 103-122.

Zen E. (1959) Clay mineral–carbonate relations in sedimentary rocks. *Amer. J. Sci.* **257,** 29–43.

Zen E. (1959) Mineralogy and petrography of marine bottom samples off the coast of Peru and Chile. *J. Sediment. Petrol.* In preparation.

Geochimica et Cosmochimica Acta, 1960, Vol. 18, pp. 72 to 80. Pergamon Press Ltd. Printed in Northern Ireland

Räumliche Verteilung der Edelgasisotope im Eisenmeteoriten Treysa

H. Fechtig,* W. Gentner* und G. Kistner†
Physikalisches Institut der Universität Freiburg i. Br.

(*Received* 3 *June* 1959)

Abstract—The rare gases He, Ne and Ar and their isotopic composition were investigated in the iron meteorite Treysa. The meteorite showed a He^4-content of $\sim 21 \times 10^{-6}$ cm³/g, an Ar^{36}-content of $\sim 15 \times 10^{-8}$ cm³/g and a Ne-content of $\sim 6 \times 10^{-8}$ cm³/g. In dependence of depth the isotopic ratio of Ar^{38}/Ar^{36} and He^4/He^3 varied about 20% in the investigated disk. This variation of the isotopic ratio may be qualitatively explained by the results of spallation investigations on copper with 0·34 and 2·2 GeV protons and on steel with 0·16, 0·43 and 3·0 GeV protons. Assuming the ratio of the average post-atmospheric radius to the average pre-atmospheric radius of Treysa is 0·44 and the spectrum of the cosmic radiation extends down to 500 MeV, we found by calculation that the variation of the Ar^{38}/Ar^{36}-ratio will be caused only by the primary component. The variation of the He^4/He^3-ratio is presumably a consequence of a secondary radiation. The amount of Ar^{38} found in the disk allowed us to calculate a radiation age of $\sim 10^9$ years.

Einleitung

Aus Untersuchungen der Höhenstrahlung mit photographischen Platten berechneten Bauer (1947, 1948) und Huntley (1948) die Menge des gebildeten Heliums als Reaktionsprodukt in Spallationprozessen. Sie stellen fest, dass eine vergleichbare Menge von Helium, wie sie in Meteoriten gefunden wird, durch Kernprozesse dieser Art erzeugt werden kann. Bauer (1947, 1948) konnte weiterhin voraussagen, dass in Meteoriten neben He^4 auch He^3 auftreten sollte. Ausserdem sollte entsprechend einer mittleren freien Weglänge der kosmischen Strahlung in Eisen eine Abnahme der Heliummenge mit zunehmender Tiefe zu finden sein. Neben den stabilen Kernen sollten nach Bauer auch radioaktive Isotope enstehen.

Diese Überlegungen konnten in den letzten Jahren von Paneth, Gentner, Fireman, Gerling, Reynolds u.a. durch umfangreiche Untersuchungen bestätigt werden. Paneth und Mitarbeiter zeigten durch massenspektrometrische Analyse, dass ein grosser Teil des Meteorheliums aus He^3 besteht. Die Mengenabnahme mit zunehmender Durchstrahlungstiefe konnte durch Chackett, Reasbeck und Wilson (1953) nachgewiesen werden. Schliesslich fanden Firemann und Schwarzer (1957) und Ehmann und Kohman (1958) die radioaktiven Isotope H^3 bzw. Co^{60}, Al^{26} und Be^{10}.

Darüber hinaus konnten Gentner und Zähringer (1955, 1957) das in Eisenmeteoriten gefundene Argon, Reasbeck und Mayne (1955) das gefundene Neon als Restkerne aus hochenergetischen Spallationprozessen deuten.

Beim Durchdringen von Materie erfährt das Energiespektrum der Höhenstrahlung eine Verschiebung, welche eine Änderung der Isotopenverhältnisse verursachen sollte. Dieser Effekt wurde von Chackett, Reasbeck und Wilson (1953) für das He^3/He^4- Verhältnis beim Meteoriten Carbo beobachtet. In der vorliegenden Arbeit wird über die Änderung der Isotopenverhältnisse Ar^{38}/Ar^{36} und He^4/He^3 berichtet, wie sie von uns beim Meteoriten Treysa gefunden wurde.

* Jetzt Max-Planck-Institut für Kernphysik Heidelberg.
† Jetzt Smithsonian Institution Cambridge Mass. U.S.A.

Der Meteorit Treysa

Der Meteorit fiel am 3 April 1916 mit den typischen Leucht- und Schallerscheinungen in der Nähe der hessischen Gemeinde Treysa (50°57′ nördl. Br. 9°10′ östl. L.). Durch die sorgfältige Auswertung von Augenzeugenberichten konnte Wegener (1917) die Bahnelemente, die Geschwindigkeit und den Hemmungspunkt berechnen, sodass der Meteorit 11 Monate später nicht weit von der berechneten Stelle aufgefunden werden konnte. Bei dem Meteoritenfall handelt es sich um einen einzigen kugelförmigen Eisenbrocken mit einem Gewicht von 63 kg und einem Durchmesser von 24 bis 36 cm. Der Meteorit zeigt beim Anätzen einer polierten, plangeschliffenen Fläche die Widmanstättenschen Figuren. Die gleichmässige Ausbildung der Oberfläche deutet darauf hin, dass der Meteorit bei seinem Flug durch die Atmosphäre rotiert hat. Eine Zuordnung zu einem der bekannten Meteorströme aufgrund der Bahnelemente ist nicht möglich. Für die vorliegenden Untersuchungen war es wichtig, den Abbrand des Meteoriten zu kennen, um die Absorptionsverluste der kosmischen Ultrastrahlung abzuschätzen.

Nach Wipple (1943) besteht zwischen der Anfangsmasse m_0 und der Anfangsgeschwindigkeit v_0 ausserhalb der Atmosphäre und der Endmasse m und Endgeschwindigkeit v des Meteoriten folgende Beziehung:

$$m = m_0 \exp\left[\frac{\lambda}{4\gamma\zeta}(v^2 - {v_0}^2)\right]$$

Hierin ist $\gamma = 0{,}5$ eine Konstante, die den Wirkungsgrad der Impulsübertragung und $\lambda = 0{,}015$ eine Konstante, die den Wirkungsgrad der Energieübertragung beschreibt; $\zeta = 1{,}2 \times 10^{10}$ erg/g ist die Schmelzwärme des Eisens, da bei Eisenmeteoriten der Massenverlust durch Wegblasen einer geschmolzenen Flüssigkeitsschicht vor sich geht (Thomas und Wipple, 1951). Die Endgeschwindigkeit von *ca.* 1 km/sec kann vernachlässigt werden. Nach obiger Formel ergibt sich mit der von Wegener (1917) bestimmten Geschwindigkeit $v_0 = 20$ km/sec ein Massenverhältnis $m/m_0 = \frac{1}{12}$ und entsprechend ein Radienverhältnis $r/r_0 = 0{,}44$. Allerdings ist die Bestimmung der Geschwindigkeit v_0 nach Wegener ungenau, sodass diese einen Fehler von $\pm 36\%$ besitzt und damit das Radienverhältnis zwischen 0,22 und 0,71 liegen kann. Mit diesem Verhältnis lässt sich aus dem Gewicht des Meteoriten ein ursprünglicher Durchmesser von 54 cm und ein ursprüngliches Gewicht von *ca.* 600 kg berechnen.

Zur Durchführung der Messungen stand eine Platte (siehe Abb. 2) mit einem mittleren Durchmesser von *ca.* 18 cm zur Verfügung, die im extraterrestrischen Meteoriten *ca.* 8 cm vom vermutlichen Mittelpunkt entfernt gelegen war. Diese Platte wurde zuerst in 8, dann zur genaueren Lokalisierung einer Mittelzone in 12 Felder eingeteilt. Von jedem Feld wurde 10 g Material abgenommen und auf die Isotopenzusammensetzung der Edelgase untersucht.

Aufschluss- und Messmethode

Die früher beschriebene Hochvakuum–Glasapparatur (Gentner und Zähringer, 1955, 1957) wurde weiter verbessert. Die anfangs verwendeten Fetthähne und -schliffe, die während längerer Zeit mit dem Gasen in Berührung standen, wurden durch Quecksilbersperren und Araldittkittungen ersetzt.

Durch induktives Erhitzen im Vakuum mittels eines 12 kW-HF-Senders wird die Meteoritenprobe zum Schmelzen gebracht. Als Ofen dient ein Graphittiegel, der zusammen mit der Induktionsspule in einem Hartglaskolben (10 l) untergebracht ist. Die in Al- Folie eingepackte Probe hängt zunächst an einem Al- Band über dem Tiegel, der *ca.* 6 Stunden bei maximaler Leistungsabgabe des Senders ausgeheizt wird. Schliesslich wird das Band induktiv durchgeschmolzen und die Probe fällt in den Tiegel, wo sie nach 5 bis 10 Minuten vollständig schmilzt. Es erwies sich als notwendig, die Probe noch 2 Stunden flüssig zu halten, um sie vollständig zu entgasen. Die austretenden Gase werden fortlaufend in den Reinigungsteil der Apparatur gepumpt. Mittels eines geheizten Palladiumröhrchens können Wasserstoff und Tritium abgetrennt werden, wodurch gleichzeitig eine wirksame Reinigung der Gase erfolgt. Ferner ist eine Tantallampe zur Krackung der Kohlenwasserstoffe vorgesehen. Zur Reinigung dienen Ca- und Cu-CuO-Öfen, welche die unedlen Gase chemisch abbinden. Aus dem restlichen Edelgasgemisch wird das Argon durch Adsorption an Aktivkohle bei der Temperatur der flüssigen Luft abgetrennt. Das He-Ne-Gemisch kann jetzt einer Fraktionierungskolonne nach Glückauf (1945) zugeführt und nach seinen Bestandteilen getrennt werden.

In einem Massenspektrometer (Smits und Zähringer, 1955) wurden die Mengen und die Isotopenzusammensetzung der einzelnen Gase gemessen. Das Mengen und Isotopenzusammensetzung der einzelnen Gase gemessen. Das Massenspektrometer ist ein einfach-fokussierendes Niersches 60°-Spektrometer mit Doppelauffänger und Elektronenstossionenquelle. Ein Zweikanal-Schwingkondensatorverstärker und ein Doppelschreiber erlaubten, zwei Linien gleichzeitig zu schreiben. Die Ionenquelle war besonders zur Messung kleiner Gasmengen konstruiert. Ein Strömungskanal zwischen Ionenquelle und Ionenrohr bewirkte einen exponentiellen Abfall des Ionenstromes. Es wurde auf den Zeitpunkt des Gaseinlasses extrapoliert, der durch einen elektrischen Impuls auf dem Schreiberdiagramm markiert war. Die Messung der Gasmengen erfolgte mit einer vergleichbaren Eichmenge, für die Volumen und Druck bekannt war, und welche unter denselben Bedingungen wie die Probe in die Ionenquelle eingelassen wurde. Vor und nach jeder Messung wurde eine Eichmessung durchgeführt. Die Isotopenverhältnisse wurden mit einem Standardgemisch verglichen. Als Mass für die unvermeidliche Beimischung von Luft konnte die Linienhöhe von Ar^{40} angesehen und infolge des hohen Ar^{40}/Ar^{36}- Verhältnisses zur Korrektur von Ar^{36} und Ar^{38} verwendet werden. Eine ähnliche Korrektur war bei Helium nicht notwendig.

Messergebnisse

In Abb. 2 sind die Mengen und Isotopenverhältnisse von Argon und Helium in die Feldeinteilungen eingetragen. Für die Isotopenverhältnisse von Ar^{38}/Ar^{36} ist eine deutliche Zunahme in den rechten inneren Feldern gegenüber den äusseren Feldern zu erkennen. Ebenso sieht man eine Abnahme der Gasmengen von aussen nach innen. Der messtechnische Fehler betrug für die Isotopenverhältnisse von Argon und Helium 2%, für die Mengen 10%. Die manchmal beobachteten grösseren Abweichungen sind auf die groben Späne zurückzuführen, die keine homogene Mischung der Felder garantieren.

Das gemessene Ar^{36}/Ar^{40}-Verhältnis betrug im Mittel 1 : 60. Da durch die Höhenstrahlung ungefähr ebensoviel Ar^{40} wie Ar^{36} gebildet wird, kann angenommen werden, dass praktisch die gesamte gemessene Ar^{40}-Menge aus Luft stammt. Diese Ar^{40}- Menge wurde zur Korrektur von Ar^{36} und Ar^{38} verwendet mit einem Isotopenverhältnis in Luft von $Ar^{36} : Ar^{38} : Ar^{40} = 1 : 0{,}187 : 296$. Nach Abschätzungen von Gentner und Zähringer (1955, 1957) kann die durch K^{40}- Zerfall gebildete Ar^{40}-Menge vernachlässigt werden.

Die korrigierten Mengen und Isotopenverhältnisse sind in Abb. 2 eingetragen. Die Mengen nehmen von den äusseren zu den innern Feldern ab. Die Isotopenverhältnisse Ar^{38}/Ar^{36} und He^4/He^3 zeigen für die Innenfelder höhere Werte als für die Randfelder. Bei eingehender Betrachtung aller Messwerte kann ein "Bestrahlungsmittelpunkt" abgelesen werden. Die Änderung der Isotopenverhältnisse Ar^{38}/Ar^{36} und He^4/He^3 von diesem Bestrahlungsmittelpunkt zum Rande beträgt *ca.* 20%.

Bei den Neonmessungen konnte kein Tiefeneffekt nachgewiesen werden. Für die Auffindung eines solchen Effektes war die Apparatur mit einem Messfehler von 5% für das Neonverhältnis zu ungenau. Die Neonmenge betrug im Mittel $6{,}1 \times 10^{-8}$ cm³/g. Das korrigierte Verhältnis Ne^{22}/Ne^{21} zeigte statistische Streuungen um den Mittelwert 1,08. Bemerkenswert ist hierbei, dass unter den Neonisotopen das Ne^{21}-Isotop stets mit der kleinsten Linienhöhe auftrat. Dies ist in Übereinstimmung mit Ergebnissen von Schaeffer und Zähringer (1958). Dagegen messen Reasbeck und Mayne (1955) am Meteoriten Thunda ein Neonverhältnis $Ne^{20} : Ne^{21} : Ne^{22} = 43 : 36 : 21$, doch steht dieses Ergebnis ebenfalls in Widerspruch zu neueren Messungen von Wänke und Hintenberger (1958).

Nach den vorliegenden Messungen (z.B. linkes unteres Feld) entspricht einer Ar^{36}-Menge von $15{,}39 \times 10^{-8}$ cm³/g eine He^4-Menge von $21{,}05 \times 10^{-6}$ cm³/g und eine Ne^{21}-Menge von $6{,}1 \times 10^{-6}$ cm³/g. Dies ist in guter Übereinstimmung mit neueren Messungen von Schaeffer und Zähringer (1958), nach welchen zu einer Ar^{36}-Menge von 15×10^{-8} cm³/g eine He^4-Menge von 20×10^{-6} cm³/g und eine Ne^{21}-Menge von 6×10^{-8} cm³/g gehört.

In das Ar^{36}-He^3-Diagramm (siehe Gentner und Zähringer, 1955, 1957) fügt sich der Messpunkt Treysa mit den Koordinaten 45×10^{-7} cm³/g He^3 und 15×10^{-8} cm³/g Ar^{36} sehr gut ein.

Chackett, Reasbeck und Wilson (1953) messen am Meteoriten Treysa einen mittleren Heliumgehalt von $26{,}2 \times 10^{-6}$ cm³/g. Dieser Wert wird bei der vorliegenden Arbeit nur an den Randpunkten erreicht. Bei den vorliegenden Untersuchungen ändert sich das He^3/He^4-Verhältnis von 0,29 (aussen) bis 0,23 (innen). Dies verträgt sich gut mit Messungen von Paneth und Mitarbeiter (1953), die für das He^3/He^4-Verhältnis an verschiedenen Meteoriten Werte zwischen 0,17 und 0,315 gemessen haben.

Für den Meteoriten Treysa ergeben sich (z.B. für das linke untere Feld) die Isotopenverhältnisse: $Ar^{38}/Ne^{21} = 3{,}8$; $He^3/Ne^{21} = 95$; $He^3/Ar^{38} = 25$ und $He^3/He^4 = 0{,}27$. Bieri (1958) beobachtet für Carbo die entsprechenden Verhältnisse 5,1; 98; 19 und 0,24, also durchaus vergleichbare Werte. Ferner erhält man für Treysa ein He^3/Ne-Verhältnis von 31,5. Messungen von Ebert und Wänke

(1957) ergeben für eine Reihe von Meteoriten He^3/Ne-Verhältnisse zwischen 32,5 und 38,5. Eine genaue Übereinstimmung ist wegen der unterschiedlichen Tiefenlage der Proben und der dadurch bedingten Isotopenverschiebung auch nicht zu erwarten.

Diskussion

Die in den Meteoriten gefundenen Edelgase sind die Reaktionsprodukte der hochenergetischen Spallationprozesse, die die Höhenstrahlung in den Eisenkernen auslöst. Die Änderung der Isotopenverhältnisse mit der Tiefe wird offenbar durch die Energieverschiebung des Spektrums verursacht. Infolge der Ionisationsverluste im abgebrannten Teil des Meteoriten und infolge des starken Abfalls des Spektrums der Höhenstrahlung bei hohen Energien handelt es sich wohl hauptsächlich um Reaktionen im Energiebereich von 0,5 bis 10 GeV. In diesem Energiebereich liegen mit Protonen aus Beschleunigern nur für zwei Energien Messungen vor, die zum Vergleich herangezogen werden können.

Batzel, Miller *et al.* (1951) bestrahlten Kupfer mit 0,34 GeV Protonen und bestimmten die Ausbeuten einer grossen Anzahl von Restkernen mit Hilfe radioaktiver Methoden. Nach Berücksichtigung des $\beta^{\pm}$-Zerfalls auf den Isobaren ergibt sich für 0,34 GeV ein Ar^{38}/Ar^{36}-Verhältnis von 1,8. Gemessen wurde ein Ar^{38}/Ar^{36}-Verhältnis von 1,75 an einem inneren Punkt des Meteoriten, der noch am ehesten dieser niederen Energie entspricht.

Friedländer *et al.* (1954) untersuchten die Restkernverteilung in Kupfer, die bei Beschuss mit 2,2 GeV Protonen entsteht. Für diese Energie lässt sich mit den Ergebnissen von Friedländer *et al.* (1954) ein Ar^{38}/Ar^{36}-Verhältnis von 1,35 ausrechnen. Dieser Wert würde bei dem Meteoriten dem Ar^{38}/Ar^{36}-Verhältnis 1,52 entsprechen, der an einem äusserem Punkt gemessen wurde. Die Spallationuntersuchungen liefern also eine Änderung des Ar^{38}/Ar^{36}-Verhältnisses im gleichen Sinne, wie sie am Meteoriten gemessen wurde.

Einen ähnlichen Vergleich für die He^4/He^3-Verhältnisse gibt eine Untersuchung von Schaeffer und Zähringer (1958; 1959). Es wurden Eisentargets mit 0,16; 0,43 und 3,0 GeV bestrahlt und die Ausbeuten von He^4, He^3 und Tritium bestimmt. Die Ergebnisse sind in Tabelle 1 zusammengefasst.

Tabelle 1. Wirkungsquerschnitte und Isotopenverhältnisse von Helium an Eisentargets bei 0,16, 0,43 und 3,0 GeV

E (GeV)	σ He^4 (mb)	σ He^3 (mb)	He^3/He^4	$He^4/He^3 + H^3$
0,16	120	11	0,09	8
0,43	450	45	0,10	5,85
3,0	1300	240	0,18	3,8

Die Werte in der letzten Spalte entsprechen den in Meteoriten gefundenen He^4/He^3-Verhältnissen. Es zeigt sich, dass das He^4/He^3-Verhältnis mit abnehmender Energie deutlich zunimmt. Dieses würde bei einem Meteoriten dem Übergang von einem äusseren Punkt zu einem inneren entsprechen.

Aus den oben erwähnten Messungen mit Protonen aus Beschleunigern kann eine Abschätzung der Isotopenverhältnisse in verschiedenen Tiefen gemacht werden. Im folgenden wird eine Berechnung der Isotopenverhältnisse für Protonen aus der Höhenstrahlung durchgeführt. Hierzu werden die Wirkungsquerschnitte aus Spallationuntersuchungen und das Spektrum der Höhenstrahlung verwendet. Weiterhin wird angenommen, dass die Höhenstrahlung eine isotrope Raumverteilung besitzt, nur aus Protonen besteht und ein differentielles Energiespektrum hat von der Form:

$$N(E)\,dE = 0{,}3\,.\,E^{-2{,}16}\ \text{Teilchen/cm}^2\text{-sec-sterad}$$

Hinsichtlich des Meteoriten wird angenommen, dass er aus reinem Eisen besteht, die Protonen geradlinige Bahnen durchlaufen und der extraterrestrische Meteorit eine kugelförmige Gestalt hatte. Beim Durchdringen der Eisenmaterie verlieren die Protonen der Höhenstrahlung durch Ionisation einen Teil ihrer kinetischen Energie. Die Zahl der Protonen nimmt entsprechend dem effektiven Wirkungsquerschnitt des Eisens ab. An einer bestimmten Stelle des Meteoriten erzeugen die primären Protonen Restkerne, deren Ausbeute durch den Wirkungsquerschnitt und durch das Energiespektrum gegeben wird. Es folgt somit:

$$S(A) = \frac{K \int_0^{4\pi} \int_{E_c - E_c(d)}^{\infty} e^{-\mu d(\vartheta)} \cdot \sigma(A, E) \cdot f(E, \vartheta)\,dE\,dO}{\int_0^{4\pi} \int_{E_c - E_c(d)}^{\infty} f(E, \vartheta)\,dE\,dO}$$

Hierbei bedeuten

$S(A)$: Anzahl der durch Spallation gebildeten Restkerne der Masse A pro g Fe;

$K = L \times I \times t \times f/A$; $L = 6{,}02 \times 10^{23}$, $A = 56$, $I = 0{,}3\ T/\text{cm}^2\text{-sec-sterad}$. t = Bestrahlungsdauer, f = Abschirmung auf der Isobaren. Da im folgenden nur Verhältnisse betrachtet werden, geht diese Konstante nicht weiter in die Rechnung ein.

μ : linearer Absorptionskoeffizient: 0,074 cm^{-1};

$d(\vartheta)$: Abstand eines Punktes der Oberfläche des Meteoriten von dem betreffenden Punkt bei dem Winkel ϑ;

$\sigma(A, E)$: Wirkungsquerschnitt für die Restkerne in Abhängigkeit von der Massenzahl und der Energie. Es wurde der Ausdruck von Rudstam (1956) benutzt: $\sigma(A, E) = \exp\,[P(E) \cdot A - Q]$;

$f(E, \vartheta) = dE/[E + \varepsilon(d)]^2$ das differentielle Spektrum der Höhenstrahlung. $\varepsilon(d)$ ist die Energieverschiebung, die ein Proton beim Durchlaufen der Strecke d infolge Ionisationsverluste erleidet.

E_C = "cut-off" Energie der Primärstrahlung.

Der Integralausdruck kann nicht geschlossen integriert werden. Es wurde eine numerische Integration durchgeführt. Die Werte von $P(E)$ wurden bei Rudstam (1956) entnommen. Die Energieverschiebung konnte auf graphischem Wege mittels der Energie-Reichweitebeziehung für Kupfer (Rich und Madey, 1954) ermittelt werden.

Nach Einführung von Schwellenenergien für die einzelnen Isotope und der Annahme, dass sich das Spektrum der Höhenstrahlung bis herunter zu 500 MeV

erstreckt, ergibt sich für das Ar^{38}/Ar^{36}-Verhältnis eine Aufspaltung von 2,9 aussen auf 3,6 innen, die in der Grössenordnung der gemessenen Werte liegt. Das Ne^{22}/Ne^{21}-Verhältnis zeigt eine Aufspaltung, die kleiner ist als der Messfehler, sodass es verständlich erscheint, warum bei Neon kein Tiefeneffekt gefunden wurde. Die Rechenergebnisse zeigen, dass die Änderung der Isotopenverhältnisse mit der Verschiebung des Energiespektrums und den verschiedenen Einsatzenergien der einzelnen Isotope verknüpft ist. Neben der Primärstrahlung, die diesen Effekt schon hervorruft, können auch Sekundärprozesse, die durch die schnellen Kaskadenteilchen und Mesonen der primären Spallationprozesse ausgelöst werden, zur Bildung von Argon und besonders von Helium beitragen. Für Neon sind die Wirkungsquerschnitte im Energiebereich der Sekundärteilchen klein, sodass die Sekundären bei Neon keinen Betrag liefern. Jedoch reichen bei Argon die Einsatzenergien für Ar^{38} und Ar^{36} noch in das Spektrum der Sekundärteilchen hinein, sodass die Sekundärteilchen einen Beitrag liefern können. Obwohl das Energiespektrum der Sekundärteilchen nach Metropolis u.a. (1958) unempfindlich ist gegenüber der Beschussenergie, ist der Anteil dieser Sekundärteilchen schwer abzuschätzen, da bei einer Berechnung nicht nur die Energiespektren der Sekundärgenerationen, sondern auch bei geladenen Teilchen die Energieverschiebung durch Ionisation und schliesslich auch eine Richtungsabhängigkeit berücksichtigt werden muss. Dennoch ist einzusehen, dass die Sekundärteilchen ebenfalls einen Anstieg des Ar^{38}/Ar^{36}-Verhältnisses mit zunehmender Durchstrahlungstiefe bewirken.

Eine Berechnung des He^4/He^3-Verhältnisses ist schwieriger, da hierzu das Energiespektrum, die Anzahl und Art der Sekundärteilchen bekannt sein muss. Die Änderung des He^4/He^3-Verhältnisses wird wohl durch die Entstehung des niederenergetischen Sekundärflusses hervorgerufen. Bei den hohen Energien der Primärteilchen machen sich die verschiedenen Einsatzenergien für He^4 und He^3 nicht mehr bemerkbar und das He^4/He^3-Verhältnis bleibt konstant; bei den niederen Energien der Sekundärteilchen überwiegt He^4 infolge der tieferen Einsatzenergie. Das He^4/He^3-Verhältnis steigt demnach in gleichem Masse wie der sekundäre Teilchenfluss zunimmt.

Die in Abb 2 eingetragenen Mengen der Edelgasisotope nehmen von den äusseren zu den inneren Feldern ab. Diese Abnahme der Gasmengen wird hervorgerufen durch die Abnahme des Primär- und Sekundärflusses infolge des effektiven Wirkungsquerschnittes und durch die Änderung der Spallation-Wirkungsquerschnitte infolge der Verschiebung des Energiespektrums mit zunehmender Durchstrahlungstiefe.

Mit Hilfe der gebildeten Edelgasmengen, der Wirkungsquerschnitte und dem Teilchenfluss der Höhenstrahlung kann auch ein "Bestrahlungsalter" des Meteoriten berechnet werden. Hierbei wird angenommen, dass der Teilchenfluss im Raum- und Zeitmittel konstant ist. Zur Berechnung wurde ein Gesamtfluss von 0,27 Teilchen/sec sterad und die Energieverteilung der Höhenstrahlung aus einer Zusammenstellung von Neher (1958) verwendet. Die Wirkungsquerschnitte von Ar^{38} wurden aus Arbeiten von Schaeffer und Zähringer (1958, 1959) bzw. Fireman und Zähringer (1957) entnommen. Es ergab sich bei einem Radienverhältnis von $r/r_0 = 0{,}44$ und einer mittleren Tiefe von 15 cm ohne "cut-off" ein

Bestrahlungsalter von $1{,}2 \times 10^9$ a, mit einem cut-off bei 1 GeV ein solches von $1{,}7 \times 10^9$ a.

Infolge des Fehlers in der Fallgeschwindigkeit des Meteoriten kann das Radienverhältnis zwischen 0,71 und 0,22 liegen. Bei einem Radienverhältnis von 0,71 und einer mittleren Tiefe von 5 cm ergibt sich ohne cut-off ein Bestrahlungsalter von $0{,}6 \times 10^9$ a mit einem cut-off bei 1 GeV ein solches von $1{,}1 \times 10^9$ a. Bei einem Radienverhältnis von 0,22 ist ein Alter $> 1{,}7 \times 10^9$ a zu erwarten.

Diese Überlegungen zeigen, dass der Meteorit Treysa ein Bestrahlungsalter zwischen 0,5 und 2×10^9 Jahren hat. Der Fehler wird verursacht durch die Unsicherheit im Radienverhältnis und durch die Schwankungen in der Teilchenzahl der Höhenstrahlung, vorausgesetzt, dass sich diese Schwankungen auch auf den Meteoriten längs seiner Bahn, ausgewirkt haben. Die Schwankungen sind nämlich eine Folge der Sonnenaktivität, die während einer aktiven Periode im Spektrum der Höhenstrahlung einen cut-off bei 1 GeV bewirkt. Auch dann, wenn die Wirkungsquerschnitte genauer bekannt sein werden, kann das Bestrahlungsalter von Treysa wegen der Unsicherheit im Abbrand kaum genauer angegeben werden.

Literatur

Batzel R. E. und Miller J. M. *et al.* (1951) The high energy spallation products of copper. *Phys. Rev.* **84,** 671.

Bauer C. A. (1947) Production of helium in meteorites by cosmic radiation. *Phys. Rev.* **72,** 354.

Bauer C. A. (1948) The absorption of cosmic radiation in meteorites. *Phys. Rev.* **74,** 225.

Bauer C. A. (1948) Rate of production of helium in meteorites by cosmic radiation. *Phys. Rev.* **74,** 501.

Bieri H. R. (1958) Rare gases in meteorite CARBO and a Cu-target exposed to 6,2 BeV protons. *Bull. Amer. Phys. Soc.* **3,** 221.

Chackett K. F., Reasbeck P. und Wilson E. A. (1953) Recent studies on iron meteorites—II. Determination of the helium content. *Geochim. et Cosmochim. Acta* **3,** 261.

Ebert G. R. und Wänke H. (1957) Uber die Einwirkung der Höhenstrahlung auf Eisenmeteoriten. *Z. Naturf.* **12,** 766.

Ehman W. D. und Kohman T. P. (1958) Cosmic-ray-induced radioactivities in meteorites. *Geochim. et Cosmochim. Acta* **14,** 340.

Fireman E. L. und Schwarzer D. (1957) Measurements of Li^6, He^3 and H^3 in meteorites and its relation to cosmic radiation. *Geochim. et Cosmochim. Acta* **11,** 252.

Fireman E. L. und Zähringer J. (1957) Depth variation of tritium and A^{37} produced by high energy protons in iron. *Phys. Rev.* **107,** 1695.

Friedländer G. *et al.* (1954) Nuclear reactions of copper with 2,2 BeV protons. *Phys. Rev.* **94,** 727.

Gentner W. und Zähringer J. (1957) Argon und Helium als Kernreaktionsprodukte in Meteoriten. *Geochim. et Cosmochim. Acta* **11,** 60.

Gentner W. und Zähringer J. (1955) Argon- und Heliumbestimmungen in Eisenmeteoriten. *Z. Naturf.* **10a,** 498.

Gerling E. K. (1956) On the origin of inert gases in stony meteorites. *Dokl. Akad. Nauk USSR* **110,** 5, 750.

Glückauf E. (1945) A micro-analysis of the helium and neon contents of air. *Proc. Roy. Soc.* A **185,** 98.

Huntley H. E. (1948) Production of helium by cosmic rays. *Nature, Lond.* **161,** 356.

Martin G. R. (1953) Recent studies on iron meteorites—IV. The origin of meteoric helium and the age of meteorites. *Geochim. et Cosmochim. Acta* **3,** 288.

Martin G. R. *et al.* (1954) Isolation and measurement of the He^4, He^3 and tritium produced in steel by 340 MeV proton bombardment. *Phil. Mag.* **45,** 410.

Metropolis N., *et al.*, Turkevich A. *et al.* und Friedländer G. (1958) Monte Carlo calculations on intranuclear cascades—I and II. *Phys. Rev.* **110,** 185.

Neher H. V. (1958) The primary cosmic radiation. *Ann. Rev. Nuclear. Sci.* **8.**

Paneth F. A. (1953) Mikroanalyse der Edelgase. *Endeavour* **12,** 5.

Paneth F. A. (1953) Recent studies on iron meteorites—I. *Geochim. et Cosmochim. Acta* **3,** 257.

Reasbeck P. und Mayne K. J. (1955) Cosmic radiation effects in meteorites. *Nature, Lond.* **176,** 733.

Reynolds J. H. und Lipson J. I. (1957) Rare gases from the Nuevo Laredo Stone meteorite. *Geochim. et Cosmochim. Acta* **12,** 330.

Richarz F. (1918) Auffindung, Beschreibung und vorläufige Untersuchung des Meteoriten von Treysa. *Ges. z. Bef. d. gesamt. Naturw. Marburg* **14,** 91.

Rich M. and Madey R. (1954) *Range-Energy Tables.* U.S. Atomic Energy Commission, Rad. Lab., University of California.

Rudstam G. (1956) *Spallation of Medium Weight Elements.* Appelbergs Boktryckeri, Uppsala.

Schaeffer O. A. und Zähringer J. (1958) Private Mitteilung. Im Druck bei *Geochim et Cosmochim. Acta.*

Schaeffer O. A. und Zähringer J. (1958) Helium- und Argon-Erzengung in Eisentargets durch energiereiche Protonen. *Z. Naturf.* **13**a, 346.

Schaeffer O. A. und Zähringer J. (1959) High-sensitivity mass spectrometric measurement of stable helium and argon isotopes produced by high-energy protons in iron. *Phys. Rev.* **113,** 674.

Smits F. und Zähringer J. (1955) Ein Massenspektrometer für kleinste Gasmengen. *Z. angew. Phys.* **7,** 313.

Thomas R. N. und Whipple F. L. (1951) The physical theory of meteors—II. Astroballistic heat transfer. *Astrophys. T.* **114,** 448.

Wänke H. und Hintenberger H. (1958) Helium und Neon als Reaktionsprodukte der Höhenstrahlung in Eisenmeteoriten. *Z. Naturf.* **13**a, 895.

Wegener A. (1917) Das Detonierende Meteor. *Ges. z. Bef. d. ges. Naturw. Marburg* **14,** 1.

Whipple F. L. (1943) Meteors and the earth's upper atmosphere. *Rev. Mod. Phys.* **15,** 246.

Geochimica et Cosmochimica Acta, 1960, Vol. 18, pp. 81 to 93. Pergamon Press Ltd. Printed in Northern Ireland

A method of analysis of oxygen isotopes in orthophosphate—its use in the measurement of paleotemperatures

A. P. Tudge*
Jones Laboratory, Department of Chemistry, University of Chicago, Chicago 37, Illinois, U.S.A.

Abstract—An analytical procedure is presented for the determination of the O^{18}/O^{16} ratio in orthophosphate and condensed phosphate. In the described procedure the phosphate is first purified, and then finally precipitated as $BiPO_4$. The phosphate oxygen is released by the following reaction; then it is purified, and analysed mass spectrometrically:

$$BiPO_{4(s)} + 8/3\ BrF_{3(l)} \rightarrow BiF_{3(s)} + PF_{5(g)} + 4/3\ Br_{2(g)} + 2\ O_{2(g)}$$

The method is quantitative, free from isotopic fractionation and exchange, and precise to $\pm 0{\cdot}15‰$. A correction can be made for the contaminating effect of water oxygen introduced during the hydrolysis of the condensed phosphates.

The possibilities are given for the use of this procedure in the measurement of paleotemperatures.

Introduction

In 1947 H. C. Urey published calculated equilibrium constants for many isotopic exchange reactions of the light elements. Several of these reactions dealt with the isotopic exchange of oxygen between water and various oxyanions such as CO_3^{2-} and SO_4^{2-}. Because these equilibrium constants varied slightly with temperature, it was decided to establish a paleotemperature scale from a knowledge of the difference in the isotopic composition of oxygen between the carbonate shells and the environmental waters of marine animals (Urey, 1948). Remarkable results have been accomplished in the $CaCO_3$–CO_2–H_2O oxygen exchange system since 1947. In order to be able to measure paleotemperatures to $\pm 1°C$, a mass spectrometer was developed which had ten times the precision of other contemporary models (McKinney *et al.*, 1950). The temperature variation in the exchange reaction between calcite and water was checked experimentally for the slow inorganic precipitation of $CaCO_3$ from solution (McCrea, 1950). Then a method was carefully developed for the reproducible analysis of oxygen isotopes in "organically" precipitated carbonates, and a relative temperature scale was prepared from data on shells deposited by marine organisms living in controlled conditions (Urey *et al.*, 1951; Epstein *et al.*, 1951 and 1953).

In order to determine the growth temperature of a shell by the Epstein *et al.* (1953) method, it is necessary to obtain oxygen isotope data *both* on the carbonate of the shell and on the water in which the calcareous animal grew. However, a sample of the water is often unobtainable even for modern shells; in the case of fossil shells it is obvious that no sample of environmental water can be obtained. Several workers have made estimates of the O^{18}/O^{16} ratio in past environmental waters, but they have been forced to restrict their paleotemperature investigations to those ocean regions where isotopic deviations were both small and slow. Absolute paleotemperature errors will result when the assumed O^{18}/O^{16} ratio of the water

* Present address: California Research Corporation, La Habra, California.

does not coincide with the true (unknown) ratio. Epstein *et al.* (1951) and Epstein and Mayeda (1953) investigated the variation in the O^{18} content of present-day marine waters. These variations were found to be large enough to cause paleotemperature errors of $\pm 5°C$ in truly marine regions, and much greater errors in marginal environments where melt water flowed or where excessive evaporation took place. In addition to these variations around the average O^{18}/O^{16} ratio of ocean water, this average itself may have changed slowly in the past geologic age due to the changes in the area of the ice caps, the formation of sedimentary rocks, and the addition of juvenile water.

This uncertainty in paleotemperatures can be removed by establishing a temperature scale based upon the temperature-dependent equilibrium constant for some isotopic exchange reaction which does not involve water. A convenient example is the hypothetical exchange of O^{18} and O^{16} atoms between solid carbonate and solid phosphate, both of which occur in shell material. Of course isotope exchange cannot occur directly between these two solids, but equilibrium could be established by many intermediate steps, almost all of which would involve water. However, the final isotopic exchange between these two solid oxides is independent of the intermediate steps if isotopic equilibrium is established in each of these steps. Once a relationship is established between growth temperature and isotopic abundance of oxygen in the carbonates and phosphates of modern shells, then by an analysis of fossil shells it would be possible to obtain accurate values of temperature in former geological time. Then by inserting this value of temperature (together with the shell carbonate O^{18} abundance) into the Epstein *et al.* (1953) equations, the O^{18} content of the ancient environmental water can be obtained.

Based upon this reasoning, a new paleotemperature project was started in order to derive a temperature scale based upon the O^{18} content of carbonate and phosphate in shells. The precise measurement of the O^{18}/O^{16} ratio of phosphate oxygen proved to be no easy task. Several methods were studied extensively by Craig and Steinberg at this laboratory; these methods included (a) the direct fluorination of $Ca_3(PO_4)_2$ to yield O_2, and (b) the high temperature reduction of $BiPO_4$ by graphite to yield CO_2 and CO. However, both these methods were eventually abandoned because of low yields and poor precision. Based upon the success of Emeléus and Woolf (1950), and of Hoekstra and Katz (1953) in using BrF_3 to liberate O_2 quantitatively from $BiPO_4$, it was decided to try to perfect this method in an attempt to obtain phosphate oxygen for mass spectrometric analysis.

A Phosphate–Carbonate Paleotemperature Scale

The variation with temperature of the equilibrium enrichment of O^{18} in carbonate and phosphate with reference to liquid water has been calculated by Urey *et al.* (1951). This variation is shown graphically in Fig. 1. The calculations were based on a free rotational model for the carbonate ion and the phosphate ion. Hence, the calculations will be only approximations to the situation with solid carbonates and phosphates which we must consider. However, there are reasons to believe that the temperature *coefficients* are close to the predicted values (McCrea, 1950). From Fig. 1 it can be seen that in order to determine paleotemperatures

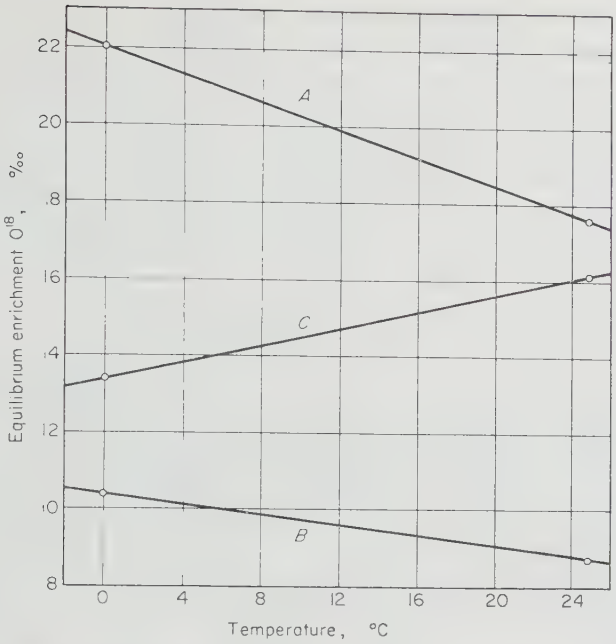

Fig. 1. Calculated relation between O^{18} equilibrium enrichment and temperature for the isotopic exchanges:
$A, CO_3^{2-}{}_{(g)}$—$H_2O_{(l)}$; $B, PO_4^{3-}{}_{(g)}$—$H_2O_{(l)}$; $C, PO_4^{3-}{}_{(g)}$—$CO_3^{2-}{}_{(g)}$ + 25‰. O^{18} concentrates in the first member of exchange pair. Slopes of lines A, B, C are −0·176, −0·068, and +0·108‰ per °C, respectively. Inverse slopes are −5·7, −14·7 and +9·3°C‰, respectively.

to ±1°C, one must determine the isotopic abundance of oxygen in both the carbonate and phosphate to ±0·07‰.

In order to attain such fine precision in isotopic work, it is necessary to devise experimental procedures so that laboratory fractionation, exchange and contamination of oxygen are eliminated.

The choice of shell material is important because most marine animals deposit very little phosphate in their skeleton. This will limit the applicability of a CO_3^{2-}–PO_4^{3-} paleotemperature scale since the ideal situation would be to analyse a shell containing moderate amounts of both carbonate and phosphate. However, it would be permissible to use two different shells, one of high carbonate content and the other of high phosphate content, if it could be established that the marine organisms producing them were completely cohabitant; and, hence, that the shells were deposited in an environment having identical thermal and isotopic conditions. This might be extremely hard to prove. In either case, an essential requirement is that both the carbonate and the phosphate are deposited in isotopic equilibrium with the surrounding water. The question of the isotopic equilibrium in the $CaCO_3$–H_2O case has been discussed before (Urey *et al.*, 1951; Epstein *et al.*, 1951), and it is thought to occur readily since the freshly deposited film of $CaCO_3$ is constantly bathed by environmental water. The phosphate case is different in that, unlike the carbonate, there is no oxygen exchange with water under purely

inorganic conditions (Winter *et al.*, 1940). However, in the complex reactions involved in phosphate metabolism, where P—O bonds are constantly being formed and broken, it is believed that mechanisms exist whereby oxygen equilibrium between H_2O and PO_4^{3-} can occur. Using water enriched in O^{18}, Koshland and Clark (1953) have demonstrated that oxygen exchange occurs between H_2O and the PO_4^{3-} produced in the hydrolysis of adenosinetriphosphate when catalysed by lobster muscle enzymes. Oxygen exchanges in the PO_4^{3-}–H_2O system have been observed by Cohn (1953) in mitochondrial preparations, and by Stein and Koshland (1952) using alkaline phosphatase as catalyst.

General Aspects of the Analytical Method

The phosphate of shells is contaminated mainly by such oxygen-containing compounds as H_2O, CO_3^{2-}, SO_4^{3-} and SiO_4^{4-}; and by the cations Ca^{2+}, Mg^{2+}, Al^{3+} and Fe^{3+}. The phosphate must be purified of these contaminants and put in a form of definite composition that contains no non-phosphate oxygen. It was decided to precipitate the phosphate first as $(NH_4)_3PO_4{\cdot}12MoO_3{\cdot}2HNO_3{\cdot}H_2O$, then as $MgNH_4PO_4{\cdot}6H_2O$, and finally as $BiPO_4$. All these precipitations are quantitative.

The removal of oxygen from bismuth phosphate by bromine trifluoride is based on the reaction

$$BiPO_{4(s)} + \tfrac{8}{3}\,BrF_{3(l)} \rightarrow BiF_{3(s)} + PF_{5(g)} + \tfrac{4}{3}\,Br_{2(g)} + 2\,O_{2(g)}$$

Bromine trifluoride has advantages over other fluorinating agents. Since BrF_3 is a liquid (m.p. 8·8°C; b.p. 125·8°C) (Oliver and Grisnard, 1952), fluorinations take place readily at convenient temperatures and so it is better than F_2, ClF_3 or BrF_5 which are gases and require high temperatures for good yields. It can be distilled readily from any of its possible halogen impurities (Br_2, BrF, BrF_5, HF, F_2, metal fluorides) and, furthermore, it can be purchased free of any oxygen-containing impurities. Tank F_2 contains small amounts of oxygen. Also, whereas ClF_3 would produce as a side reaction some thermally stable chlorine oxides or oxyfluorides, the corresponding bromine analogues are thought to be unstable (Hoekstra and Katz, 1953; Baertschi and Silverman, 1951).

Apparatus and Materials

The fluorination apparatus, shown in Fig. 2, was a modification of the one described by Hoekstra and Katz (1953). The reaction system of the line was constructed entirely of nickel and the fluorine-inert plastics, Fluorothene and Teflon. Details of the reaction tube and traps are given by Hoekstra and Katz (1953). The components were silver soldered together with American Platinum Works solder no. 355 and flux no. 1200. This solder is recommended since it is resistant to attack by BrF_3. It is also recommended that Teflon-gasketed diaphragm valves be used; soldered diaphragm valves (soldered during manufacture) often corroded and leaked. Another reaction line was built in which copper and brass were substituted for the nickel; this second line proved to be just as good as the nickel line.

The BrF_3 was obtained from Harshaw Chemical Company, and was distilled

from trap to trap in the fluorination line before it was used. The high-purity (99·99 per cent) dry nitrogen used to flush the fluorination tube was purchased from the Linde Company. The nitrogen was further dried before use by passing it through an efficient trap at −196°C.

Before any experiments were started, it was necessary to prefluorinate the metallic and plastic parts of the line several times to remove completely any grease, flux or oxide films. This treatment also covered the metal with a metal fluoride film which prevented the removal of any of the O_2 as nickel or copper oxide during experimentation.

Analtyical Procedure

Dissolution of phosphate sample

The sample of phosphatic shell, after being washed and air dried, was crushed in a steel mortar and then ground finer in an agate mortar. The resulting powder was mixed carefully, and two samples (each containing about 100 mg PO_4^{3-}) were selected and weighed. In the dissolution step one sample was dissolved in solutions containing water of normal isotopic abundance, while the other sample was dissolved in solutions enriched with a known excess of O^{18}. The sample was added slowly (excessive CO_2 evolution) to about 15 ml of 10 M nitric acid and allowed to remain in this acid medium for 6 hr in order for dissolution to be complete. In certain cases when the sample was particularly difficult to dissolve, it was necessary to add a few millilitres of concentrated hydrochloric acid and to warm the mixture. In order to prevent the contamination of later precipitates, the mixture was warmed and the organic matter was oxidized by the dropwise addition of 0·3 M $KMnO_4$ solution. Any excess permanganate was reduced with 1·0 M KNO_2 solution.

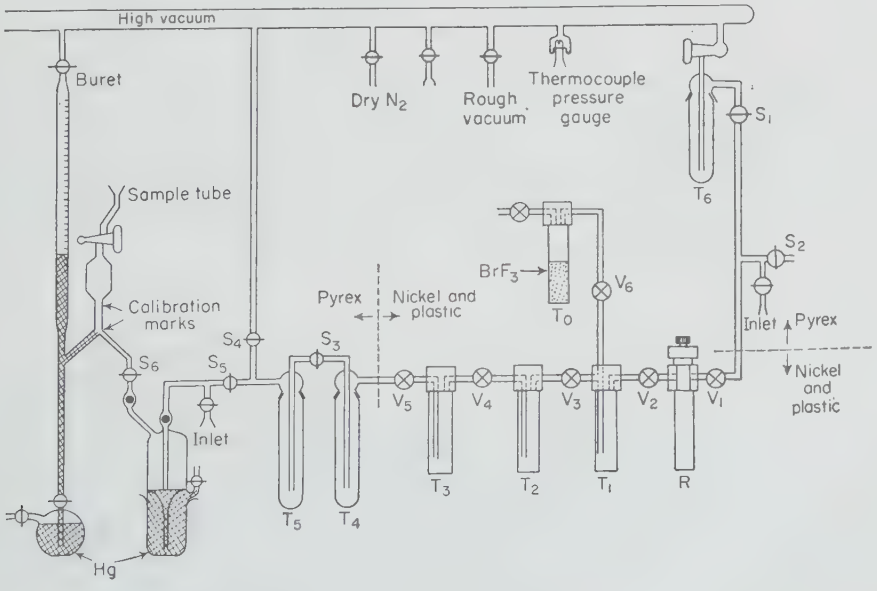

Fig. 2. Fluorination apparatus.

At this point all the powder was dissolved except for any small amounts of sulphates or silica, and the solution was colourless and free from organic impurities. The mildest treatment, consistent with the composition of the phosphatic material, was used in each case to dissolve the sample. Excessive evaporation of water was avoided, and the heated mixture was never allowed to become syrupy.

Precipitation of phosphate

The PO_4^{3-} was precipitated first as $(NH_4)_3PO_4 \cdot 12MoO_3 \cdot 2HNO_3 \cdot H_2O$ and then once as $MgNH_4PO_4 \cdot 6H_2O$ using well known procedures. The latter precipitate was filtered on a medium porosity, sintered-glass filter funnel and was washed with dilute ammonium hydroxide (0·7 M NH_4OH) until free from chloride ion. By means of the above two precipitations, which were quantitative and without analytical difficulties, the phosphate was removed from its contaminating impurities.

The precipitate was dissolved carefully from the filter by the dropwise addition of 6·5 ml of 5·4 M nitric acid and the filtrate allowed to run into a 250 ml, wide-mouthed, Erlenmeyer flask. The flask was placed in an 80 ± 2°C water bath for 75 sec. Then 10·0 ml of hot, bismuth reagent solution (0·2 M $Bi(NO_3)_3$; 2·0 M HNO_3) was added, and 45 sec later 95 ml of hot, distilled water was added dropwise from a burette. Thus the concentration of nitric acid was 3·34 M at the start of precipitation and 0·5 M after dilution. This method of precipitation is similar to that given by Kešans (1943, 1948). During these additions the flask was kept in the water bath and was swirled gently to prevent concentration gradients in the precipitation mixture. In order to obtain a denser precipitate and also to allow time for complete precipitation to occur, the mixture was digested on the water bath for 90 min and then allowed to stand at room temperature for a day. The precipitate was collected on a previously weighed, small, fine porosity, sintered-glass filter crucible; washed twice with small amounts of *freshly prepared*, dilute bismuth solution (0·0086 M $Bi(NO_3)_3$; 0·12 M HNO_3); and then washed once with water. The crucible and precipitate were dried overnight at 90°C, cooled in a P_2O_5-containing desiccator, and weighed immediately. Then the precipitate was completely removed from the crucible with a small, camel's-hair brush; transferred to a small, quartz boat; and dried in the vacuum furnace at 140 ± 5°C for 3 hr or more. Dry nitrogen was admitted to the furnace, the $BiPO_4$ removed, and a 30–40 mg sample quickly weighed into a tiny Teflon cup. The sample was ready to be put into the fluorination system.

Fluorination reaction

The valve V_2 and stopcock S_1 were closed, and dry nitrogen at a pressure of about 860 mm was admitted to R through S_2. The screw cap at the top of the reactor head was removed to permit the introduction of the Teflon cup containing the $BiPO_4$ sample; then the top was quickly replaced. The slow stream of nitrogen emerging from the top of the reactor prevented the entry of air-oxygen or water vapour. The reactor was evacuated through S_1 for at least 4 hr in order to remove completely any air or water vapour that had become adsorbed on the fine $BiPO_4$ powder after its removal from the vacuum furnace. This evacuation period was shortened considerably, if necessary, by heating the reaction tube.

Meanwhile, the BrF_3 (about 0·2 ml) in T_2 was frozen; V_4, V_3 and V_2 opened to evacuate thoroughly T_2 and T_1; V_2 and V_4 closed; a middle fraction of the BrF_3 distilled into T_1; and V_3 closed. When the sample was to be fluorinated, R was tapped to spill the powder from the cup, T_1 was heated, V_1 was closed, and R cooled in liquid nitrogen. Then V_2 was opened for about 5–10 sec to allow a very small amount of BrF_3 to distill into R; V_2 was closed and the reactor heated. As R reached room temperature, the BrF_3, which had frozen in a faint ring about the upper part of the Fluorothene tube, flowed down the sides and mixed with the $BiPO_4$ powder. Oxygen evolution began at once and, although the reaction seemed complete within a few minutes, the temperature was maintained at 90°–100°C for 30 min.

Before the fluorination was complete, the traps T_1, T_2 and T_3 were cooled in liquid nitrogen and opened to the vacuum manifold. Then the reactor was cooled by an air blast, and the above traps closed. In order to separate the O_2 completely from other volatile impurities (some of which might be low boiling) the gases were held in each trap at liquid nitrogen temperatures before being allowed to expand into the next trap. The gases were held in the Fluorothene and glass traps for 3 and 5 min, respectively. The oxygen was then toeplered into the calibrated volume. When all of the oxygen was removed from the fluorination system, the trap T_1 was heated in order to melt the BrF_3–Br_2 mixture that had escaped from R and had solidified near the top of the trap. This precaution was necessary to release any small amount of O_2 that might have been trapped as the mixture solidified. The system was again evacuated with the Toepler pump, and any additional gas placed in the calibrated volume. After the gas pressure and temperature were recorded, the yield of O_2 was calculated. Since the pressure, temperature, and the standard volume calibration were all accurate to $\pm 0{\cdot}2$ per cent, the oxygen volume (4–5 cm^3 at NTP) was known to within 0·02 cm^3. The oxygen was then moved into the evacuated sample tube.

Mass analysis of phosphate oxygen

The gaseous oxygen samples were analysed on a 60 degree, double-collecting, null-type mass spectrometer previously described by McKinney *et al.* (1950). The relative permil (‰) difference was determined between the O^{18}/O^{16} ratio (from masses 34 and 32) of the sample and an arbitrary standard of O_2 gas,

viz:
$$\delta = 1000 \times \frac{(O^{18}/O^{16})\ \text{sample} - (O^{18}/O^{16})\ \text{standard}}{(O^{18}/O^{16})\ \text{standard}}$$

Discussion

Precipitation of $BiPO_4$

Bismuth phosphate must be precipitated from an acid solution. It is convenient to use nitric acid since most other anions precipitate with bismuth. The nitric acid concentration is important; above 0·5 N the yields are low due to the increased solubility of $BiPO_4$, and below 0·16 N the results are affected by the presence of basic bismuth salts (Silverman and Shideler, 1954). The solubility of $BiPO_4$ in nitric acid is given in Table 1 (Kešans, 1943).

Table 1. Solubility of bismuth phosphate in nitric acid

Acidity (N)	Solubility (mg/100 ml)	Solubility (moles/l.)
0·25	2·5	$8{\cdot}2 \times 10^{-5}$
0·50	10·1	$3{\cdot}3 \times 10^{-4}$
1·00	92·6	$3{\cdot}0 \times 10^{-3}$

Bismuth phosphate is insoluble in water (Zharovskiĭ, 1951):

$$[Bi^{3+}][PO_4^{3-}] = 1{\cdot}3 \times 10^{-23} \text{ at } 18°C \text{ (solubility product constant)}$$

The loss of PO_4^{3-} in dilute acid solutions can be prevented by using an excess of Bi^{3+}. In spite of this low solubility, however, a large degree of supersaturation can occur unless the precipitation mixture is digested near the boiling point and is shaken at frequent intervals (Kešans, 1943). Also, the precipitate is very fine and hard to filter unless the precipitation occurs in hot solutions.

A promising technique appeared to be the precipitation in hot, acid solutions (1–5 N HNO_3) followed by slow dilution with water until the correct final acidity was reached. It was found that this technique made it possible to form a large size, grainy precipitate which did not creep up the walls of the flask, and which was easily filtered and washed.

A systematic investigation was made of the experimental variables in the precipitation step. The concentration of nitric acid present at the *start* of the precipitation was found to have an effect on the purity of the $BiPO_4$. When the nitric acid concentration was 1·0 N, a fine precipitate formed immediately upon the addition of $Bi(NO_3)_3$ to the H_3PO_4. This precipitate, even after considerable digestion, was too heavy by 1 per cent. The excess weight was probably due to the presence of $Bi(NO_3)_3$, which had been trapped and occluded during the rapid precipitation. At acid concentrations of 3·3 N and higher, the addition of Bi^{3+} did not start to produce a precipitate until after an induction period of 30–60 sec; then the precipitate formed slowly. Bismuth phosphate precipitated slowly from solutions 3·3 N in nitric acid had no occluded $Bi(NO_3)_3$. When 5·3 N acid was used, the product was again heavy by 0·3 per cent. The presence of Mg^{2+} and NH_4^- ions (from $MgNH_4PO_4{\cdot}6H_2O$) had no effect upon the precipitation. As long as the precipitation was done in reasonably hot solutions, minor changes in temperature had no effect (e.g. changing from 90° to 75°C). It was found that the dilution of the precipitation mixture (from 3·3 N to 0·5 N HNO_3) must be done slowly in order to form a grainy precipitate. The decision to dilute to 0·5 N HNO_3 was arbitrary. With the excess of Bi^{3+} used, dilution to 0·5 N HNO_3 allowed only 0·2 per cent of the PO_4^{3-} to remain in solution. Although this small loss could have been reduced by further dilution to 0·25 N HNO_3, it was felt that any such change in procedure would also increase the possibility for the co-precipitation of basic bismuth salts.

Drying of $BiPO_4$

Water vapour was strongly adsorbed upon the powdery $BiPO_4$ precipitate. Even over "Drierite" in a desiccator, dry $BiPO_4$ powder absorbed 3 per cent water in one day. It was not possible to dry the $BiPO_4$ precipitate in an ordinary oven or furnace, since considerable water remained at temperatures which caused decomposition. The only alternative was to heat in a vacuum furnace below the decomposition temperature. When samples were heated in air, it was not obvious at first that decomposition was occurring since the $BiPO_4$ remained white even up to 460°C. Probably the solid decomposition products were oxidized to other white compounds. However, when samples were heated in vacuum to 250°C, they slowly turned grey-brown due to the accumulation of bismuth–phosphorus decomposition products.

The decomposition temperature is difficult to define. This is because the decomposition of $BiPO_4$ in vacuum is a rate effect, and becomes more rapid as the temperature is raised. It was thus necessary to define certain limits of decomposition within a certain time interval. Since we were interested in avoiding isotopic changes, we defined "decomposition temperature" as that temperature which changed the O^{18}/O^{16} ratio of $BiPO_4$ (in a vacuum) by 0·2‰ in 5 hr time. This temperature was found to be 215–230°C. Table 2 lists the data for some drying experiments. Two different samples of $BiPO_4$, no. S-10 and no. S-13, were precipitated directly from the same parent H_3PO_4 solution. The precipitates were air dried, and then small representative samples were dried further in a vacuum oven. The $BiPO_4$ was reacted with BrF_3 to release molecular O_2 for mass spectrometric analysis. The data in Table 2 also serve to indicate the precision of the analytical method.

Table 2. Effect of heating in vacuum on the O^{18} content of bismuth phosphate

Drying conditions		O^{18} Analysis of $BiPO_4$ (δ in ‰)*	
Temperature (°C)	Time (hr)	Sample no. S-10	Sample no. S-13
32	36	+0·30 +0·23†	—
92	21	—	+0·03
144	38	+0·00	+0·17
195	$10\frac{1}{2}$	+0·03	−0·07
280	2	+0·77‡	+0·85‡

* Permil difference from an arbitrary standard of O_2 gas.

† Data indicate that room temperature evacuation was not sufficient to remove the strongly adsorbed water.

‡ Samples had decomposed and turned grey in colour.

The method finally adopted for the drying of $BiPO_4$ was to heat it in vacuum at 140 ± 5°C for at least 3 hr. This temperature was low enough to avoid any decomposition, yet high enough to cause the complete desorption of water in a short time.

The fluorination reaction

According to the fluorination equation given earlier, about 36 mg of BrF_3 (0·013 ml liquid) is required for 30 mg $BiPO_4$. When five to ten times this theoretical amount was used, the yields of liberated O_2 were quantitative and the O^{18} analyses precise. The use of lesser amounts of BrF_3 caused incomplete reaction, while the use of very large amounts caused both the O^{18} analyses and the per cent yields of O_2 to be erratic.

Isotopic contamination

In precise isotopic work all sources of contamination must be scrupulously avoided. In order to attain a precision of 0·1‰, two conditions must be fulfilled:

(A) The O_2 for mass analysis must not contain any non-oxygen impurities which interfere significantly in the *m/e* "mass positions" 32 and 34. In particular, any mass 34 impurity must be less than 4×10^{-5} volume per cent.

(B) At least 99·5 per cent of the O_2 must come from the $BiPO_4$. This assumes that the O^{18}/O^{16} ratio of different compounds does not vary by more than 20‰.

In order to meet condition (A) the following steps were found to be necessary:

(1) The phosphate from the phosphatic sample must be purified by three different precipitations;

(2) The fluorination reaction must be done carefully;

(3) The O_2 released in the fluorination step must be purified by the complete removal of impurities and other reaction products at —196°C.

Many samples of O_2 from different phosphates were analysed and then converted to CO_2 by reaction with hot carbon in an induction furnace (98 per cent yield). The CO_2 was carefully purified and then analysed in the mass spectrometer to determine again the O^{18}/O^{16} ratio. All the samples retained their relative differences on O^{18}/O^{16} ratio. This test was considered proof that the O_2 released from $BiPO_4$ had no significant mass 34 impurities.

The $BiPO_4$ must be free of impurities containing oxygen, because BrF_3 will also release O_2 from such impurities. Therefore to meet condition (B), the following steps must be observed:

(4) The $BiPO_4$ must not contain any H_2O.

(5) The $MgNH_4PO_4 \cdot 6H_2O$ precipitate must be washed carefully to remove all Cl^- ion and so prevent the formation of BiOCl.

(6) The $BiPO_4$ must be precipitated slowly under the correct conditions to prevent the occlusion of $BiONO_3$ and $Bi(NO_3)_3$.

No increase in O^{18}/O^{16} was observed for $BiPO_4$ samples precipitated from water enriched in O^{18}. This proved that BiOCl, $BiONO_3$, and H_2O were absent. Since NO_3^- ions do not exchange oxygen with water under the experimental conditions (Bunton, 1953), it was not possible to prove the absence of $Bi(NO_3)_3$ by the enriched water experiments. However, based upon the observed percentage yields of $BiPO_4$ and on the fact that deviations of O^{18}/O^{16} in nature rarely exceed 20‰, it was concluded that the presence of $Bi(NO_3)_3$, if it existed at all, could not affect the isotopic analyses by more than 0·1‰.

During blank fluorinations (no $BiPO_4$), about 0·05 standard cm^3 of gas was collected. This gas was mainly air that had diffused through the Fluorothene

tubes and Teflon diaphragms during the course of the fluorination and toeplering. A calculation based on the air permeability of Teflon and Fluorothene, the thickness of the plastic, and the time of diffusion yielded a gas volume value in very close agreement with the above observed value. All of the yields of O_2 were corrected for this blank. Since the volume of the blank was about 1 per cent of the volume of the oxygen sample, then the phosphate-oxygen was contaminated with 0·2 per cent of air-oxygen. Since air-oxygen analysed about 10‰ heavier than phosphate-oxygen, we see that the isotopic error due to this contamination was only 0·02‰.

The $BiPO_4$ samples dried in vacuum had a high adsorption capacity. During the short period between removal from the vacuum furnace and introduction into the fluorination line, the $BiPO_4$ adsorbed a considerable amount of water vapour and air. If the sample was not evacuated for more than 4 hr (a shorter time if R heated) in the reactor before the fluorination was started, then the oxygen yield was high and the O^{18} was erratic.

Fractionation and exchange of oxygen isotopes

By means of many experiments the analytical procedure was proven to be free from isotopic fractionation and exchange. The result of these experiments can be summarized as follows:

(1) Providing the transfer of O_2 was complete, no fractionation occurred when the gas was passed over prefluorinated copper or nickel, Fluorothene at —196°C, or BrF_3 either at its boiling point or at —196°C.

(2) There was no fractionation in the sample inlet system of the mass spectrometer. Some fractionation always occurred in the mass spectrometer "leaks". However, since this fractionation was identical for each sample, the relative differences between samples were still precise.

(3) Because of the fractionation of the O_2 in the mass spectrometer leak and immediately in front of the leak, these fractionated gases were excluded (by turning the appropriate stopcock) when a sample in the inlet system was put back into the sample tube for future mass analysis. If this precaution was not taken, the value of δ at the next analysis might increase by as much as 0·3‰ especially with small O_2 samples.

(4) There was no oxygen exchange between phosphate and water in any of the precipitation or purification steps.

(5) Apparent oxygen exchange between phosphate and water occurred *when the phosphatic sample was dissolved* if the proper procedure was not followed. If the heated phosphate solution became too concentrated, some orthophosphate polymerized (by loss of water) to pyrophosphate and triphosphate (Keisch and Wahl, 1958; Higgins and Baldwin, 1955). Upon subsequent dilution these latter compounds hydrolysed back to orthophosphate again and so incorporated oxygen from the water (Osterheld, 1958),

viz: $$2PO_4^{3-} + 2H^+ = P_2O_7^{4-} + H_2O$$

(6) Above 235°C $BiPO_4$ began to exchange its oxygen with air O_2.

Table 3 gives some representative data on the investigation of oxygen exchange in the various steps of the purification procedure. Each step under investigation

was studied twice—once with normal water (laboratory distilled water) and once with O^{18}-enriched water. In all other steps of the procedure, normal water was used. The $BiPO_4$ samples from each pair of experiments was analysed to determine whether any oxygen exchange had occurred. The last column in Table 3 gives the difference in O^{18} content between these two $BiPO_4$ samples.

Table 3. Investigation of oxygen isotope exchange in chemical treatment of phosphate

Phosphate source	Step investigated	Enrichment of water in O^{18} (‰)	Special reaction conditions	Enrichment of phosphate in O^{18} (‰)
Shark teeth	Sample dissolved	500	Dissolved in hot, dilute aqua regia; heated almost to dryness	+166·0
Reagent $Ca_3(PO_4)_2$	Sample dissolved	500	Dissolved in hot, dilute HNO_3; heated to syrupy condition	+10·9
Reagent $Ca_3(PO_4)_2$	Sample dissolved	800	Dissolved in cold HNO_3 solution	+0·3
Reagent $Ca_3(PO_4)_2$	Sample dissolved	380	Dissolved in warm, aqua regia	+0·2
H_3PO_4 soln.	Pptn. of amm. phosphomolybdate	380	—	+0·0
H_3PO_4 soln.	Pptn. of $MgNH_4PO_4$	155	—	+0·2
H_3PO_4 soln.	Pptn. of $BiPO_4$	140	—	−0·2
H_3PO_4 soln.	All pptn. steps	140	—	+0·2
H_3PO_4 soln.	Final washing of $BiPO_4$ (to study if water removed by drying procedure)	6000	—	+0·2

The presence of condensed phosphates in the phosphatic specimens

The dissolution step in the analytical procedure hydrolysed most of the condensed phosphate and organic phosphate in the specimen to PO_4^{3-}. This newly formed PO_4^{3} contained some water oxygen (Barnard *et al.*, 1955). In order to correct for this contamination, duplicate samples of the phosphatic specimen were dissolved—one in O^{18} enriched water and the other in normal, distilled water (about 22‰ light with respect to phosphate oxygen). Thus it was possible to calculate the true O^{18}/O^{16} ratio in the original phosphates.

Acknowledgements—The writer is very grateful to Professor H. C. Urey who suggested the problem, and who generously gave permission for the use of his laboratory and mass spectrometer in this research. The most sincere thanks are due Mrs. T. Mayeda for her valuable assistance in the laboratory, and Dr. J. J. Katz for advice with the BrF_3 reaction line. The

writer acknowledges the financial assistance of the Shell Oil Fellowship Committee and the U.S. Office of Naval Research, Task Order XXVIII, Contract N6 Ori-02028.

References

Baertschi P. and Silverman S. R. (1951) *Geochim. et Cosmochim. Acta* **1,** 317.
Barnard P. W. C., Bunton C. A., Llewellyn D. R., Oldham K. G., Silver B. L. and Vernon C. A. (1955) *Chem. & Ind. (Rev.)* 760.
Bunton C. A. (1953) *Mémor. Serv. Chim. État* **38,** 417.
Cohn M. (1953) *J. Biol. Chem.* **201,** 735.
Emeléus H. J. and Woolf A. A. (1950) *J. Chem. Soc.* 164.
Epstein S., Buchsbaum R., Lowenstam H. A. and Urey H. C. (1951) *Bull. Geol. Soc. Amer.* **62,** 417.
Epstein S., Buchsbaum R., Lowenstam H. A. and Urey H. C. (1953) *Bull. Geol. Soc. Amer.* **64,** 1315.
Epstein S. and Mayeda T. (1953) *Geochim. et Cosmochim. Acta* **4,** 213.
Higgins C. E. and Baldwin W. H. (1955) *Analyt. Chem.* **27,** 1780.
Hoekstra H. R. and Katz J. J. (1953) *Analyt. Chem.* **25,** 1608.
Keisch B. and Wahl A. C. (1958) *J. Amer. Chem. Soc.* **80,** 4778.
Kešans A. (1943) *Z. anal. Chem.* **125,** 6.
Kešans A. (1948) *Z. anal. Chem.* **128,** 215.
Koshland D. E. and Clark E. (1953) *J. Biol. Chem.* **205,** 917.
McCrea J. M. (1950) *J. Chem. Phys.* **18,** 849.
McKinney C. R., McCrea J. M., Epstein S., Allen H. A. and Urey H. C. (1950) *Rev. Sci. Instrum.* **21,** 724.
Oliver C. D. and Grisnard J. W. (1952) *J. Amer. Chem. Soc.* **74,** 2705.
Osterheld K. (1958) *J. Phys. Chem.* **62,** 1133.
Silverman L. and Shideler M. (1954) *Analyt. Chem.* **26,** 911.
Stein S. S. and Koshland D. E. (1952) *Arch. Biochem. Biophys.* **39,** 229.
Urey H. C. (1947) *J. Chem. Soc.* 562.
Urey H. C. (1948) *Science* **108,** 489.
Urey H. C., Lowenstam H. A., Epstein S. and McKinney C. R. (1951) *Bull. Geol. Soc. Amer.* **62,** 399.
Winter E. R. S., Carlton M. and Biscoe H. V. A. (1940) *J. Chem. Soc.* 31.
Zharovskĭi F. G. (1951) *Trud. Kom. Anal. Khim., Akad. Nauk SSSR* **3,** 101.

Geochimica et Cosmochimica Acta, 1960, Vol. 18, pp. 94 to 100. Pergamon Press Ltd. Printed in Northern Ireland

The effect of formation pressures on sheet structures—a possible case of Al-Si ordering*

M. S. Crowley and Rustum Roy
The College of Mineral Industries, The Pennsylvania State University, University Park, Pennsylvania

(*Received* 9 *March* 1959)

Abstract—Experimental evidence is presented to show that a real change in the b and c dimensions of the unit cell of muscovite occurs as a function of the pressure at which it is synthesized. The contraction caused by changes of pressure from 5000 to 50,000 lb/in² is in the range from 0·1 to 0·5 per cent. The effect is demonstrated as being independent of "leaching," hydronium substitution, starting materials, etc. Phlogopite and pyrophyllite do not show the same effect. Chlorite solid solutions with composition near clinochlore show a similar though smaller effect.

The explanation offered for this phenomenon is the progressive ordering of Al–Si at higher pressures. Ordering appears to be enhanced (or made possible) by the presence of a vacancy or substitutional defect in the octahedral layer.

Introduction

The effect of formation conditions on micas was investigated as part of a larger problem involving the determination of the extent of solid solution of various ions in the micas in the system K_2O–MgO–Al_2O_3–SiO_2–H_2O. The compositions which were studied are plotted in Fig. 1, and represent the addition of Mg^{2+} to the dioctahedral muscovite family and Al^{3+} to the trioctahedral phlogopites.

Since the limits of solid solution can be most easily determined by measuring the change in unit cell dimensions with changing compositions, accurate cell spacings for all the members were necessary. In working with synthetic micas of the muscovite composition, it was found that the b and c axes (as measured on the 060 and 005 peaks) were not consistent from one run to the next, using the same starting material. The muscovite cell dimensions were found to vary as a function of the pressure of formation with the unit cell size decreasing at high formation pressures. It is not difficult to visualize a slight contraction in a mica structure at 60,000 lb/in² water vapour pressure, but it seems unlikely that such a "condensed structure" could be frozen in by a simple quenching. If this was simply a function of the compressibility of the mica, it would be expected that the pressure would allow the cell to return to its normal size since quasi "plastic" behaviour on the unit cell scale is unknown.

This phenomenon has been noticed earlier in these laboratories by Hill and Gillery who studied septechlorites and chlorites of various compositions. They noticed that increased formation pressures caused a decrease in the cell size of the synthetic chlorite but could find no explanation for the phenomenon. Previous studies on synthetic micas (Yoder and Eugster, 1954, 1955) and synthetic chlorites (Nelson and Roy, 1958) did not mention this phenomenon. However, it could be easily missed if all the cell measurements were made on material

* Contribution No. 58–83 The College of Mineral Industries, The Pennsylvania State University, University Park, Pennsylvania.

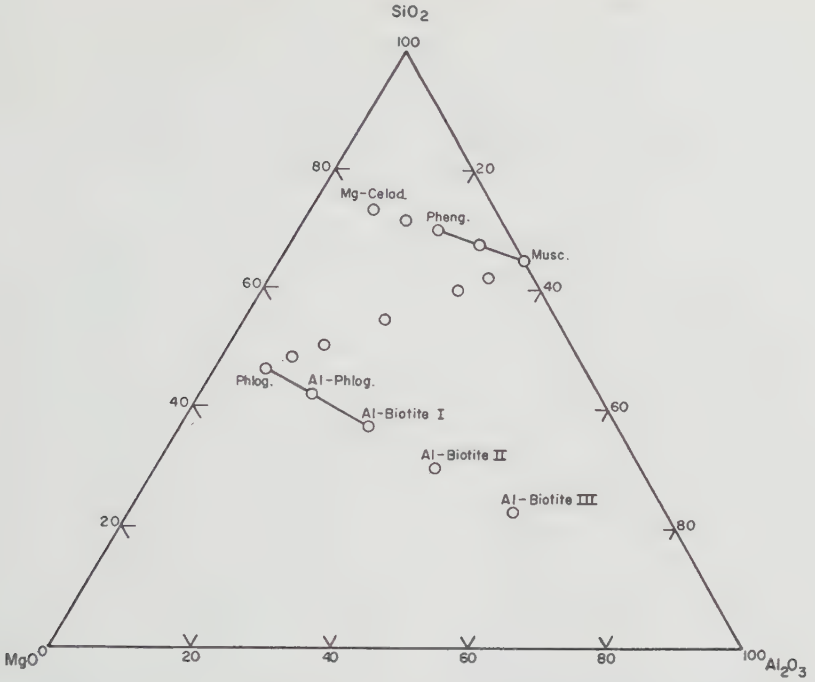

Fig. 1. The anhydrous compositions of the muscovite and phlogopite mica families plotted on a molar basis on a "constant K_2O mole faction" plane in the system K_2O–MgO–Al_2O_3–SiO_2. The circles indicate the compositions studied in detail and the limits of the solid solution actually found in the two families is shown by the solid lines. Although good evidence was found for considerable solid solution in phlogopite "towards" the muscovite composition, this is not shown since the extent cannot be decided from the present data.

synthesized at the same time. Since micas and chlorites are clay-like structures, it is felt that observations on the better crystallized micas may allow inferences to be drawn about the behaviour of the less well crystallized montmorillonites.

Method of Investigation

This study was conducted with conventional hydrothermal apparatus and techniques described in the literature (e.g. Roy and Osborn, 1952; Roy and Tuttle, 1956). It was found necessary to make most of the runs in sealed gold or platinum tubes instead of in gold envelopes because of the possibility of having the bulk composition changed due to preferential leaching of material from the envelopes.

Starting materials were (1) gels made from ethyl orthosilicate and nitrates of the desired cations, (2) mixtures of natural minerals (i.e. feldspar and gibbsite or hydromagnesite) or (3) other mixtures such as kaolinite and potassium carbonate or $K_2O{\cdot}6SiO_2$ plus alumina.

Products were identified with a Norelco X-ray Diffractometer, using an internal quartz standard for precise spacing measurements; these were shown to be accurate to $\pm 0{\cdot}01°2\theta$/ on the basis of statistical checks run for this purpose.

Results and Discussion

The effect of increasing formation pressure and temperature on the 060 spacing of muscovite made from a gel is shown in Fig. 2. The temperature of formation appears to have little effect on the cell dimensions as compared to the pressure of formation (see Table 1). The 060 peak for the 600°C run on muscovite gel varies from 61·78° ± 0·01° 2θ at 4000 lb/in² to 61·99° 2θ at 40,000 lb/in², a change

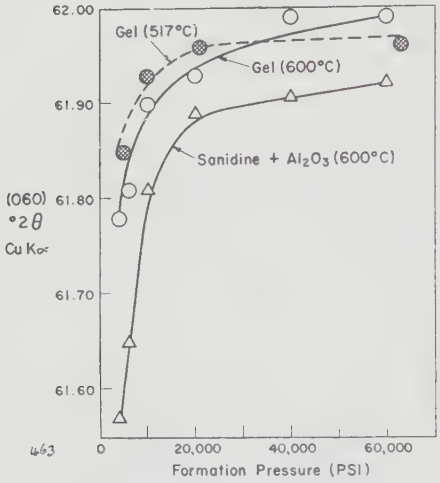

Fig. 2. The change of the 060 spacing of muscovite with pressure of formation. The effects are illustrated for different sets of starting materials and correspond to a change in the b dimension of the unit cell of muscovite from $9{\cdot}009_6$ Å to $8{\cdot}982_0$ Å for the pure gel at 600°C and a change from $9{\cdot}036_6$ to $8{\cdot}992_2$ when starting from sanidine and corundum—a change of nearly ½ per cent.

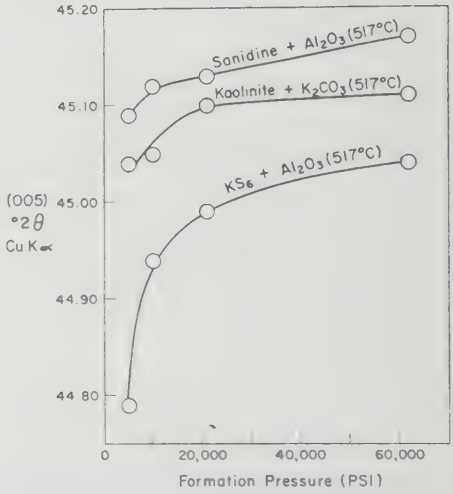

Fig. 3. Diagram illustrating the effect of the various starting materials on the 005 spacing of muscovite when pressure of synthesis is changed. Neither the (kaolinite + K_2CO_3) nor (sanidine + Al_2O_3) give exact stoichiometric equivalence to the $K_2O{\cdot}6SiO_2$ (glass) + Al_2O_3 synthetic composition. Hence absolute comparison of value is not worthwhile. However, note the difference in the change of spacing with pressure. In the (KS_6 + Al_2O_3) case this amounts to a change in 001 spacing from $10{\cdot}117_0$ to $10{\cdot}061_5$.

of 0·21° 2θ completely outside the range of experimental error. Moreover entirely separate runs made under identical conditions give spacing values within ±0·02°. In order to eliminate the type of starting material as the cause of cell contraction a number of different starting materials were tried, each with total compositions equal to muscovite. The materials used, gel, sanidine plus gibbsite, kaolinite plus potassium carbonate, $K_2O{\cdot}6SiO_2$ glass plus alumina, represent a wide range of types, crystalline, amorphous, framework structures, sheet structures and glass. Throughout most of the temperature range the polytype obtained is the $1M$ phase. In the shortest runs at the lowest temperatures Mica$_d$ (equivalent to Yoder's $1M_d$) and true $1M_d$ patterns are obtained, while the $2M$ polytype was obtained only a few times just below the decomposition limit. No $3T$ polytype was ever obtained with the pure muscovite composition, whereas "phengitic" substitutions shown in Fig. 1 made it possible to obtain $3T$ polytypes in the low temperature region (see Crowley and Roy). The results reported here deal only

with those phases with well resolved 112 and $11\bar{2}$ peaks that can be classified as 1*M* (Smith and Yoder, 1956). The 005 peaks for muscovite made from these materials are plotted as a function of pressure in Fig. 3. The curve for the gel was essentially identical with that for the kaolinite plus potassium carbonate mixtures so it is not shown. The total change in the muscovite 060 peak for mica made from sanidine and gibbsite is 0·34° 2θ. The term Al_2O_3 is used in Fig. 2 because the gibbsite actually mixed with the sanidine converts to Al_2O_3 very quickly on heating in the bomb (as shown by actual experimental checking).

There was no change in peak position with time (from 5 h to 3 weeks) for muscovites made at high pressures (from 40,000 to 60,000 lb/in²); however, at lower pressures (approximately 10,000 lb/in²) several days were required for the cell to attain equilibrium size. Runs of several hours duration were as much as 0·06° 2θ below "equilibrium" values.

With respect to other compositions, a gel of the clinochlore composition showed a shift in the 001 peak of 0·20° 2θ (from 12·28° 2θ at 5000 lb/in² to 12·48° 2θ at 62,000 lb/in²) as a function of pressure. However, numerous attempts to produce a "condensed phlogopite" were unsuccessful. Phlogopites made from gels or sanidine plus basic magnesium carbonate were synthesized at various pressures (from 4000 lb/in² to 48,000 lb/in²) with time and temperature held constant. The measured 060 and 005 peaks were remarkably constant and within the limits of accuracy established ($\pm$0·01° 2θ).

Several possible causes for this contraction effect in certain layer silicates come to mind:

(1) Leaching out of some of the ions in the starting material;

(2) Interlayering of potassium mica with hydronium (H_3O^+) mica;

(3) Collapse of the silica tetrahedra to different extents around the vacant octahedral site in muscovites. This is the reason given by Smith and Yoder (1956) for the fact that the *b* axis in natural and synthetic muscovites is 3 per cent smaller than the calculated value, assuming the tetrahedra are in nearly parallel arrays, while the phlogopite values agree quite well with the ideal value.

(4) Formation of a new polytype, indistinguishable by powder methods from the "usual" muscovite.

(5) An order–disorder phenomenon involving either the AlO_4 and SiO_4 tetrahedra or the vacant octahedral position and the potassium ion. It is also possible that ordering of the Al–Si would lead to an ordering of the octahedral hole-potassium so that the effects of both were additive.

The hypotheses listed above were investigated and the following additional data obtained:

(1) Leaching plays no part since the effect is independent of leaching conditions (open or closed tubes), starting materials varying from K_2CO_3 to Al_2O_3 in solubility, and can be obtained in sealed systems with a very small amount of total solution. Nearly every run, except where intentionally otherwise, was made in a sealed gold tube weighed before and after the run. The total volume of water was about one-fourth that of the solids.

(2) Interlayering with hydronium micas is not possible since Dr. C. Warshaw

Table 1. Muscovite spacings—temperature sequence

Run	Temperature (°C)	Pressure (lb/in²)	Time (days)	060(2θ)	
459	517	62,000	4	61·96	
231	540	60,000	¼	61·95	
849	604	44,000	7	61·94	61·94
694	613	45,000	2	61·94	± 0·02°
689	622	40,000	1	61·95	2θ
707	718	55,000	5	61·92	
		Time Effect—High Pressure			
			(h)		
218	550	63,000	0·5	61·95	61·96
231	540	60,000	5	61·95	±0·02°
230	543	57,000	65	61·98	2θ
132	539	63,000	480	61·97	
		Time Effect—Low Pressure			
891	656	8000	9	61·82	
333	680	10,000	288	61·87	

Recommended accurate cell spacing for maximum ordered synthetic muscovite based on:

Peak	°2θ	dÅ	
005 =	45·11	2·0098	$c \sin \beta = 001 = 10{\cdot}0490$ Å
060 =	61·96	1·4970	$b = 010 = 8{\cdot}9820$ Å

(1958), in this laboratory, has shown that no hydronium mica can persist beyond 300°C and also that all illites and other mixed layer phases are decomposed above 400°C. Most of the runs in the present study were above 500°C.

(3) If it is a case of structural collapse of the silica tetrahedra around the vacant octahedral site, a mineral like pyrophyllite which has a vacant octahedral site and a structure similar to muscovite should exhibit cell contraction as a function of formation pressure. To check this, pyrophyllite was synthesized from a gel at four different pressures, 5000 lb/in², 10,000 lb/in², 20,000 lb/in² and 50,000 lb/in² (at 500°C for 48 h). The measured 060 spacing showed no shift as a function of pressure.

(4) Formation of a new muscovite polytype is improbable if the limitations on polytype formation given by Smith and Yoder (1956) are followed. No evidence such as changing intensity ratios, new peaks, etc., were found in the wide variety of samples studied. In any event, it would be impossible to detect a new polytype of this type since no crystals large enough for single crystal diffraction patterns could be grown.

Infra-red absorption spectra of the extremes of variation in muscovite showed only a slight spreading in width of the Si—O absorption peak at 10μ for the more disordered (i.e. low pressure) structure. This in itself is not a contra-indication for ordering since this minor change was all that was found in the infra-red spectra of microline and sanidinized microline, and since recent infra-red work in this

laboratory suggests that the Al—O bond in fourfold co-ordination does not absorb in this region at all.

To sum up, an analysis of the data reveals the following facts:

(1) Muscovites, which can have ordering of Al—Si in the tetrahedral layer and octahedral hole-interlayer potassium positions or can have silicatetrahedra collapse into the octahedral hole, *do* exhibit cell contraction with increasing formation pressures.

(2) Phlogopites, capable of ordering in the Al—Si positions but not hole-K ordering or silica-tetrahedra collapse, *do not* exhibit marked cell contraction with increasing formation pressure.

(3) Chlorites (clinochlore), capable of Al—Si ordering in the tetrahedral layer, Mg—Al ordering in the interlayer, but allowing only partial collapse of the silica tetrahedral layer, because of the difference in size of Mg^{2+} and Al^{3+}, *do* exhibit cell contraction with increasing formation pressure.

(4) Pyrophyllites, capable of silica-tetrahedra collapse into the vacant octahedral site but not capable of Al—Si ordering or hole-potassium ordering, *do not* exhibit cell contraction as a function of formation pressure.

The common denominator for the contracting structures is Al–Si ordering in the tetrahedral layer but since phlogopite does not show any cell contraction, this ordering effect must apparently be coupled with a defect in the structure such as a hole in the octahedral layer or a substitution of the smaller Al^{3+} for Mg^{2+} in the octahedral layer.

The larger variation in the 060 peak of "sanidine-muscovite" as compared to the "gel-muscovite" (Fig. 2) may now be explained on the basis of greater Al—Si ordering made possible by the non-ideal composition of the feldspar, including the effect of the Ca^{2+} and Na^{+} present in the feldspar.

The effect of pressure on Al—Si ordering in framework structures has been investigated by MacKenzie (1957) who reported that increased pressure had the same effect as increased time in prompting better Al—Si ordering in hydrothermally synthesized albites. In this study the possibility of order–disorder phenomena in the sheet silicates is demonstrated for the first time. As in the case of "low albite," it is possible that synthetic muscovite has never been prepared with the same degree of ordering as is present in natural muscovite. This point is not easily susceptible of proof owing to the compositional variation in natural muscovite. Careful X-ray study of a carefully analysed muscovite with a composition which is nearly ideal would be very rewarding. The implication of the data with respect to a thermodynamically stable order–disorder transformation are clear. Up to the dissociation temperature of muscovite the reaction appears to be going toward the compressed (= more ordered, ?) state, so that there may be no true stability range for the open (= disordered, ?) structure.

This finding casts doubt on the validity of determining solid solution limits or compositional changes in such synthetic phases by simply measuring a shift in cell dimensions. Correlations with natural minerals based on data from the synthetic phases is likewise suspect. In the present state of knowledge it is advisable that all the data on starting materials and conditions of formation should be given when reporting precise cell constants on synthetic minerals.

Acknowledgements and note—This research was supported by the American Petroleum Institute as part of its American Petroleum Institute Project 55 at The Pennsylvania State University.

This work forms part of a larger study on the effect of solid solubility on the stability, properties and polytypism of micas, submitted by M. S. Crowley in partial fulfillment of the requirements for the Ph.D. degree in geochemistry at The Pennsylvania State University, January 1959. Over 900 runs were made in this study, 150 of them specifically to attempt to answer the present problem. The writers feel that graphical presentation of the data is adequate for most purposes. Those interested in more details on the experiments may obtain them from the University Library, or University Microfilms, Ann Arbor, Michigan.

References

Crowley M. S. and Roy R. Solid solubility in synthetic muscovite and phlogopite groups. *Amer. Min.* To be published.

MacKenzie W. S. (1954) The orthoclase-microline inversion. *Miner. Mag.* **30,** 354–366.

MacKenzie W. S. (1957) The crystalline modifications of $NaAlSi_2O_8$. *Amer. J. Sci.* **255,** 481–516.

Nelson B. W. and Roy R. (1958) Synthesis of the chlorites and their structural and chemical constitution. *Amer. Min.* **43,** 707–725.

Roy R. and Osborn E. F. (1952) Some simple aids in hydrothermal investigation of mineral systems. *Econ. Geol.* **47,** 717–721.

Roy R. and Tuttle O. F. (1956) Investigations under hydrothermal conditions. *Physics and Chemistry of the Earth* Vol. I, Chap. 6. Pergamon Press, New York.

Smith J. V. and Yoder H. S. (1956) Experimental and theoretical studies of the mica polymorphs. *Miner. Mag.* **31,** 209–235.

Warshaw C. M. (1958) Experimental studies of illite. *Proc. Seventh Nat. Clay Conf. Washington D.C.* (Abstract.) To be published. Pergamon Press, London.

Yoder H. S. and Eugster H. P. (1954) Phlogopite synthesis and stability range. *Geochim. et Cosmochim. Acta* **6,** 157–185.

Yoder H. S. and Eugster H. P. (1955) Synthetic and natural muscovites. *Geochim. et Cosmochim. Acta* **8,** 225–280.

Geochimica et Cosmochimica Acta, 1960, Vol. 18, pp. 101 to 107. Pergamon Press Ltd. Printed in Northern Ireland

Scandium, chromium and europium in stone meteorites by simultaneous neutron activation analysis*

G. L. Bate,† H. A. Potratz‡ and J. R. Huizenga
Argonne National Laboratory, Lemont, Illinois

(*Received* 20 *March* 1959)

Abstract—Analyses of five chondrites by simultaneous neutron activation yielded average concentrations of $(9{\cdot}4 \pm 0{\cdot}3) \times 10^{-6}$ g Sc/g meteorite, $(2{\cdot}2 \pm 0{\cdot}1) \times 10^{-3}$ g Cr/g meteorite and $(7{\cdot}8 \pm 0{\cdot}3) \times 10^{-8}$ g Eu/g meteorite. Following the assumptions of Urey, these results lead to cosmic abundances of 32, 6400 and 0·078 (per 10^6 Si atoms) for Sc, Cr and Eu, respectively. Except for lowering the europium abundance by a factor of 2, the Suess–Urey abundances based on chondrite analyses are not materially altered. The present results are consistently lower than the solar abundances reported by Aller, approaching nearly an order of magnitude in the case of europium. The concentrations of the three elements in two achondrites varied markedly; the Sc/Eu atom ratio, for example, decreased from an average of 410 for the chondrites to 190 for Nuevo Laredo but increased to 5700 for Johnstown, Colorado.

Introduction

The abundances of the elements have become increasingly significant in recent years, not only from the standpoint of classical geochemistry, but perhaps more so as regards possible implications for nuclear structure and for nucleo-genesis of the elements in particular. Further, astrophysical data on solar elemental abundances and stellar elemental abundances in general, promote understanding of nuclear processes in stars. These data, however, are subject to considerable uncertainty for many elements (Aller, 1958), and comparisons with terrestrial and meteoritic abundances aid in establishing valid data together with the appropriate implications for stellar processes, genesis of the solar system, and cosmogony in general.

Recently conflicting elemental abundances from solar and meteoritic sources are (among others) those of iron, chromium, scandium and europium, the Fe/Cr and Sc/Eu ratios in particular. Iron falls at a prominent maximum in the abundance curve. Scandium and europium are of particular interest since the odd–even mono-isotope of scandium falls at a major minimum and the two odd–even isotopes of europium comprise a minor minimum in the abundance vs. Z curve of the elements. With the macroscopic amounts of iron present in chondrites, there has seemed little reason to question the conventional wet chemical analyses for iron in chondrites. Hence if the meteoritic Fe/Cr ratio is in error, greater suspicion must be attached to the chromium analyses, although the apparent concentration levels of ~1 mg Cr/g are not highly suspect. Scandium concentrations are reported to approach the 10 μg/g level in chondrites, at which level emission spectrographic data should be reasonably valid. Earlier meteoritic europium analyses seemed most susceptible to error since the indicated concentration levels

* Based on work performed under the auspices of the United States Atomic Energy Commission.
† Permanent address: Department of Physics, Wheaton College, Wheaton, Illinois.
‡ Permanent address: Department of Chemistry, Washington University, St. Louis 5, Missouri.

were below 1 μg/g and the analyses of Noddack (1935), difficult as they are with conventional rare-earth chemistry, have not been verified in recent times.

Since the neutron-induced activities of scandium, chromium and europium all have rich γ-intensities (permitting γ-pulse-height analysis in favour of greater ease of discrimination against extraneous activities from impurities) and appropriate half-lives, the present work was undertaken to establish the scandium, chromium and europium abundances in stone meteorites by the independent technique of neutron activation analysis. This technique has the advantages of high sensitivity and freedom from reagent contamination during radiochemical processing. The number of elements which may be simultaneously determined by neutron activation analysis is limited only by the requisite development of coherent radiochemical separation procedures, by the physical aspects of adequate monitoring of neutron flux during activation (involving separate flux monitors for each element), and by certain radioactive properties.

The possibility of simultaneous multiple-element assay is especially appropriate for meteorite analysis since a further economy of limited meteorite material is permitted. Moreover, the intrinsic difficulty of obtaining homogeneous sampling for samples of 0·2–0·4 g size (which becomes especially severe in the case of the highly variable achondrites) is partially overcome by the added control afforded by simultaneous analysis. Further, simultaneous analysis permits sharper resolution of possible "fine structure" effects in the distribution of the elements, which might otherwise escape detection in separate analysis of small samples.

Since the abundance of thorium had previously been subject to question, simultaneous activation analysis was made of the four elements, scandium, chromium, europium and thorium. The thorium results have been presented and discussed earlier (Bate, *et al.*, 1959). The present paper reports the completed analyses of scandium, chromium and europium.

Procedure and Results

The preparation of the samples for activation has been described in our previous report (Bate *et al.*, 1959), noting here in addition that after grinding and powdering, the samples were heated in a drying oven at 110°C for $\frac{1}{2}$ hr and weighed. This weight agreed very well with the weight of the sample after activation. Separate physical flux monitors containing about 1 μg each of Sc, Cr and Eu were prepared in the manner reported for the thorium analysis. Three sets of the Sc, Cr and Eu flux monitors with appropriate blank foils were centrally located in each of the two groups of samples listed in the thorium paper. This was done for convenience of packaging, but such an arrangement occasioned some loss in control of the flux exposure. Individual monitoring obtained in the case of thorium has been shown superior for greater accuracy, but the uncertainty introduced by the poorer geometry is probably within 5 per cent, and not greater than 10 per cent.

After activation, about 30 mg each of Sc, Cr and Eu in the respective compounds of Sc_2O_3, $Na_2Cr_2O_7$ and Eu_2O_3 were added as carriers and to monitor the chemical yields. The basic supernate (containing CrO_4^{2-}) which was obtained after separating insoluble hydroxides, $SiO_2{\cdot}H_2O$, etc., from the aqueous solution of the Na_2O_2 fusion mixture (see radiochemical procedure *B* in our thorium report), was analysed for radiochromium by following a modified form of a procedure described by Burgus (1954). This solution was allowed to age about 4 months since there was a copious Cr^{51} activity and many shorter-lived impurities would be eliminated by the ageing process. At the end of the ageing period, inspection of the γ-spectrum of the supernate showed no activity extraneous to the Cr^{51} 300 keV photopeak.

Chromium chemistry. About one-quarter to one-half of the supernate was taken for analysis. The solution was acidified with HCl, treated with 3 ml of saturated $Ba(NO_3)_2$ solution, and digested on the steam bath to precipitate $BaSO_4$. After centrifuging, the clear supernate was decanted, discarding the $BaSO_4$ precipitate. Excess NH_4OH was added to the supernate to precipitate $BaCrO_4$. The precipitate was washed once with water and was then dissolved in a minimum amount of HCl. The solution was diluted to 20 ml, to which was added 1 ml 1 M $HC_2H_3O_2$. $BaCrO_4$ was precipitated by adding from 2 to 4 ml 1 M $NH_4C_2H_3O_2$ solution. One or two drops of NH_4OH were added, if necessary, to complete precipitation. The $BaCrO_4$ precipitate was washed with hot water, transferred to a tared filter, washed once more with about 20 ml of water and was finally washed with about 10 ml of ethyl alcohol. It was then dried in an oven for about 10 min, weighed and mounted.

Scandium chemistry. After removal of protactinium (again following radio-chemical procedure *B* in our thorium report), the aqueous solution containing scandium and europium carriers was treated with 3 ml of concentrated HNO_3 and heated to boiling. Excess NH_4OH was added to precipitate scandium and europium hydroxides. Zirconium hydroxide, from zirconium which had been introduced during fusion in zirconium crucibles (10–20 mg weight lost per fusion due to Na_2O_2 attack), also precipitated. The precipitate was washed with water and dissolved in excess 6 N HNO_3. One drop of 85% H_3PO_4 was added to precipitate the bulk of the zirconium as phosphate. The mixture was heated on the steam bath and after centrifuging, the supernate was decanted and the precipitate discarded. Excess ammonium molybdate was added to the supernate and the mixture was heated to precipitate ammonium phosphomolybdate which was discarded. The supernate was treated with excess NH_4OH and the hydroxide precipitate was washed once with water. It was then dissolved in 1 ml of 6 M HCl and the solution was diluted to 10 ml. To remove the last traces of zirconium and iron, 2 ml of aqueous 6% cupferron solution was added and the mixture was extracted three times with 10 ml portions of chloroform. The chloroform extracts were discarded. The aqueous phase was heated on the steam bath for 10 min. Excess NH_4OH was added. The hydroxide precipitate was washed once with water and was then dissolved in 25 ml of concentrated HCl. Scandium was now removed from the concentrated HCl solution by extracting it into 25 ml of tributyl phosphate (Eberle and Lerner, 1955). The HCl phase was reserved for europium analysis. The tributyl phosphate phase, which contained the scandium, was washed three times with 20 ml portions of concentrated HCl. Scandium was then back-extracted into 30 ml of water. The aqueous solution containing the scandium was washed with 20 ml of diethyl ether to remove tributyl phosphate. After heating on the steam bath to remove ether, excess NH_4OH was added to precipitate scandium hydroxide. The precipitate was washed with water and was then dissolved in a few drops of 6 M HCl. The solution was evaporated to dryness. The residue was taken up in about 5 ml of hot water. The solution was centrifuged and decanted to a clean tube. Five millilitres of 10% ammonium tartrate was now added and the solution was heated to near boiling. Ammonium scandium tartrate was precipitated by adding two drops of concentrated NH_4OH (Fischer and Bock, 1942). The mixture was allowed to stand for 10 min after which the precipitate was filtered out, washed with water, ignited to Sc_2O_3, weighed and mounted.

Europium chemistry. The concentrated HCl solution containing the europium carrier was evaporated to 10 ml, diluted and treated with excess NH_4OH. The europium hydroxide precipitate was washed once with water and was then dissolved in 0·5 M HCl. The solution was heated on the steam bath, centrifuged and decanted. A small amount of residue, possibly silica, which remained behind was discarded. Radioeuropium was separated from other activities in the solution by a procedure developed by Keller (1954) for the determination of radioeuropium in fission product material. In this procedure barium and strontium activities are removed as sulphates. Rare earths are then separated from other activities by fluoride precipitations in the presence of zirconium holdback carrier. The solution containing the rare earths is treated with zinc dust which reduces europium to the 2+ state. The other rare earths are removed from the solution by precipitation of their hydroxides. Ce^{3+} serves as carrier for the unreduced rare earths. The Eu^{2+} remaining in the solution is oxidized to the tripositive state and precipitated as the oxalate. The oxalate is ignited to Eu_2O_3, which is weighed and mounted.

The purity of the $BaCrO_4$, Sc_2O_3 and Eu_2O_3 samples was checked by emission spectrograph analysis. No evidence of contaminants, especially those of silica in $BaCrO_4$, zirconium in Sc_2O_3 and rare earths in Eu_2O_3, was found. Gamma counting was accomplished by means of a 200 channel pulse-height analyser, energized by pulses of varying height from a photomultiplier tube optically coupled with a 3 in. × 3 in. NaI crystal detector. The γ-spectra of the Sc, Cr and Eu samples were identical to those of the corresponding flux monitors. Half-life measurements further confirmed the correct identification of the activities of the samples. The scandium concentration was determined from the 1·12 MeV photo-peak produced by the decay of Sc^{46}. Eu^{152} and Eu^{154} produce a number of γ-rays, but it was found most convenient to base the calculations on the intense, sharp K X-ray at 48 keV. That this line was free from X-rays of other possible rare earth activities was demonstrated by: (a) the intensity ratio of K X-rays to 120 keV γ-rays (from Eu^{152} and Eu^{154} decay) in the sample was the same as that for the flux monitor; and (b) no detectable broadening of the line could be discerned on comparison with the width of the K X-ray line of the flux monitor. Further, the scandium and europium solutions aged for nearly a year before final processing so that the ageing factor would strongly discriminate against most other rare-earth activities.

Results

By counting the flux monitors immediately before or after sample counting at the same geometry, the amounts of Sc, Cr and Eu in the meteorites were determined from their proportionate activities. All counting involved at least 10,000 integrated counts so that statistical errors were of the order of 1 per cent. The results are tabulated in Table 1. The average experimental deviation of a little over 3 per cent for Sc and Eu in chondrites is quite acceptable for these concentrations although as pointed out earlier, the absolute uncertainty may be

Table 1. Scandium, chromium and europium contents of meteorites by neutron activation analysis

Sample*	Sample number	Scandium 10^{-6} g/g	Chromium 10^{-3} g/g	Europium 10^{-8} g/g	Sc/Eu (atom ratio)
Achondrites:					
Nuevo Laredo	1	45	1·2	75	200
Nuevo Laredo	2	41	1·0	77	180
Johnstown, Colo.	7	17	3·2	0·98	5700
Chondrites:					
Modoc	3	9·2	2·2	8·0	390
Modoc	4		2·4	7·9	
Richardton	5	9·9	2·4	7·9	420
Richardton	6	9·6		8·0	400
Forest City	8	8·9	2·0	7·3	410
Holbrook	9	9·7	2·1	8·1	410
Holbrook	10		2·2	8·1	
Beardsley	14	9·2	2·3	7·4	420
Chondrite average:		9·4 ± 0·3	2·2 ± 0·1	7·8 ± 0·3	410

* Sources for these samples are stated in our thorium report (1959).

somewhat larger due to lack of better geometry for flux monitor control. Moreover, since most of the final Sc_2O_3 samples weighed less than 10 mg, an allowable uncertainty of 0·1 mg in weighing could account for an added scatter in the scandium results. In any event, the final average of the scandium concentrations should be relatively free of systematic error so caused, due to the statistical nature of weighing errors of this kind.

The average experimental deviation of 5 per cent for Cr in chondrites may be attributed in part to real variations from sample to sample and also to chemical impurities in the final precipitate. The latter effect arises from the possibility that the washings of the final $BaCrO_4$ precipitate may fail to remove all of such impurities as nitrate or chloride salts; and there remains the further possibility of incomplete moisture removal on oven drying. Effects of these kinds are systematic in nature and the final average Cr concentration shown may be suppressed below the true value.

The transition in content of these elements from chondrites to achondrites is most variable. Thorium and europium are enhanced by about an order of magnitude in Nuevo Laredo (relative to average chondrite) and are suppressed by the same magnitude in Johnstown, Colorado. Scandium and chromium are almost equally enriched by a factor of about 1·6 in Johnstown, Colorado, while in Nuevo Laredo scandium is further enriched but chromium is suppressed below the chondrite average. The considerable variations in the two analyses of Nuevo Laredo are possibly attributable to sample inhomogeneity rather than to experimental error. It may be observed in this connexion, that our supply of Nuevo Laredo, having been previously ground, was not further ground, to avoid the added possibility of contamination; but in Nuevo Laredo a sprinkling of grains small fractions of a millimetre in diameter was noticed, so that a statistical variation in the distribution of these grains could account for the observed variations (sample 1 weighed 0·264 g and sample 2 weighed 0·223 g).

Discussion of Results

The abundances of scandium, chromium and europium as deduced by various investigators are displayed for comparison in Table 2. In the absence of completely reliable samples of cosmic matter, it is an open question as to which of the sources cited is the best approximation to the primitive abundances of the elements; the different abundance values for a given element need not therefore be rigorously comparable and may reflect real variations, over and above errors of chemical analysis. The data of Suess and Urey (1956) are deduced from best analyses of chondrites and accordingly may be expressly compared with the Argonne chondrite averages. The data of Cameron (1959) are a revision of the Suess–Urey abundances based on nucleogenetic criteria, and are changed only for europium of the three elements cited. The solar values of Aller (1958) deduced from spectra originating in the sun's atmosphere may depart from their primitive relative concentrations by alterations due to subsequent nuclear reactions and by mixing of the surface and interior, as Suess and Urey (1956) observe. The meteoritic averages of Levin *et al.* (1957) are subject to continuing uncertainty as to the proper relative amounts of the various meteorite phases.

Table 2. Comparison of "cosmic" abundances of Sc, Sr and Eu from various sources

Source	Abundance, Si = 10^6			Sc/Eu (atom ratio)
	Sc	Cr	Eu	
Suess–Urey	28	7800	0·187	150
Cameron	28	7800	0·115	240
Aller (solar)	40	13,000	0·6	60
Levin, Kozlovskaia and Starkova (average meteorites)	20	7600	0·3	60
Argonne (average chondrites)	32	6400	0·078	400

Considering the diversity of sources, it is perhaps encouraging that the scandium abundances agree to within less than a factor of 2. The accuracy of the solar value for scandium is difficult to assess (Aller, 1958). The Suess–Urey value is attributed to Wiik (a separately published datum has not been located) and most nearly agrees with the Argonne value, which is 50 per cent higher than that reported by Pinson *et al.* (1953).

Except for the solar value, which may indicate an actually high value in the sun's atmosphere, the chromium abundances seem compatible. However, considering the relatively large concentrations of this element, one would expect a better agreement between the conventional chemical analysis of Suess and Urey (1956) attributed to Wiik and the Argonne analysis, the difference between the two results amounting to nearly 20 per cent. Due to the sources of error previously noted for chromium, the Argonne value is possibly low and Wiik's result may be regarded as more probable.

The variations between the reported values are greatest for the abundances of europium, and experimental sources of error may account for the greater part of these differences, due to the inherent analytical difficulties in determining very low-level europium concentrations. That the abundance datum for europium of Ida Noddack reported by Suess and Urey differs by only a factor of 2 from the Argonne result, is a tribute to the excellence of her analytical techniques of over two decades ago. The solar abundance of europium is subject to considerable uncertainty because of the lack of laboratory data of *f*-values (Aller, 1958). Cameron's (1959) revision of the europium abundance from 0·187 to 0·115 in order to make a more regular variation in the odd–even effect in the rare-earth region provides better agreement with the Argonne value of 0·078. It would seem that until improvements in solar data and in the relative weighting factors for various meteorite phases can be made, the cosmic abundances of scandium and europium are best approximated by their content in chondrites as determined by neutron activation analysis, and Wiik's value for chromium in chondrites may similarly best serve for the cosmic abundance of chromium.

In the two achondrites analysed, the irregular distribution pattern of scandium,

chromium, europium and thorium is not easily accounted for. Although the mineralogical composition of the specific samples analysed was not determined, the literature classifies Johnstown (PRIOR, 1953) as a diogenite (pyroxene MgO/FeO = 4) and Nuevo Laredo (PATTERSON, 1955) as a chondritic howardite (pyroxene with anorthite). If these particular samples are consistent with VINOGRADOV's (1958) generalization that feldspar achondrites contain less silica than do achondrites low in feldspar, then Nuevo Laredo exhibits an enrichment in thorium and europium with a lower silica content whereas Johnstown with a higher silica content is impoverished in these elements. This variation is contrary to normal terrestrial differentiation but is consistent with the anomalous variation of certain trace elements and of alkalis in achondrites as observed by VINOGRADOV (1958) and by CASSIDY (1958). The increased concentration of scandium in both Johnstown and Nuevo Laredo over the average chondrite content is not easily explained in the absence of detailed mineralogical analysis, especially since with enrichment of aluminum in Nuevo Laredo over Johnstown, scandium should be suppressed in the former under "normal" trends of crystallization. The suppression of chromium in Nuevo Laredo as compared to Johnstown is consistent with the presence of feldspar in the former.

The question of the origin of achondrites has been discussed by CASSIDY (1958) and by VINOGRADOV (1958). As the present data are supplemented by additional trace element abundances, better understanding of this problem will be obtained.

REFERENCES

ALLER L. H. (1958) *Handbuch der Physik* Vol. 51. 324. Springer Verlag, Berlin.

BATE G. L., POTRATZ H. A. and HUIZENGA J. R. (1959) *Geochim. et Cosmochim. Acta.* **16,** 88.

BURGUS W. H. (1954) Los Alamos Scientific Laboratory Report LA-1721, p. 54.

CAMERON A. G. W. (1959) *Astrophys. J.* **129,** 676.

CASSIDY W. A. (1958) *Geochim. et Cosmochim. Acta* **14,** 304.

EBERLE A. R. and LERNER M. W. (1955) *Analyt. Chem.* **27,** 1551.

FISCHER W. and BOCK R. (1942) *Z. anorg. Chem.* **249,** 161.

KELLER R. N. (1954) Los Alamos Scientific Laboratory Report LA-1721, p. 179.

LEVIN B. Y., KOZLOVSKAIA S. V. and STARKOVA A. G. (1957) *Geochim. et Cosmochim. Acta* **13,** 76.

NODDACK I. (1935) *Z. anorg. Chem.* **225,** 337.

PATTERSON C. C. (1955) *Geochim. et Cosmochim. Acta* **7,** 151.

PINSON W. H., AHRENS L. H. and FRANCK M. L. (1953) *Geochim. et Cosmochim. Acta* **4,** 251.

PRIOR G. T. (1953) *Catalogue of Meteorites.* British Museum (Natural History). London.

SUESS H. E. and UREY H. C. (1956) *Rev. Mod. Phys.* **28,** 53.

VINOGRADOV A. P. (1958) *Second United Nations International Conference on the Peaceful Uses of Atomic Energy.* Paper 2523. United Nations, Geneva.

Geochimica et Cosmochimica Acta, 1960, Vol. 18, pp. 108 to 129. Pergamon Press Ltd. Printed in Northern Ireland

The sedimentary geochemistry of the beryllium isotopes

J. R. Merrill,* E. F. X. Lyden,† M. Honda‡ and J. R. Arnold‡
Department of Chemistry, Princeton University, Princeton, N.J.

(*Received* 6 *April* 1959)

Abstract—The sedimentary geochemistry of beryllium has been investigated with a view toward the use of cosmic-ray-produced Be^{10} for geochronology. Analyses of some Pacific ocean water samples give an average total Be content of 6×10^{-13} parts per part (p.p.p.), less than half of which is retained by a Millipore filter. The concentration of Be^{9} in five deep ocean sediment cores ranges from 2 to 3 p.p.m. These data indicate an ocean residence time for Be of the order of a few hundred years. Analyses of river water give concentrations of about 10^{-10} p.p.p., substantiating this residence time. An abrupt change in Be^{10} content with depth in a Pacific sediment core correlates with a change in the ionium–thorium ratio reported by Goldberg and Koide for the same core.

I. Introduction

Three years ago the existence of beryllium-10 in nature, produced by the action of cosmic rays on the atmosphere, was verified by Arnold (1956) and by Goel and co-workers (1957). The gap in radioactive age methods in the million year region, and the possibility of studying variations in the intensity of primary cosmic radiation, and in the earth's magnetic field, on this time scale, have provided strong incentives to both groups to continue work with this species. The difficulties which have been experienced in developing age methods with other isotopes have caused us to proceed cautiously, however.

Except in the unusually straightforward case of carbon-14, the early history of each method in turn has been marred by a series of illusory successes. Outside of difficulties of technique, the main problem has been the geochemistry of the species and its daughters, which is seldom as simple as is supposed at first. This affects not only the interpretation of data but also the selection of samples.

Beryllium-10 (a β-emitter of 0·56 MeV energy and half-life $2{\cdot}5 \times 10^{6}$ years) occurs in sediments and, we suppose, in the ocean. Since the sedimentary and marine geochemistry of beryllium was at the start of our work virtually unknown, and since it was unlikely on chemical grounds to be simple, we have tried to learn something in this field. Concurrently we have continued beryllium-10 measurements on selected cores.

Beryllium is a rare element in the earth's crust, and in the universe (Goldschmidt and Peters, 1932). Early efforts to study its concentration were hampered by analytical difficulties. The modern study of the subject may be dated from the work of Sandell (1952); later workers have used his analytical method either directly or to verify results of spectrographic analysis, which as usually carried out has a sensitivity limit of about 5 p.p.m.

In order to establish the beryllium content of the earth's crust, Sandell analysed a series of American granitic rocks, and found a range of from 2·4 to

* Present address: Experimental Station, E. I. du Pont de Nemours & Co., Wilmington, Del.
† Present address: Dept. of Geology, Princeton University, Princeton N.J.
‡ Present address: School of Science and Engineering, University of California, La Jolla, California.

5·5 p.p.m. in different composites. His granitic average was close to 3 p.p.m. while basalts yielded a value of ~1 p.p.m. Diorites contained around 1·5 p.p.m. Beus and Sazhina (1956) studied granitic rocks and their minerals from various parts of the U.S.S.R. The beryllium content of individual samples varied from 1 to 32 p.p.m. An average content of 4 p.p.m. was shown by 130 samples of biotite granites; forty samples of two-mica and muscovite granites showed 9 p.p.m. The writers' grand average is 5 p.p.m. Twenty samples of acid effusive rocks showed an average of 6 p.p.m. Granites in the neighbourhood of beryl-containing pegmatite fields or hydrothermal deposits of beryllium showed no marked enrichment. They also studied the distribution of beryllium in major minerals. Quartz showed a very low beryllium content; feldspars had a content about equal to the rock average, while concentrates of muscovite, biotite and hornblende showed about fourfold higher values.

Goldschmidt and Peters (1932) found a high beryllium content in nepheline syenites. Borodin (1956) has recently found very low values, of the order of 0·7 p.p.m., which brings the older values into question.

Kuroda and Gorai (1956) have made extensive studies of the beryllium content of the igneous rocks (in particular the acidic rocks) of Japan.

Andesites of Tertiary age ranged from 1·0 to 7·3 p.p.m. Be, with a mean of 3·1. A group of twenty-one Paleozoic granites and granodiorites ranged from 1·0 to 5·9 p.p.m. with a mean of 3·5. Seventeen Mesozoic rocks of these types showed a similar range with a mean of 2·7 p.p.m. A small group listed as granites and granodiorites of late Mesozoic or Tertiary are higher in beryllium; the mean is 8·9 with a range from 3·0 to 11·8 p.p.m.

Among the banded gneisses and "granitic rocks" of these areas the beryllium content is of the same order as in other previously described areas, with one notable exception: a granitic rock from Yamaguchi Prefecture which had 20·0 p.p.m.

In a detailed study of the banded gneisses separate analyses of the "granitic" and "gneissic" parts show a striking concentration of Be in the "gneissic" part, with the ratio of concentrations ranging as high as 13 to 1. Beryllium contents as high as 20 p.p.m. were noted in these gneissic parts.

Among metamorphic rocks two slates showed 0·5 and 0·8 p.p.m.

Beryllium-10 must be produced in igneous rocks in very small amounts. Secondary reactions in the earth which can produce it are $Li^7(\alpha,p)Be^{10}$, and the much less important $Be^9(n,\gamma)Be^{10}$, and $B^{10}(n,p)Be^{10}$. The value for the activity of Be^{10} induced in an average granite by the first reaction is less than 10^{-3} d.p.m./kg, an undetectable amount, corresponding to a ratio of Be^{10}/Be^9 of less than 10^{-11}. Because both lithium and uranium tend to segregate in large crystals of minor minerals in granite, the true value will be much lower than this (Holland, 1958). The inventory of Be^{10} produced by secondary reactions must be at most of the order of a hundred tons, less than the amount produced by cosmic rays (see below). In any case, it is so diffusely distributed that it is unimportant for sedimentary age studies at this stage of their development.

However, in minerals or fine-grained rocks high in lithium and in uranium or thorium, Be^{10} should be easily observable.

Be^{10} must also be made in surface rocks by penetrating cosmic rays. This sort of process has been discussed by Schaeffer and Davis (1956) in connexion with the production of Cl^{36}. Only at extreme altitudes, however, would this effect be observable for Be^{10}. It is quantitatively unimportant.

The source of Be^{10} of chief interest is the bombardment of the atmosphere by cosmic rays. The best current estimate of its rate of production is 0·08 atom cm^{-2} sec^{-1} (Lal *et al.*, 1958). On this basis, assuming constancy of the cosmic radiation over millions of years, the world inventory of cosmic-ray-produced Be^{10} is about 1000 tons. It is produced partly in the troposphere and mostly in the stratosphere but in a minute fraction of one half-life it will have reached the surface, chiefly in rain (Arnold, 1956). Rama and Zutshi (1958) have shown that Be^{7} in rain is in soluble form; this presumably holds for Be^{10} also. Be^{10} which falls on land will mainly be removed by the soil; its history will be complex and the soil specific activity will generally be very low. River sediment should contain no observable Be^{10}.

That which falls on the ocean is mixed with the normal beryllium (Be^{9}) there. This is constantly being removed in sediments and replenished by rivers and other sources. For age determination a crucial question is: are the two isotopes mixed uniformly?

The completeness of mixing depends on the time available. Goldberg and Arrhenius (1958) have defined a mean residence time T for an element given by the equation:

$$T = \frac{A}{J} \qquad (1)$$

where A is the inventory of the element and J its rate of introduction which in steady state equals the rate of removal. As a first approximation they consider only a single cycle of introduction and deposition. Arnold (1958) has explored the usefulness of some more complex models, in particular one where a "soluble" fraction (including exchangeable sorbed ions) moves independently from a "particulate" fraction. He concludes that one or the other usually dominates the transport. Values obtained for the "soluble" mean life on this model are longer than those obtained by Goldberg and Arrhenius, but of the same order of magnitude. Critical comparison of models is limited now by scarcity of data.

The quantity obtained from equation 1 or its variants is an essential parameter in the geochemistry of Be. We may compare it with a rather ill-defined quantity, the "mixing time" of the oceans (Craig, 1957; Revelle and Suess, 1957; Arnold and Anderson, 1957). If T is long compared with the mixing time (which is of the order of 10^3 years), the element will be rather uniformly distributed throughout the ocean, and the isotope ratio Be^{10}/Be^{9} will be constant, at any time. If it is short on this time scale there will be inhomogeneities in both amount of Be and isotope ratio.

In glacial periods, which last for times of the order of 10^4–10^5 years, the pattern of erosion on the continents may be significantly altered, and J will be altered somewhat (though this alteration may well be small). If T is less than about 10^5 years, the quantity A for a stable element will be altered during such a climatic fluctuation. Unless the cosmic ray flux varies proportionately with A (which is

extremely unlikely), the ratio Be^{10}/Be^{9} will change somewhat at such times. Variations of the cosmic ray intensity with times between T and a few million years will also affect the ratio. We will assume for discussion that the flux is constant.

If T is long compared with the time scale of climatic fluctuations, A and the ratio Be^{10}/Be^{9} will not be affected by such fluctuations.

In this last case, the problem of age determination using Be^{10} will reduce to the measurement of isotope ratio, just as in the case of C^{14}. If T is of the order of 10^4 years, this will also be true if J remains sensibly constant, but not otherwise. If T is less than 10^3 years, we will be forced to introduce another assumption. For example, we may assume that the local rate of sedimentation, in a particular core, is constant. This assumption is not so bad as it may appear for two reasons. First, we are interested only in fluctuations whose time scale is not very small or large compared with the half-life of Be^{10}. Very short or long term fluctuations do not concern us. Second, we can demand that the activity of the core decrease exponentially with depth, making the method largely self-checking.

Nonetheless, a small value of T will restrict seriously the number of cases where Be^{10} dating can be applied.

We have attempted to measure the quantities needed for computing T for beryllium: the rate of removal, the rate of introduction, and the inventory.

II. Beryllium-9 Content of Ocean Sediments

A. Sediment cores

Five ocean sediment cores have been analysed for Be^{9} content with a spectrophotometric method developed for this investigation and described in detail elsewhere (Merrill *et al.*, 1959). In all cases except core Capricorn 50BG1 the division into different portions along the length of the core is the same as for the Be^{10} determinations. Core length represents depth from the top of the sediment column removed by the coring apparatus. No correction has been applied for possible distortion of the core in the coring process.

Core Capricorn 50BG1, Wigwam 3, and Wigwam 6 (referred to as "*I*", "*J*" and "*G*" in earlier publications) were collected by the Scripps Institution of Oceanography of the University of California, and supplied by Dr. E. D. Goldberg. Core Capricorn 50BG1 was collected on 16 February 1953 at latitude 14°55′N and longitude 124°12′W from a depth of 4270 m. It was originally divided into five equal portions for Be^{10} determinations. At the time of Be^{9} analyses a thin lengthwise section was available. There was visible particle-size sorting at a depth of 12 to 18 cm, and a discontinuity in colour, from buff-grey to reddish-brown, below 29 cm. Dr. Goldberg suggested that the lower portion might consist of sediment much older than the upper. It was decided to make a measurement for the very top of the column. What remained of the core was further subdivided with regard to these features. The results in Table 1 are the averages of two or three analyses on each portion.

Core Wigwam 3 was obtained from latitude 28°N and longitude 125°W at a depth of 2200 m. There were no obvious features outside the original five equal

Table 1. Distribution of Be^9 in sediment core Capricorn 50BG1

Depth (cm)	Be (p.p.m.)
0–5	2·5
5–12	3·0
12–18	2·0
18–24	2·0
24–29	2·8
29–36	2·3
36–48	3·0
48–60	2·5

Table 2. Be^9 in core Wigwam 3

Depth (cm)	Be (p.p.m.)
0–22	2·7
22–44	3·0
44–66	3·0
66–88	2·9
88–111	2·9

Table 3. Be^9 in core Wigwam 6

Depth (cm)	Be (p.p.m.)
0–25	2·5
25–50	2·7
50–75	2·6
100–125	2·6
125–135	2·5

Table 4. Be^9 in core A-172-19

Depth (cm)	Be (p.p.m.)
0–15	2·8
180–200	2·8
380–400	2·9
480–500	2·7

subdivisions for Be^{10} determinations. The 44–66 cm portion showed sorting. The results in Table 2 represent single analyses of each section.

Core Wigwam 6 came from latitude 25°09·5′N, longitude 123°04·3′W, at a depth of 4310 m. No sample had been retained for the 75–100 cm section. Since only about 1 g had been saved from the other sections, no further subdivisions were possible. Single analyses are given in Table 3.

Samples of core A-172-19 were obtained from Mr. D. G. Ericson of the Lamont Geological Observatory of Columbia University. It was the only Atlantic core analysed. Its position was latitude 24°35′N and longitude 64°02′W at a depth of 5400 m. Samples were taken at the intervals shown in Table 4. Since the sedimentation rate is believed to be higher than in the Pacific, a core of considerable length was chosen. Single analyses were made on each portion.

Core 77 was obtained for a co-operative project with the workers at the Tata Institute at Bombay led by Dr. B. Peters. Dr. B. Kullenberg, of the Oceanografiska Institutet at Gothenburg, Sweden, had ten consecutive samples of this long Pacific core carefully divided into two equivalent portions. Both groups are analysing this core for Be^9 and Be^{10}. The core was taken from latitude 9°30′N and longitude 148°40′W at a depth of 5384 m.

The results of our analyses are given in Table 5. The results for the top two

Table 5. Be^9 in core 77

Depth (cm)	Be (p.p.m.)
0–100	2·38
100–200	2·46
200–300	2·3
300–400	2·2
400–500	2·2
500–600	2·2
600–800	2·2
800–1000	2·4
1000–1200	2·48
1200–1400	2·20

Table 6. Be^9 in size fractions

Particle size range (μ)	Be (p.p.m.)
10–32	2·1
3·2–10	2·1
1–3·2	2·9
less than 1	3·9

sections and the bottom two sections are averages of duplicate determinations. The rest are single analyses. The results are consistent with a uniform concentration of beryllium in the core.

All the cores have a similar Be content. The lowest value for any portion is 2·0 p.p.m., the highest, 3·0 p.p.m. The overall average is about 2·6. If the rate of sedimentation for the Pacific cores is taken as 0·1 cm per 1000 years, then these cores sample sediments deposited in a time of about 14 million years.

B. Sediment components

The mechanisms by which stable Be becomes part of the pelagic sediments have yet to be worked out. That portion which is present in true solution may be removed by adsorption or ion exchange, or may participate structurally in the formation of authigenic minerals. Some portion of the beryllium on surfaces of particles in the sea may be readily exchanged with the beryllium in solution, and thus be effectively available for this process. On the other hand, some beryllium in particles transported to pelagic areas by wind and currents must remain fixed in those particles. Submarine volcanic material may play a significant role. This section describes some studies relating to these questions.

Dr. G. O. S. Arrhenius furnished samples of core material which had been separated into several particle-size ranges by sedimentation velocity. These preparations came from the upper portion of Scripps core Y7P. Table 6 contains the results of duplicate analyses.

The smaller particle sizes have a higher Be concentration. Dr. Arrhenius has suggested that the smaller particles have a higher authigenic mineral content.

Dr. Arrhenius also supplied four samples of variously prepared authigenic phillipsite, a natural zeolite. Microscopic crystals of phillipsite are common in Pacific pelagic sediments.

Because of the very small samples used, and the early state of development of the analytical method when these measurements were made, the results can be given only as ranges (Table 7).

Table 7. Phillipsite samples

Number	Description	Probable limits of Be (probable value) (p.p.m.)
16-165-5	Not of high purity	0·3–1·0
16-518	From cores Capricorn 21–25 H and 33 BG; size >10 μ; density <2·25; subjected to chelative dissolution; about 95% phillipsite.	0·6–1·0 (0·7)
16-549-B	From core Capricorn 30 BG, 36–40 cm; size >3·2 μ; density <2·9; subjected to chelative dissolution; probably 95% phillipsite.	0·0–1·4 (0·2)
16-510	From core Capricorn 21–25 H; size 80–350 μ; density <2·16; at least 90% phillipsite, plus MnO_2 and opal.	0·4–0·8 (0·6)

No definite conclusions can be drawn here, except that the beryllium content of authigenic phillipsite is low.

The beryllium content of manganese nodules may well originate from beryllium in solution. The large surface areas of nodules and the presence of disordered layers in the mineral structures may account for the inclusion of small amounts of many other metals. Beryllium was detected in a sample of complete nodule, as well as in selected fractions of a nodule.

A random sampling of Scripps nodule MP-25-F2, supplied by Dr. Goldberg, was analysed for total Be content. This nodule was collected 2 September 1950, at latitude 19°07′N and longitude 169°44′W at a depth of 1710 to 1760 m. Duplicate analyses gave results averaging 5·0 $\pm$ 0·2 p.p.m. Be, or almost twice the value obtained for the sediments analysed.

Dr. Arrhenius supplied samples of fractions derived from 79 g of Horizon nodule 16–800. Results are shown in Table 8.

Table 8. Manganese nodule fractions

Identification	Description	% of weight	% of nodule Be
800-7	Weakly or non-magnetic part of 3–10 μ fraction. Consists of Fe and Al silicate and silica.	0·27	0·10 $\pm$ 0·02
800-8	Strongly magnetic part of 3–10 μ fraction. Contains ferromanganese minerals.	3·1	3·2 $\pm$ 0·2
800-15	Concentrate of nodule network silica.	2·2	0·7 $\pm$ 0·1

None of the samples had been treated with EDTA. Samples 800–7 and 800–15 contain only about one-third of the Be to be expected on the basis of a completely uniform distribution.

C. Extraction of beryllium from sediments

There is interest in finding a simple method for removing Be from sediments, since the treatment of hundreds of grammes of clay with hydrofluoric acid is a slow, unsatisfactory process. The problems of Be removal and mineral structure are of course related. One of the simplest experiments is the acid leaching of sediment with a determination of the amount of Be removed.

Untreated sediment samples of known Be content from the 36–48 cm portion of core Capricorn 50BG1 were subjected to mild and vigorous extractions with hydrochloric acid. In the first case, about a gramme of sediment was agitated for 10 min in 30 ml of 3 N hydrochloric acid at room temperature. About 30 per cent of the Be was removed by the acid. In the second experiment a gramme of sediment was boiled for 10 min in 30 ml of 6 N hydrochloric acid. About 50 per cent of the Be was removed.

Experiments by Goel and others indicate about 50 per cent of the Be^{10} (private communication) and Be^{9} (Peters, 1958) in a sediment are removed by prolonged treatment with hydrochloric acid. The results suggest that about half the Be is tightly bound.

The effect of chelative dissolution on sediment Be was determined by analysis of three samples prepared by Dr. G. Arrhenius. The original sediment sample came from a chocolate-brown clay core, Capricorn 33 BG, collected on 22 January 1953, at latitude 12°46′S and longitude 143°33′W at a depth of 4380 m.

The sediment was washed with water and then heated 1 hr with 3% lithium hydroxide solution to exchange sorbed species. The residue was then sorted into size fractions, and part of the 1–3·2 μ portion was subjected to chelative dissolution. The sample was stirred for 2 hr in a 5% EDTA solution buffered to pH 8 with ammonia, and kept at 100°C. A sample of material removed just before the chelation, a sample of the residue after chelation, and the evaporated and ashed chelate solution were all analysed in duplicate (Table 9).

Apparently most of the original sediment Be resisted extraction in the preliminary lithium hydroxide treatment. This is judged from the 3 p.p.m. content of the sample taken after the lithium hydroxide step, but before chelation. This figure is typical of the Be content of the untreated sediments described in

Table 9. Removal of Be with EDTA

Sample	Total weight (g)	Be (p.p.m.)	Total Be (10^{-6} g)	Be (%)
Chelate solution	2·20	2·67	5·9	21
Residue	6·96	3·07	21·4	79
Original material	9·17	3·02	27·6	100

Section IIA. About 20 per cent of the Be was removed by the chelation step. Chelation dissolves readily soluble phases such as manganese oxide minerals and microcrystalline apatite (calcium fluophosphate).

The 1–3·2 μ sediment fraction consisted mainly of amorphous ferric oxide-silicates and clay minerals. Goldberg and Arrhenius (1958) report that the removal of Mg, Sr, B, Cu and V from this fraction by chelation was markedly less than in the case of the larger grain size fractions. They correlate the increasing insolubility of these elements with the increasing clay mineral content of the smaller size fractions. They note that only a fraction of 1 per cent of the aluminium in sediments is removed by chelation, in contrast to the result for beryllium.

The results for mineral fractions do not indicate any marked excess concentrations of Be. The most suggestive result is that for the manganese nodule. If particulate matter in pelagic regions is not enriched in Be, this is proof that much of the Be in nodules passes through the solution cycle. If current theories for the growth mechanism of nodules are valid (Goldberg and Arrhenius, 1958), it is likely that Be is removed from solution at the nodules by the same process we exploit in the laboratory method described below.

III. Beryllium-9 Content of Ocean Water

The second part of our programme was the determination of the average concentration of Be in ocean water.

A. Sampling techniques

Ideally, the Be concentration in many samples of ocean water from different locations should be determined. In practice, only a few measurements have been feasible. Through the co-operation of the Scripps Institution of Oceanography of the University of California, La Jolla, it was possible to collect four samples totalling 168 l. expressly for this purpose. The sampling location chosen was at latitude 31°40·0′N and longitude 119°35·0′W. This is an area of deep water with access to general Pacific circulation. The total depth at this point is about 3300 m. To avoid surface effects samples were taken from a depth of 1000 m. Van Dorn samplers made from polyvinyl chloride were used to collect the deep water.

A tracer experiment was performed with a sampler prior to the ocean water collection. The sampler was filled with sea-water containing a known activity of carrier-free Be^7, and allowed to stand for $2\frac{1}{2}$ hr. The recovery of Be^7 still in solution was at least 90 per cent, indicating that a negligible adsorption of Be in solution would occur while the collected samples were being brought to the surface.

The possibility of adsorption of trace elements on container walls or precipitates has been occasionally neglected in sea-water analyses. Considerable attention has been given throughout the present work to monitoring any adsorption losses of Be. The adsorption of Be^7 from slightly basic solution is slower on polyethylene surfaces than on glass. Since the natural pH of sea-water is about 8, plastic containers have been used whenever feasible. The analyses have been designed to account for the sample Be from the time of collection to the final measurements.

We wished to maintain the natural condition of the water to preserve the original balance of Be in solution and that associated with particulate matter.

Lowering the pH with acid, for example, probably would have avoided wall adsorption losses, but would most likely have upset the natural distribution.

To measure the recovery, a known activity of carrier-free Be^7 (in 2 ml of 0·1 N hydrochloric acid) was added to each sample at the time of collection as tracer for the Be in true solution. The sample containers were 50 l. polyethylene carboys. When each carboy was half filled with sea-water, the tracer was added. The motion of the ship was adequate to ensure rapid stirring.

In addition to the ocean water collected specifically for this study, two 50 l. samples were donated by Dr. T. R. Folsom of Scripps. These samples had been stored 4 months in polyethylene carboys. Although no tracer had been present in these samples, it was felt they might yield additional information. Tracer was added to each at the time of analysis, and the same procedures applied as for the special collections. Sample D–5 is Scripps E–1, collected 16 April 1957, at latitude 37°39·4′N and longitude 123°17·1′W from a depth of 1000 m. Sample D–6 is Scripps F–1, collected 18 April 1957, at latitude 40°14·3′N and longitude 128°00·1′W, also from 1000 m.

B. Analytical apparatus

A series of four analyses was first made on the relatively more accessible surface water obtainable from the Scripps 1000 ft pier (*P* series). The apparatus which served in essentially the same form for all the sea-water analyses is shown in Fig. 1. The water was led by a polyethylene tubing siphon into a Büchner funnel through a rubber stopper. A Millipore filter, sandwiched between two filter supports, was placed in the funnel bottom. A special polyethylene holder kept the filters in place. Experiments were made with visible amounts of fine precipitates, and on the flow rate of water through the assembled filter funnel. It is believed the filtration was highly effective. The operational definition of Be in solution is that which passed through the filters. The particulate matter in suspension was caught on the filters; the rest was assumed to collect on the container walls. The pore size of the Millipore filters used (type HA) is 0·45 μ, according to the manufacturer.

Be in solution was removed by special ion-exchange columns following the filters. Each polyethylene column contained 5 ml of specially prepared Dowex 50-X8 resin of 200–400 mesh. The resin in hydrogen form was first completely converted to the ferric form with concentrated ferric chloride solution. Then, after the column was washed with water, 1·5 M ammonia was passed through it, followed by sufficient wash water to bring the effluent to pH 7. This "adsorption column" was developed after that of McIsaac and Voigt (1952) to meet the special requirements of the removal of traces of Be from sea-water. About 90 per cent of the Be in solution in untreated sea-water could be removed at flow rates up to 150 column volumes per hour (1·5 l./hr). Use of a pair of columns and filters running simultaneously allowed samples to be processed in about 40 hr.

Although the Be can be eluted selectively, total elution of cations with 3 N hydrochloric acid was chosen for completeness and expediency. The large amount of iron dissolved from the column was removed by extraction into diethyl ether.

C. Analytical blanks

Despite a vigorous attempt to improve the sensitivity of the spectrophotometric method (Merrill *et al.*, 1959), no Be could be detected in the series of pier water samples. Only an upper limit of about 5×10^{-12} parts per part (p.p.p.) could be set. The analytical blanks were of major concern. To obtain adequate

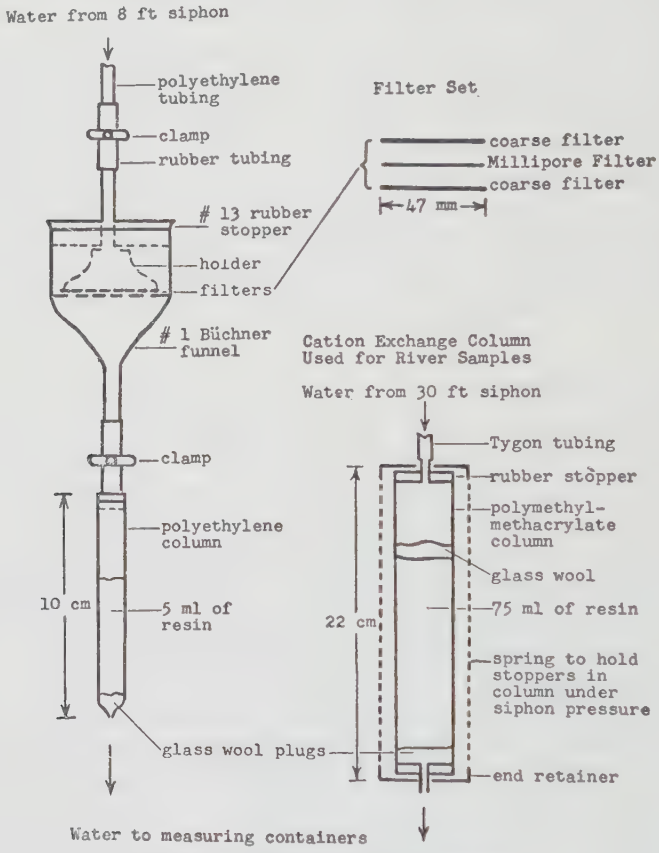

Fig. 1. Apparatus for water analyses.

data for blanks, the first ocean sample (D–1) was saved after passage through the filters and rerun as a completely new analysis (DB–1). A partial blank was also run using a large column of iron hydroxide-resin.

In addition to the determinations of Be in solution, two other analyses were made for each run. The storage carboys were rinsed for 24 hr with 0·5 N nitric acid, which was analysed for Be that had collected on the walls. The filter sets for a given run were combined. To these were added paper wipes of the plastic container used at the head of the siphon, and filter papers used to collect the small amounts of heavy particulate matter that settled in the final few millilitres of each run. This combined collection of particulate matter was ashed and treated with the hydrofluoric acid and fusion steps of an ordinary mineral analysis. In

preparation for spectrographic analysis, the twenty-seven resulting samples were purified by multiple solvent extractions (MERRILL *et al.*, 1959).

D. Detection of beryllium

Dr. N. H. NACHTRIEB of the Institute for the Study of Metals of the University of Chicago kindly agreed to examine our samples by their spark emission spectra on copper electrodes. Impurities were reduced to the microgramme level by

Table 10. Beryllium content of Pacific water samples

Sample	Volume (l.)	Dissolved Be (10^{-9} g)	Dissolved Be content ($10^{-4}\mu$g/kg)	Total Be in filters (10^{-9} g)	Total Be from container walls (10^{-9} g)	Particulate Be content* ($10^{-4}\mu$g/kg)	Total Be content ($10^{-4}\mu$g/kg)
P–2	23	1·5	0·7	3·4	—	1·5	2·2
P–3	61	14	2·3	4·9	—	0·8	3·1
P–4	69	15	2·2	3·6	—	0·5	2·7
D–1	50	38	7·5	6·9	68	1·3†	8·8
D–2	50	28	5·5	10	2·3	2·0	7·5
D–3	50	17	3·4	7·9	3·0	1·7	5·1
D–4	18	3·6	2·0	1·5	4·5	3·0	5·0
D–5	43	16	3·8	4·7	7·3	1·6‡	5·4
D–6	50	19	3·7	6·9	4·8	1·3‡	5·0
DB–1**	49	<1·7§	<0·4	<0·5	—	<0·1	<0·5

* Particulate Be was computed as the sum of filter Be plus container wall Be, minus the dissolved Be adsorbed on the walls and on the filters, as calculated from their tracer contents.

† For D–1, all the wall Be was considered contamination and not used in the calculation of particulate content. This figure is based only on the filter Be.

‡ D–5 and D–6 were stored without tracer. It was assumed that 30 per cent of the Be originally in solution was adsorbed on the walls.

§ After subtraction of 2 per cent of the solution Be in D–1, removed in the rerun.

** Blank rerun.

solvent extraction procedures so that the sensitivity of detection of Be was enhanced. The purified solutions of Be were evaporated on to the flat end of short copper electrodes about 6 mm in diameter. All of the samples were divided into two for duplicate determinations. One microgramme of molybdenum was added to each sample as an internal standard. In all cases, minimal amounts of Be^7 were added (if not already present) to monitor the transfer to the electrodes. The Be^7 on each electrode was counted in a well-type scintillation detector. Since the chemical and mechanical yields permitted by the long sequence of manipulations were variable, the use of tracer was indispensable.

E. Results

The spectrographic results, obtained by Dr. NACHTRIEB and Mr. A. J. LEONI, have first been corrected to 100% yield with tracer data. The scatter between results with duplicate electrodes is often considerable at such low levels, some pairs differing by as much as a factor of 2. The duplicate results have been averaged in Table 10.

Because the fraction of tracer found on the carboy walls was significant (7–30 per cent), a model had to be chosen for calculating final results. The distribution of tracer has been interpreted as proportional to that of the Be^9 originally in

solution at the time of collection. The Be^7 on the carboy walls is considered equivalent to loss of "solution Be" either by adsorption on the walls, or by adsorption on particulate matter which adhered to the walls. The analyses of wall Be have been corrected to 100 per cent from analytical yields of either the solution tracer initially present, or (for D–5, D–6, and DB–1) tracer added to the wall samples for this purpose. These analyses of wall Be represent the sum of adsorbed solution Be plus true particulate Be. From this corrected sum has been subtracted that part of the weight of total solution Be as indicated by the percentage of adsorbed solution tracer.

The Be^9 found on the filter sets is also considered as particulate, so the sum of corrected wall Be plus filter Be is the total particulate content of the sea-water samples. Additional tracer was added to the filter samples after ashing so that subsequent analytical yields could be determined. As in the case of the container wall elution analyses, the 1–8 per cent of original solution Be present (indicated by the tracer) has been subtracted. The results in Table 10 are calculated according to this model, but do not depend strongly on its correctness. In these calculations, and throughout this paper, the density of water samples has been taken as 1 g/cm^3.

The results bring to light some unforeseen problems. The carboy used for D–1 was not available for cleaning before use. Unfortunately it appears to have been contaminated with Be on its walls. (It should be noted that only 2 mg of ordinary soil could contribute all the Be found in sample D–1.) As a result, the wall Be figure for D–1 is markedly high. The nearly normal solution Be content indicates that only a small amount of Be from the contamination could have dissolved. Apparently none found its way to the filters.

D–1 was therefore a poor choice for the blank rerun DB–1. The average of four spectrographic analyses (two duplicate pairs, one pair stated only as upper limits) indicates a total of $<2{\cdot}5 \times 10^{-9}$ g of Be in solution in DB–1. However, accounting of the tracer from D–1 recovered in DB-1 indicates that about 2 per cent of the solution Be in D–1 was removed in the rerun. Subtracting 2 per cent of the Be in solution in DB–1 leaves a blank of $<1{\cdot}7 \times 10^{-9}$ g. This upper limit for the blank is relatively insignificant in comparison with the total amount of solution Be in each sample, except for D–4 and P–2.

The reagent blank experiment gives further evidence of a negligible blank. It differs from DB–1 in that there was little exposure to the air of the room, only 100 ml of pier water was run, and the filtering apparatus was not used. The detection limit of $<0{\cdot}1 \times 10^{-9}$ g was reported for this experiment, which included the same volume of Be^7 tracer solution as used in the ocean analyses.

The amount of Be reported for the DB–1 filter set was a detection limit of $<0{\cdot}5 \times 10^{-9}$ g.

Since no positive blanks could be measured, and the limits found correspond to a correction of only a few per cent in most samples, the blank in all cases has been assumed equal to zero.

The series D–1 through D–4 represents essentially the same sample, as does the pier water series P–2 through P–4. Samples D–5 and D–6 represent two other, distinct locations, although all the locations are within 800 miles of one another.

The similarities are striking. Some ambiguity exists with D–5 and D–6, the samples stored 4 months without tracer. From data on the other runs, it is estimated that from 30 to 40 per cent of the solution Be might have been adsorbed in that time. A figure of 30 per cent has been assumed.

To obtain average values for the calculation of residence time, the results for D–2, D–3, D–4, D–5, and D–6 have been averaged in the ratio 50 : 50 : 18 : 43 : 50 (Table 11). This weighting is in proportion to the sample volumes. All three unambiguous samples of the special collection have been used for the average to counterbalance the uncertainty of D–5 and D–6 caused by their storage without

Table 11. Averaged deep ocean results

Be in solution	$3{\cdot}9 \times 10^{-13}$ p.p.p.	68%
Particulate Be	$1{\cdot}8 \times 10^{-13}$ p.p.p.	32%
Total Be concentration	$5{\cdot}7 \times 10^{-13}$ p.p.p.	100%

tracer. The latter have been included because they represent different sampling locations and times.

Although the pier samples gave similar results, they could not be expected to be typical of the deep ocean and have not been included. Actually, the mean results are not very sensitive to the method of averaging, since the values for all samples are similar.

Before considering the use of these concentrations for further calculations, some comment on the order of magnitude itself may be appropriate. Table 12

Table 12. Concentrations in ocean water

Element	Concentration (mg/kg)
Cl	19,000
Mg	1300
Fe	0·02
Mn	0·001
Au	0·000,006
Be	0·000,000,6
Ra	0·000,000,000,3

gives some typical concentrations of elements in the ocean (following Sverdrup, *et al.*, 1942, except for Be).

Radium is detected by its radioactivity. The analyses of Be probably represent the lowest concentration of any stable element yet determined in ocean water.

It is of interest to speculate on the form of the dissolved Be. At pH 8, based on the solubility product $(Be_2(OH)_2{}^{2+})(OH^-)^2 = 10^{-18{\cdot}6}$ (Bjerrum *et al.*, 1957, 1958), the concentration of Be would be 5×10^{-9} g/g in water, or rather more in sea-water (because of the high ionic strength). Actually it is much less, a typical

situation (Krauskopf, 1956). Because of the very low concentration, only monomeric species should occur, even though the polynuclear cations $Be_n(OH)_n^{n+}$ dominate at higher concentrations. According to studies of the hydrolysis of Be (Bjerrum, 1957, 1958), Be^{2+} should be negligible at a pH higher than 6. $Be(OH)^+$ or $Be(OH)_2$ should be the stable species in very dilute solution. Anions would not be important below pH 9.

Common inorganic anions do not have high complex formation constants with Be (Bjerrum, 1957, 1958), and others such as fluoride are too low in concentration to be significant. It is possible but unlikely that the formation of complexes with organic ligands dissolved in the sea might play a role.

The removal of beryllium in tracer amounts on glass walls and on our columns at high pH, as well as other evidence discussed below, suggests that beryllium can be removed from the sea on hydrous iron oxide or similar materials.

Table 13. Residence times of elements in the sea

Element	Time (years)
Si	10,000
Mn	700
Ti	160
[Be	150]
Fe	140
Al	100

F. Residence time

The residence time can now be calculated in the manner indicated by Goldberg and Arrhenius (equation 1).

$$T = \frac{5{\cdot}7 \times 10^{-13}\ \text{g Be/cm}^3\ H_2O \times 1{\cdot}37 \times 10^{24}\ \text{cm}^3}{2{\cdot}6 \times 10^{-6}\ \text{g Be/g sediment} \times 2 \times 10^{15}\ \text{g sediment/year}} = 150\ \text{years}$$

The Be concentrations in ocean and sediments are taken from this paper. The total volume of the ocean ($1{\cdot}37 \times 10^{24}$ cm^3) is taken from Sverdrup, *et al.* (1942). The total amount of sediment deposited per year is calculated from estimates of Goldberg and Arrhenius.

Here the rate of removal of Be by sedimentation has been used, with the assumption that a steady state exists between rates of introduction and removal. There are many uncertainties about the numbers used, and this residence time can be considered correct only to a factor of a few at best. The average concentration of Be in sediments is based on only a few locations. The concentration in water is based on a limited series of measurements in a small area of the Pacific. The estimate of the total amount of sedimentation per year is also uncertain, but any percentage of error it introduces will be common to all element residence times calculated with it.

Some element residence times calculated in this manner by Goldberg and Arrhenius are quoted in Table 13 for comparison. The similarity of the residence

times of Ti, Be, Fe and Al suggests the possibility of similar mechanisms of deposition in sediments.

An alternative method of calculation can be used (Arnold, 1958). This approach considers an average square centimetre column in the ocean and its underlying sediment. The equation used is the same as before, but the numbers are obtained differently. The reader is referred to this paper for a detailed discussion.

Substitution of concentrations, estimated sedimentation rate for pelagic sediments, and the average weight of water over a square centimetre (mean ocean depth) gives:

$$T = \frac{3{\cdot}9 \times 10^{-13}\ \text{g Be/g } H_2O \times 3{\cdot}8 \times 10^5\ \text{g } H_2O/\text{cm}^2}{2{\cdot}6 \times 10^{-6}\ \text{g Be/g clay} \times 10^{-4}\ \text{cm/yr} \times 1\ \text{g/cm}^2} = 570\ \text{years}$$

The assumed rate of sedimentation (0·1 cm per 1000 years) is a common estimate. The actual amount of (dry) sediment contained per cubic centimetre of wet sediment varies. An average of 1 g/cm^3 has been taken (again following Goldberg and Arrhenius). The average depth of the ocean has been taken as $3{\cdot}8 \times 10^5$ cm. Only the concentration of Be in solution has been used here, on the assumption that we are interested only in Be^9 passing through the solution cycle, and that it does not exchange with particulate matter. Both methods of calculation indicate a residence time of the order of a few hundred years.

IV. Beryllium-9 Content of River Water

This short residence time suggests that Be transport through the ocean is actually in a steady state (unless man-made contamination is important). Consequently it should be possible to determine the rate of introduction, and with it calculate an independent residence time. However, the rate of introduction is also difficult to measure experimentally. It is probable that the majority of Be is carried into the ocean by rivers through the process of land erosion. The amount of Be carried off the land by wind, or introduced by submarine volcanoes, is assumed to be a small fraction of the total. Within these assumptions, knowledge of the average total influx of river water to the ocean and the average Be content of river water would permit calculation of the rate of introduction.

Wüst (1942) has estimated the total annual run-off of water from land to be 37,000 km^3. No measurements of Be in rivers have been published. Ideally the major rivers of the earth should be analysed over a period of time to obtain a weighted-average Be content. We have been content at this stage with a few analyses.

A. Sampling techniques

Precautions similar to those employed with the ocean samples were taken with the river analyses. All samples represent water collected at the surface in the river channel. Be^7 was added at the time of collection. The apparatus used for filtration and removal of dissolved Be was similar to that for the ocean analyses. However, despite the much lower salt content of river water, the removal of Be by a ferric hydroxide adsorption column proved to be less efficient. During

analysis of sample R–1, only 40 per cent of the Be in solution was recovered on two 5 ml adsorption columns. In the case of river water, the higher dissolved silica content may preferentially adsorb on the ferric hydroxide, preventing complete removal of Be. In all succeeding runs a single 75 ml column of Dowex 50-X8 in the hydrogen form was used. The use of 50–100 mesh resin allowed a high flow rate to be maintained. The recoveries were about 75 per cent. Virtually all cations are expected to be removed with a hydrogen-form resin. The total salt concentration of river water is small enough to make this method of collection feasible.

Samples R–1 and R–2, taken from the lower Delaware river, were taken at 10 a.m. on 24 April 1958, from the Lambertville, New Jersey–New Hope, Pennsylvania bridge.

The upper Delaware river is represented by sample R–4, taken from the U.S. Highway 209 bridge at Port Jervis, New York. The water was collected at 2 p.m. on 13 May 1958. According to New Jersey State Geologist, Dr. M. Johnson, there is little pollution of the Delaware at this location.

Two samples of the Hudson river were taken in midstream from the deck of a Newburgh-Beacon, New York ferryboat, at 7 p.m. on 13 May, 1958. This was the last of an ebb tide, which would ensure that the samples were typical of river water. These samples were labelled R–3 and R–5.

Visible amounts of suspended matter fell to the bottom of all the storage containers in about a day. This detrital material is important both for its Be content and its relation to Be in solution. The river detrital material was collected by resuspending it in the last few millilitres of a sample and filtering through medium porosity paper. Filter papers used to clean the container walls were added to the major portion of solids. These solids plus the Millipore filter sets were defined as particulate matter. The total amounts of Be^7 associated with the particulate matter were appreciable (15–38 per cent).

B. Calculation of results

It can be assumed, as was done for the ocean samples, that Be^7 is adsorbed from solution on to the particulate matter, and that a directly equivalent proportion of Be^9 originally in solution accompanies it. Calculated with this *adsorption model*, the data yield the results in Table 14.

On the other hand, it is possible that the transfer of 15–40 per cent of the Be^7 to particulate matter represents not loss, but *exchange*. A portion of the particulate Be may be exchangeable, in times of the order of a day, with the Be in solution. The relative size of the reservoir of Be in solution at all times, compared with the reservoir of readily exchangeable particulate Be, might be determined from the distribution of tracer after a time sufficient for equilibrium to have become established. Limiting exchange values have been estimated by extrapolating percentage tracer exchanged vs. time for each location. These values have been used to estimate the relative amounts of solution and exchangeable Be for a *three-reservoir model* (Table 15).

The adsorption and exchange models lead to the same total Be contents. Only the classification of Be by source differs.

Table 14. Beryllium content of river water samples with absorption model

Sample	Volume (l.)	Dissolved Be (10^{-6} g)	Dissolved Be content ($10^{-1}\mu$g/kg)	Particulate Be (10^{-6} g)	Particulate Be content ($10^{-1}\mu$g/kg)	Total Be content ($10^{-1}\mu$g/kg)
Delaware at Lambertville						
R–1	62·7	24·5	3·91	11·5	1·82	5·73
R–2	69·9	29·6	4·24	10·2	1·46	5·70
Delaware at Port Jervis						
R–4	54·8	0·59	0·11	0·58	0·11	0·21
Hudson at Newburgh						
R–3	51·4	0·86	0·17	1·85	0·36	0·53
R–5	43·8	0·76	0·18	1·51	0·35	0·52

Table 14 (*contd*). Beryllium content of river water samples with absorption model

Sample	Particulate matter (g)	Particulate matter (p.p.m.)	Be content of particulate matter (p.p.m.)	Per cent of sample Be in solution	Per cent of sample Be particulate
R–1	1·3	21	8·6	68	32
R–2	1·1	16	9·1	75	25
R–4	0·18	3	3·2	50	50
R–3	0·69	13	2·7	32	68
R–5	0·73	17	2·1	34	67

Table 15. Beryllium content of river water samples with three-reservoir model

Sample	Dissolved Be (10^{-6}g)	($10^{-1}\mu$g/kg)	Exchangeable Be (10^{-6}g)	($10^{-1}\mu$g/kg)	Non-exchangeable Be (10^{-6}g)	($10^{-1}\mu$g/kg)
Delaware at Lambertville						
R–1	17·9	2·86	13·5	2·15	4·6	0·72
R–2	18·4	2·62	13·8	2·01	7·5	1·07
Delaware at Port Jervis						
R–4	0·50	0·09	0·09	0·02	0·57	0·10
Hudson at Newburgh						
R–3	0·71	0·14	0·30	0·06	1·68	0·33
R–5	0·53	0·12	0·23	0·05	1·51	0·35

Table 15 (*contd.*) Beryllium content of river water samples with three-reservoir model

Sample	Sample Be in solution (%)	Sample Be exchangeable (%)	Sample Be non-exchangeable (%)	Total Be content ($10^{-1}\mu$g/kg)
R–1	50	38	12	5·73
R–2	46	35	19	5·70
R–4	43	8	49	0·21
R–3	26	11	63	0·53
R–5	23	10	67	0·52

The Be content of the Delaware river at Lambertville is markedly higher than that in the upper Delaware or the Hudson river. The Lehigh river, which joins the Delaware 35 miles above Lambertville, is the most likely source of the increase. A cursory investigation has uncovered no definite industrial Be contamination of the Lehigh, although this river passes through an area of coal and steel industry. However, Be ore is currently mined at Hazelton, Pennsylvania, at the headwaters of the Lehigh. The river Be content may be quite natural, but perhaps unusually high because of the minerals in this particular watershed. In any case, the Be content of the particulate matter collected at Lambertville is notably high, about 9 p.p.m. The other particulate samples contain about 3 p.p.m., a value close to the estimated lithosphere average. There is no reason to suspect Be contamination at the other sampling points.

C. Residence time

The residence time can now be computed using the input rate.

$$T = \frac{A}{J} = \frac{\text{total Be in ocean}}{\text{rate of Be input}}$$

$$T = \frac{3{\cdot}9 \times 10^{-13}\ \text{g Be/cm}^3\ \text{water} \times 1{\cdot}37 \times 10^{24}\ \text{cm}^3}{(\text{soluble conc. in rivers}) \times 3{\cdot}7 \times 10^{19}\ \text{cm}^3/\text{year} \times 1\ \text{g/cm}^3}$$

$$T \times (\text{soluble conc. in rivers}) = 1{\cdot}4 \times 10^{-8}\ (\text{g Be/g water})\ \text{years}$$

With the above inverse relation between residence time and concentration, a table can be set up with the river data. The "soluble" concentrations chosen are the sums of solution and exchangeable Be calculated with the three-reservoir model. The non-exchangeable particulate Be is considered to be precipitated rapidly near the continental shelf.

A precise residence time cannot be determined from such limited data, but they do tend to confirm the order of magnitude derived from the sediments.

V. Beryllium-10 Content of Ocean Sediments

The beryllium-10 content of two more Pacific cores has now been measured. The first, Scripps Wigwam 3, is similar in character to a previously analysed core (Wigwam 6) from the same general area. There are definite disturbances in the core, and the heterogeneity of the Be^{10} is not surprising (Table 17).

The high value for the top sample of core 50BG1 is striking. Because of the high activity, we were able to recycle this sample three times, using a different chemical method each time, to check that it was at constant activity. The first recycle gave a higher value, which was traced to contamination of a platinum crucible with fission products, but the second and third gave specific activities which agreed with the original value within 10 per cent. Absorption data were also consistent with expectations, and thus we have a more rigorous proof than heretofore available that we are really observing Be^{10}.

Goldberg and Koide (1958) have published ionium/thorium measurements for core Capricorn 50BG, obtained at the same station as 50BG1. These data

show a smooth decrease of ionium activity with depth, corresponding to a rate of sedimentation of about 1 mm per thousand years, down to more than 20 cm (values for greater depths require correction for U-supported ionium). This is quite different from the behaviour expected for 50BG1 from Be^{10} measurements. We are indebted to Dr. GOLDBERG for the measurements on core 50BG1 given in Table 18.

The appearance of a sharp break in the ratio at 12 cm is gratifying. This core

Table 16. Residence time from river Be concentrations

Location	Soluble Be (10^{-10} p.p.p.)	Residence time (years)
Delaware river at:		
Lambertville	4·8	30
Port Jervis	0·11	1300
Hudson river	0·19	740

also shows much more variability in total Th than 50 BG. From previous work Dr. GOLDBERG estimates that all the ionium below 24 cm may be uranium-supported; there may be some excess ionium in the 12–24 cm fraction.

Although taken close together, these cores must have had quite different histories.

If cores undisturbed for several half-lives of ionium can be found, there seems more reason to be optimistic about the possibility of finding suitable cores for Be^{10}

Table 17. Beryllium-10 content of two cores

Wigwam 3		Capricorn 50BG1	
Depth (cm)	Be^{10} (d.p.m./g wet clay)	Depth (cm)	Be^{10} (d.p.m./g wet clay)
0–22	$4{\cdot}1 \pm 0{\cdot}7 \times 10^{-3}$	0–12	$61 \pm 3 \times 10^{-3}$
22–44	$3{\cdot}8 \pm 0{\cdot}4$	12–24	$1{\cdot}3 \pm 0{\cdot}3$
44–66	$9{\cdot}2 \pm 0{\cdot}7$	24–36	$-0{\cdot}5 \pm 0{\cdot}5$
66–88	$1{\cdot}6 \pm 0{\cdot}5$	36–48	$1{\cdot}6 \pm 0{\cdot}4$
88–111	$4{\cdot}8 \pm 0{\cdot}6$	48–60	$7{\cdot}7 \pm 0{\cdot}4$

dating. The simultaneous measurement of both species in cores should be particularly useful.

VI. Summary and Conclusions

(1) The beryllium content of all pelagic clay sediment samples analysed lies between 2 and 3 p.p.m. This is not far from the average for igneous rocks.

(2) Among authigenic minerals phillipsite is low in beryllium, while manganese nodules and their iron-manganese-oxide minerals are high.

(3) The total beryllium content of some Pacific deep water samples is 6×10^{-13}; less than half of this is apparently particulate (retained by a Millipore filter). Residence times for beryllium in the ocean calculated from these data by two models are 150 and 570 years, respectively. This is rather short compared with the "mixing time" of the ocean.

(4) Analyses of the beryllium content of the Delaware and Hudson rivers show values of the order of 10^{-10}. The residence time for beryllium in the ocean

Table 18. Ionium and thorium activities in core Capricorn 50BG1
(Data of E. D. Goldberg and M. Koide)

Depth (cm)	d.p.m. Io / d.p.m. Th	Th (p.p.m.)
0–5	27·0	9·5
5–12	22·9	8·6
12–18	4·8	7·8
18–24	5·5	14
24–30	2·8	13
30–36	1·4	5·9
36–48	2·2	6·4
48–60	1·6	5·6

estimated from these data and the ocean concentration are of similar magnitude to those given above.

(5) Analyses of Be^{10} in core 50BG1 show a sharp change of concentration with depth. This indicates that vertical migration of beryllium in sediments is unimportant. Data of Goldberg and Koide show a break in ionium concentration at the same point.

Acknowledgements—The many specific contributions of samples, information and measurements supplied by other workers have been indicated in the text. It remains to acknowledge helpful discussions with E. D. Goldberg, G. Arrhenius, N. H. Nachtrieb, D. Lal and M. Fleischer. This work was supported by the Office of Ordnance Research, U.S. Army, and the National Science Foundation.

References

Arnold J. R. (1956) Beryllium-10 produced by cosmic rays. *Science* **124**, 584.

Arnold J. R. (1958) Trace elements and transport rates in the ocean. *Proc. Second Int. Conf. Peaceful Uses Atomic Energy, Geneva.* **18**, 344, P/411.

Arnold J. R. and Anderson E. C. (1957) The distribution of carbon-14 in nature. *Tellus* **9**, 28.

Beus A. A. and Sazhina D. I. (1956). The average beryllium content of acidic magmatic rocks of the U.S.S.R. *Dokl. Akad. Nauk SSSR* **109**, 807.

Bjerrum J., Schwarzenbach G. and Sillén L. G. (Compilers) (1957 and 1958) *Stability Constants* Vol. I and II. Chemical Society, London.

Borodin, L. S. (1956) On the distribution of beryllium in the Khibina alkalic massif and on the clarke of beryllium in nepheline syenites. *Dokl. Akad. Nauk SSSR* **109**, 811.

Craig H. (1957). The natural distribution of radiocarbon and the exchange time of carbon dioxide between atmosphere and sea. *Tellus* **9**, 1.

Goel P. S., Kharkar D. P., Lal D., Narsappaya N., Peters B. and Yatirajam V. (1957) The beryllium-10 concentration in deep-sea sediments. *Deep-Sea Res.* **4,** 202.

Goldberg E. D. and Arrhenius G. O. S. (1958) Chemistry of Pacific pelagic sediments. *Geochim. et Cosmochim. Acta* **13,** 153.

Goldberg E. D. and Koide M. (1958) Ionium-thorium chronology in deep-sea sediments of the Pacific. *Science* **128,** 1003.

Goldschmidt V. M. and Peters C. (1932) The Geochemistry of Beryllium. *Nachr. Ges. Wiss. Göttingen* 377.

Holland H. D. (1958) Personal communication.

Krauskopf K. B. (1956) Factors controlling the concentration of thirteen rare metals in sea water. *Geochim. et Cosmochim. Acta* **9,** 1.

Kuroda R. and Gorai M. (1956) Geochemical investigations on the granitic rocks—III. *Nippon Kagaku Zasshi* **77,** 609; (1955) *Ibid.* **76,** 919.

Lal D., Malhotra P. K. and Peters, B. (1958) On the production of radio-isotopes in the atmosphere by cosmic radiation and their application to meteorology. *J. Atmosph. Terr. Phys.* **12,** 306.

McIsaac L. D. and Voigt A. (1952) *A new technique for the separation of radiophosphorus from sulfur.* Ames Lab. Report ISC-271.

Merrill J. R., Honda M. and Arnold J. R. (1959) Methods for separation and determination of beryllium in sediments and natural waters. In press.

Peters B. (1958) Personal communication.

Rama Thor and Zutshi P. K. (1958) Annual deposition of cosmic-ray-produced Be^7 at equatorial latitudes. *Tellus* **10,** 99.

Revelle R. and Suess H. E. (1957) Carbon dioxide exchange between atmosphere and ocean. *Tellus* **9,** 18.

Sandell E. B. (1952) Beryllium content of igneous rocks. *Geochim. et Cosmochim. Acta* **2,** 211.

Schaeffer O. and Davis R., Jr. (1956). *Chlorine-36 in nature.* Nat. Acad. Sci.–Nat. Res. Coun. Publ. No. 400, p. 172.

Sverdrup H. V., Johnson M. W. and Fleming R. H. (1942) *The Oceans.* Prentice-Hall, New York.

Wüst G. As quoted in Sverdrup H. V., Johnson M. W. and Fleming R. H. (1942) *The Oceans* p. 120. Prentice-Hall, New York.

Geochimica et Cosmochimica Acta, 1960, Vol. 18, pp. 130 to 142. Pergamon Press Ltd. Printed in Northern Ireland

Studies in the geochemistry of gold—I

The distribution of gold in rocks and minerals of the Skaergaard intrusion, East Greenland

E. A. Vincent and J. H. Crocket*
Department of Geology and Mineralogy, University Museum, Oxford

(*Received* 6 *May* 1959)

Abstract—Gold has been determined by neutron activation analysis in a suite of rocks from the strongly differentiated Skaergaard gabbroic complex and in some of the constituent silicate, oxide and sulphide minerals. The chilled marginal gabbro (taken as representative of the initial magma) contains 0·0046 p.p.m. Au and with four exceptions all rocks and minerals analysed carry between half and twice this amount. The uncharged gold atom shows no preference for any one of the various silicate, oxide and iron sulphide minerals, but is very strongly concentrated in the copper sulphides, emphasizing the chemical similarity of the Cu and Au atoms rather than any general chalcophile tendency on the part of gold.

Introduction

The distribution and geochemical behaviour of gold in the igneous rocks is poorly known, due chiefly to the difficulties which have hitherto existed in the analytical determination of very small quantities of this element. Attempts to determine the gold content of rocks and minerals have been few, and often seem to have been made on a somewhat oddly chosen assortment of materials—perhaps where relatively high concentrations of gold were anticipated. The availability in recent years of the neutron activation method of analysis (which is particularly sensitive for gold because of this element's very high activation cross-section for thermal neutrons) enables us for the first time to provide reliable data on the distribution of gold in common igneous rocks and silicate minerals. The present paper reports the results of analyses made by this method on certain rocks and constituent minerals from the strongly-differentiated layered gabbroic complex of the Skaergaard intrusion in East Greenland, and discusses some aspects of the geochemistry of gold which they reveal.

Analytical Method

The procedure used for irradiating and analysing the rock and mineral samples was that of Vincent and Smales (1956), except that the steps for the simultaneous determination of palladium were omitted. In the earlier account the assumption was made that errors due to self-shielding in the 5 mg fragments of gold foil (0·002 in. thick) irradiated as standards along with the rock samples could be neglected (see also Goldberg and Brown, 1950). Further work on the neutron activation method for the estimation of gold has, however, shown that gross errors are introduced unless very small amounts of gold are irradiated as standards. In the present work, therefore, the gold foil standards were replaced by silica ampoules in which a strongly acid solution containing an accurately known weight (not more than 10 μg) of gold had been evaporated to dryness and sealed. Careful experiments showed that for a given neutron flux no appreciable variation in

* Present address: Department of Geology and Geophysics, Massachusetts Institute of Technology.

specific activity with weight of gold irradiated was encountered, provided that the latter was kept below 10 μg. In the rock and mineral samples analysed, the gold is in such small amounts and distributed so evenly throughout the sample that no error due to self-shielding would be anticipated; this is borne out by the reproducibility of the gold determinations in duplicate samples of widely differing weight.

In an experiment designed to assess the analytical error introduced by using gold foil as the irradiated standard, it was found that an evaporated acid solution containing a few micrograms of gold gave a specific activity some 37 per cent higher than a gold foil 0·002 in. in thickness irradiated alongside in the identical high neutron flux (*c.* 10^{11} neutrons cm^{-2} sec^{-1}). The results for gold previously reported by Vincent and Smales are likely to be high, therefore, by about this percentage. Vincent's (1956) values for gold in the standard granite and diabase samples G–1 and W–1 were 0·0095 p.p.m. and 0·018 p.p.m., respectively. Decreased, rather arbitrarily, by 37 per cent these become 0·006 p.p.m. and 0·01 p.p.m., figures which may be compared with new analyses (in duplicate) giving values of 0·0046 and 0·0043 p.p.m. for G–1, and 0·0085 and 0·0083 p.p.m. for W–1.

Further experiments have been devised to check whether any errors might be introduced by self-absorption or self-scattering in the gold samples finally counted. In most of the analyses, between 10 and 25 mg out of 30 mg of gold carrier added was recovered; provided that the gold is plated out evenly on the counting tray in a fine state of subdivision, specific activity is independent of the weight of gold recovered, at least between the above limits.

In all determinations the radiochemical purity of the recovered gold was checked by plotting a decay curve and, in cases where the counting rate was sufficient, by constructing an absorption curve and deducing the maximum energy of the emitted β-particles.

A further possible source of error in the analyses is that platinum, if present in the rocks, may on irradiation give rise to traces of another active isotope of gold, Au^{199}, which decays with a half-life of 3·15 days. It has not been possible to take this into account in the present work, since the platinum content of our rocks is unknown. Theoretically, it is found that a Pt/Au ratio of more than 4 : 1 could be tolerated as such a ratio would introduce an error of only 1 per cent in the determination of gold; it is considered most improbable that the results quoted in this paper are seriously in error from this cause.

Gold in the Rocks

A full account of the geology and petrology of the Skaergaard intrusion has been given by Wager and Deer (1939), and the distribution of a number of significant trace elements in the intrusion has been described by Wager and Mitchell (1951). In this latter paper, and also in a more recent one by Wager *et al.* (1957) summaries are given of the principal features of the Skaergaard intrusion and the sequence and origin of its chief rock types. Gold has been determined in seventeen rocks from the intrusion, representing all significant horizons in the differentiated sequence. The constituent minerals of two of the

rocks have also been analysed individually for gold, as have two examples of iron sulphide minerals appearing near the top of the sequence. The positions of the analysed rocks on the arbitrary height scale adopted for the intrusion are indicated in Fig. 1, which also shows the variations in occurrence and composition of the principal mineral phases.

The results of the analyses are set out in Table 1. The Chilled Marginal Gabbro

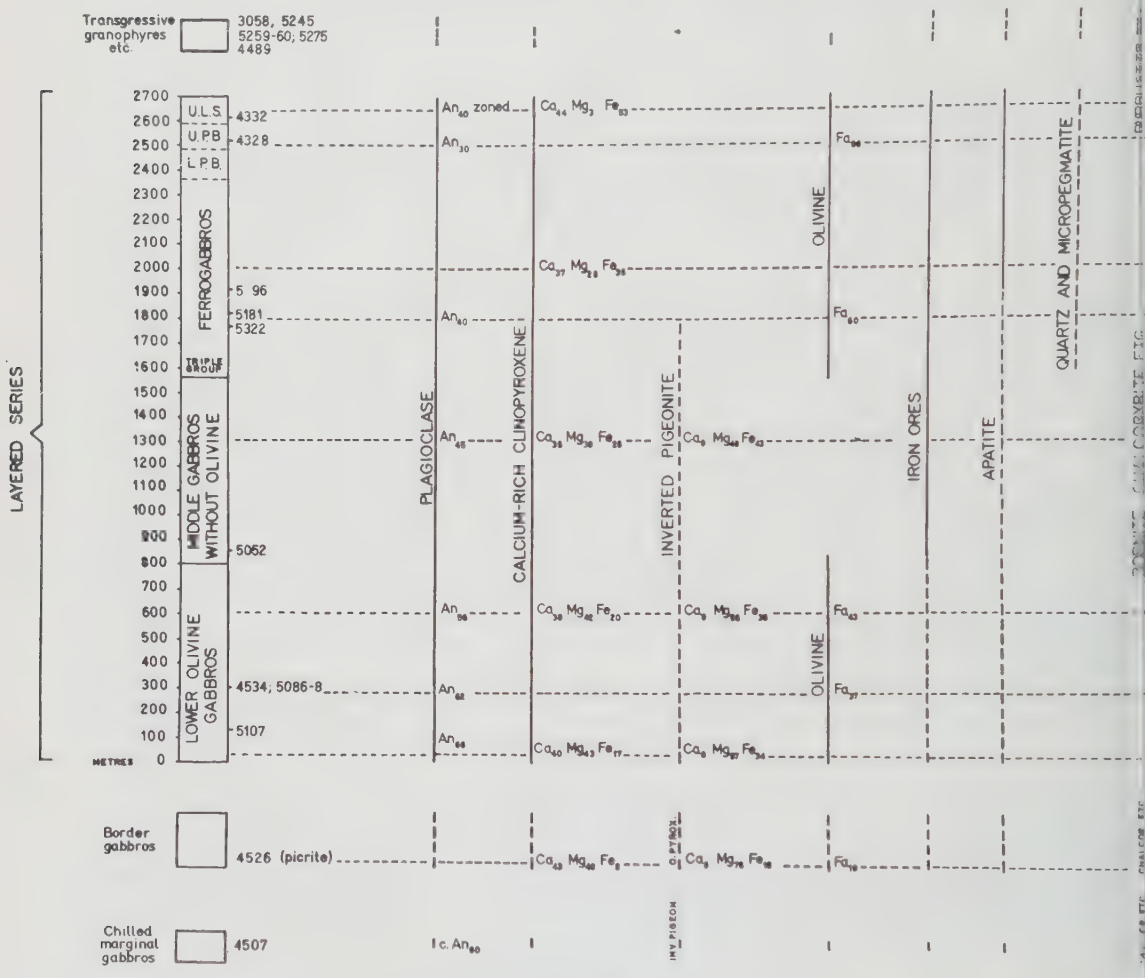

Fig. 1. Variations in the minerals of the Skaergaard rocks. Continuous vertical lines indicate primary precipitate minerals, broken vertical lines interprecipitate or undifferentiated minerals. The numbers and horizons of rocks analysed for gold are inserted. (The rock number at approximately 1900 m should read 5196.)

(4507),* taken to represent the composition of the 300 km^3 of initial magma from which the intrusion crystallized contains 0·0046 p.p.m. Au, and a glance at the table shows that the gold contents of all the other rocks analysed throughout the differentiated series are within a factor of 2 of this amount, with four exceptions indicated in italic figures.

The gabbro-picrite of the northern Border Group, interpreted as the result of accumulation of early olivine, pyroxene and plagioclase by sinking, contains a little less gold than the original magma. It is possible that this material may approximate in composition to some of the Hidden Layered Series representing the first 60 per cent of the magma to crystallize.

Table 1. Gold in rocks of the Skaergaard intrusion

Rock no. E.G.	Type	Structural height (m)	Au content determined (replicate samples) (p.p.m.)	Average Au content Normal rocks (p.p.m.)	Anomalous rocks (p.p.m.)	Remarks
Late Differentiates						
5260	Transgressive		0·0040, 0·0037 (J. H. C.)	0·0039		
5259	acid		0·0030, 0·0032 (J. H. C.)	0·0031		
3058	granophyres		0·0039, 0·0041 (E. A. V.)	0·0040		
4489			0·071, 0·074 (J. H. C.)		*0·073*	
Layered Series						
4332	Basic hedenbergite granophyre (Unlaminated Layered Series)	2590	0·0083, 0·0087 (J. H. C.)	0·0085		
4328	Fayalite ferrogabbro, Upper Purple Band	2500	0·0029, 0·0029 (J. H. C.)	0·0029		Rock carries *c.* 2 per cent by weight of iron sulphides
5196	Hortonolite ferrogabbro, melanocratic band	1900	0·028, 0·028, 0·027 (E. A. V.)		*0·028*	Rock carries *c.* 0·4 per cent by weight of copper sulphides
5181	Hortonolite ferrogabbro, average rock	1800	0·0029, 0·0033 (J. H. C.)	0·0031		Rock carries 0·03 per cent by weight of copper sulphides
5322	Hortonolite ferrogabbro	c.1750	0·011, 0·011 (E. A. V.) and J. H. C.)		*0·011*	Rock relatively rich in copper sulphides (amount not measured).
5052	Middle gabbro (olivine free)	825	0·0023, 0·0024 (J. H. C.)	0·0024		
5086	Lower olivine gabbro	280	0·034, 0·031 (E. A. V.) 0·034, 0·025 0·025, 0·043 (J. H. C.)		*0·032*	
5087	Lower olivine gabbro	280	0·0042, 0·0053 (E. A. V.)	0·0048		
5088	Lower olivine gabbro, melanocratic band	280	0·0060, 0·0059 (E. A. V.)	0·0060		
4534	Lower olivine gabbro	270	0·0054, 0·0047 (E. A. V.) and J. H. C.)	0·0051		
5107	Lower olivine gabbro	110	0·0083, 0·011 (E. A. V. and J. H. C.)	0·009		
Marginal Rocks						
4526	Gabbro picrite		0·0033, 0·0033, 0·0038 (E. A. V.)	0·0035		
4507	Chilled marginal gabbro		0·0047, 0·0045 (J. H. C.)	0·0046		

The lowest exposed olivine gabbros of the differentiated Layered Series contain plagioclase (*c.* An_{60}), augite, inverted pigeonite and olivine (*c.* Fa_{40}) together with opaque iron ores and small traces of sulphides—predominantly of copper. The lowest rock from this division analysed for gold (5107) was taken from a height of 110 m on the arbitrary height scale, and contains 0·009 p.p.m. Au, twice as much as in the initial magma. Three examples (4534, 5088, 5087) taken from a somewhat higher horizon (270–280 m) all have 0·005–0·006 p.p.m. Au. The rock 5088 is a melanocratic band, rich in dark minerals (especially ores) and poor in

* The catalogue numbers refer to the collection of East Greenland rocks housed in the Department of Geology and Mineralogy, Oxford.

plagioclase; the similarity in gold content with the adjacent average rock 5087 indicates no particular concentration of gold in the mafic minerals at this horizon.

Another nearby average rock, 5086, is anomalous. This was the rock at first chosen to represent the lower olivine gabbros, and proved on analysis to contain 0·03 p.p.m. Au—six or seven times that in the initial magma. This contrasted so strikingly with the general distribution of gold in the remainder of the Layered Series that the further specimens (4534, 5087–8) from the same horizon were analysed and proved to have much lower contents of gold. We can offer no convincing explanation at present for the high gold content of this rock. It may merely represent a local chance concentration of the element or, since complete melting of acid gneiss inclusions derived from the basement complex is thought to have taken place in these lower gabbros, the extra gold may conceivably have been derived from the gneiss, although hand specimens and thin sections of the rock 5086 give no indication of gneiss having been incorporated. Specimens of the gneiss have not been analysed for gold but would have to contain very many times as much as the Skaergaard magma if the abnormally high gold contents of this rock and of the granophyre 4489 (see below) are to be explained in this way.

Only one example (5052, from a height of 825 m) of the middle gabbros has been analysed; it has about half the gold content of the initial magma.

In the hortonolite–ferrogabbros at a structural height of 1750–1900 m in the Layered Series, copper-rich sulphide minerals locally become noteworthy accessories (up to *c.* 0·4 per cent by weight), while higher still (2500 m) there is a narrow horizon with more abundant iron sulphides (up to 2 per cent by weight) (Wager *et al.*, 1957). The abnormally high gold content of the melanocratic ferrogabbro 5196 appears to be directly connected with its relative richness in accessory copper sulphides, and the same is true of the rock 5322. The fayalite ferrogabbro 4328, on the other hand, has the usual low concentration of gold, despite its carrying about 2 per cent by weight of iron sulphides.

As an example of the basic hedenbergite granophyre which comes at the top of the differentiated Layered Series, specimen 4332 has been analysed; its gold content is about twice that of the initial magma. The rock contains a small quantity of iron sulphide (Wager *et al.*, 1957, p. 869).

The latest differentiates of all are acid granophyres, forming transgressive sill-like masses cutting earlier rocks; the field relations are none too clear. A transgressive hedenbergite granophyre, 4489, is also abnormally rich in gold, which could once more conceivably be due to the incorporation into the residual magma at this late stage of appreciable quantities of the acid gneiss of the basement complex. Three other examples, however, of the ultimate acid differentiates all carry 0·003–0·004 p.p.m. Au. There is thus no evidence of any appreciable overall concentration of gold in the late magmatic fractions responsible for these acid rocks. The slight possibility remains that gold might have become appreciably concentrated in the very last hydrothermal solutions remaining from the latest acid granophyres, and subsequent precipitation from these solutions, quite fortuitously, in the earlier transgressive hedenbergite granophyres may account

for the high gold content of 4489. This rock does indeed show some evidence of hydrothermal alteration.

The distribution of gold in the rocks of the intrusion is summarized in Fig. 2, in which the analytical results are plotted against percentage of the magma solidified. A horizontal line has been drawn through Au = 0·0046 p.p.m.—the gold content of the initial magma, and as remarked earlier it will be clearly seen that with the four exceptions already noted (two of them copper sulphide rich rocks) all the analyses fall between the broken lines representing half (0·0023) and

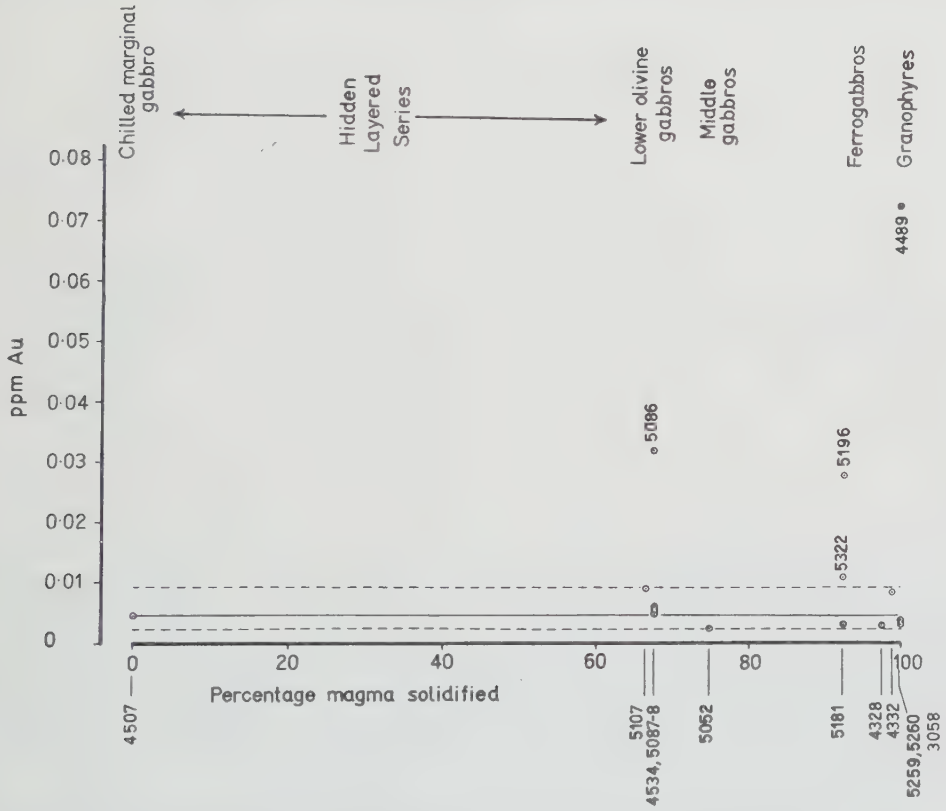

Fig. 2. Gold in the Skaergaard rocks plotted against percentage of the magma solidified. The full horizontal line is drawn through Au = 0·0046 p.p.m. (initial magma) and the broken lines at half (0·0023 p.p.m.) and twice (0·0092 p.p.m.) this value.

twice (0·0092) this initial value. The constancy of the gold content of these very strongly fractionated rocks is the most remarkable result of this work, and implies that throughout the entire crystallization of the intrusion the gold contents of the successive residual liquid fractions can scarcely have deviated significantly from that of the original magma. The amplitude of the variation is so small that any attempt at comparing the gold contents of the rocks and the magmatic liquids at various stages (in the manner outlined for S, Cu, Co and Ni in Wager *et al.*, 1957, pp. 881–883) proves to be artificial and probably misleading.

Gold in the Minerals

Apart from the observed concentration of gold in melanocratic rocks at the copper sulphide horizon in the ferrogabbros, the general uniformity of gold content of the Layered Series rocks suggests that the element is fairly evenly distributed among the predominant silicate and oxide minerals, and that the gold content of these shows little change with progressive fractionation. These suggestions are confirmed by direct analyses for gold made on pure samples (at least 99–99·5 per cent) of the component minerals separated* from rocks at two different horizons, the results of which are given in Tables 2 and 3.

Table 2. Gold in constituent minerals of middle gabbro, E.G.5052 (anal. J. H. C.) (structural height in layered series: 825 m)

Mineral	Modal % by weight	Au content, by analysis (p.p.m.)		Au content contributed to rock by mineral (p.p.m.)
Plagioclase, An_{50}	48	0·0013	0·0015	0·00067
Pyroxene, $Ca_{37}Mg_{41}Fe_{22}$	29	0·0028	0·0031	0·00088
Titaniferous magnetite	9	0·0030	0·0030	0·00027
Ilmenite	14	0·0028	0·0030	0·00041
Whole rock		0·0023	0·0024	$\Sigma = 0·00223$

With the exception of the olivine in 5181, the gold contents of the chief constituent minerals in both rocks all agree again within a factor of 2, and no particular mineral, silicate or oxide, can be singled out as an exceptionally favourable or unfavourable host for the element. Most of the gold found by direct analysis of the whole rock specimens is accounted for by the contributions made by the primary minerals, and the agreement between the sums of these contributions and the gold contents of the rocks as determined is regarded as satisfactory. In the case of the hortonolite ferrogabbro 5181, the difference (0·0007 p.p.m.) may possibly be due to traces of sulphides and some interstitial secondary minerals which have not been distinguished from the chief phases in the modal analyses. The rock 5051 is cleaner, and carries much less secondary material; the fair agreement between the total gold in the rock and the sum of that in the constituent primary minerals of 5181, however, indicates that even in this rock the interstitial liquid was not very significantly enriched in gold relative to the early crystallized phases.

Comparing the minerals of one rock with those of the other, the greatest difference is to be observed in the gold contents of the plagioclases–0·0014 and

* The separations were made using an isodynamic magnetic separator, final purification being done by hand-picking. The use of Clerici's solution was avoided because of the danger of its containing traces of other heavy metals including gold.

0·0027 p.p.m., respectively, though this two-fold increase probably has little geochemical significance.

It appears, then, that a variety of different crystal-structural types are able to accommodate occasional atoms of gold with equal facility, a result which might perhaps have been forecast on the assumption that the noble metal gold is likely to remain as uncharged atoms in the magma, rather than forming charged ions whose admission into the crystal lattices of silicates and oxides would be much more rigidly controlled by crystal chemical factors.

Table 3. Gold in constituent minerals of hortonolite ferrogabbro, E.G.5181 (anal. J. H. C.) (structural height in layered series: 1800 m)

Mineral	Modal % by weight	Au content, by analysis (p.p.m.)		Au content contributed to rock by mineral (p.p.m.)
Plagioclase, An_{40}	54	0·0029	0·0025	0·00146
Pyroxene, $Ca_{35}Mg_{34}Fe_{31}$	23	0·0021	0·0018	0·00046
Olivine, Fa_{60}	13	0·0008	0·0009	0·00012
Titaniferous magnetite	4·5	0·0043	0·0040	0·00019
Ilmenite	5·5	0·0029	0·0029	0·00016
Whole rock		0·0029	0·0033	$\Sigma = 0·00239$

The olivine of the hortonolite ferrogabbro 5181 contains appreciably less gold—three or four times less—than the other minerals, which may suggest that the densely-packed olivine structure provides fewer favourable opportunities for gold atoms to be incorporated during crystallization. Both the spinel and ilmenite structures, on the other hand, are also densely packed, and yet these minerals carry as much gold as do the rest of the silicates. The middle gabbro 5112 carries no olivine as a primary precipitate phase and no analyses for gold have been made on olivines from other horizons in the intrusion.

The melanocratic hortonolite ferrogabbro 5196 has been mentioned as containing 0·4 per cent by weight of copper sulphide globules and having a gold content of 0·028 p.p.m.—about ten times that in the adjacent average rocks. Apatite forms a conspicuous primary precipitate phase at this horizon, and is particularly abundant in the melanocratic rocks. Although it seemed unlikely that apatite would prove to be a favoured host mineral for gold, the possibility existed and a sample was extracted from a nearby ferrogabbro, 4312, rather higher in the sequence at a structural height of 1920 m. This apatite contains only 0·004 p.p.m. Au, and it seems that the high gold content of the ferrogabbros 5196 and 5322 is very probably due to its concentration in the sulphide minerals. It is impossible to separate the accessory copper sulphides from the rock and so verify this conclusion by direct analysis and in view of the unexplained anomalously high values for gold in the sulphide-free rocks 5086 and 4489 (Table 1) some doubt

must inevitably remain as to whether the gold is in fact concentrated in the copper sulphides.

Optical examination of the constituent minerals of the melanocratic hortonolite ferrogabbro 5196 indicates that they are almost identical in composition with those in the average rock 5181, the only significant difference in the rocks is in the relative proportions of the minerals. The analyses presented above show that there can be but negligible differences in the gold contents of the same mineral in the two rocks, or of the different minerals in one rock. The modal proportions of copper sulphides in the average and melanocratic rocks are approximately 0·03 and 0·4 per cent by weight, respectively, and the gold contents of the two rocks are 0·0031 and 0·028 p.p.m. The tenfold increase in gold in the melanocratic rock is approximately in proportion to its increased content of copper sulphide. It appears likely that the sum of the gold contents of silicates and oxides in the average rock 5181 (0·003) p.p.m. equals the sum of the gold contents of silicates, oxides and apatite in the melanocratic rock 5196, so that the gold not accounted for in these latter minerals (0·028 — 0·003 = 0·025 p.p.m.) is presumably concentrated in the 0·4 per cent of copper sulphides in the rock. This gives as a very rough estimate 0·025 × 100/0·4 = 6 p.p.m. for the gold content of the copper sulphide globules. These copper sulphides are considered (Wager *et al.*, 1957, p. 860, Fig. 3) to represent droplets of an immiscible sulphide liquid in the silicate magma, so that the ratio of gold in the sulphide (6 p.p.m.) to gold in the silicates (0·003 p.p.m.) gives a value of 2000 for the partition coefficient of gold between copper sulphide and silicate liquids at this stage in the intrusion.

The analysed fayalite ferrogabbro 4328, at a structural height of 2500 m in the intrusion, carries about 2 per cent by weight of iron sulphides (pyrrhotite and marcasite replacing it), again undoubtedly originally in the form of immiscible liquid droplets (Wager *et al.*, 1957, p. 866, Figs. 9, 10). In contrast to the copper sulphide bearing ferrogabbros its gold content is only 0·0029 p.p.m., and there can have been no tendency whatever for gold to enter the iron sulphide matter in preference to the silicate minerals. This is to some extent confirmed by the direct estimation of gold in pyrrhotite and pyrite separated pure from two of the uppermost granophyres of the intrusion, representing the latest residual magmatic fractions. Both these rocks carry sulphides —very locally and sporadically—in pieces large enough to separate from the enclosing rock (Wager *et al.*, 1957, p. 870, Figs. 12, 13).

	Au, (p.p.m.)
Pyrrhotite from acid granophyre, 5275	0·0027; 0·0029
Pyrite from acid granophyre, 5245	0·015; 0·017

The fivefold greater concentration of gold in the pyrite compared with the pyrrhotite is probably significant, but neither of these iron sulphide minerals apparently compares with the bornite, digenite and chalcopyrite in the lower ferrogabbros as a favoured host for gold.

Aspects of the Geochemistry of Gold Exemplified by the Skaergaard Intrusion

Apart from somewhat rare occurrences as the telluride or in mixed tellurides with silver and bismuth, gold is found in nature as the native metal; Clarke (1924) in the 5th Edition of his *Data of Geochemistry* cites several instances where native gold has been identified as a primary constituent of igneous rocks as diverse as granite, pitchstone and dunite. The geochemistry of gold is in most respects quite different from the other group IB metals, Cu and Ag, and in particular the first ionization potential for Au (9·22 V) is much greater than for Cu or Ag (7·7 and 7·57 V, respectively). Ahrens (1953) is of the opinion that were it not for this high ionization potential—a direct consequence of the lanthanide contraction—the chemical and geochemical properties of gold would lie midway between those of monovalent silver and monovalent thallium.

Gold, therefore, is oxidized to the aurous or auric state only with considerable difficulty, and then tends to bond with suitable anionic partners, such as S^{2-} and Cl^- to form stable complexes, in which form it is generally transported in natural mineralizing solutions. Krauskopf (1951) in discussing the solubility of gold under various conditions shows that in even weakly acid solution in the presence of enough Cl^- and an oxidizing agent such as MnO_2, O_2, Fe^{3+} or Cu^{2+} the stable tetrachloroaurate ion, $AuCl_4^-$, is readily formed. In alkaline solutions containing the S^{2-} ion, gold is probably present as the AuS^- complex ion. From a consideration of the appropriate standard electrode potentials, Krauskopf states that neither of the *simple* ions Au^+ or Au^{3+} can exist in solution in geological environments.

The clear conclusion to be drawn from the nearly constant amount of gold in the rocks and minerals of the Skaergaard intrusion is that gold was present in the magma, and became incorporated into the various crystallizing minerals, in the form of uncharged atoms. It seems unlikely that conditions in the magma could possibly have led to the formation of either the $AuCl_4^-$ or the AuS^- complexes to any significant extent; Goldschmidt (1954) points out moreover that the tendency for elements to form complex ions is greatly reduced at high temperatures.

Krauskopf's statement that simple aurous or auric ions could not exist under geological conditions may be illustrated by a rough calculation of the oxidation potential of the Skaergaard magma at some stage in its fractionation, as estimated from the ferric-ferrous iron ratio, and applying the result to the gold/aurous ion and gold/auric ion oxidations. The Skaergaard fourth liquid, remaining after 95 per cent of the initial magma had crystallized, may be considered; the ultimate result would be little altered if any other stage were chosen. According to Wager and Deer (1939) this liquid contained about 19 per cent FeO and 4 per cent Fe_2O_3, corresponding to 14·8 per cent Fe^{2+} and 2·8 per cent Fe^{3+}; we will consider this liquid, arbitrarily, at a temperature of 1000°C.

Making the usual assumptions that activities are more or less proportional to concentrations, the oxidation potential of the liquid is given by

$$E_h = -E^\circ + \frac{RT}{nF} \ln \frac{[Fe^{3+}]}{[Fe^{2+}]} \quad \text{(see Garrels, 1953)}$$

where E° for the couple $Fe^{2+} = Fe^{3+} + e = -0{\cdot}771$ V;

$R = 8{\cdot}314$ absolute joules per degree-mole;
$T = 1273°K$;
$n = 1$ (the number of electrons transferred in the reaction);
$F = 96{,}500$ C.

Substituting the Fe^{3+}/Fe^{2+} ratio for the Skaergaard 4th liquid in this equation, we obtain:

$$E_h = 0{\cdot}555 \text{ V}$$

Now, for the reaction $Au = Au^+ + e$, $E^\circ = -1{\cdot}68$ V (Latimer, 1952), and $n = 1$, so that, in the Skaergaard fourth liquid at 1000°C:

$$0{\cdot}555 = 1{\cdot}68 + \frac{8{\cdot}314 \times 1273 \times 2{\cdot}303}{1 \times 96{,}500} \log \frac{[Au^+]}{[Au]}$$

whence

$$\log \frac{[Au^+]}{[Au]} = -4{\cdot}4453$$

and

$$Au = 2{\cdot}8 \times 10^4 \, Au^+$$

In view of the considerable inaccuracies and assumptions involved (for example the application of Latimer's E° values for aqueous solutions at 25°C to a basic rock melt at 1000°C), we may only say that the ratio of metallic gold to aurous ion in the Skaergaard fourth liquid was very high indeed, possibly about 10,000 : 1. A similar calculation for the oxidation of gold to the Au^{3+} ion leads to a ratio Au/Au^{3+} of about 10^{10}. From these considerations then, also, it may be concluded with some confidence that we are dealing in this intrusion with uncharged atoms of gold.

The concentration of gold observed in the Skaergaard silicate and oxide minerals is lower, generally by a factor of 1000–100,000, than the concentrations of many other trace elements, such as nickel, cobalt, copper, gallium, etc. (Wager and Mitchell, 1951). No matter how low its concentration, however, we would expect the entry of any trace element *ion* into a rock-forming mineral to be governed by the usual considerations such as radius, charge and ionization potential. The incorporation of an uncharged atom, on the other hand, seems to be a much more random process. Throughout the differentiation series, the proportion of gold atoms in the rock-forming silicate and oxides remain of the same order as in the liquid, and a growing crystal will probably include such neutral atoms as are in the immediate vicinity. Being uncharged, there will be no particular forces tending to attract or repel the gold atoms to or from lattice sites in the growing crystals, and of the usual factors governing the entry of trace elements into crystals only the comparatively large radius of the gold atom (1·44 Å) may possibly be significant.

It is impossible to say precisely where the gold atoms are located in crystals of any particular mineral. In general, the common minerals have imperfect mosaic structures in which blocks of a finite number (say, 10^4–10^{12}) unit cells are arranged in a parallel or, more commonly, a sub-parallel pattern throughout the

crystal. The geometrically perfect structure of the lattice within each block may in some minerals provide spaces large enough for a gold atom to lodge there; in others there are no such spaces and in general it is perhaps more likely that the occasional gold atoms are situated in the spaces left between adjacent blocks of the mosaic, and in this sense cannot be regarded as occupying any specific sites in the crystalline structure. At the concentrations with which we are dealing here, the incorporation of an occasional large atom of gold into any of the crystal structures would be an insignificant matter. In an augite, for example, with 0·0025 p.p.m. Au, a single gold atom would be associated with approximately every hundred million unit cells.

There remains to discuss the interesting observation that while the gold contents of the accessory iron sulphide minerals of the Skaergaard intrusion are not very different from those of the silicates and oxides, there is some evidence of a spectacular concentration (by a factor of 2000–3000) in the copper and copper–iron sulphides. The vertical interval in the Layered Series where immiscible droplets of copper sulphides formed noteworthy accessories is small, and the preferential entry of gold into these droplets cannot so have depleted the magma in this element that much less was available to enter the iron sulphides forming later. Analyses of the higher rocks in the series—above the copper sulphide horizon—show that the gold content of the magma was virtually unchanged.

Gold is a classic example of a siderophile element in its general geochemistry, as was stressed by Goldschmidt, but the frequent occurrence of appreciable traces of gold in sulphide minerals (pyrite, for example) has sometimes led geochemists to regard it as having certain chalcophile tendencies also. Although on an extremely small scale, the Skaergaard result suggests that gold is here exhibiting a strong coherence with copper in the sulphides, rather than a general chalcophilic tendency.

Interatomic bonding in most of the common sulphide minerals has generally been regarded as dominantly covalent in character, and Ahrens (1953) points out that the application of ionic radii and ionization potentials has only limited usefulness in dealing with their structures; while Frueh (1954) views the crystal structures in the copper-rich part at least of the Cu–Fe–S system from the metallic bond side of covalency, so to speak, rather than from the ionic. If this latter view be accepted, it might be appropriate for the present discussion to bear in mind the close similarity in radius (Cu 1·28 Å; Au 1·44 Å) and electronic configuration between the uncharged copper and gold atoms, and the different configuration of the transition metal iron. Traces of gold may possibly enter these copper sulphide minerals on much the same terms as when gold forms metallic alloys with copper.

The actual Skaergaard silicate and oxide minerals analysed for gold were not also analysed for copper, but spectrographic and colorimetric determinations of copper are available for some of the minerals of the melanocratic copper-sulphide rich ferrogabbro 5196 (Wager *et al.*, 1957, Table VII) and for the ferrogabbro 4318 occurring some 400 m higher in the layered series (*ibid.* Table VI). These figures, and others previously published by Wager and Mitchell (1951) show that the copper contents of the various non-sulphide minerals vary considerably from one mineral to another in the same rock, and in the same mineral species from bottom

to top of the differentiated series. The uniform distribution of gold is in striking contrast, presumably because copper is bound in the silicates and oxides by forces having a greater degree of ionic character than in the sulphides.

Acknowledgements—We wish to record our gratitude to Professor L. R. Wager for selecting and providing representative material from the Skaergaard intrusion and for valuable discussions we have had with him during the course of the work. Mr. A. A. Smales of AERE, Harwell, has given us much help and advice over analytical problems, and we would also thank Drs. H. D. Holland, G. M. Brown and M. G. Bown for helpful discussions. One of us (J. H. C.) gratefully acknowledges the award of a Rhodes Scholarship. The neutron irradiations required for this work were carried out in the Harwell pile BEPO, by arrangement with the Isotope Division of the Atomic Energy Research Establishment.

References

Ahrens L. H. (1953) The use of ionization potentials—II. Anion affinity and geochemistry. *Geochim. et Cosmochim. Acta* **3,** 1–29.

Bragg W. L. (1937) *Atomic Structure of Minerals.* Cornell University Press, New York.

Clarke F. W. (1924) *The Data of Geochemistry.* (5th Ed.). USGS. Bull. 770.

Frueh A. J., Jr. (1954) The use of zone theory in problems of sulphide mineralogy. *Geochim. et Cosmochim. Acta* **6,** 79–89.

Garrels R. M. (1953) Some thermodynamic relations among the vanadium oxides, and their relation to the oxidation state of the uranium ores of the Colorado Plateau. *Amer. Min.* **38,** 1251–1265.

Goldberg E. D. and Brown H. (1950). Radiometric determination of gold and rhenium. *Analyt. Chem.* **22,** 308–311.

Goldschmidt V. M. (1954) *Geochemistry* (Edited by Muir A.). Clarendon Press. Oxford.

Krauskopf K. B. (1951) The solubility of gold. *Econ. Geol.* **46,** 858–870.

Latimer W. M. (1952) *The Oxidation States of the Elements and their Potentials in Aqueous Solutions.* (2nd Ed.). Prentice Hall, New York.

Vincent E. A. and Smales A. A. (1956) The determination of palladium and gold in igneous rocks by radioactivation analysis. *Geochim. et Cosmochim. Acta* **9,** 154–160.

Wager L. R. and Deer W. A. (1939) The petrology of the Skaergaard intrusion, Kangerdlugssuaq, East Greenland. *Medd. om Grønland* **105,** No. 4, 1–352.

Wager L. R. and Mitchell R. L. (1951) The distribution of trace elements during strong fractionation of basic magma—a further study of the Skaergaard intrusion, East Greenland. *Geochim. et Cosmochim. Acta* **1,** 129–208.

Wager L. R., Vincent E. A. and Smales A. A. (1957) Sulphides in the Skaergaard intrusion, East Greenland. *Econ. Geol.* **52,** 855–903.

Geochimica et Cosmochimica Acta, 1960, Vol.1, pp. 143 to 148. Pergamon Press Ltd. Printed in Northern Ireland

Studies in the geochemistry of gold—II

The gold content of some basic and ultrabasic rocks and stone meteorites

E. A. Vincent and J. H. Crocket*
Department of Geology and Mineralogy, University Museum, Oxford

(*Received* 6 *May* 1959)

Abstract—Analyses by the neutron activation method reveal about 0·002 p.p.m. Au in two basalts from the British Tertiary igneous province and in one Recent Hawaiian flow. From 0·001 to 0·01 p.p.m. Au has been found in dunites and olivine-rich nodules included in basalts, the majority of results being appreciably higher than for the basalts analysed. Four chondritic meteorites carry from 0·1 to 0·3 p.p.m. Au, which appears most probably to be concentrated in the dispersed metallic phase.

In a previous paper (Vincent and Crocket, 1959) the writers discussed the geochemical significance of the gold contents, as estimated by neutron activation analysis, of rocks and minerals from the Skaergaard gabbroic complex. The same method has also been used to determine gold in a few basalts, dunites and chondritic meteorites, and the object of the present paper is to discuss these further results briefly. A far greater number of analyses would be required in order to arrive at a sound average for the gold content of basic and ultrabasic rocks in general and to determine its upper and lower limits and the pattern of its distribution.

Gold in Basalts

Samples of three much-described and typical Tertiary and Recent basalts have been analysed for gold (Table 1).

Table 1. Gold content of three typical basalts (analyst: J. H. Crocket)

	Au content (duplicate analyses) (p.p.m.)	Mean Au content (p.p.m.)
Tertiary olivine basalt ("Plateau magma type"), Morvern, Scotland.	0·0021, 0·0023	0·0022
Tertiary tholeiitic basalt, Giant's Causeway, Co. Antrim, N. Ireland.	0·0021, 0·0019	0·0020
Tholeiitic olivine basalt, eruption of 1919, Mauna Loa, Hawaii	0·0024, 0·0027	0·0026

* Present address: Department of Geology and Geophysics, Massachusetts Institute of Technology.

The strikingly close agreement between the results was not anticipated, and, of course, may very well prove to be fortuitous when further analyses become available. The chilled marginal gabbro representing the parent magma of the Skaergaard Complex, and broadly comparable with tholeiitic basalt in composition, contains 0·0046 p.p.m. Au—just twice the amount in the three basalts analysed (Vincent and Crocket, 1960). The standard diabase sample of the U.S. Geological Survey, W–1, from Centerville, Virginia, contains 0·0084 p.p.m. Au, four times that found in the basalts, and twice that in the standard granite sample G–1, from Westerly, Rhode Island (Table 2; see also Vincent and Crocket, 1960, p. 130).

Table 2. Gold contents of USGS standard granite and diabase samples (new analyses by J. H. Crocket)

	Au content (duplicate samples) (p.p.m.)	Mean Au content (p.p.m.)
Granite, G–1	0·0046 0·0043	0·0045
Diabase, W–1	0·0085 0·0083	0·0084

Macgregor (1951) has drawn attention to the close association often observed between basaltic igneous rocks (or their metamorphosed equivalents) and invading granite masses in regions where economic deposits of gold are found. He suggests that the primary source of the gold is in the sima where it is diffused in the basaltic materials. Reactions between the extruded or intruded products of basaltic magma and later molten granite or granitizing fluids could perhaps provide fluxes able to dissolve the gold out of the incorporated basic material and then later to transport it into the mineral deposits. It would be interesting to find out whether basaltic rocks in the neighbourhood of such gold deposits carry roughly the same proportions of the element as we have found in our analyses. Further, it might be possible in some favourable instance to test Macgregor's hypothesis by direct analysis.

Gold in Dunitic Materials

Bowen (1928) argued the case for the production of basalt magma by partial melting of peridotitic material in the upper regions of the mantle, rather than by local remelting of a vitreous basalt layer as postulated by Daly, and his ideas have recently been elaborated by Wager (1958). A comparison of the gold content of materials which may conceivably have come from the mantle with those of the basalts is therefore of some interest.

Hess (1955) considers the alpine type of peridotite mass, occurring in orogenic belts, to represent material from the mantle pushed into the crust in a down-buckle, or tectogene. Other peridotites and dunites, very similar petrographically to the alpine type, undoubtedly represent the early accumulation of olivine from a normal basaltic magma subsequent to its injection into the upper parts of the crust; they are autochthonous cumulites, as defined by Wager (1958, p. 35).

The dunitic nodules occasionally found in basalts in various parts of the world may also represent fragments derived directly from the mantle and carried up during local volcanic activity, as believed for the majority of cases by Ross, Foster and Myers (1954); such an origin, however, is by no means proved for all cases, and some of the nodules in basalts may well represent fragments of autochthonous olivine cumulites.

Table 3. Gold content of dunitic materials (analyst: E. A. Vincent)

	Au content (duplicate samples) (p.p.m.)	Mean Au content (p.p.m.)
Peridotites:		
Alpine type dunite, Balsam, N. Carolina (coll. by G. M. Brown)	0·0023, 0·0021	0·0022
Autochthonous olivine cumulite, average Rhum peridotite (H5328–34; Brown, 1956, p.47)	0·011, 0·011	0·011
Olivine nodules from basalts:		
Dreiser Weiher, Eifel, Germany (Ross *et al.* No. 4)	0·0099, 0·0094	0·0097
Kapfenstein, Styria, Austria (Ross *et al.* No, 5)	0·0060, 0·0061	0·0061
Camargo, Chihuahua, Mexico (Ross *et al.* No. 1)	0·00096, 0·00082	0·0009
Ludlow, California (Ross *et al.* No. 2)	0·0014, 0·0020	0·0017
Peridot Cove, near Globe, Arizona (Ross *et al.* No. 3)	0·0063, 0·0061	0·0062
Salt Lake Crater, Oahu, Hawaiian Islands (Ross *et al.* No. 8)	0·0058, 0·0064	0·0061

Gold has been determined in six olivine nodules kindly provided by Dr. C. S. Ross and described in Ross, Foster and Myers (1954); in an alpine type peridotite from the Appalachian fold belt, and in an undoubted autochthonous olivine cumulite from the Island of Rhum. The results are given in Table 3.

The Appalachian dunite has the same gold content as the Tertiary and Recent basalts analysed; the Rhum peridotite five times as much. The nodules from basalts show a far greater range in gold content than any other materials so far analysed, even though the results for three out of six are identical; unfortunately, no analyses have been made of a nodule and the actual enclosing basalt in which it was found.

In the case of the Skaergaard intrusion it was found that, with very few exceptions, the gold contents of rocks formed at all stages during the extreme fractional crystallization of the magma remained surprisingly constant (within half and twice the amount in the initial magma) and that the uncharged gold atoms were equally evenly distributed among all the constituent silicate and oxide minerals. This inert, non-selective behaviour would be expected also on fractional melting, so that basalt produced by partial melting of the peridotite of the upper mantle would probably have about the same gold content as this peridotite. The results we have obtained contribute little to solving the question of the origin of the olivine nodules; if some or all represent material from the mantle, then the distribution of gold in the upper parts of the mantle is not very uniform, in a lateral or a vertical sense, or both. The fact that most of the dunites analysed contain three or four times more gold than the basalts seems perhaps at variance with the postulate that they represent the parent material for the basalts, but no conclusion on this extremely important question is justified from these very few disconnected observations on the distribution of a single element.

Gold in Chondritic Meteorites

Table 4 gives the results of analyses for gold made on four meteorites (all observed falls) from the collection in the Oxford University Museum; the powdered samples used were prepared under the direction of Mr. A. A. Smales, of the Atomic Energy Research Establishment, Harwell.

As might be anticipated, these materials contain a far higher proportion of gold than the basic and ultrabasic rocks, and the element, in accordance with its strongly siderophile nature, is almost certainly concentrated in the dispersed

Table 4. Gold content of stone meteorites (analyst: E. A. Vincent)

Meteorite	Type	Au content (duplicate samples) (p.p.m.)	Mean Au content (p.p.m.)
Faha (Limerick) (fell 10/9/1813)	Veined grey bronzite–chondrite	0·29, 0·28	0·29
Bjurböle, Finland (fell 12/3/1899)	Spherical hypersthene–chondrite	0·102, 0·097	0·10
Château Renard, Montargio, Loiret, France (fell 12/6/1841)	Veined intermediate hypersthene–chondrite	0·13, 0·12	0·13
Tabory, Ochansk Perm, Russia (fell 30/8/1887) (4·5% metal phase extracted before analysis)	Polymict brecciated spherical bronzite–chondrite	0·13, 0·15	0·14

metallic phase of the chondrites. If we assume the gold contents of the various silicate phases to be only about the same as found in the dunites (0·001–0·01 p.p.m.), we may ignore them and derive the approximate gold content of the metallic phase (Table 5).

The higher gold content of Limerick (Faha) is in proportion to its higher metal content as compared with Bjurböle and Château Renard; assuming as a first approximation that all the gold is in the metal phase the nickel–iron portion

Table 5. Approximate gold content of metallic phase of chondrites

Meteorite	Au content found (p.p.m.)	Metal phase (%)	Approx. Au content in metal phase (p.p.m.)
Faha	0·29	20·3*	1·4
Bjurböle	0·10	7·7*	1·3
Château Renard	0·13	~8·5†	1·5
Tabory	0·14	~24‡	(0·74)

* From analyses quoted and accepted as reliable by Urey and Craig (1953).
† Prior (1919)
‡ Tchirvinsky (1921) } Analyses discarded by Urey and Craig.

of all these three chondrites contains about 1·4 p.p.m. Au. This is in agreement with the results of Goldberg *et al.* (1951) who found an average of 1·44 p.p.m. Au in forty-five iron meteorites. The range reported by these writers is 0·45–2·54 p.p.m. Au (excluding one at 0·09 p.p.m. and another at 8·74 p.p.m.), with the majority carrying between 1 and 2 p.p.m. The sample of the Tabory (Ochansk) meteorite had about 4·5 per cent of metal phase extracted from it at Harwell, and microscopic examination of a polished sample of the analysed grains indicated that not more than about 10 per cent of metal phase remained. The figure of 0·7 p.p.m. Au in the metal phase of Tabory, given in Table 5, however, is based upon Tchirvinsky's analysis, showing 24 per cent metal, less the 4·5 per cent. Since the sample now analysed for gold almost certainly had far less metal than this (though no accurate estimate has been attempted) the true gold content of the metal phase of Tabory is probably closer to that of the other chondrites.

Acknowledgements—We are grateful to Professor L. R. Wager, Dr. C. S. Ross and Dr. G. M. Brown for providing samples for analysis, and to Professor Wager for useful discussion during the course of the work. Mr. A. A. Smales, of AERE, Harwell, has freely given his advice on analytical matters; the neutron irradiations required were carried out in the Harwell pile BEPO, by arrangement with the Isotope Division of the Atomic Energy Research Establishment.

References

Bowen N. L. (1928) *Evolution of the Igneous Rocks* Ch. 17. Princeton University Press.
Brown G. M. (1956) The layered ultrabasic rocks of Rhum, Inner Hebrides. *Phil. Trans.* B**240**, 1–53.

Goldberg E., Uchiyama A. and Brown H. (1951) The distribution of nickel, cobalt, gallium, palladium and gold in iron meteorites. *Geochim. et Cosmochim. Acta* **2,** 1–25.

Hess H. H. (1955) Serpentines, orogeny and epeirogeny. *Geol. Soc. Am. Special Paper* **62,** 391–407.

Macgregor A. M. (1951) The primary source of gold. *S. Afr. J. Sci.* **47,** 157–161.

Prior G. T. (1919) A method for the quick determination of the approximate amount and composition of the nickeliferous iron in meteorites; and its application to seventeen meteoric stones. *Min. Mag.* **18,** 349–353.

Ross C. S., Foster M. D. and Myers A. T. (1954) Origin of dunites and of olivine-rich inclusions in basaltic rocks. *Amer. Min.* **39,** 693–737.

Tchirvinsky P. (1921) Étude de la météorite d'Okhansk. *Bull. Soc. franç. Miner.* **44,** 162–169.

Urey H. C. and Craig H. (1953) The composition of the stone meteorites and the origin of the meteorites. *Geochim. et Cosmochim. Acta* **4,** 36–82 (especially Table 2).

Vincent E. A. and Crocket J. H. (1960) The distribution of gold in rocks and minerals of the Skaergaard intrusion, East Greenland. *Geochim. et Cosmochim. Acta.* **18,** 130–142.

Wager L. R. (1958) Beneath the earth's crust. *Advanc. Sci. Lond.* **15,** 31–45.

Geochimica et Cosmochimica Acta, 1960, Vol. 18, pp. 149 to 150. Pergamon Press Ltd. Printed in Northern Ireland

LETTER TO THE EDITOR

Neutron activation results for vanadium and scandium in G-1 and W-1

THE vanadium content of the "standard" rocks G–1 and W–1 has been measured by several workers, mainly by emission spectroscopy, with reported results ranging from 8 to 38 p.p.m. for G–1 and 170 to 340 p.p.m. for W–1 (AHRENS, 1954; HAWLEY and MACDONALD, 1956; MCKENZIE *et al.*, 1958).

Recently SHAW (1958) has commented that "the vanadium content of W–1 is at present quite uncertain" because of the possibility that a calcium–vanadium spectral line coincidence at 3185 Å has contributed to errors in reported vanadium results. He prefers to use the 3102 Å vanadium line, which still, however, requires compensation for a calcium coincidence. He reports new figures, 230 p.p.m. and 120 p.p.m., respectively, using both lines.

SCOTT and SWAINE (1959) agree with SHAW that V 3185 Å should not be used for vanadium determinations in calcium rich samples, but point out that the coincidence at this wavelength is not a new observation, and that the result from their laboratory, reported by AHRENS, was obtained using not the 3185 Å line but one at 4379 Å.

Continuing the neutron activation work on G–1 and W–1 in this laboratory, we have recently determined vanadium (and scandium) and our results are given in Table 1 together with those of others.

Our results for vanadium on W–1 (CaO 10·96 per cent) clearly favour that obtained by SHAW using V 3185 Å, i.e. the line he does *not* recommend, and differ notably from his result obtained using his recommended V line. They also agree with, *inter alia*, that from SCOTT and SWAINE's laboratory (analyst 1 in Table 1), and with the "recommended" value of AHRENS although agreement in the latter case is somewhat fortuitous as the "recommended" value is an

Table 1. Analytical results for G–1 and W–1 (p.p.m.)

Element		Analyst (1)	(2)	(3)	(4)	(5)	(6)	(7)	(8)	(9)	SHAW (1958) using V 3102 Å	SHAW (1958) using V 3185 Å	AHRENS' recommended value	This work: Individual determinations	This work: Average
Vanadium	G–1	17	26	18	20	8	20		19 16	38	11·5	14	18	13·4, 13·2, 12·9, 13·1, 13·0, 13·0, 13·0, 12·7	13
	W–1	220	220	340	250	170	220		260 310	310 320	120	230	240	250, 244, 244, 246, 247, 244	246
Scandium	G–1	n.d.	2	4	–	<3	–						3	2·72, 2·86, 2·77, 2·84, 2·76	2·8
	W–1	15	34	51	50	35	–	36					37	34·1, 34·8, 33·5 33·5	34

Analysts: (1)–(6) taken from AHRENS (1954); (7): KVALHEIM quoted by AHRENS (1954); (8): HAWLEY and MACDONALD (1956); (9): MCKENZIE *et al.* (1958).

10A—(4 pp)

average of figures which, according to AHRENS "are in very satisfactory agreement" but which in fact range from 170 to 340 p.p.m.

Our results for scandium reinforce the values recommended by AHRENS for both G–1 and W–1.

Atomic Energy Research Establishment D. M. KEMP
Harwell, England A. A. SMALES

REFERENCES

AHRENS L. H. (1954) *Quantitative Spectrochemical Analysis of Silicates* pp. 25–29. Pergamon Press, London.
HAWLEY J. E. and MACDONALD G. (1956) *Geochim. et Cosmochim. Acta* **10,** 197–223.
MCKENZIE R. M., OERTEL A. C. and TILLER K. G. (1958) *Geochim. et Cosmochim. Acta* **14,** 68–72.
SCOTT R. O. and SWAINE D. J. (1959) *Geochim. et Cosmochim. Acta* **16,** 195.
SHAW D. M. (1958) *Geochim. et Cosmochim. Acta* **15,** 159.

Geochimica et Cosmochimica Acta, 1960, Vol. 18, pp. 151 to 153. Pergamon Press Ltd. Printed in Northern Ireland

GEOCHEMICAL NOTE

On the chemical evolution and densities of the planets

In a recent paper, Ringwood (1959) has presented an explanation for the variable densities of the terrestrial planets depending on a variable degree of reduction of silicon dioxide as well as iron oxide by carbon. He succeeds in getting a plausible agreement between the earth's elementary composition and that of the chondritic meteorites. However, there are difficulties in this theory which I have not been able to resolve during the last year since Dr. Ringwood very kindly allowed me to read his paper, and I should like to record these difficulties.

(1) No means is provided for the escape of the higher atomic weight gases from the earth. Very early in my own studies this problem was discussed. These gases must have escaped very early before any appreciable sized bodies accumulated since there is no known method by which they could be lost from a planet as massive as, or more massive than, Mars. Possibly some such loss could have occurred during the early stages of a process of planetary evolution which would be consistent with Ringwood's theory, but no such process has been suggested by him.

(2) The amount of carbon needed to produce the amounts of silicon and iron is quite large and the mass of carbon monoxide which would be produced is very appreciable, i.e. 11·3 per cent of the earth's mass of carbon monoxide to produce the silicon and 23 per cent to produce both the iron and silicon. It is obvious that these gases must have escaped from the earth and no satisfactory mechanism for the loss of gases of molecular weight 28 from the earth or even a planet like Mars is known. Ringwood makes some general suggestions but some numerical calculations show that really remarkable processes are required to produce the required losses. Thus, he suggests that energy from the continuous accumulation of dust may remove these gases, but collisions of this kind can hardly result in the removal of some 20 or 25 per cent of their own mass completely from the earth's field!

One might assume that the reduction processes occurred in objects of smaller mass than the earth, say of lunar mass for example, and that the carbon monoxide was lost *before* the earth accumulated. In this case one notes that the Moon and meteorites did not go through this strongly reducing process.

We assume that the source of heat for the reduction process was the gravitational energy of accumulation of the earth. Reduction in lunar sized objects could not occur because of the smaller gravitational energy involved. A temporary immersion of the lunar objects in cosmic gases which were lost before the earth accumulated is a possible explanation, but the absence of the reduction process in the Moon remains a difficulty. Also, the absence of such reduction in Mars raises further questions of a similar kind.

(3) The trend of density from the high density of Mercury to the low density of Mars suggests a solar origin for the high temperatures required for the reduction process. If the Sun at some stage had a luminosity some 10^4 times that of the present time, this might account for the required high temperature. In some ways this would be a convenient way of accounting for other difficulties in the evolution of the system (Urey, 1954). However, no explanation of the low density of the Moon is secured in this way and there is no evidence from current astrophysical theory that the Sun ever had such a high temperature.

(4) RINGWOOD postulates the meteorite planet in order to explain the structures of the meteorites. These objects surely cannot be explained by such a simple model for reasons much too complex to review briefly. In a paper in press, UREY and MAYEDA (1959) present many details in regard to the metallic fragments of the chondrites which require processes wholly lacking in RINGWOOD's model (see UREY, 1956).

The amount of carbon required for the reduction of the iron in the earth's core is 5 per cent of the earth's mass. If some additional carbon were present and dissolved in the iron, the low density of the earth's core indicated by the seismic data would be explained. Also, RINGWOOD and others who discuss this subject ignore the sulphur which should be present somewhere in the earth and which should further decrease the density if it is dissolved in the core. Whether sulphur would dissolve in the core at high pressures and temperatures is quite unknown so far as my information extends. It seems to me that some amounts of carbon and sulphur would give a reasonable explanation of the fact that the earth's core is not pure iron nickel according to reliable evidence.

In regard to the variable densities of the terrestrial planets, the suggestion previously made seems to be a feasible one and causes no difficulty in understanding the density of the Moon. A break-up of lunar objects produced finely divided silicates which were lost with the gaseous elements (UREY, 1956) and subsequent accumulation into the planets resulted in variable proportions of metal and silicate with the Moon remaining as one of the primary unfractionated objects. Recent data on the cosmic ray ages of the stone and iron meteorites indicate that the silicate and iron phases as represented by these objects have become separated from each other (UREY, 1959).

Two suggestions to account for this have been made: (1) The stones come from the Moon and the irons from the asteroidal belt. (2) Both come from the asteroidal belt, but the stones are destroyed by collisions some twenty-five times as rapidly as the irons. In either case we note that the separation of silicate and metal fractions has occurred.

RINGWOOD's theory for the composition of the earth is impressive but many other features of the problem must be considered. One most disturbing problem is posed by the abundances of the elements in the Sun. ALLER (1958) gives iron an abundance of $\frac{1}{7}$ that of silicon and 0·3 that of magnesium in the Sun.* The low density of the moon is consistent with a low solar abundance of iron providing the higher abundance of iron in the earth and terrestrial planets was produced by a fractionation of the silicate and metallic phases.

The writer proposed that the chondritic meteorites were a more nearly average sample of the non-volatile solar matter than any other samples which are available. It should be noted that there is no proof that these objects furnish a *true* average sample. In fact, the existence of at least two groups of chondrites should warn us that the *true* average sample may well be different from either of them. There is a great tendency for people to take averages and to believe that the average is highly reliable. This has been done by RINGWOOD in the paper under discussion, but a more sceptical attitude toward averaged data is probably desirable. Especially is this true when we have so little information in regard to the cause of the variations observed. It seems possible to me that the relative abundance of any element may differ from the values of SUESS and UREY (1956) by a factor of 2 or 3 and, in fact, there is evidence that even more serious discrepancies may exist, e.g. the maximum at Sn^{120}, the very low abundances of In, Tl, Bi and Pb. We should not take meteoritic abundances as more than an approximation to true primitive values.

University of California
La Jolla, California, U.S.A.

H. C. UREY

* I have consulted other specialists on solar and stellar abundances and find considerable agreement with respect to this low value for the solar abundance of iron.

References

Aller L. H. (1958) *Handbuch der Physik* Vol. 51, p. 324. Springer Verlag, Berlin.
Ringwood A. E. (1959) *Geochim. et Cosmochim. Acta* **15,** 257.
Suess H. E. and Urey H. C. (1956) *Rev. Mod. Phys.* **28,** 53.
Urey H. C. (1954) *Astrophys. J.* Suppl. Ser. **1,** 147.
Urey H. C. (1956) *Astrophys. J.* **124,** 623.
Urey H. C. (1959) Primary and secondary objects. Symposium on Space Exploration, Washington, 1959. *J. Geophys. Res.* November.
Urey H. C. and Mayeda T. (1959) *Geochim. et Cosmochim. Acta* **17,** 113.

Geochimica et Cosmochimica Acta, 1960, Vol. 18, p. 154. Pergamon Press Ltd. Printed in Northern Ireland

BOOK REVIEW

The Planet Earth. Edited by D. R. Bates. Pergamon Press, London. 312 pp., 35s.

In this book fifteen distinguished specialists describe the state of their fields and in conjunction give an excellent account of the state of geophysics at the beginning of the IGY, and more particularly of the state of knowledge of the upper atmosphere and ionosphere while it still had to be attained by those indirect methods which are the delight of the profession. Although no mathematics is allowed and processes such as thermal conduction are described in footnotes, the range of argument is so wide and of necessity so condensed that few scientists could read more than one or two chapters without pause—or without profit.

The book is addressed to that mysterious layman who has had no scientific or mathematical training but must yet be capable at the end of twenty or so pages of appreciating the different views taken over the origin of mountains or magnetic storms, of the earth or of life itself. Some graduates of the older British schools might qualify; at any rate the authors succeed admirably in catering for him and provide a bibliography to guide his further reading.

H. Hughes

Geochimica et Cosmochimica Acta, 1960, Vol. 18, pp. 155. Pergamon Press Ltd. Printed in Northern Ireland

ERRATA

R. G. COLEMAN: New occurrences of ferroselite ($FeSe_2$). *Geochim. et Cosmochim. Acta* **16,** 296–301.

On p. 296 "rammelsbergite ($FeAs_2$)" should read "rammelsbergite ($NiAs_2$)."

K. S. HEIER and S. R. TAYLOR: Distribution of Ca, Sr and Ba in southern Norwegian pre-Cambrian alkali feldspars. *Geochim. et Cosmochim. Acta* **17,** 286–304.

Page 302, Table 6: the following sentence should be deleted: "The source of this data is not clear from the text of Goldsmith's paper." The following sentence should be substituted:

"J. R. GOLDSMITH (personal communication) states that the sources of the melting point data quoted are: OSBORN E. F. (1942) *Amer. J. Sci.* **240,** 781 (for $CaAl_2Si_2O_8$); DITTLER E. and LASCH H. (1931) *S. B. Akad. Wiss. Wien*, Abt. I, **140** (8), 633–74."

Page 292, Table 2: the following figures should be substituted for those appearing in Table 2

Sample number	K	Na
65	76·72	23·60
66	82·53	16·02
69	77·64	21·75
70	77·08	22·09
71	71·15	27·84

Geochimica et Cosmochimica Acta, 1960, Vol. 18, p. 156. Pergamon Press Ltd. Printed in Northern Ireland

Papers to be published in future issues

R. E. MARINGER and G. K. MANNING: Aerodynamic heating of the Grant meteorite.

R. R. BROOKS, L. H. AHRENS and S. R. TAYLOR: The determination of trace elements in silicate rocks by a combined spectrochemical–anion exchange technique.

E. A. VINCENT and J. H. CROCKET: Studies in geochemistry of gold—I. The distribution of gold in rocks and minerals of the Skaergaard intrusion.

E. A. VINCENT and J. H. CROCKET: Studies in the geochemistry of gold—II. The gold content of some basic and ultrabasic rocks and stony meteorites.

F. A. PANETH: The discovery and the earliest reproductions of the Widmanstätten figures.

E. L. FIREMAN and J. DEFELICE: Argon-39 and tritium in meteorites.

P. E. BROWN and B. J. RUSHTON: Some chemical data on the Mourne Mountain granite G2.

K. H. WEDEPOHL: Spurenanalytische Untersuchungen an Tiefseetonen aus dem Atlantik.

H. HAMAGUSHI, R. KURODA and H. ISHIKAWA: The distribution of minor elements in the rocks of Sakura-Jima volcano.

P. M. HURLEY, H. W. FAIRBURN, W. H. PINSON and G. FAURE: K–A and Rb–Sr minimum ages for the Pennsylvanian section in the Narragansett Basin.

K. KREJCI-GRAF and F. E. WICKMAN: Ein geochemisches Profil durch den Lias alpha.

A. T. WILSON and G. J. FERGUSSON: Origin of terrestrial tritium.

W. G. ERNST: The stability relations of magnesioriebeckite.

R. E. MARINGER: Ablation deposits on iron meteorites.

P. W. GAST: Alkali metals in stone meteorites.

R. D. RUSSELL and R. M. FARQUHAR: Dating galenas by means of their isotopic constitutions—II.

A. P. VINOGRADOV, E. I. DONTSOVA and M. S. CHUPAKHIN: Isotopic ratios of oxygen in meteorites and igneous rocks.

D. A. SCHAEFFER and J. ZAHRINGER: Helium, neon and argon isotopes in some meteorites.

E. ANDERS: The record in the meteorites—II. On the presence of aluminium-26 in meteorites and tektites.

S. R. TAYLOR: The abundance of the rare-earth elements in relation to their origin.

P. G. JEFFERY: The silica and aluminium content of the standard rocks G-1 and W-1.

D. F. C. MORRIS and R. A. KILLICK: Silver and thallium contents of rocks.

H. W. FAIRBAIRN, W. H. PINSON, P. M. HURLEY and R. F. CORMIER: A comparison of the ages of co-existing biotite and muscovite in paleozoic granitic rocks.

J. L. HORWOOD: Gamma-ray analysis of atmospheric dust samples.

W. S. FYFE: The possibility of *d* electron coupling in olivine at high pressures.

J. F. LOVERING, L. J. PARRY and J. C. JAEGER: Temperatures and mass losses in iron meteorites driving ablation in the Earth's atmosphere.

E. A. VINCENT and L. I. BILEFIELD: Cadmium in rocks and minerals from the Skaergaard intrusion, East Greenland.

G. G. GOLES, R. A. FISH and E. ANDERS: The record in the meteorites—I. The former environment of stone meteorites as deduced from K^{40}–Ar^{40} ages.

INFORMATION FOR CONTRIBUTORS

I. GENERAL

1. Papers on *geochemistry* should be submitted to the appropriate Executive Editor—Prof. L. R. WAGER for papers from the United Kingdom and British Commonwealth, and for papers in English from Europe; Prof. C. W. CORRENS for papers in German or French; Prof. E. INGERSON for papers from the American continents. Papers on *cosmochemistry* should be sent to Prof. W. A. WAHL. Papers submitted for publication will naturally be judged from the standpoint of scientific originality and novelty. Technical details of apparatus used in scientific investigation can, however, be presented in brief notes. Critical comments or preliminary results requiring early publication should be submitted as letters to the editors. Where possible, letters should be confined to 500 words. The preparation of progress reports and review articles will be invited by the editors from time to time. The journal appears as independent and complete numbers, which are combined into volumes of about 300 pages.

2. Only papers which have not been previously published can be accepted. Authors must agree not to publish elsewhere a paper submitted to and accepted by *Geochimica et Cosmochimica Acta*.

3. Fifty reprints of each paper are provided free. Additional copies can be purchased if ordered at the time the first proofs are returned. A reprint order form will accompany first proofs.

II. SCRIPT REQUIREMENTS

1. Scripts must be written in one of the three official languages—English, French or German.

2. The script should be typed (not a carbon copy). The text must be ready for printing and should be carefully checked for errors. Authors will receive proofs for correction.

3. Illustrations should accompany the script, mounted on separate sheets. Line diagrams that require to be redrawn should include all relevant details. Half-tone illustrations should be restricted to the minimum necessary. Photographs should be enlarged sufficiently to permit their clear reproduction, and if words or numbers appear on them, two copies should be sent, one clearly printed and the other without inscription. All illustrations should be provided with descriptive legends, which should be given on a separate sheet. Any lettering on diagrams—other than Greek letters, symbols, etc.—should be stencilled and should be sufficiently large and bold to permit reproduction when the diagram has been reduced to a size suitable for inclusion in the journal.

4. References in the text should be given by quoting the author's name and year of publication, i.e.

AHRENS (1952). *Full references should be listed at the end of each paper, in alphabetical order, in the following manner.*

AHRENS, L. H. (1952). The use of ionization potentials—I. Ionic radii of the elements. *Geochim. et Cosmochim. Acta* **2**, 155–169.

and should include the full title of the article, standard abbreviated title of the journal, year, volume, number and inclusive page numbers.

5. The text of articles submitted should be concise and in a readily understandable style. The technical description of the methods used should only be given in detail when such methods are new. The essential contents of each paper should be briefly recapitulated in an abstract in English. Such an abstract, may, however, be submitted by the author in the language of the original typescript for translation into English by the editorial staff.

6. To conserve space, authors are requested to mark less important portions of the paper (such as description of methods, record of experimental results, etc.) for printing in smaller type.

7. Indices of refraction should be denoted by the symbols α, β, γ, ω, ε, n, and vibration directions by X, Y, Z, O and E.

Pergamon Press are also publishers of the following Journals:

JOURNAL OF NUCLEAR ENERGY (*including* THE SOVIET JOURNAL OF ATOMIC ENERGY*). PART A: REACTOR SCIENCE; PART B: REACTOR TECHNOLOGY; PART C: PLASMA PHYSICS—ACCELERATORS—THERMONUCLEAR REACTORS
HEALTH PHYSICS (*The Official Journal of the Health Physics Society*)
JOURNAL OF INORGANIC AND NUCLEAR CHEMISTRY
TETRAHEDRON (*The International Journal of Organic Chemistry*)
TALANTA (*An International Journal of Analytical Chemistry*)
INTERNATIONAL JOURNAL OF APPLIED RADIATION AND ISOTOPES
BIOCHEMICAL PHARMACOLOGY
ARCHIVES OF ORAL BIOLOGY
* BIOPHYSICS
* JOURNAL OF MICROBIOLOGY, EPIDEMOLOGY AND IMMUNOBILOGY
* PROBLEMS OF HEMATOLOGY AND BLOOD TRANSFUSION
* PROBLEMS OF VIROLOGY
* PROBLEMS OF ONCOLOGY
* SECHENOV PHYSIOLOGICAL JOURNAL OF THE U.S.S.R.
* PAVLOV JOURNAL OF HIGHER NERVOUS ACTIVITY
* ELECTRIC TECHNOLOGY, U.S.S.R.
* RADIO ENGINEERING
* RADIO ENGINEERING AND ELECTRONICS
* TELECOMMUNICATIONS
* PHYSICS OF METALS AND METALLOGRAPHY
* THE ABSTRACTS JOURNAL OF METALLURGY
* APPLIED MATHEMATICS AND MECHANICS
CHEMICAL ENGINEERING SCIENCE
JOURNAL OF ATMOSPHERIC AND TERRESTRIAL PHYSICS
PLANETARY AND SPACE SCIENCE
BULLETIN GÉODÉSIQUE
ANNALS OF THE INTERNATIONAL GEOPHYSICAL YEAR
SPECTROCHIMICA ACTA
JOURNAL OF THE MECHANICS AND PHYSICS OF SOLIDS
ACTA METALLURGICA (*for the Board of Governors of Acta Metallurgica*)
INTERNATIONAL JOURNAL OF THE PHYSICS AND CHEMISTRY OF SOLIDS
DEEP-SEA RESEARCH
JOURNAL OF NEUROCHEMISTRY
JOURNAL OF PSYCHOSOMATIC RESEARCH
JOURNAL OF INSECT PHYSIOLOGY
INTERNATIONAL JOURNAL OF AIR POLLUTION
INTERNATIONAL ABSTRACTS OF BIOLOGICAL SCIENCES (*for Biological and Medical Abstracts Ltd.*)
RHEOLOGY ABSTRACTS
VACUUM
OPERATIONAL RESEARCH QUARTERLY
ANNALS OF OCCUPATIONAL HYGIENE
ELECTROCHIMICA ACTA

* *Translations of Russian journals published on behalf of the Pergamon Institute, a division of Pergamon International Corporation*

Leaflets giving further details and subscription rates of each of these journals are available on request

4Apr1960R 28Mar 64F
FILED IN STACKS

THE GEOCHEMICAL SOCIETY

OFFICERS

J. Frank Schairer, President
Tom F. W. Barth, Vice-President
Konrad B. Krauskopf, Secretary
George T. Faust, Treasurer

COUNCILLORS

John A. S. Adams, 1957–1959
Alfred O. Nier, 1957–1959
E. F. Osborn, 1958–1960
H. G. Thode, 1958–1960
Albert E. J. Engel, 1959–1961
Friedrich G. Hontermans, 1959–1961

REGIONAL VICE-PRESIDENTS

Louis H. Ahrens
Rui Ribeiro Franco
Ing. Georges Ordoñez
C. W. Correns
William S. Fyfe
Ken Sugawara

COMMITTEES

Auditing Committee:
Joseph J. Tregoning, Chairman
William L. Hill
C. R. Nasser

Constitution and By-Laws Committee:
Michael Fleischer, Chairman
Julian R. Goldsmith
Denis M. Shaw

Education Committee:
H. D. Holland, Chairman
J. A. S. Adams
D. M. Henderson
Kurt E. Lowe
G. D. Nicholls
Hans P. Eugster

Membership Committee:
R. M. Garrels, Chairman
Harvey C. Diebl
Chester B. Slawson
James E. Slosson
Irving Breger

Nominating Committee:
Wm. T. Pecora, Chairman
T. G. Sahama
C. E. Tilley
G. Tunell

Programme Committee:
H. T. Evans, Chairman
Gordon J. F. MacDonald
H. E. Lowenstam

Publications Committee:
E. W. Heinrich, Chairman
Julian R. Goldsmith
John C. Maxwell
N. W. Rakestraw
S. C. Robinson
L. R. Wager
Earl Ingerson

Research Committee:
C. G. Dodd, Chairman
W. F. Bradley
R. A. Rowland
T. G. Thompson

Russian Translations Committee:
Earl Ingerson

Standards Committee:
Alvin Van Valkenberg, Chairman
Michael Fleischer
Loren Stieff
George Switzer
George Tilton

Tellers Committee:
Charles Meyer, Chairman
Henry R. Cornwall
Colin O. Hutton